



**AN INVESTIGATION OF THE RESPONSE OF AN FPSOV STRUCTURES
TO EXTERNAL AIR BLAST: A CASE STUDY OF FPSOV OPERATING IN
THE NIGER DELTA**

BY

KAZEEM DOLAPO SHITTU

A Thesis submitted for the degree of Doctor of Philosophy (Integrated)

School of Marine Science and Technology

The University of Newcastle upon Tyne

April 2013

DEDICATION

TO

**ALHAJI DOLAPO SHITTU, DEACONESS JULIANA SHITTU AND
OMOBOLA SHITTU**

Acknowledgements

First, I would like to express my gratitude to Almighty God for taken me this far in the search of knowledge and to have seen me through my academic pursuit at the University of Newcastle upon Tyne.

Secondly, I am grateful to my supervisors Dr Peter Wright and Professor Robert Dow for their support, understanding, help and guidance. Despite the numerous challenges I went through, their guidance and support was one thing I never lacked. My special thanks go to Professor Robert Dow who stood in for Dr Peter Wright when he took ill. To both of you, I say a big thank you sir.

Thirdly, I am grateful to the Petroleum Trust Development Funds who paid my 3years tuition fees and to the Nigerian Navy where I am serving an officer of the rank of a Commander, to have released me for this study.

Furthermore, I am very grateful to the Head of school Professor Richard Birmingham to have encourage me to undertake a doctoral studies of the University of Newcastle upon Tyne, I am indeed proud of this citadel of learning. I will encourage other international student to come to this great University.

Additionally, I am also grateful to all the staff members of the University of Newcastle, School of Marine Science and Technology for the support they gave me as an international student throughout my studies at Newcastle. Also special thanks to John Garside for going through some of my initial scripts .Also to Mr BolajiAkinyemi and Musa Bashir who out of no time assisted in going through some of my work. God reward you all.

Being away from home, the support of my extended family was crucial to my success, therefore, I am indeed very grateful to my children, mum, uncles and siblings. Finally, to my loving and kind Wife who has put up with those late evenings and weekends to pick me up at school and for her help, patience, understanding, assistance and support throughout the course of my stay at Newcastle upon Tyne.

Abstract

Floating production storage and offloading systems, otherwise known as FPSOs in the oil and gas industry, are high risk structures because of their exposure to hazardous and flammable hydrocarbons which they carry and in some situations, because of their vulnerability to terrorist attack especially in their areas of operation. These structures have been widely used for the development of offshore oil and gas fields all over the world, especially in most part of Africa, because of their attractive features such as large work area and storage capacity, relative lower cost of construction and good stability. They are either converted from existing tankers or bulk carriers or purposely built. However the recent wave of terrorism across the Nigerian Niger Delta has necessitated the study for the need for offshore structures especially FPSO to be protected from the activities of terrorist. One of the worst case scenarios that is likely to occur on an FPSO is an attack by terrorist resulting in an above water external air blast on the side plate of a midship section of an FPSO. The resulting damage effects that would be caused by this form of attack can be devastating in terms of loss of revenue to a nation, loss of life, assets and degradation to the local environment. This was tragically demonstrated in the North Sea with the loss of the Piper Alpha Platform mentioned by (lees, 1996), albeit initiated by an accidental internal blast, unrelated to terrorist activities. At present, most design methods on the midshipsection structural members of a merchant vessel are based on working stress design concepts that are safe and suitable for normal pre-commissioning and operating conditions and which emphasize the minimum acceptable requirement for the classification society. However, design under extreme air blast loading especially those typical of terrorist/Militant attack, whose magnitude would be far higher than ordinary operating load, are desirable. In order to make it a major design consideration, this study addressed this issue on minimizing the effects of blast overpressure through the evaluation of the 3 types of T stiffeners and 3 L stiffeners to local structural response of such blast pressure on the side shell of the midshipsection of a typical FPSO code named FPSO Nigeria. The Nigerian Niger Delta accounts for over 95% of Nigerian oil and foreign reserve earning, and has been a source of attack and insurgence by militant of the Niger Delta. The objective of this study is to examine an above water air blast pressure attack to the side plate of a midshipsection of an FPSO code named FPSO Nigeria. This blast pressure is converted to an equivalent amount of TNT explosive typical to that which may be used by the militants of the Nigeria Niger delta or other parts of the world and to

recommend ways by which an FPSO operating in this area could be made more resilient to terrorist attack to a larger extent or at least to minimize terrorist caused damage to the barest minimum by the selection of the best of the 3 types of T and L stiffeners considered. Additionally, blast resistant anti-ballistic material was recommended and a cost benefit analysis carried out in order to justify the need and the importance of using such blast resistance anti-ballistic materials. In order to achieve the aim of the thesis, the study commenced with the investigation of the displacement and stresses of plates and stiffened plates using Abaqus software code and compared the results of displacement and stresses generated from Abaqus with that of classical theory in order to validate the accuracy of the Software code by considering different plate thickness and boundary conditions, frequency extraction analysis were generated for plates and stiffened plates in order to obtain frequencies at which resonance could occur and to prevent such. The results generated from Abaqus software code were found to correlates with those generated from classical theory. Actual FPSO Nigeria stiffened panel were then considered and subjected to non-linear blast analysis under different boundary conditions where effects of mesh refinement were considered in details. The mid ship section of the above water side of the FPSO Nigeria was then subjected to blast pressure attack considering the different type of stiffeners with a view to determine the best stiffener configuration and to determine the rupture strain consequently an anti-ballistic blast resistant material was recommended as an aftermath of Cost Benefit analysis was carried out to validate the need for such anti-ballistic blast resistance material on the above water side of FPSOs operating in the Nigeria Niger Delta and the cost savings to nigerian Government was highlighted vis a vis the loss that would have been incurred by the Government should such attack occurs. The research concentrates mainly on developing an appropriate methodology and an illustrating the behavior of typical ship structures to high rate transient air blast loading effects, rather than undertaking a specific detail design study as such. Consequently the research has made modest contribution to knowledge by the determination of all of the above including the cost benefit analysis carried out.

DECLARATION

No portion of the work presented in this thesis has been submitted in support of an application for another degree or qualification of this or any other university or other institute of learning.

Table of Contents

DEDICATION.....	ii
Acknowledgements.....	iii
Abstract.....	iv
DECLARATION.....	vi
Table of Contents.....	vii
List of Figures.....	ix
List of Tables.....	xvi
Nomenclature.....	xviii
CHAPTER 1.....	1
1. Introduction.....	1
1.1 Introduction.....	1
1.2 Background of Study.....	2
1.3 Word Energy Demand.....	5
1.4 Word Oil and Gas Overview.....	5
1.41 Oil and Gas Reserve.....	6
1.42 Crude Oil Production.....	6
1.43 Concept of Deepwater Development and Floating System.....	7
1.44 African Oil: A Brief Survey.....	8
1.51 Major Oil Consumer And Africa.....	9
1.52 Development of Nigeria’s Oil Industry.....	10
1.6 Study Objectives.....	11
1.61 Research Methodology.....	11
1.7 Overview of the Chapter.....	13
CHAPTER 2.....	15
An Introduction to Blast Analysis Methods.....	15
2.2 Introduction to Blast Analysis.....	15
2.1 Literature Reviews on Blast Loading and Plate Deformation.....	16
Chapter 3.....	26
3.0 Structural Vibration and Frequency Extraction Analysis.....	26
3.1 Introduction.....	26
3.2 Determination of stresses and displacement using Abaqus Code and classical theories (Roark’s formula).....	27
3.3 Introduction to Structural Vibration.....	28
3.4 Frequency Extraction Analysis of Unstiffened Plate.....	29
3.5 RESULTS AND DISCUSSIONS.....	49
3.6 CONCLUSION.....	50
Chapter 4.....	52
4. Non-linear Analysis of Stiffened Plates Subjected to Uniform Blast Pressure Load....	53
4.1 Introduction to Non-linear Analysis of Stiffened Plates Subjected to Uniform Blast Pressure Load.....	53
4.2 INTRODUCTION.....	53
4.1 NUMERICAL MODELS.....	53
4.2 DESCRIPTION OF PLATES.....	54
4.3 MODEL GEOMETRY.....	54
4.4 Finite Element Modelling.....	54
4.5 FUNDAMENTAL FREQUENCY EXTRACTION AND PERIOD.....	56
4.6 THE EXPLOSION PHENOMENON.....	57
4.7 Idealisation of Blast Pressure Loading.....	58

Table of Contents

4.8. Effect of Mesh Refinement on the Displacement of the central node, Energy terms of the model and Von Misses Stress.....	65
4.9 EFFECT OF DAMPING ON THE ARTIFICIAL ENERGY OF THE SYSTEM.....	71
4.10 EFFECT OF RATE DEPENDENCE ON CENTRAL NODE ON MODEL 1, 2 AND 3	72
4.12 RESULTS AND DISCUSSIONS.....	99
4.4 Effect of Rate Dependence.....	100
4.5 Conclusions.....	101
Chapter 5.....	103
5. Blast Analysis and Determination of Rupture Strain.....	103
5.1 Introduction to Blast Analysis and Determination of Rupture Strain.....	103
5.2 Introduction.....	105
5.2 Definition of Stress and Strain.....	106
5.3 Strain.....	107
5.4 Relationship Between Stress and Strain.....	107
5.4 COMPUTATIONAL MATERIAL MODEL.....	110
5.5 NUMERICAL SIMULATIONS.....	115
5.7 Simulation of Blast Analysis Results.....	118
5.8 DISCUSSION AND CONCLUSION.....	136
5.9 Conclusions.....	138
Chapter 6.....	140
6. A Cost Benefit Analysis of Installing Anti Ballistic Material on the above water sides of FPSO Nigeria.....	140
6.1 Introduction.....	140
6.2 Nigeria as an Oil Producing Nation.....	140
(Millions of barrels per day).....	143
6.3 Floating Production Storage and Offloading (FPSO).....	144
6.4 Technical Advantages of FPSO For Oil Field Development.....	144
6.5 Cost Benefit Analysis on whether to Protect the Above Water Side of an FPSO Operating In Nigerian Water or not.....	146
6.6 Parameters of FPSO Vessel Nigeria in which Cost Benefit Analysis was Carried out and other Related Parameters.....	147
6.9 Benefits Expected from the Study.....	150
6.10 Ballistic Protection Material.....	151
6.11 Conclusion.....	154
Chapter 7.....	156
8. Conclusion and Recommendations for further work.....	156
8.1 Introduction.....	156
8.2 Rationale of the Research.....	156
8.3 Summary.....	157
8.3 Main Conclusions.....	159
8.4 PASSIVE PROTECTION.....	161
8.5 Recommendations.....	161
Appendix.....	162
References.....	188

List of Figures

Figures	Pages
1 The damaged hull of the U.S.S Cole.....	3
1.1 The M/V Limburg on fire.....	3
3 (a) and (b): Frequency extraction analysis modes 1 and 2 respectively for a 2mx2mx5mm plate fixed at all edges.....	31
3.1 (a) and (b): Frequency extraction analysis modes 1 and 2 respectively for a 2mx2mx8mm plate fixed at all edges.....	32
3.2 (a) and (b): Frequency extraction analysis modes 1 and 2 respectively for a 2m x 2m x 25mm plate fixed at all edges.....	32
3.3 (a) and (b): Frequency extraction analysis modes 1 and 2 respectively for a 2m x 2m x 30mm plate fixed at all edges.....	32
3.4: FPSO panel (4.86mx4.86m).....	33
3.5: FPSO Panel with fix fix boundary conditions.....	33
3.6: FPSO panel-Fundamental Extraction frequency for 5mm plate.....	34
3.7. Mode 1 for the 4.86m x 9.72 x 5mm thick plate with a point supported boundary condition.....	34
3.9 Mode 1 for the 4.86m x 12.15m x 5mm thick plate with a point supported boundary condition.....	35
3.10 Mode 1 for the 4.86m x 12.15m x 10mm thick plate with a point supported boundary condition.....	36
3.11 Mode 2.....	36
4. Model 1-Configuration of Stiffeners-(1x1).....	55
4.1 Configuration of Stiffeners-Model 2-[2x2].....	55
4.2. Configuration of Stiffeners -Model 3-[3x3].....	56
4.3. Showing the effect of mesh refinement on the displacement of the central node.....	62
4.4 Showing the effect of mesh refinement on the displacement of the central node.....	63
4.5: Showing the effect of mesh refinement on the displacement of the central node.....	64
4.6: Effect of coarse mesh on internal energy and plastic dissipation energy of the system.....	67

List of Figures

4.7: Effect of fine mesh on internal energy and plastic dissipation energy of the system.....	67
4.10 Effect of coarse mesh on internal energy and plastic dissipation energy of the system.....	68
4.11 Showing the effect of fine mesh on internal energy and plastic dissipation energy of the system.....	68
4.12 Effect of coarse mesh on internal energy and plastic dissipation energy of the system.....	69
4.13 Showing the effect of Damping on the Displacement of the central node on model 1.....	70
4.14: Showing the effect of Damping on the Displacement of the central node on model 2.....	70
4.15: Effect of Damping on the Displacement of the central node on model 3.....	71
4.16: Effect of material damping on internal energy of the system for model 1.....	71
4.17: Showing the effect of material damping on internal energy of the system for model 2.....	72
4.18: Showing the effect of material damping on internal energy of the system for model 3.....	72
4.19 Showing the effect of material damping on artificial energy of the system for model 1.....	73
4.20 Showing the effect of material damping on artificial energy of the system for model 2.....	73
4.21 Showing the effect of material damping on artificial energy of the system for model 3.....	74
4.22 Showing the effect of material damping on Plastic dissipation energy of the system for model 1.....	74
4.23 Showing the effect of material damping on Plastic dissipation energy of the....	75
4.24 Showing the effect of material damping on Plastic dissipation energy of the system for model 3.....	75
4.25 Showing the effect of rate dependence on the displacement of the central node for model 1.....	76

List of Figures

4.26 Showing the effect of rate dependence on the displacement of the central node for model 2.....	76
4.27 Showing the effect of rate dependence on the displacement of the central node for model 3.....	77
4.28 Effect of material damping on Artificial Strain dissipation energy of the system for model 1.....	77
4.29 Effect of material damping on Artificial Strain dissipation energy of the system for model 2.....	78
4.30 Effect of material damping on Artificial Strain dissipation energy of the system for model 3.....	78
4.31 Showing the effect of material damping on Internal Energy of the system for model 1.....	79
4.32 Showing the effect of material damping on Internal Energy of the system for model 2.....	79
4.33 Showing the effect of material damping on Internal Energy of the system for model 3.....	80
4.34 Showing the effect rate dependence on the plastic dissipation energy model 1.....	80
4.35 Showing the effect rate dependence on the plastic dissipation energy model 3.....	81
4.36 Showing the effect of material damping on Strain Energy of the system for model 1.....	81
4.37 Showing the effect of material damping on Strain Energy of the system for model 2.....	82
4.38 Showing the effect of material damping on Strain Energy of the system for model 3.....	82
4.39 Comparison of the Displacement History of the central node for Model 1, 2 and 3.....	83
4.40 Comparison of the Undamped Displacement History of the central node For Model 1, 2 and 3.....	86
4.41 Showing comparison of the damped Displacement History of the central node For Model 1, 2 and 3.....	87
4.42 Showing the effect of Rate Dependency on the Displacement of the central node for model 1, 2 and 3.....	88

List of Figures

4.43 Comparison of the Effect of Artificial Energy on the Displacement of the central node for model 1, 2 and 3.....	88
4.44 Showing comparison of the Effect of Undamped Artificial Energy on the Displacement of the central node for model 1, 2 and 3.....	89.
4.45 Showing comparison of the Effect of damped Artificial Energy on the Displacement of the central node for model 1, 2 and 3.....	90
4.46 Showing comparison of the Effect of Internal Energy on the Displacement of the central node for model 1, 2 and 3.....	90
4.47 Showing comparison of the Effect of Undamped Internal Energy on the Displacement of the central node for model 1, 2 and 3.....	91
4.48 Showing the comparison of the Effect of Damped Internal Energy on the Displacement of the central node for model 1, 2 and 3.....	92
4.49 Showing the comparison of the Effect of Internal Energy with rate of Dependence on the Displacement of the central node for model 1,- 2 and 3.....	92
4.50 Showing the comparison of the Effect of Kinetic Energy on the Displacement of the central node for model 1, 2 and 3.....	93
4.51 Showing the comparison of the Effect of Undamped Kinetic Energy on the Displacement of the central node for model 1, 2 and 3.....	93
4.52 Showing the comparison of the Effect of damped Kinetic Energy on the Displacement of the central node for model 1, 2 and 3.....	94
4.53 Showing the comparison of the Effect of Kinetic Energy with rate of dependence on the Displacement of the central node for model 1, 2 and 3.....	94
4.54 Showing the comparison of the Effect of Undamped Plastic Dissipation Energy on the Displacement of the central node for model 1, 2 and 3.....	95
4.55 Showing the comparison of the Effect of damped Plastic Dissipation Energy on the Displacement of the central node for model 1, 2 and 3.....	95
4.56 Showing the comparison of the Effect of Plastic Dissipation Energy with rate of dependence on the Displacement of the central node for model 1, 2 and 3.....	96
4.57 Showing the comparison of the Effect of strain Energy on the Displacement of the central node for model 1, 2 and 3.....	96
4.58 Showing the comparison of the Effect of undamped strain Energy on the Displacement of the central node for model 1, 2 and 3.....	97
4.59 Showing the comparison of the Effect of damped strain Energy on the Displacement of the central node for model 1, 2 and 3.....	97

List of Figures

4.60 Showing comparison of the Effect of strain Energy with rate of dependence on the Displacement of the central node for model 1, 2 and 3.....	98
5.0 Panel of the FPSO Nigeria subjected to blast pressure loading.....	98
5.1: STRESS CURVE FOR STRUCTURAL STEEL.....	104
5.2: Example Test on 2 grades of Steel (Curled from Stress-Strain note-Newcastle University).....	107
5.3a-T Stiffener (150mm x14mm.....	108
5.3b: T Stiffener (200mm x10.5mm).....	111
5.3C: T Stiffener (250mm x8.4mm)	111
5.3e-L Stiffener (200mmx10.5mm).....	112
5.3d-L Stiffener (150mm x14mm)	112
5.3: Midship section of the FPSO showing blast area and boundary condition applied which is fixed in all direction.....	116
5.4 (a and b): Showing blast simulation result of the impact of blast Pressure of 1e+6 Pascal on the above water side of the FPSO Nigeria (Type A Stiffened Plate)...	118
5.4 (c and d): Showing blast simulation result of the impact of blast Pressure of 1e+7 Pascal on the above water side of the FPSO Nigeria (Type A Stiffened Plate)...	118
5.4 (c and d): Showing blast simulation result of the impact of blast Pressure of 1e+8 Pascal on the above water side of the FPSO Nigeria (Type A Stiffened Plate)..	119
5.5 (a and b): Showing blast simulation result of the impact of blast Pressure of 1e+6 Pascal on the above water side of the FPSO Nigeria (Type B Stiffened Plate).	120
5.5 (c and d): Showing blast simulation result of the impact of blast Pressure of 1e+7 Pascal on the above water side of the FPSO Nigeria (Type B Stiffened Plate).	120
5.5 (e and f): Showing blast simulation result of the impact of blast Pressure of 1e+8 Pascal on the above water side of the FPSO Nigeria (Type B Stiffened Plate)...	121
5.7 (a and b): Showing blast simulation result of the impact of blast Pressure of 1e+6 Pascal on the above water side of the FPSO Nigeria (Type C Stiffened Plate)...	121
5.7(c and d): Showing blast simulation result of the impact of blast Pressure of 1e+7 Pascal on the above water side of the FPSO Nigeria (Type C Stiffened Plate)..	122
5.7 (e and f): Showing blast simulation result of the impact of blast Pressure of 1e+8 Pascal on the above water side of the FPSO Nigeria (Type C Stiffened Plate)..	122
5.8 (a and b): Showing blast simulation result of the impact of blast Pressure of 1e+6 Pascal on the above water side of the FPSO Nigeria (Type D Stiffened Plate)...	123

List of Figures

5.8 (c and d): Showing blast simulation result of the impact of blast Pressure of 1e+7 Pascal on the above water side of the FPSO Nigeria (Type D Stiffened Plate)....	123
5.8 (e and f): Showing blast simulation result of the impact of blast Pressure of 1e+8 Pascal on the above water side of the FPSO Nigeria (Type D Stiffened Plate)...	124
5.9 (a and b): Showing blast simulation result of the impact of blast Pressure of 1e+6 Pascal on the above water side of the FPSO Nigeria (Type D Stiffened Plate)....	125
5.9 (c and d): Showing blast simulation result of the impact of blast Pressure of 1e+7 Pascal on the above water side of the FPSO Nigeria (Type D Stiffened Plate).....	125
5.9 (e and f): Showing blast simulation result of the impact of blast Pressure of 1e+8 Pascal on the above water side of the FPSO Nigeria (Type D Stiffened Plate)....	126
5.91 (a and b): Showing blast simulation result of the impact of blast Pressure of 1e+6 Pascal on the above water side of the FPSO Nigeria (Type F Stiffened Plate)....	127
5.91 (a and b): Showing blast simulation result of the impact of blast Pressure of 1e+7 Pascal on the above water side of the FPSO Nigeria (Type F Stiffened Plate)....	127
5.91: A True Stress Strain Curve Of The Area Blasted (For T Stiffeners).....	129
5.93: a. The stress strain curve.....	130
6.94: A TRUE STRESS STRAIN CURVE OF THE AREA BLASTED.....	130
5.95: True Stress-strain curve for type A –T stiffener-150mm x14mm with the application of 1e7pascal blast pressure.....	131
5.96: True Stress-strain curve for type A –T stiffener-200mm x10.5mm with the application of 1e8pascal blast pressure.....	131
5.97: COMBINED ENERGY GRAPH FOR STIFFENNER T AND L when Blast Pressure of 1e8 Pascal was applied.....	132
5.98: COMBINED ENERGY GRAPH FOR STIFFENNER T AND L when Blast applied Pressure of 1e7 Pascal was applied.....	133
5.99: COMBINED ENERGY GRAPH FOR STIFFENNER T AND L when Blast Pressure of 1e6 Pascal was applied.....	134
5.9.1: COMBINED ENERGY GRAPH FOR STIFFENNER T AND L when Blast Pressure with 1e6Pascals, 1e7Pascals and 1e8 Pascal was applied.....	135
6.1: Nigerian Oil and Gas Fields	141
6.2: Typical arrangement of a composite ballistic protection material.....	152
6.3: Isometric view of the typical arrangement of a composite ballistic protection material.....	153

List of Figures

6.4: Vertical view of a typical arrangement of a composite ballistic protection material.....	153
6.5: Simple Schematic diagram of a bar armour for the protection against shaped charger.....	154

List of Tables

1. Showing selected Gulf of Guinea countries-Oil production and Projections 1990- 2033-----	4
1.1: African Proven Oil Reserve-----	8
1.2: African oil production mb (1995-2005) -----	9
3.1: Showing Comparison of Stress and Displacement results obtained from Abaqus Software and Classical Theory using a Blast Pressure loading of 1E06 Pascal-----	27
3.2: Showing Comparison of Stress and Displacement results obtained from Abaqus Software and Classical Theory using a Blast Pressure loading of 1E+06 Pascal---	28
3.3: Result of Natural frequency Analysis carried out for Simple Plate 2mx2m with AR=1 and with all edges fixed using Abaqus software code and validated against Classical theory.-----	30
3.4: Result of Natural frequency Analysis for FPSO Plate Panel 4.86mx4.86m validated from Abaqus software against Classical Theories-point supported boundary condition----- -----	34
3.5: Result of Natural frequency Analysis for FPSO Plate Panel 4.86mx7.29m-----	35
3.6: Result of Natural frequency Analysis for FPSO Plate Panel 4.86mx9.72m (AR=2.0) validated from Abaqus software against Classical Theories-point supported boundary condition-----	37
3.7: Result of Natural frequency Analysis for FPSO Plate Panel 4.86mx 12.5m (AR=2.5)-- -----	39
3.8: Comparison of frequency extraction analysis for FPSO plate with AR 1 resulting from 2 different boundary conditions-----	41
3.9: Comparison of frequency extraction analysis for FPSO plate with AR 1.5 resulting from 2 different boundary conditions-----	42
3.10: Comparison of frequency Extraction Analysis for FPSO Plate with AR 2.5 resulting from 2 Different Boundary Conditions.-----	42
4: Fundamental Frequencies and Period for the 3 cases in view-----	56
5.1: Standard Conversion Factor for Some Explosives-----	60
4.2: Material Properties Used for the Analysis.-----	61
4.3: BLAST LOAD AMPLITUDE-----	61
4.4: Showing the effect of mesh refinement on Von –Misses Stresses for Model 1, 2 and 3-----	65

List of Tables

4.5: Effect of Mesh refinement on internal energy and plastic dissipation energy of the system.....	66
4.6: Showing the effect of rate dependence on all the energy given terms.....	84
5: Properties of Steel.....	110
5.1: Detailed Size of T-stiffeners Considered	114
5.2: Detailed Size of L-Stiffeners Considered.....	143
6: Showing Top World Oil Producers, Exporters, Consumers, and Importers as at 2006----	145
6.1: Some of the FPSOs operating in the Nigerian Water.....	149
6.2 Annual Benefits.....	149
6.3 Annual cost (outgoings).....	149
6.4 : Present Value of Benefit.....	150

Nomenclature

A	Area of the plate (m ²)/explosive constant
B, R1, R2, U	Explosive constants
C	Structural damping matrix
ca	Ambient speed of sound in air (m/s)
cp	Peak wind velocity (m/s)
csa	Velocity of shock wave in air (m/s)
cw	Velocity of sound in water (m/s)
D	Material constant
E	Young's modulus of the plate material
Es	Energy of the shock wave per unit area (J/m ²)
ETNT	Energy of TNT explosive (J)
F	Peak load on the plate (N)
F(t)	Time-dependent load on the plate (N)
K	Structural stiffness matrix
k	Stiffness of the plate (N/m)
M	Structural mass matrix
m	Mass per unit area of the plate (kg/m ²)
n	Material parameter
Pm	Peak pressure/peak overpressure (MPa)
Po	Atmospheric pressure (MPa)
p	Exponent of power-type strain law/pressure (MPa)
pi	Incident pressure (MPa)
q	Dynamic pressure (MPa)/material constant
re	Radius of the explosive (m)
S	Stand off (m)
S0	Scaled distance (m/m)
T	Kinetic energy of the plate (J)
t	Time (s)/thickness (m)
tc	Cavitation time (m/s)

Nomenclature

t_d	Positive duration of the blast wave (s)
U	Internal energy of the explosive per unit volume (J/m ³)
V	Volume (m ³)/impact velocity (m/s)
V_m	Maximum velocity attained by the plate (m/s)
A_i	Element area
b	Plate breath
B	Ship breadth
b_e	Plate effective width
b_f	Stiffener flange width
C	Hull girder applied moment curvature
C_B	Block coefficient
D	Ship moulded depth
E	Young's modulus
$f(x)$	Probability density function
$fe(x)$	External finite element model definition
$g(x)$	Limit state or performance function
h	Subscript /superscript for hogging load condition
I	Second moment of inertial
I_N	Transverse neutral axis
J	Contour J-integral
K_a	Applied stress intensity factor
K_G	Geometry stress concentration factor
$K_{I,II,III}$	Stress intensity factor for mode I, II, and III loading
K_{IC}	Plane strain fracture toughness
K_{plt}	Plate stress intensity factor
K_{web}	Stiffener web stress intensity factor
L	Ship length
L^*	Load at design point
L'	Characteristic value of load
M^*	Hull girder ultimate strength at the design point
M'	Characteristic value of hull girder ultimate strength
M_{0H}	Horizontal hull girder ultimate bending capacity
M_{0V}	Vertical hull girder ultimate bending capacity
M_H	hull girder horizontal bending component

Nomenclature

M_{sw}	Still water bending moment
M_u	Ultimate hull girder strength
M_v	Hull girder vertical bending component
M_{wH}	Horizontal component of wave-induced bending moment
M_{wV}	Vertical component of wave-induced bending moment
M_y	Hull girder horizontal bending moment
N	Total number of samples
S^*	Strength at design point
t	Plate thickness
t_f	Stiffener flange thickness
t_w	Stiffener web thickness
T	Ship draft
w_0	Plate initial deflection
y_i	Hull girder element horizontal ordinate
z	Section modulus
α	Importance factors
β	Reliability index, plate slenderness ratio
β_E	Effective plate slenderness ratio
ε_i	Element strain
λ	Column slenderness ratio
σ_{max}	Maximum tensile stress
σ_{rc}	Residual stress amplitude
σ_{xx}	Principal normal stress in the x-direction
σ_Y	Yield strength
σ_{yy}	Principal normal stress in the y-direction
σ_{zz}	Principal normal stress in the z-direction
τ_{xz}	Shear stress in the x-z plane
τ_{yz}	Shear stress in the y-z plane
ν	Poisson ratio

CHAPTER 1

1. INTRODUCTION

1.1 PREAMBLE

Floating production storage and offloading systems, otherwise known as FPSOs in the oil and gas industry, are high risk structures because of their exposure to hazardous and flammable hydrocarbons which they carry and in some situations, because of their vulnerability to terrorist attack especially in their areas of operation. These structures have been widely used for the development of offshore oil and gas fields all over the world, especially in most part of Africa, because of their attractive features such as large work area and storage capacity, relative lower cost of construction and good stability. They are either converted from existing tankers or bulk carriers or purposely built. However the recent wave of terrorism across the Nigerian Niger Delta has necessitated the study for the need for offshore structures especially FPSO to be protected from the activities of terrorist. One of the worst case scenarios that is likely to occur on an FPSO is an attack by terrorist resulting in an above water external air blast on the side plate of a midship section of an FPSO. The resulting damage effects that would be caused by this form of attack can be devastating in terms of loss of revenue to a nation, loss of life, assets and degradation to the local environment. This was tragically demonstrated in the North Sea with the loss of the Piper Alpha Platform mentioned by (lees, 1996), albeit initiated by an accidental internal blast, unrelated to terrorist activities. At present, most design methods on the midshipsection structural members of a merchant vessel are based on working stress design concepts that are safe and suitable for normal pre-commissioning and operating conditions and which emphasize the minimum acceptable requirement for the classification society. However, design under extreme air blast loading especially those typical of terrorist attack, whose magnitude would be far higher than ordinary operating load, are desirable. In order to make it a major design consideration, this study would address this issue on minimizing the effects of blast overpressure through the evaluation of the 3types of T stiffeners and 3 L stiffeners to local structural response of such blast pressure on the side shell of the midshipsection of a typical FPSO. The Nigerian Niger Delta accounts for over 95% of Nigerian oil and foreign reserve earning, and has been a source of attack and insurgence. The objective of this study is to examines an above water air blast pressure attack to the side plate of a midshipsection of an FPSO code

named FPSO Nigeria. This blast pressure is converted to an equivalent amount of TNT explosive typical to that which may be used by the militants of the Nigeria Niger delta or other parts of the world and to recommend ways by which an FPSO operating in this area could be made more resilient to terrorist attack to a larger extent or at least to minimize terrorist caused damage to the barest minimum by the selection of the best of the 3 types of T and L stiffeners considered. Additionally, blast resistant material would be recommended and a cost benefit analysis would be carried out in order to justify the need and the importance of using such blast resistance materials. This research concentrates mainly on developing an appropriate methodology and an illustrating the behavior of typical ship structures to high rate transient air blast loading effects, rather than undertaking a specific detail design study as such.

1.2 BACKGROUND OF STUDY

This study examines alternative methods of improving a typical FPSO design to minimize the effect of blast overpressures on the side shell of the FPSO experiencing the effect of an external explosion. Explosions produce expanding circular front shock waves which induce transient overpressures over short period of time, Assuming that the propagation of the pressure waves are not obstructed, the strength and its impact on a surface depend its rise time, maximum peak pressure, the duration and the distance of explosion to the point on an object. As the magnitudes of the blast load are usually many times greater than the more conventional loads on the sides of shell of the midship section of an FPSO, there is thus the need to make alternative design methodology and analysis techniques for the type of stiffeners in order for them to be able to withstand, or minimize the effects of external blast over pressures. A typical midship side shell of an FPSO vessel code named FPSO Nigeria would for the purpose of this study be modelleled and subjected to blast overpressures using the Abaqus finite element programme in order to evaluate the extent and form of damage that would result from the blasting of the side shell. Thus the study will look into the present arrangement where L stiffeners are used with a view to comparing them with 3 types of T stiffeners having a constant web size but with variable flange length and flange thickness in order to get a structural configuration of stiffeners with better performance so as to improve the capabilities to withstand blast over pressures and or to minimize the effect of terrorist/Militant attack. Figures 1 and 1.1 shows various form of attack by terrorist on USS Cole



Figure 1: The damaged hull of the U.S.S Cole after being hit by suicide bombers in a small boat while in the port of Yemen. (Source: www.washingtonpost.com)



Figure 1.1- The M/V Limburg on fire after being hit by suicide bombers in small boats at port in Yemen. (Source: <http://timriley.com/LimburgOilTankerFire.jpg>)

Table 1 : Selected Countries in the Gulf of Guinea: Oil Production and Projections, 1990-2033						
in thousands of barrels per day						
	Angola	Cameroon	Congo, Rep. of	Equat. Guinea	Gabon	Nigeria
1990	473	145.8 (†)	165.7	0	270.0	1,812
1991	497	136.7 (†)	160.8	0	296.0	1,894
1992	549	129.9 (†)	172.8	3.1	294.0	1,959
1993	504	113.7 (†)	189.8	4.5	312.0	2,038
1994	550	107.9 (†)	180.8	4.9	356.0	1,897
1995	617	101.1 (†)	180.0	6.2	368.0	1,990
1996	679	107.7 (†)	196.0	16.9	364.0	2,179
1997	698	114.8 (†)	238.0	56.6	368.0	2,271
1998	739	119.5 (†)	252.8	82.9	350.0	2,231
1999	746	113.4 (†)	259.4	103.1	312.0	2,110
2000	748	114.2 (†)	268.0	117.9	272.0	2,261
2001	740	103.3 (†)	235.2	205.1	260.0	2,238
2002	903	102.5	231.6	247.0	252.0	1,960
2003*	n/a	97.3	218.0	n/a	270.0	2,450
Projections :						
2004	n/a	90.1	n/a	n/a	266.0	2,500
2005	n/a	85.8	n/a	n/a	220.0	2,630
2006	n/a	81.4	n/a	n/a	204.0	2,700
2007	n/a	n/a	n/a	n/a	n/a	2,750
2008	n/a	n/a	n/a	n/a	n/a	2,810
2009	n/a	n/a	n/a	n/a	n/a	2,880
2010	n/a	n/a	n/a	n/a	154.0	n/a
2015	n/a	n/a	n/a	n/a	112.0	n/a
2020	n/a	n/a	n/a	n/a	82.0	n/a
2025	n/a	n/a	n/a	n/a	60.0	n/a
2030	n/a	n/a	n/a	n/a	44.0	n/a
2033	n/a	n/a	n/a	n/a	36.0	n/a
Note: (*) Estimations. (†) Production corresponds to the fiscal year beginning in the year specified, e.g., 1990 stands for fiscal year 1990/91.						
Source: IMF Country Reports						

Table 1-Selected Gulf of Guinea countries-Oil production and Projections 1990-2033 (In thousands of barrel per day)

1.3 WORLD ENERGY DEMAND

Oil and gas are still the world's most common sources of energy supply. Over 100 countries around the world are producing oil at the moment. The world oil consumption which reached 75mbl/day in 1999 will probably grows to 120mbl/day in 2030 (**International Energy Agency, 2002**). Around 40% of the world's oil consumption at the moment are produced by eleven OPEC countries namely Algeria, Indonesia, Iran, Iraq, Kuwait, Libya, Nigeria, Qatar, Saudi Arabia, The United Arab Emirate Republic and Venezuela, the rest is produced by Non-Opec countries such as United states, Mexico, Denmark, Norway, the United Kingdom, the Russian Federation, China and Vietnam (**ILO,2002**). The last seven years have been characterized by an unprecedented, sharp and steady rise in oil prices albeit with major fluctuation. Prices have risen for a record setting consecutive years from \$26 per barrel in 2001 to over \$140 in July 2008 (**IEA,2008**).The reality of the market forces of demand and supply including the uncertainties and political development is steadily putting upward pressure on the prices. World oil consumption rose by 9million barrels per day over the period. China, Middle East and India are major contributors to this growth thus offshore platforms, particularly floating types, are of fundamental importance to oil producing nations as they pave the ground for the exploration and exploitation of oil and gas in deep water areas in order to help meet increase in demand . Consequently, the need for FPSO and other offshore field exploration facilities could not be overemphasized.

1.4 WORLD OIL AND GAS OVERVIEW

The population of the world continues to grow, as does the average standard of living, increasing demand for food, water and energy are placing increasing pressure on the environment. The population of the world doubled from 3.2 billion in 1962 to 6.4 billion in 2005 and is forecasted to grow to 9.2 billion in 2050. (**BP Statical energy survey, 2008**), hence the dependence of the world population on oil could not be overemphasized.

Thus Oil accounts for between 34% and 37% of the world's primary energy. Components of crude oil are feedstocks to the chemicals, plastics and fertiliser industries. Crude oil is extracted from the earth and refined to create a range of gas (liquefied petroleum gas - LPG), liquid (gasoline, diesel, jet aviation fuel, paraffin, etc) and solid (bitumen) petroleum

products. The most sought after crudes are those that are "light" (i.e. contain a high proportion of short chain molecules) and "sweet" (i.e. low sulphur content) as they are easier and cheaper to refine. Therefore the world is highly dependent on oil.

1.41 OIL AND GAS RESERVE

According to the 2008 BP Statistical Energy Survey, the world had proven oil reserves of 1237.875 billion barrels at the end of 2007, while consuming an average of 85219.7 thousand barrels a day of oil in 2007. OPEC members hold around 75% of world crude oil reserves. The countries with the largest oil reserves are, in order, Saudi Arabia, Iran, Iraq, Kuwait, United Arab Emirates (UAE), Venezuela, Russia, Libya, Kazakhstan and Nigeria. The world had proven natural gas reserves of 177.35 trillion cubic metres and natural gas production of 2939.99 billion cubic metres in 2007 **(BP Statistical energy survey, 2008)**

In June 2007, OPEC announced plans to invest US\$ 130 billion in expanded production between then and 2012. Excluding Iraq, production is forecasted to increase from 35.7 million bpd to 39.7 million bpd in 2010. Between 2013 and 2020 OPEC plans to spend a further US\$ 500 billion provided bio fuels doesn't change economics. Saudi Arabia alone is investing US\$ 50 billion to increase crude production capacity from 10.5 million barrels a day in 2007 to 12 million bpd in 2009 and 15 million bpd after 2025 **(BP Statistical energy survey, 2008)**. The oil and Gas reserve around the world are pointers to indicate that the FPSO and other offshore structures for oil and gas exploration plays important role hence the need for her protection is worth it.

1.42 CRUDE OIL PRODUCTION

Crude oil production averaged 82 million barrels per day (mbpd) in 2006, a change of 413 tbpd compared to 2005, and 85.7 mbpd in 2007. In 2006, OPEC crude oil production was 43.5% of the world total. Excess OPEC capacity dropped from 6 mbpd in 2002 to 2 million barrels a day in 2006. The countries with the largest 2006 oil production were, in order, Saudi Arabia, Russia, the USA, Iran, China, Mexico, Canada, the UAE, Venezuela, Norway, Kuwait and Nigeria **(IEA reports 2008)**. Consequently Nigerian is a major player in the oil and gas sector

1.43 CONCEPT OF DEEPWATER DEVELOPMENT AND FLOATING SYSTEM

The history of exploration and production of oil and gas started in 1947, when three oil companies drilled out sight of land in the Gulf of Mexico. Shortly after the termination of the Tidelands controversy in 1953, activities in the Gulf of Mexico increased several important innovations in technology significantly, particularly that of exploration took place **(Veldman and Lagers, 1997)**. The innovations and technology developed during these era were gradually applied in a much wider field than drilling alone, encompassing such activities as heavy lifting, pipelaying and ultimately in floating production facilities. From the gulf of Mexico offshore operations spread over the globe in the sixties and the Groningen gas field having been discovered in 1959, the prospect of the north sea were reconsidered **(Veldman and Lagers, 1997)**. Low oil and gas market prices and the harsh environmental conditions of the North Sea deterred many operators for sometimes and so did the gas absence of a settlement on the territorial rights of surrounding countries in the mid-sixties, therefore, exploration expanded and the BP discovered gas in the southern North Sea **(BP Report 2008)**. The Northern part of the sea remained relatively unexplored until Phillips hit oil at Ekofisk in 1967. They and other operators found that Gulf of Mexico technology was not appropriate for the North sea environment and its application led to equipment damage or worsen the condition. In the late 1960s however, adaptation of the technology did not appear to be economically viable. Rises in the oil prices due to the crises of 1973 and 1978 made expensive offshore technologies in the North Sea more profitable and strong offshore sectors began to develop in the UK, Norway, France and the Netherlands **(BP 2006)**. As a result, the North Sea became a breeding ground for the new technology, which consisted mostly the improvements on the existing concepts, but also included breakthroughs, like the gigantic concrete platforms and the first full size tension leg platform[TLP]. At this point, typical European developments, like tankers shaped floating production ships[FPSO], were exported to other continents **(BP 2006)**. Then disasters of Ekofisk, Alexander Kielland semi-submersible and Piper Alpha platform, along with reduction of oil prices in 1985, redirected the advance of technology towards inexpensive methods and equipment. Consequently, investments in giant platforms like Bullwinkle or Troll did not seem likely to continue and FPSO's became popular as a competitive method for fast track development in deeper waters, both in the North sea and worldwide **(Veldman and Lagers, 1997)**. Deepwater developments have been identified as a major source of

economic growth thus the new technologies in deepwater areas have drastically reduced the cost of producing a barrel of crude oil.

1.44 AFRICAN OIL: A BRIEF SURVEY

African producers enjoy several advantages. The region holds substantial oil reserve. Unlike reservoirs in the US, China, the North Sea and Russia most African reservoirs are largely untapped. Upon development, these African reservoirs have the potential to make significant contribution to world oil supply. Furthermore, most of Africa's oil is of low-sulphur high quality especially that of Nigeria. Finally, the traditional production from shallow-water has been declining in recent years. Since the mid-1990s, most of the discoveries have been in deep-water. The location of most oil fields is convenient for shipment to almost all major consuming regions. Given these characteristics (substantial reserves, high quality, and easy transportation) Africa has attracted massive investment from international oil companies. These huge and growing investments have contributed to the rise of both proven reserves and production as shown in the table below:

Table 1
Proven reserves, 1995–2005
(mb)

Country	1995	2005
Angola	3.1	9.0
Chad	0.0	0.9
Republic of Congo	1.3	1.8
Equatorial Guinea	0.6	1.8
Gabon	1.5	2.2
Nigeria	20.8	35.9
Sudan	0.3	6.4
Other African countries	0.7	0.6
Total	28.3	58.6

Source: British Petroleum, BP Statistical Review of World Energy, London, 2006, p. 6.

Table 2: African Proven Oil Reserve (1995-2005)

Table 2
Production, 1995–2005
(1,000 b/d)

Country	1995	2005
Angola	633	1,242
Cameroon	106	58
Chad	0	173
Republic of Congo	180	253
Equatorial Guinea	7	355
Gabon	356	234
Nigeria	1,998	2,580
Sudan	2	379
Other African countries	51	72
Total	3,833	5,346

Source: British Petroleum, BP Statistical Review of World Energy, London, 2006, p. 8.

Table 3: African oil production (1995-2005)

The figures show that proven reserves have more than doubled and production level has substantially risen from 1995 to 2005. Three countries were responsible for this significant surge and are the leading oil producers in sub-Saharan Africa Nigeria, Angola and Gabon.

1.51 MAJOR OIL CONSUMERS AND AFRICA

The Africa's proven oil reserves and the substantial rise in the continent's production have been of great interest to major consuming regions and countries in their efforts to secure badly-needed supplies. The US, EU and China are dependent on Africa's oil, at different degrees, and have been actively involved in the oil industry all over the continent. Over the last half century, US consumption of oil has grown consistently, except for a short period of time in the late 1970s and early 1980s. Parallel to this rise in consumption is the steady decline in production. Indeed, US crude oil production in the mid-2000s is at 50-year lows.¹⁶ As a result, net imports of oil and petroleum products have increased steadily since 1982 to fill the growing gap between indigenous supply and demand. Despite efforts to restrain import dependence, the US imports around 60 per cent of its oil needs. Africa holds steadily increasing significance for future US energy supplies. High levels of exploration and production investment in Nigeria and Angola, along with significant growth in other countries along West Africa's Gulf of Guinea, have transformed the region into a strategic supplier of crude oil, and prospectively also of natural gas, to the US and global energy markets. The region is important to the diversity of US oil supplies as well. The top oil suppliers to the US are Canada, Mexico, Saudi Arabia,

Venezuela and Nigeria. US energy investment in West and Central Africa, particularly in Nigeria and Angola, has been on the rise for several years. Investment by foreign companies in the Gulf of Guinea energy sector is already substantial – \$50 billion in this decade.¹⁷ nearly all of this investment is to develop deep offshore oil and gas fields (Organization of the Petroleum Exporting Countries, 2007) OPEC Review This figure is likely to grow considerably over the next decade as new offshore discoveries of oil are brought into production and as West Africa becomes a new major global exporter of natural gas. Africa provides several incentives to American oil companies. First, the region's sweet, low-sulphur oil has advantages from an environmental standpoint. This high-quality oil is particularly suitable for US refineries. Second, the region provides an attractive investment framework. Over the last few decades international oil companies have been able to negotiate and sign joint ventures and production sharing agreements with their national companies' counterparts. Third, oil from West Africa is easily transported to the eastern US seaboard. Given these incentives, a recent report by the Washington-based Centre for Strategic and International Studies on the rising US energy stakes in Africa has recommended that the US government should pursue sustained, high-level engagement, bilaterally and multilaterally with African oil producing nations. **(Organization of the Petroleum Exporting Countries, 2007)**. All these facts further indicate that the presence of FPSO will be on the increase in Africa and the need to make adequate provision for their protection is of vital importance

1.52 DEVELOPMENT OF NIGERIAL'S OIL INDUSTRY

Nigeria is the most populous country in Africa and has been active member in OPEC since 1971. The country is the largest oil producer in the region and plans to increase its proven reserves and production in the next few years. In order to achieve these ambitious plans, the Nigerian National Petroleum Corporation (NNPC), created in 1977, is working with several international oil companies. The NNPC has been involved in joint ventures and production sharing contracts with multinationals such as Shell Petroleum, ExxonMobil, Total, Chevron, Agip and ConocoPhillips. Since the mid-2000s, Chinese corporations have aggressively pursued oil deals with Nigeria **(Organization of the Petroleum Exporting Countries, 2007)**. Most of the oil exploration and development operations are focused along the country's Niger River Delta and increasingly in deepwater. Nigerian crude oil production is light and sweet (low sulphurs). The majority of

Nigerian crude exports go to markets in the US and Western Europe, with Asia and Latin America becoming increasingly important destinations (**Organization of the Petroleum Exporting Countries, 2007**).

The advent of the oil industry can be traced back to 1908 when a German entity and the Nigeria bitumen corporation, commenced exploration activities in the Araromi area, west of Nigeria (NNPC 2008). These pioneering efforts ended abruptly with the out break of the first world war in 1914.Oil was discovered in Nigeria in 1956 in oloibiri in the Niger delta after half a century of exploration. The discovery was made by the Shell-BP. Nigeria joined the ranks of oil producers in 1958 when its first oil field came on stream producing 5,100 bpd.After 1960,exploration rights inshore and offshore areas adjoining the Niger delta were extended to other foreign companies. Nigeria joined the Organisation of petroleum Exporting countries (OPEC) IN 1971 (**NNPC 2008**).By the late sixties and early seventies, Nigeria had attained a production level of 2million barrels of crude oil a day. Current development strategies are aimed at increasing production to 4million barrels per day by the year 2010 (**NNPC 2008**).

1.6 STUDY OBJECTIVES

The aim and objective of this study is to come out with a modest improvement in the design of an FPSO that would be resilient to a larger extent to an above water attack by considering different sizes of T Stiffeners and Stiffeners and to focus on how to minimize the effects of an Air blast pressure attack on an FPSO and to recommend passive means and strategies to further achieve a design that would check mate the activities of terrorist in the Niger Delta of Nigeria

1.61 RESEARCH METHODOLOGY

In order to achieve the set objectives, the following areas will be looked into:

- a. A detailed look at the world Energy, oil demand and production, and oil production in Nigeria in order to justify the study.
- b. Concept of deep water development of floating system
- c. African oil survey and Development of Nigerian oil

- d. Identification of certain threats to an FPSO replica to the threat that could cause economic sabotage.
- e. Identification of unique blast pressure load capable of causing economic damage to the structural members of the midship section of an FPSO when attacked or exploded from the above water point specifically the stiffened plate panel.
- f. Identification of the weakest and strongest type of stiffener considered at the midship section.
- g. Assessment of standard FPSO structure using Abaqus finite element analysis to benchmark inherent resistance to identified the blast pressure load that could cause rupture.
- h. Identification of structure failure resulting from blast loading and recommendation of structural features that will provide enhanced capabilities to withstand or minimize blast.
- i. Prediction of rupture strain

In order to reach the set goals, firstly an analysis of a simple plate subjected to lateral blast pressure will be analyze in linear and non-linear analysis, and Non-linear explicit dynamic analysis with inclusion of plasticity, this exercise will be carried out in order for the scholar get familiar with the various finite element modeling techniques and thereafter stiffened plate panel will be subjected to a non-dynamic lateral pressure. In addition to the finite element analyses, The scholar will compare the displacement and stresses obtained by numerical solutions to analytical solutions. Frequency extraction analysis of simple plate and stiffened plates will be carried out and the results generated from Numerical analysis will be compare with classical method in order to enhance the scholar with the Abaqus tool and software. Active and passive protection modes will be advised. {Passive i.e. patrol, floating booms, etc, active, i.e. inherent blast resistant structure and systems.}

1.7 OVERVIEW OF CHAPTERS

This section presents an overview of the remaining chapters. The work of other authors will be referred to where necessary and works in this thesis will be dealt with chapter by chapter.

Chapter two describes a review of explosion and blast loading effects on structures and the overview of the geopolitical situation and the spectrum of the potential threats to the offshore fields. Attention shall only be focused on the midship section of the hull girders and not in the fore and aft regions. The probable response of the hull structure to such impulsive forces, from small effects to large scale damage will be mentioned. .

Chapter 3 will deal with the application of finite element analysis using ABAQUS software to analysis the displacement and stresses of simple plate progressively to stiffened panel of an FPSO and to validate the results obtained in abaqus with that obtained from classical theory (Roark's formula), thus comparison of classical theory and abaqus software will be carried out under various boundary conditions and aspect ratio.

Chapter 4. Having carried out the capabilities of abaqus on simple plating and validation of the theoretical and classical theory, further analyses will be carried out in this chapter on plate and stiffened plate with much emphasis on the actual panel of the FPSO considered. Frequency Extraction Analysis of plate and stiffened plate will be carried out using Abaqus software code and classical theory. The two results will be compared with a view to ascertain the accuracy of the Abaqus software code with the classical theory. .

Chapter 5 will look into the Nonlinear Analysis of stiffened plate of the FPSO subjected to blast pressure loading in an explicit non-dynamic analysis state. Different boundary conditions will be examined. This includes frequency extraction to determine and obtain the natural frequencies of the panel with the effects of damping and the high material strain rate effects as well as the effect of plasticity were considered using the finite element code ABAQUS EXPLICIT.

The displacement and responses of the stiffened panel at the central node will be investigated including their energy terms.

CHAPTER 1: Introduction

Chapter 6 will examine the blast pressures loading on the midshipsection of the FPSO by considering different sizes of T Stiffened and L stiffened plates with a view of determining the best stiffened size amongst the once considered that would be able to withstand blast pressure loading to a greater extent. The rupture strain will also be determined and the blast pressure that would achieve this rupture strain. Consequently recommend the best option for the stiffened panel of the FPSO. Other passive and active methods of preventing terrorism will be proffered.

Chapter 7 will be the conclusion and recommendation for future works.

CHAPTER 2

2.0 An Introduction to Blast Analysis Methods

2.1 Introduction

Over the years, the analysis of the structures and its component under blast loading has received considerable attention due to various blast events all over the world especially those of terrorism. The analysis of the blast loading on structures started way back in 1960s. Thus in 1959, a technical manual titled “structures to resist the effects of accidental explosions” was released by the United States Army and in 1990, the revised edition of the manual which is TM 5-1300 used mostly by the military and civilian organization for designing structures to prevent and avoid the propagation of blast loading and to provide safety and protection for structures, personnel and valuable equipment was released.

The prediction of blast loading effects can be predicted by the following methods:

- a. Empirical (or analytical) methods: Involves correlations with experimental data. The empirical approaches are constraints by the extent of the underlying experimental database and the accuracy of all empirical equations diminishes as the explosive event becomes increasingly near field.
- b. Semi-empirical methods: These methods are hinged on simplified models of physical phenomena and the idea was to model the underlying important physical processes in a simplified way. They are dependent on extensive data and case study. The predictive outcome accuracy has been observed to be better than that provided by the empirical methods
- c. Numerical methods. This method sometimes called first-principle methods and are based on mathematical equations that describe the basic laws of physics governing a problem. These principles amongst others include conservation of mass, momentum, and energy. The physical behaviour of materials is described by their constitutive relationships **(Timoshenko et al. 1977)**.

The most important are the loads produced from air blast sources, how they interact with structures and the response of the structures to them. Blast sources include gas, high explosives, dust and nuclear materials. Review of literature in this thesis commenced with the review of books on blast loading and its effects. Furthermore, the Fundamental features of the explosion and blast wave phenomena are presented along with a

discussion of TNT (trinitrotoluene) equivalency and blast scaling laws while the characteristics of incident overpressure loading due to conventional high explosives, unconfined vapours cloud explosions are addressed. Thereafter, the reviews of blast loading effects on plates are presented.

2.2 Literature Reviews on Blast Loading and Plate Deformation

Over the years, the analysis of the structures and its component under blast loading has received considerable attention due to various blast events all over the world especially those of terrorism. Subsequently, Dynamics of blast loading and the development of blast loading models have been topics of research since many decades ago especially in academia, government and in the military. Lots of researches works on blast loading in the military and government are classified. Overview of some of the books and papers related to blast loading are highlighted below. Kinney and Graham produced a very comprehensive book, titled “Explosive Shocks in Air” **Kinney and Graham (1985)**, in that book explanation on many different aspect and characteristics of explosive loads was made. Also **Baker (1973)** published a book on blast loading titled “Explosive in Air”. This book narrated an overview of explosive loading which includes a compilation of experimental equipment and data as well as some computational methods. Most importantly, Baker et al published a comprehensive book titled “Explosion Hazards and Evaluation” **Baker et al. (1983)**. The book gave a detailed account and computation of various experimental works on explosive loads. Another slightly updated book with an excellent overview of explosive loading titled “Blast and Ballistic loading of structures” which was published by **Smith and Hetherington (1984)**. Henrych published another book on blast loading titled “Dynamic Loading and Design Structures” **Kappos (2002)**. This book is also comprehensive and was edited BY **A.J. Happos**. The book provided sections on various loadings including explosions and impacts.

Aside from books, a number of papers have also been received. Thus **Flore K and Benaroya (2005)** provided an extensive review on pulse loading effects on structures. This included review of various studies on pulse shapes and their effects on the deflection of structures. It also summarized efforts to reduce or eliminate these pulse shape effects, which can be done for much rigid – plastic geometry with a uniform load.

Furthermore, **Remennikor (2003)** gave an overview of current available analytical and numerical techniques to predict loads on structures which are subjected to explosive loading. Discussions in that paper was also made on the widely used Army Technical Manuals from US **TM 5-1300 (1990)** and **TM 5-88-1 (1986)**. These technical manuals were also discussed by **Ngo et al (2007)**. The paper provided an overview of blast loading effects on structures. **Bashara (1994)** carried out an extensive review on the analysis of unconfined blast loading from different sources for above ground rigid structures. He discussed on the use of the TNT equivalency and blast scaling laws. Also, the differences of over pressure, reflective and dynamic pressure were also discussed. Bashara asserted as a means of conclusion that blast load effects on the responses of structure does not only depend upon the magnitude of the load but also on its duration, rise time and general shape. Consequently, he concluded that the implication of having a good blast loading model is very important **Chock and Kapania (2001)** carried out the review of blast scaling i.e the Hopkinson – Cranz and the Sachs blast scaling. Two methods of calculating explosive blast in air was compared.

Baker (1973) provided the first method. This method uses Sachs-Cranz scaling while the second method was from **Kingery and Bulmash (1984)**. This method uses Hopkinson – Cranz scaling. The conclusion was that the reflected peak pressures are of a similar order of magnitude but a difference exists in the specific impulses delivered to the target.

For the case given in Chock and Kapania, Baker's method has a much lower impulse and an earlier arrival time than Kingery and Bulmash's method. Chock and Kapania asserted that the difference could be attributed to difference in time duration and a change in the way the decay values were determined. Though unable to determine the best of the two methods since the two methods were based on experimental data with little or no repeated tests.

Esparza (1986) carried out experiment on TNT and other explosives at small scaled distances. He asserted that there is insufficient verification when a single equivalent weight ratio is used at a small scaled distance. Subsequently, on TNT equivalency, he stated that an equivalence system with only one blast parameter may not be accurate. This is because TNT equivalence can differ significantly depending on the scaled distance of the explosive, even with same type of explosive.

Esparza carried out a study and comparison of data on the peak over pressure, arrival time, impulse and positive duration of the blast loads in his experiments. He observed that the TNT equivalency for few of the parameters can be heat of detonation furthermore, for small scaled distances the impulse and positive duration parameters are not as well defined as the pressure and arrival time parameter.

Hargather and Settles (2007) used the optical shadowgraphy and high speed digital imaging techniques to measure the shock wave caused by an explosion. Through this techniques, calculation of the TNT equivalence of the explosion that was sued. It was concluded that a single TNT equivalence value was inadequate to fully describe an explosive yield, rather TNT equivalence factor and over pressure duration must be presented as functions of scaled distances.

Gatto and Krznic (1996) also carried out experiments an explosive loads in an aircraft luggage containers. The pressure profile on the container panel due to explosion was measured with different amounts of luggage inside. It was observed that additional luggage reduces the pressure on the container significantly.

Veldman et al. (2006) and **Veldman et al. (2008)** carried out an experiment on pre-pressurized plates under blast loading. The plate indicted river – attached stiffeners in order to model the fuselage skin of a commercial aircraft. High speed cameras to capture the deformation and failures of plates. It was observed that for weak blast loads the pre-pressurization is not a large factor, however, for stronger blast loads the pre-pressurization causes a significant increase in panel damage.

Simmons and Schleyer (2006) carried out an experimental works with finite element analysis of the response and failure modes of stiffened, aluminum alloy panels with conventional riveting and laser welding. A pressure chamber that theoretically gives a triangular pressure pulse on the test structure. The conclusion here was that riveted joints have greater energy absorbing capacity than laser welded joints. It was noted that the joint energy absorption is sensitive to the load rate.

Several studies especially **Zhao et al.(1994)**, **Zhu(1997)** and **Zhao(1997)** on saturated impulse phenomena for pulse – loaded perfectly plastic beams and elastic – plastic plates

was carried out. The studies showed that there is a limit exists on how much impulse applied to structure well affect its deformation. This fact is due to the membrane forces, which were induced by large deflection and which gives the plate a greater capacity. The saturation duration is the time during which the loading effects the deformation of the structure. It was also confirmed that additional loads after this saturation duration time wouldn't have any further contribution on the structural deformation. **Zhu and Yu (1997)** stated that the saturation duration is a function of plate geometry and material properties and not of the pressure loading.

Brode (1956) carried out a Numerical analysis of spherical blast waves. He also undertook a computational analysis of a blast wave from a spherical charge of TNT. In that analysis, Brode the rarefaction waves and their interaction with multiple shocks.

Gantes and Pnevmatikies (2004) proposed a response spectra based on a blast pressure profile with an exponential distribution which was then compared with a triangulation distribution. In that study, the technique used was recommended by the US department of the **Army TM 5-1300 (1990)** which was based on substituting the structural element by a stiffness equivalent, single degree of freedom system, and suing elastic – plastic response spectra to predict the maximum response of the system. They concluded that a triangular distribution with time can sometimes be slightly unconservative for stiffer structures. They asserted that since exponential loading decreases faster than a triangular one, thus the differences between the two are influenced more in elastic-plastic situations than in purely elastic ones. Additionally when differences in blast loading profiles lays a significant roles in the response, range of certain parameters are traded off.

In **Watson (2002)**, the response depends on the synchronization with the rebound of the structure, therefore, a good knowledge of blast load time and space variations are critical to obtain the correct response. Watson stated that the influence of damping on these systems can be neglected.

Neuberger et al, (2007) carried out an experiment and numerical simulations on circular plates to determine whether scaling laws are valid for large and close rang spherical explosions in air. Their results proved validity of the scaling laws.

Bogosiam et al. (2002) compared experimental data to variety of simplified models, including Blast X, Van Wep and shock, and to measure the inherent uncertainty in these blast model codes. The data used in analysing this experiment was analysed was restricted to a scaled range of 3 to 100ft/16). Though their final test data base comprised of 303 individual gage records, they noted that not all were of sufficient duration and/or quality. Some have bad peak pressure readings and therefore could not produce reliable impulses. Additionally, the test data comprised a wide range of configuration from cylindrical to spherical to hemispherical charges. Different types of explosives were used including TNT C-4 and ANFO, which were all converted into their TNT equivalent load before computing the scale factors. This shows how difficult it is to obtain a complete and accurate set of experimental work to analyse and understand the entire spectrum of blast loadings. However, Bogosian et al. Were able to show that of the tools they analysed, ConWep best represented the test data in an overall sense. Their researches also showed that BlastX provides values that are close to the data set, stock significantly under predict reflected positive pressure and over predicts reflected positive impulse. By calculating the standard deviation of the rest da, they noticed that two sigma values range from 1/3 to 2/3 in magnitude which indicates a very wide range of uncertainty.

ABS consulting Ltd prepared a **Research Report (2006)** that uses a tool they developed, called Blasts TAR, to perform multiple analyses of simple structures that are subject to blast loadings with different geometries durations and peak pressures. Blast STAR finds the force displacement and equipment mass characteristics of an equivalent simplified system by utilising the results of a state FE analysis. Their result analyses the maximum displacements obtained from a variety of loading scenario acting on various structures.

Nansteel and Chen (2009) discuss a procedure using high speed cameras to capture plate deflection and strains. Their procedure does not incorporate any devices which are in contact to the plate. The high speed cameras are coupled with digital image correlation techniques and are. Capable of capturing the full transient motion of the entire plate

Hargather and Settles (2009) performed an experiment utilising high speed camera to measure the deformation of aluminum plates subjected to explosions. They concluded that the maximum dynamic plate deformation is a straight forward function of plate the applied explosive impulse.

Ballantyne et al. (2010) analytically analysed the effect of a blast wave hitting a structure with a finite width. Because of the finite width, clearing was created. Clearing occurs when the reflected reaches the section extremities and cause vertices to shed and a low pressure wave to generate. This low pressure wave propages inwards towards the expanding wave which causes the expanding wave to decay faster. This process reduces the impulse on the structure, however does not affect the peak reflected pressure.

Bauer (1968) and Singh and **Singh (1991)** provide mathematical models to product the deflection of an elastic plate subjected to an exponentially decaying pulse, representative of blast loads.

Trying to obtain a simplified, yet accurate model for blast loadings in a topic still being examined. These publications, which ate mainly focused on loading models, shows there is a great amount of uncertainty involved when dealing with blast loads modally. In addition, many of the publications show that the response of a structure is very sensitive to the loading model.

Fertice (1973) has extensive study of structures and computation of blast loading aboveground structures.

A. Khadid et al. (2007) studied the fully fixed stiffened plates under the effect of blast loads to determine the dynamic response of the plates with different stiffener configurations and considered the effect of mesh density, time duration and strain rate sensitivity. He used the finite element method and the central difference method for the time integration of the nonlinear equations of motion to obtain numerical solutions.

A.K. Pandey et al. (2006) studied the effects of an external blast explosion on the outer reinforced concrete shell of a typical nuclear containment structure. The analysis was made using appropriate non-linear material models till the ultimate stages. An analytical procedure for non- linear analysis by adopting the above model was implemented into a finite element code DYNAIB.

Alexander M. Remennikov (2003) studied the methods for predicting bomb blast effects on structures. When a single structure is subjected to blast loading produced by the detonation of high explosive device. He adopted the simplified analytical techniques used for obtaining conservative estimates of the blast effects on buildings structures and Numerical techniques including Lagrangian, Eulerian, Euler- FCT, ALE, and finite element modelling used for accurate prediction of blast loads on commercial and public buildings.

The property of blast waves obtained from the trajectories was studied by **Dewey (1971)** where he first introduced the effect of spherical and hemispherical TNT (trinitrotoluene) in blast waves and determined the density throughout the flow was determined by the application of the Lagrangian conservation of mass equation which was used for calculation of pressure by assuming the adiabatic flow for each air element between the shock fronts. The temperature and the sound speed found from the pressure and density, where perfect gas equation of states was assumed.

Kirk A. Marchand et al. (2005) reviewed the contents of American Institute of Steel Construction, Inc. for facts for steel structures gave a general science of blast effects with the help of numbers of case studies for structures which are damaged due to blast loading. Kirk also studied the dynamic response of a steel structure to blast loading and shows the behaviour of ductile steel column and steel connections for blast loadings.

Dharaneepathy et al. (1995) studied the effects of the stand-off distance on tall shells of different heights, with a view to study the effect of distance (ground-zero distance) of charge on the blast responses. An important task in blast-resistant design is to make a realistic prediction of the blast pressures. The distance of blast explosion from the structure is an important datum which governs the magnitude and duration of the blast loads. The distance, known as 'critical ground-zero distance', at which the blast response is a maximum.

Ronald L. Shope (2006) studied the response of wide flange steel columns subjected to constant axial load and lateral blast load. The finite element program ABAQUS was used to model the steel column where he considered different slenderness ratio and boundary conditions. Additionally, Non-uniform blast loads were considered. Changes in

displacement time histories and plastic hinge formations resulting from varying the axial load were also examined.

T. Borvik et al. (2009) studied the response of a steel container as closed structure under the blast loads where the mesh less methods based on the Lagrangian formulations was used to reduce mesh distortions and numerical advection errors to describe the propagation of blast load using LS-DYNA simulations of blast loaded structures.

Borvick et al. (2009) in a manual titled “structures to resist the effects of accidental explosions” coded as TM 5-1300 (UFC 3-340-02) provides guidance to designers, the step-to-step analysis and design procedure, including the information on such items (1) Blast, fragment and shock loading. (2) Principle on dynamic analysis. (3) Reinforced and structural steel design and (4) A number of special design considerations.

T. Ngo, et al. (2007) in their study on “Blast loading and Blast Effects on Structures” gave an overview on the analysis and design of structures subjected to blast loads phenomenon for understanding the blast loads and dynamic response of various structural elements which helps for the design consideration against extreme events such as bomb blast, high velocity impacts e.t.c.

Nurick and Martin (1989) reported the response of plates subjected to uniform impulsive loads and different types of failure modes were examined.

Cichocki and Perego (1997) carried out detailed studies on rectangular plates subjected to blast and a comparison between experimental, numerical and analytical methods were presented thus emphasizing the use of computer codes for high velocity deformation analysis .

Schubak (1991) reported a simplified rigid-plastic method for modelling beams using asymmetric beam sections and subsequently a one-way and two-way orthogonally stiffened plate. The stiffened plate was treated as a single symmetric beam with the plate acting as a large flange.

Olson (1991) reported the modelling of orthogonally stiffened plates using combination of rigid-plastic and finite element. The rigid-plastic model used a beam grillage representation of the stiffened plate where the beam sections were asymmetric.

Louca et al. (1996) had reported the results for the response of a typical wall and a T-stiffened panel subjected to hydrocarbon explosions using nonlinear finite element analysis considering plasticity, strain rate and buckling effects. Comparisons were made and presented between the numerical results, experimental data and the approximate solutions obtained with a single degree of freedom model **Louca, Punjani and Harding (1996)**.

Pan and Louca (1999) also reported the numerical studies of stiffened plates subjected to hydrocarbon explosions using simplified model of the stiffened plate considering different response aspects, such as, the contribution of stiffeners under varying stress state and loading conditions. The response of plates to a central localised blast load had been examined experimentally **Nurick and Radford (2000)**, theoretically **Wierzbicki et al. (2000)** and numerically using ABAQUS/Explicit **Jacinto et al. (2001)** by several researchers. The failure modes reported for locally loaded plates were similar to those observed for uniformly loaded plates; the main difference being existence of an additional capping mode, i.e. thinning and tearing of a central fragment, or 'cap'.

Kadid et al. (2007) and **Kadid (2008)** carried out the numerical study of stiffened plate employing the Cowper-Symonds (C-S) model in ABAQUS/Explicit and reported the usefulness of the C-S model for strain rate consideration along with the stiffeners.

Stiffened plates are amongst the most frequently used structural elements to resist high amplitude loading such as that due to the explosions, or impact. In the stiffened plates, stiffeners may be positioned facing towards or away from the blast loading. In spite of the large number of plates that are designed and built, the effect of stiffeners and their behaviour under blast loading are not well understood and properly taken into account by the designers.

Numerical analysis carried out in this thesis using ABAQUS software code aims for the study of air blast pressure analysis on a midship section of an FPSO code named FPSO Nigeria where a. Three types of T stiffened plates and 3 L stiffened plates of same flange area with varying flange length and width are considered with a view to selecting the best stiffener configuration for FPSO Nigeria b, Effect of strain rate consideration c. Frequency extraction analysis in order to determine resonance and guard against it d. Determination of rupture strain under such hostile blast pressure as against experimental tests that are

extremely very costly and dangerous. Most times the reproducibility of the experimental results is not always ensured because of the uncertainties involved, especially in case of the blast experiments. These shortcomings are addressed herein by using numerical simulation by subjecting the above water side of a midship section of an FPSO Nigeria operating in the Niger Delta of Nigeria to blast pressure responses. The Numerical analysis helps in the reduction of experimental trial and helps in the selection of better stiffeners for FPSO Nigeria amongst those considered in this thesis; furthermore it helps in the better understanding of the physics of the problem. Additionally, it helps to provide a better solution to the protection of the above water side of an FPSO subjected to blast pressure by the use of an appropriate anti-ballistic material. Thus, A cost benefit Analysis was also necessitated and was carried out bearing in mind the financial and economic cost to a nation where the FPSO is producing the crude oil or refined oil, the potential effect on personnel working on the FPSO, the potential Effect of the crude on the marine mammal's i.e environmental pollution and the potential Effect on a nation and or the owner of the FPSO. Consequently, the cost benefits to the Nigerian Government in carrying out the protection of the above water side of an FPSO against the losses that would be lost by the Government of Nigeria should an attack be carried out by the militant of the Niger Delta were discussed and contribution to knowledge was made in addition to some other passive method of alienating the effect of blast pressure on the above water side of FPSO Nigeria.

CHAPTER 3

3.0 Structural Vibration and Frequency Extraction Analysis

3.1 Introduction

Before progressing deeper into Chapter 3, which is structural vibration and frequency extraction analysis, static analysis of plates and stiffened plate were carried out and validated using Abaqus software code against classical theory. Thus the Displacement and stresses resulting from blast pressure loading of plates with different aspect ratio, different thicknesses of plates and different boundary conditions using Abaqus Software code were validated against calculations carried out using classical theory/Formula. The result of the displacement and stresses generated by Abaqus were found to correlate excellent well with the displacement and stresses calculated from classical theory/formula. This was very necessary in order to ascertain and validate that the results being obtain by the scholar is correct and the much needed confidence required by the scholar on all results generated by Abaqus is acquired. Thereafter, Chapter 3 progressed a step further by carrying out Linear perturbation Analysis of plates and stiffened plates subjected to frequency extraction analysis for about 9 different plate thicknesses under different aspect ratio and boundary conditions in order to calculate their natural frequency with a view to avoid resonance due to blast pressure or any form of impact. In this section, frequency extraction analysis generated from Abaqus code was also compared with that calculated from classical theories in a bit to further validate the accuracy of the ABAQUS CODE and to further give the researcher the most needed confidence to progress to other aspect of Finite Element Analysis. Most importantly, a panel of the FPSO plate (unstiffened and stiffened) was subjected to frequency extraction analysis. In each case, a minimum of 2 modes or more were generated even though; the most important of the modes is the fundamental modes. However, before going into the frequency extraction analysis, below in a tabular form are the result of displacement and stresses generated from abaqus software code by considering different plate thicknesses subjected to different blast pressures being validated against displacement and stresses generated by classical theory/formula under same blast pressures.

3.2 Determination of stresses and displacement using Abaqus Code and classical theories (Roark's formula)

TABLE 3.1 CASE 1-Showing Comparison of Stress and Displacement results obtained from Abaqus Software and Classical Theory using a Blast pressure loading of 1E06 Pascal Validated on 6 different plate thicknesses 5mm,10mm,15mm,20mm,25mm and 30mm with a boundary condition of all edges Fixed.

S/No	Plate thickness (m)	Classical Theory Calculated using Roark Formula		Numerical Results From ABAQUS-Software		Difference In Stress Value	Difference In Displacement Ymax (m)
		(c)	(d)	(e)	(f)		
(a)	(b)	(c)	(d)	(e)	(f)	(g)=(e-c)	(h)=(f-d)
	Plate thickness (m)	Stress Values σ (Pa)	Displacement Ymax (m)	Stress Values σ (Pa)	Displacement Ymax (m)	Difference in Stress σ (Pa)	Difference in Displacement Ymax (m)
1.	0.005	4.92E10	8.410	4.92E10	8.420	0.00	0.01
2.	0.010	1.23E10	1.050	1.23E10	1.050	0.00	0.00
3.	0.015	5.47E10	0.312	5.47E09	0.312	0.00	0.00
4.	0.020	3.08E09	0.131	3.08E09	0.132	0.00	0.001
5.	0.025	1.97E09	0.067	1.97E09	0.068	0.00	0.001
6.	0.030	1.37E09	0.039	1.37E09	0.039	0.00	0.00

Comment: The analysis type carried out here is Static linear with quadratic geometrical order involving an 8-node doubly curved thick shell with reduced integration (S8R). From the table 3.1 above. It could be seen that the stress and displacement values generated in columns c and d respectively (from classical theory) and those generated in columns e and f respectively (from ABAQUS) completely agreed. The agreement of these values showed very clearly to the researcher that ABAQUS Software code has a very high accuracy for numerical analysis. Furthermore, it gives the researcher that much needed confidence required by a researcher in the use of Abaqus software code having validated it against classical theory. The extract of the blast pressure loading from Abaqus software

code, the boundary condition picture, the displacement plot and the stress plot are shown in appendix 3

Table 3.2:Case 2:Showing Comparison of Stress and Displacement results obtained from Abaqus Software and Classical Theory using a Blast Pressure loading of 1E06 Pascal(with two edges Fixed and two other edges simply supported).

S/No	Plate thickness (m)	Classical Theory from Roark Formula		Numerical Results From ABAQUS-Software		Difference In Stress Value	Difference In Displacement Ymax (m)
(a)	(b)	(c)	(d)	(e)	(f)	(g)=(e-c)	(h)=(f-d)
	Plate thickness (m)	Stress Values σ (Pa)	Displacement Ymax (m)	Stress Values σ (Pa)	Displacement Ymax (m)	Difference in Stress σ (Pa)	Difference in Displacement Ymax (m)
1.	0.005	1.85E+10	9.26E-01	1.85E+10	9.26E-01	0.00	0.01
2.	0.010	4.63E+10	1.16E-01	4.62E+10	1.16E-01	0.00	0.01
3.	0.015	2.06E+10	3.43E-02	2.05E+09	3.44E-02	0.00	0.01
4.	0.020	1.16E+09	1.45E-02	1.16E+09	1.45E-02	0.00	0.00
5.	0.025	7.40E+08	7.41E-03	7.40E+08	7.50E-03	0.00	0.000
6.	0.030	5.14E+08	4.29E-03	5.14E+08	4.36E-03	0.01	0.000

Comment: The analysis type carried out here is Static linear with quadratic geometrical order involving an 8-node doubly curved thick shell with reduced integration (S8R).From the table 3.57 above. It could be seen that the stress and displacement values generated in columns c and d respectively (classical theory) and those generated in columns e and f respectively (ABAQUS) completely agreed.

3.3 Introduction to Structural Vibration

The need for the analysis of structural vibration of a structure could not be overemphasized in order to calculate the natural frequencies of a structure, to predict resonance and to response to the expected excitation. In this manner, it could be determined whether a particular structure will leave up to its intended function or not. Additionally, the results of the dynamic loadings acting on a structure can be predicted, such as the dynamic stresses, fatigue life and noise levels **Turkia H. (2003)**.Thus the

integrity and usefulness of a structure can be maximized and maintained. Furthermore, the analysis will afford one to know which structural parameters most affect the dynamic response of the structure so that if an improvement or change in the response is required, the structure can then be modified in the most economic and appropriate way. Because of the very serious effects that unwanted vibrations can have on dynamic systems, it is essential that vibration analyses be carried out as an inherent part of a particular design; when necessary modifications can easily be made to eliminate vibration or at least to reduce it as much as possible. It is usually much easier to analyze and modify a structure at the design stage than to modify a structure with undesirable vibration characteristics after it has been built **Dyke et al (1996)**. However, it is sometimes necessary to be able to reduce the vibration of existing structures brought about by inadequate initial design, by changing the function of the structure or by changing the environmental conditions, and therefore techniques for the analysis of structural vibration should be applicable to existing structures as well as to those in the design stage. Present-day structures or machinery components often contain high-energy sources which create intense vibration excitation problems, and modern construction methods result in structures with low mass and low inherent damping. Therefore careful design and analysis is necessary to avoid resonance or an undesirable dynamic routine. The vibration that occurs in most machines, structures and dynamic systems is undesirable, not only because of the resulting unpleasant motions, the noise and the dynamic stresses which may lead to fatigue and failure of the structure or machine, but also because of the energy losses and the reduction in performance that accompany the vibrations **Gordaninejad et al (2002)**. It is therefore essential to carry out a vibration analysis of any proposed structure. There have been very many cases of systems or structural failing or not meeting performance targets because of resonance, fatigue or excessive vibration of one component or another. In this chapter, the scholar will look into damping in structures, sources of vibration, causes and effect of structural vibration and how structural vibration could be reduced. Furthermore the researcher carried out the frequency calculation of various plates shapes with different boundary condition using ABAQUS software code and was validated against theoretical calculations. This further buttress the validity of the ABAQUS software code used in this thesis.

3.4 Frequency Extraction Analysis of Unstiffened Plate

In the frequency extraction analyses carried out in this chapter, Natural frequency of stiffened and unstiffened plate with different aspect ratio (AR) with various plate thicknesses and various boundary conditions were calculated using the classical theory which was also compared to the natural frequencies generated by the researcher from ABAQUS software code. Deductions/Comment were made.

3.41 Case 1: In Case 1, Frequency extraction analysis of a simple 5mm plate measuring 2m x2m (AR=1) and with a boundary condition of having all the edges fixed was carried out using Abaqus code. Similarly, the classical theory was used in calculating the fundamental frequencies of the plate with various thickness and boundary conditions. The results obtained in each case are tabulated in the subsequent table below for each of the cases.

Table 3.3: Result of Natural frequency Analysis carried out for Simple 5mm Plate 2mx2m with AR=1 and with all edges fixed using Abaqus software code and validated against Classical theory.

S/No	Size of Plate (m)	Plate Thickness (m)	Boundary Condition Used	Aspect Ratio	Calculated Natural Frequency From Classical theories (HZ)	Generated Natural Frequency From ABAQUS Software code. (HZ)	Difference in (f-g) (HZ)	Remarks
(a)	(b)	(c)	(d)	(e)	(f)	(g)	(h)	(i)
1.	2x2	0.005	ALL EDGES FIXED	1.0	11.244	11.244	0.000	
2.	2x2	0.008	ALL EDGES FIXED	1.0	17.99	17.988	0.002	
3.	2x2	0.01	ALL EDGES FIXED	1.0	22.488	22.483	0.005	
4.	2x2	0.012	ALL EDGES FIXED	1.0	26.986	26.976	0.010	
5.	2x2	0.015	ALL EDGES FIXED	1.0	33.733	33.711	0.022	
6.	2x2	0.018	ALL EDGES FIXED	1.0	40.479	40.442	0.027	
7.	2x2	0.02	ALL EDGES FIXED	1.0	44.976	44.925	0.051	
8.	2x2	0.025	ALL EDGES FIXED	1.0	56.221	56.119	0.102	
9.	2x2	0.03	ALL EDGES FIXED	1.0	67.465	67.288	0.197	

Comment: Frequency extraction analysis carried out by using Abaqus software code and those calculated using the classical theory (Roark's formula) are tabulated in columns g and f respectively in Table 3.3 above. As could be seen, all the values in the 2 columns compared excellently well especially for plate of lower thicknesses while those of higher thickness have very negligible error of less than 0.2 which could have been due to mesh refinement. However the two results compared excellently well. Below are the frequency extraction modes diagrams generated from Abaqus software code however the first fundamental mode (Mode 1) is the most important of these modes.

3.42: Mode Diagram of frequency Analysis for 2m x 2m x 0.005m Obtained FromAbaqus Software Code (AllEdges Fixed)

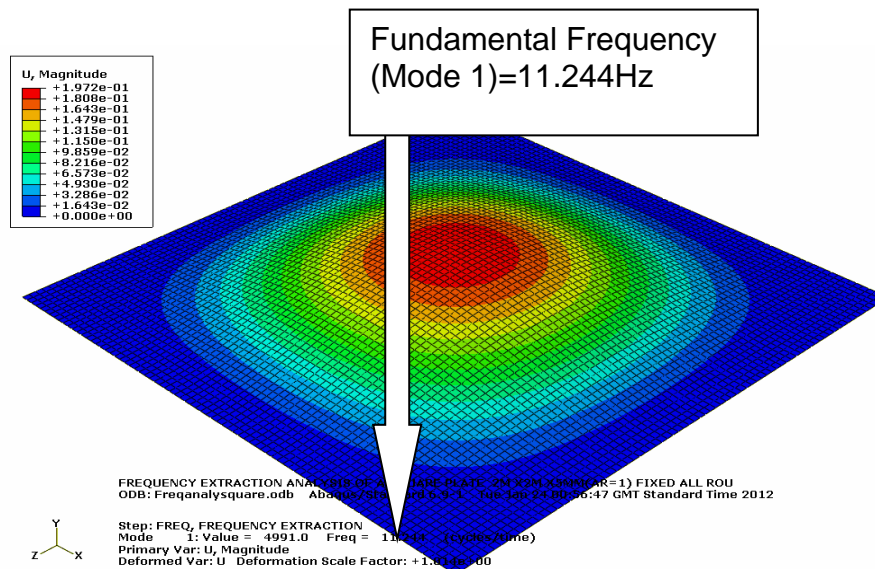


Figure 3-Mode 1 for the 2m x 2m x 5mm thick plate with all edges fixed is 11.244Hz which is the lowest frequency mode as could be seen in figure 3 above and is it is the frequency at which Resonance would occur. Other Modes increase in that order.

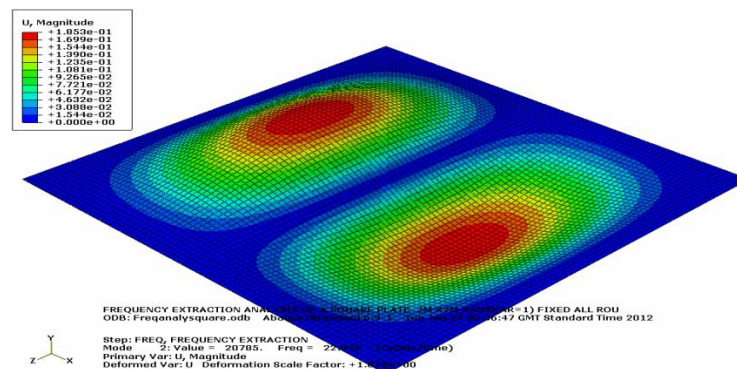


Figure 3.1-Mode 2

3.43: Mode Diagram of frequency Analysis for 2m x 2m x 0.008m Obtained FromAbaqus Software Code (All Edges Fixed)

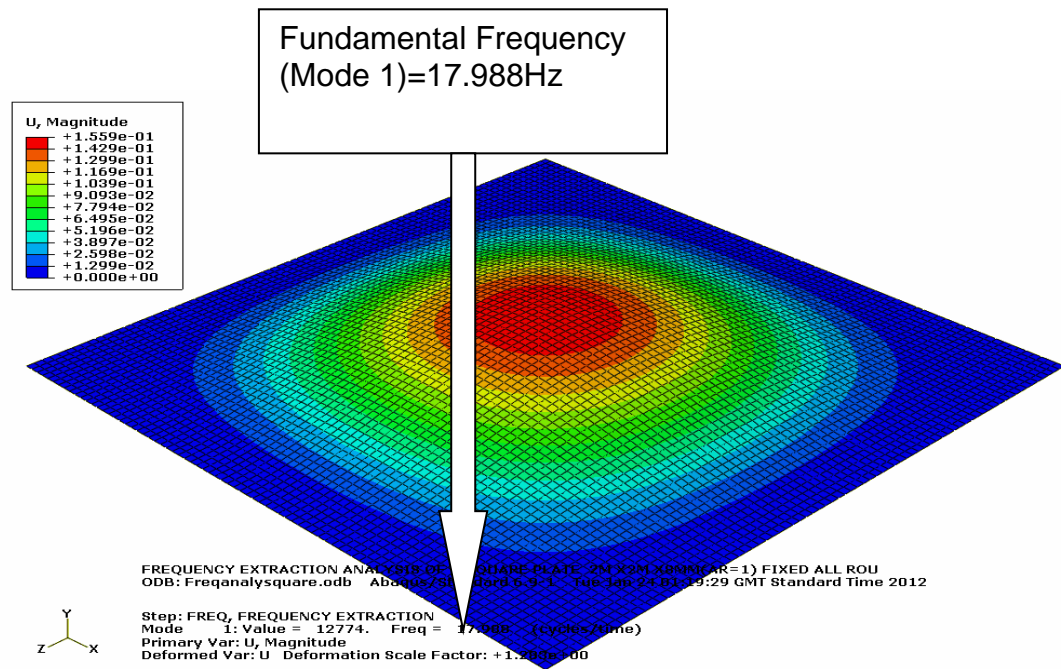


Figure 3.2 a-Mode 1 for the 2m x 2m x 8mm thick plate with all edges fixed is 17.988Hz which is the lowest frequency mode as could be seen in figure 3.2 a above and is it is the frequency at which Resonance would occur. Other Modes increase in that order

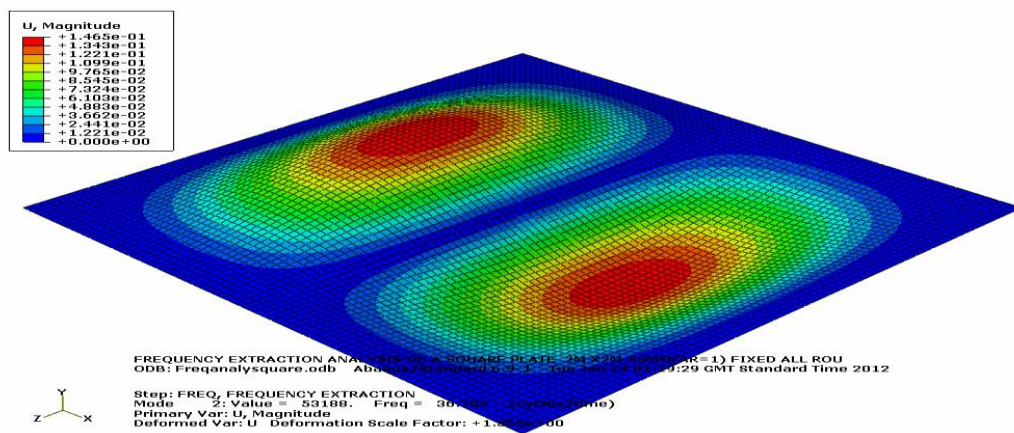


Figure 3.2b-Mode 2

3.44: Mode Diagram of frequency Analysis for 4.86m x 4.86m x 30mm Obtained From Abaqus Software Code (FIX, FREE, FREE, FREE)

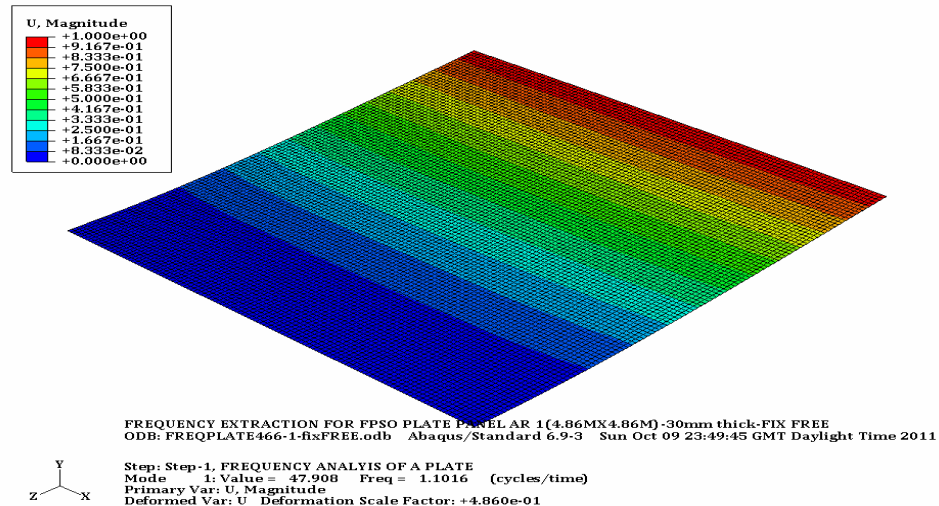


Figure 3. 3a-Mode 1 for the 4.86m x 4.86m x 30mm thick plate with all edges fixed is 1.1016Hz which is the lowest frequency mode as could be seen in figure 3. 85a above and is it is the frequency at which Resonance would occur

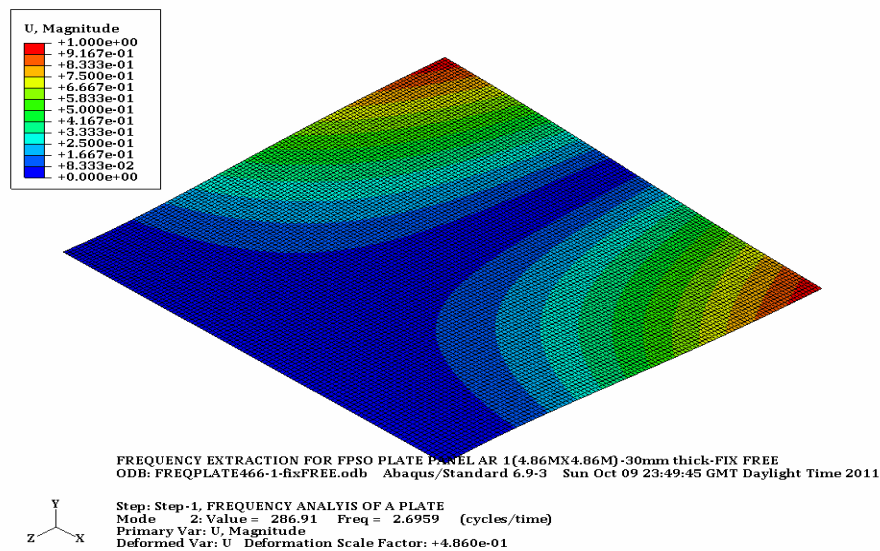


Figure 3.3b-Mode 2

Comment: Here, one full panel of the FPSO measuring 4.86m x 4.86m was subjected to frequency extraction analysis using Abaqus software code for plates with 30mm with a fix free freefree boundary condition and an aspect ratio of 1. The fundamental Frequency obtained was determined to be 1.1016Hz from ABAQUS software code and correlate favourably with the freq derived from classical theory as seen in table 3.3 above.

Table 3.4: Result of Natural frequency Analysis for FPSO Plate Panel 4.86mx4.86m validated from Abaqus software against Classical Theories-point supported boundary condition

S/No	Size of Plate (m)	Plate Thickness (mm)	Boundary Condition Used	Aspect Ratio	Calculated Natural Frequency From Classical theories (HZ)	Generated Natural Frequency From ABAQUS Software code.(HZ)	Difference in (f-g) (HZ)	Remarks
(a)	(b)	(c)	(d)	(e)	(f)	(g)	(h)	(I)
1.	4.86X4.86	0.005	Point supported at the edges	1.0	0.376	0.376	0.000	0.000
2.	4.86X4.86	0.01	Point supported at the edges	1.0	0.753	0.752	0.001	0.001
3.	4.86X4.86	0.015	Point supported at the edges	1.0	1.129	1.128	0.001	0.001
4.	4.86X4.86	0.020	Point supported at the edges	1.0	1.506	1.503	0.003	0.003
5.	4.86X4.86	0.025	Point supported at the edges	1.0	1.883	1.880	0.003	0.003

3.45: Mode Diagram of frequency Analysis for 4.86m x 4.86mm x 5mm thick Plate-Point Supported Boundary Condition

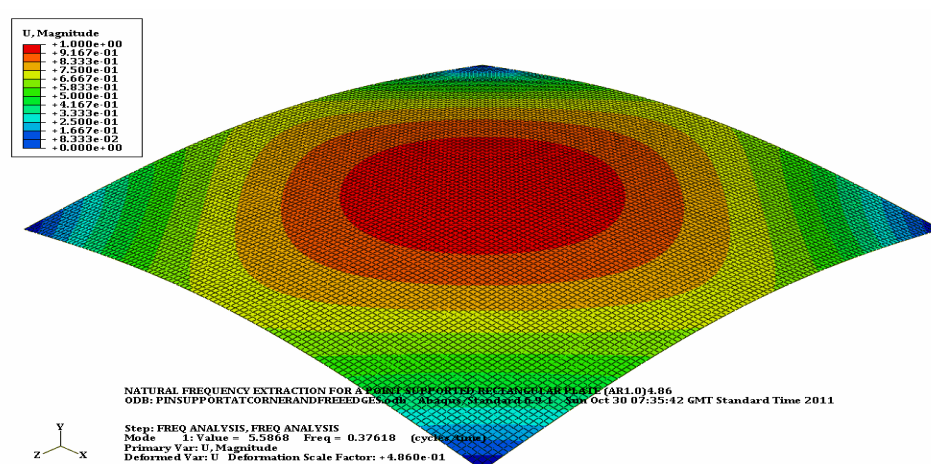


Figure 3.3c-Mode 1 for the 4.86m x 4.86m x 5mm thick plate with a point supported boundary condition the fundamental frequency was determined from abaqus to be 0.37618Hz which is the lowest frequency mode as could be seen in

figure 3. 3c above and is it is the frequency at which Resonance would occur

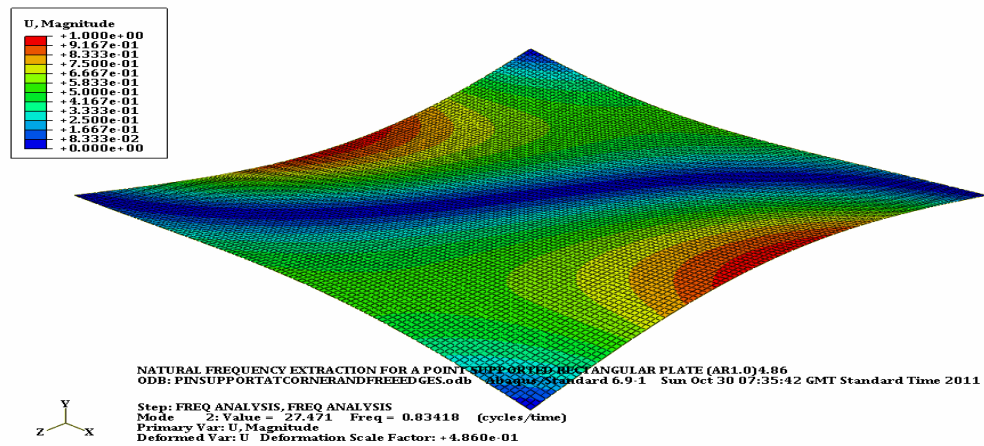


Figure 3.3d-Mode 2

Comment: Here, one full panel of the FPSO measuring 4.86m x 4.86m was subjected to frequency extraction analysis using Abaqus software code for plates with 5mm with a point supported boundary condition and an aspect ratio of 1. The fundamental Frequency obtained was determined to be 0.37618Hz from ABAQUS software code and correlate favourably with that derived from classical theory as seen in table 3.3 above.

Table 3.5: Result of Natural frequency Analysis for FPSO Plate Panel 4.86mx7.29m validated from Abaqus software against Classical Theories-point supported boundary condition.(AR=1.5)

S/No	a/b	λ^2	Plate Size(m)	Plate Thickness	Natural Frequency Calculation from Classical Theory	Natural Frequency Calculation from ABAQUS	Remarks
(a)	(b)	(c)	(d)	(e)	(f)	(g)	(h)
1.0	1.5	7.12	4.86x7.29	0.005	0.209	0.209	0.000
2.0	1.5	7.12	4.86x7.29	0.010	0.419	0.419	0.000
3.0	1.5	7.12	4.86x7.29	0.015	0.629	0.629	0.000
4.0	1.5	7.12	4.86x7.29	0.020	0.838	0.838	0.000
5.0	1.5	7.12	4.86x7.29	0.025	1.049	1.049	0.000
6.0	1.5	7.12	4.86x7.29	0.030	1.258	1.258	0.000

Comment: Here, one full panel of the FPSO measuring 4.86m x 7.29m was subjected to frequency extraction analysis using Abaqus software code for plates

with thicknesses of 5mm, 10mm, 15mm, 20mm, 25mm and 30mm with a point supported boundary condition and an aspect ratio of 1.5. All the fundamental Frequency obtained from Abaqus software code correlated absolutely well with that obtained from classical theory as seen in table 3.5 above.

3.46: Mode Diagram of frequency Analysis for 4.86m x 7.29m x 5mm thick Plate-Point Supported Boundary Condition (AR=1.5)

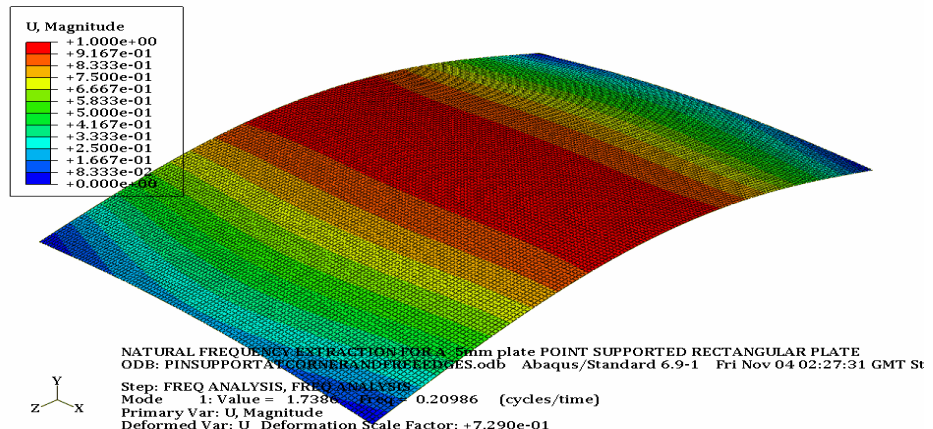


Figure 3.3e-Mode 1 for the 4.86m x 7.29m x 5mm thick plate with a point supported boundary condition the fundamental frequency was determined from abaqus to be 0.20986 HZ which is the lowest frequency mode as could be seen in figure 3.3e above and it is the frequency at which Resonance would occur.

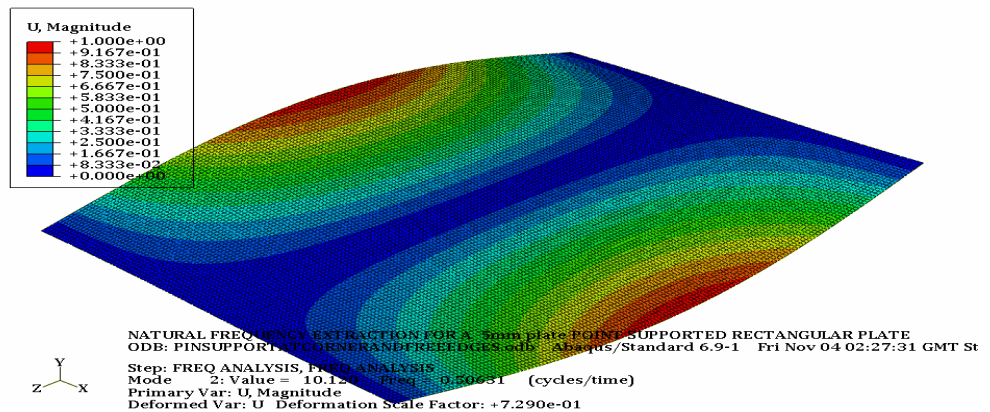


Figure 3.3f-Mode 2

Comments: Result of frequency extraction analysis from abaqus correlated well with those obtained through calculation as could be seen in Table 3.5 above

NATURAL FREQUENCY CALCULATION FOR A POINT SUPPORTED RECTANGULAR PLATE FROM BLEVINS TEXT**ASPECT RATIO 2 (PLATE SIZE 4.86m x 9.72m)**

Table 3.6: Result of Natural frequency Analysis for FPSO Plate Panel 4.86mx9.72m (AR=2.0) validated from Abaqus software against Classical Theories-point supported boundary condition

S/No	a/b	λ^2	Plate Size(m)	Plate Thickness	Natural Frequency Calculation from Classical Theory	Natural Frequency Calculation from ABAQUS	Remarks
1.0	2.0	7.12	4.86x9.72	0.005	0.123	0.123	0.000
2.0	2.0	7.12	4.86x9.72	0.010	0.246	0.246	0.000
3.0	2.0	7.12	4.86x9.72	0.015	0.369	0.369	0.000
4.0	2.0	7.12	4.86x9.72	0.020	0.491	0.491	0.000
5.0	2.0	7.12	4.86x9.72	0.025	0.614	0.614	0.000
6.0	2.0	7.12	4.86x9.72	0.030	0.737	0.737	0.000

Comment: Here, one full panel of the FPSO measuring 4.86m x 9.72m was subjected to frequency extraction analysis using Abaqus software code for plates with thicknesses of 5mm, 10mm, 15mm, 20mm, 25mm and 30mm with a point supported boundary condition and an aspect ratio of 2.0. All the fundamental Frequency obtained from Abaqus software code correlated absolutely well with that obtained from classical theory as seen in table 3.6 above.

CASE 1-5mm Plate (4.86x9.72m) A POINT SUPPORTED-AR 2

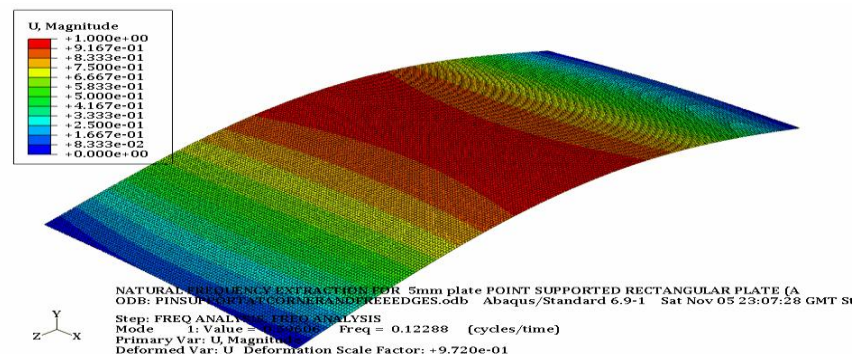


Figure 3.1.3a-Mode 1 for the 4.86m x 9.72 x 5mm thick plate with a point supported boundary condition the fundamental frequency was determined from abaqus to be 0.12288 HZ Which the lowest frequency mode is as could be seen in figure 3. 1.3a above and it is the frequency at which Resonance would occur.

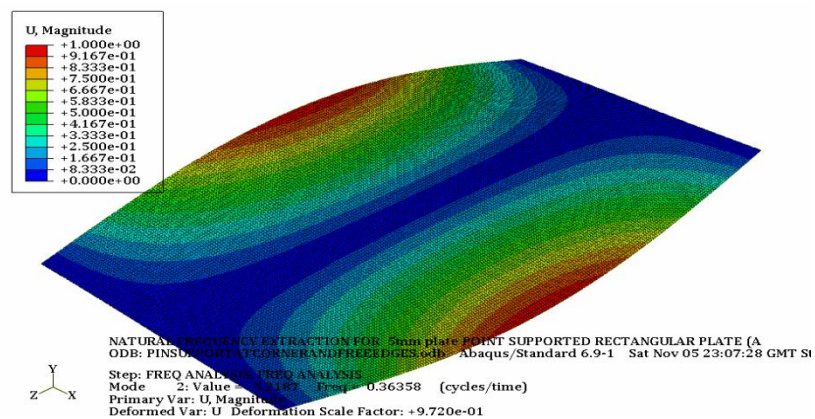


Figure 3.1.3b-Mode 2

Comments: Result of frequency extraction analysis from abaqus correlated excellently well with those obtained through calculation as could be seen in Table 3.6 above

NATURAL FREQUENCY CALCULATION FOR A POINT SUPPORTED RECTANGULAR PLATE FROM BLEVINS TEXT ASPECT RATIO 2.5

Table 3.7: Result of Natural frequency Analysis for FPSO Plate Panel 4.86mx 12.5m (AR=2.5) validated from Abaqus software against Classical Theories-point supported boundary condition.

S/No	a/b	λ^2	Plate Size(m)	Plate Thickness	Natural Frequency Calculation from Classical Theory	Natural Frequency Calculation from ABAQUS	Remarks
1.0	2.5	7.12	4.86x12.15	0.005	0.0794	0.0794	0.000
2.0	2.5	7.12	4.86x12.15	0.010	0.159	0.159	0.000
3.0	2.5	7.12	4.86x12.15	0.015	0.238	0.238	0.000
4.0	2.5	7.12	4.86x12.15	0.020	0.318	0.318	0.000
5.0	2.5	7.12	4.86x12.15	0.025	0.397	0.397	0.000
6.0	2.5	7.12	4.86x12.15	0.030	0.476	0.476	0.000

CASE 1-5mm Plate 4.86mx12.15m ASPECT RATIO 2.5

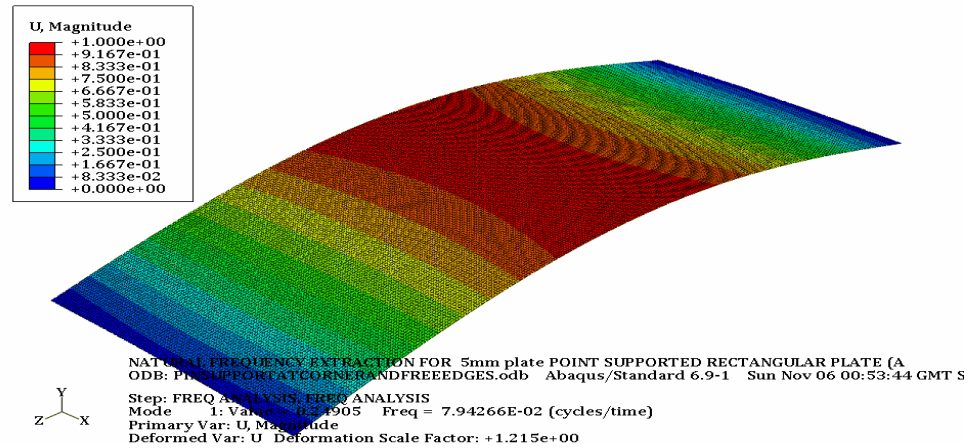


Figure 3.1.8c-Mode 1 for the 4.86m x 12.15m x 5mm thick plate with a point supported boundary condition the fundamental frequency was determined from abaqus to be 7.94266E-02 HZ which the lowest frequency mode is as could be seen in figure 3.1.8c above and it is the Frequency at which resonance would occur.

CASE 2-10mm Plate (4.86x12.15m) ASPECT RATIO 2.5

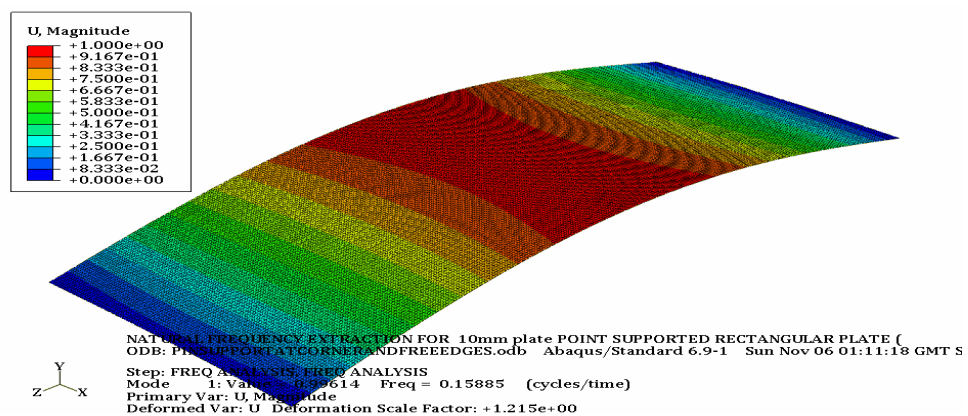


Figure 3.1.9a-Mode 1 for the 4.86m x 12.15m x 10mm thick plate with a point supported boundary condition the fundamental frequency was determined from abaqus to be 0.15885 HZ which the lowest frequency mode is as could be seen in figure 3.1.9a above and it is the Frequency at which resonance would occur.

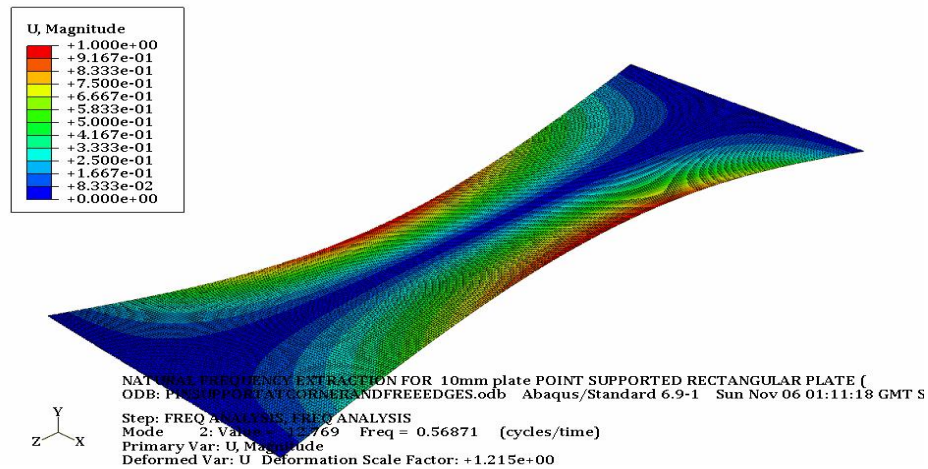


Figure 3.1.9a-Mode 2

Comments: Result of frequency extraction analysis from abaqus correlated excellently well with those obtained through calculation as could be seen in Table 3.7 above

COMPARISON OF FREQUENCY EXTRACTION ANALYSIS BETWEEN TWO TYPES OF BOUNDARY CONDITION (PIN-PIN-PIN-PIN AND FIX-FIX-FIX-FIX -AR 1.0)

Table 3.8: Comparison of frequency extraction analysis for FPSO plate with AR 1 resulting from 2 different boundary conditions

S/N o	a/b	Plate Size (m)	Plate Thickness(m)	Natural Frequency From Abaqus (pin, pin ,pin, pin)	Natural Frequency Calculation from ABAQUS(fix fix,fix,fix)	Remarks
1.0	1.0	4.86x4.86	0.005	0.376	0.441	0.0657
2.0	1.0	4.86x4.86	0.010	0.752	0.882	0.130
3.0	1.0	4.86x4.86	0.015	1.128	1.321	0.193
4.0	1.0	4.86x4.86	0.020	1.503	1.760	0.257
5.0	1.0	4.86x4.86	0.025	1.878	2.197	0.319
6.0	1.0	4.86x4.86	0.030	2.253	2.634	0.381

COMPARISON BETWEEN PIN-PIN, PIN, PIN, PIN AND FIX-FIX-FIX-FIX (AR 1.5)

Table 3.9: Comparison of frequency extraction analysis for FPSO plate with AR 1.5 resulting from 2 different boundary conditions

S/No	a/b	Plate Size(m)	Plate Thickness	Natural Frequency From Abaqus(pin-pin)	Natural Frequency Calculation from ABAQUS(fix, fix,fix,fix)	Remarks
1.0	1.5	4.86x7.29	0.005	0.209	0.250	0.041
2.0	1.5	4.86x7.29	0.010	0.419	0.497	0.078
3.0	1.5	4.86x7.29	0.015	0.629	0.743	0.114
4.0	1.5	4.86x7.29	0.020	0.838	0.988	0.150
5.0	1.5	4.86x7.29	0.025	1.049	1.231	0.182
6.0	1.5	4.86x7.29	0.030	1.258	1.474	0.216

Comparison Between Pin-Pin-Pin-Pin and Fix-Fix-Fix-Fix (AR 2.0)

Table 3.10: Comparison of frequency Extraction Analysis for FPSO Plate with AR 2.5 resulting from 2 Different Boundary Conditions.

S/No	a/b	Plate Size(m)	Plate Thickness	Natural Frequency From Abaqus(pin,pin, pin,pin)	Natural Frequency Calculation from Abaqus (fix,fix,fix fix)	Remarks
1.0	2.0	4.86x9.72	0.005	0.123	0.150	0.03
2.0	2.0	4.86x9.72	0.010	0.246	0.298	0.052
3.0	2.0	4.86x9.72	0.015	0.369	0.444	0.075
4.0	2.0	4.86x9.72	0.020	0.491	0.589	0.098
5.0	2.0	4.86x9.72	0.025	0.614	0.733	0.119
6.0	2.0	4.86x9.72	0.030	0.737	0.877	0.14

Comments: Comparison of the result of frequency extraction analysis from abaqus correlated excellently well with those obtained through calculation, however it was observed that the fundamental frequency of the plate with fix,fix,fix ,fix is higher than the ones with boundary condition of pin,pin,pin pin as could be seen from table 3.8,3.9 and 3.91 above for all the aspect ratio.

3.5 NATURAL FREQUENCY EXTRACTION FOR STIFFENED PLATE

Having carried out several analyses of frequency extraction analysis of unstiffened plate using the Abaqus code and validated the capability and accuracy of the code with the much confidence, the researcher progressed to carry out frequency extraction analysis on stiffened plates to determine and obtain the natural frequencies of the panel. The results also gave a good understanding of the response of tee-stiffened rectangular plates with an aspect ratio of 2 under fixed boundary conditions subjected to frequency extraction analysis.

3.51 PARTICULARS OF PLATES SUBJECTED TO FREQUENCY EXTRACTION ANALYSIS

All the flat rectangular plates are 25mm thick and the overall plate size is 3000mmx1500mm and were fitted with T-stiffeners 10mm thick [flange and stiffener thickness=10mm thick] and the stiffener height is 150mm, the flange width is 50mm. They are also stiffened by a flat bar of size 1500x150x10mm and all edges are fully fixed against rotation and translation in all directions. A frequency extraction analysis was carried out. Three different models consisting of shell element size of 30mm fine mesh was used to verify the accuracy of the finite element models of the panel. A total of about 5250 elements was created by Abaqus. The 3 models considered are as follows:

- a. **Model 1-Configuration of Stiffeners-(1x1).**
- b. **Model 2-Configuration of Stiffeners-(2x2)**
- c. **Model 1-Configuration of Stiffeners-(3x3)**

Model 1-Configuration of Stiffeners

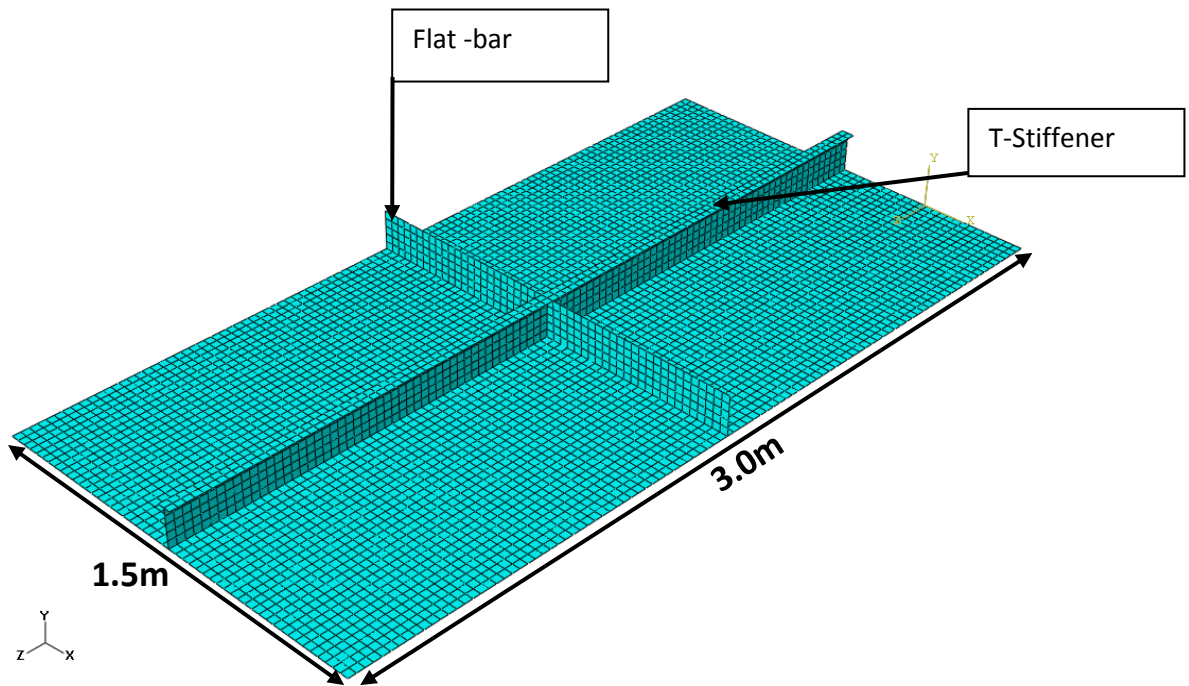


Figure 3.2: Model 1-Configuration of Stiffeners-(1x1)

CASE 1-MODE 1

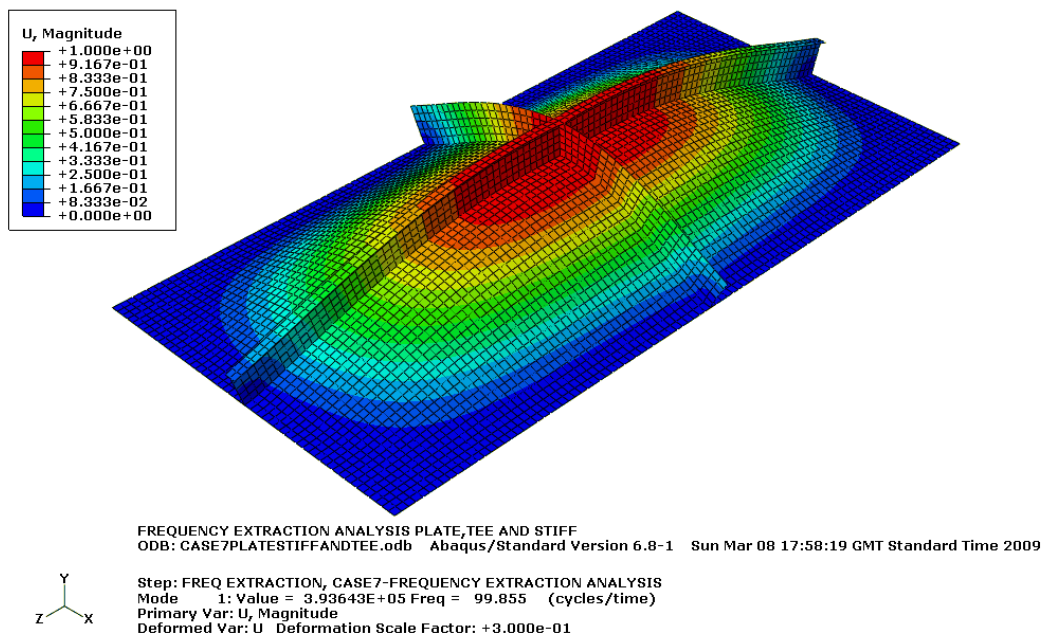


Figure 3.3: Showing the frequency extraction analysis of (1x1)-Mode 1(99.85Hz)

CASE 1-MODE 2

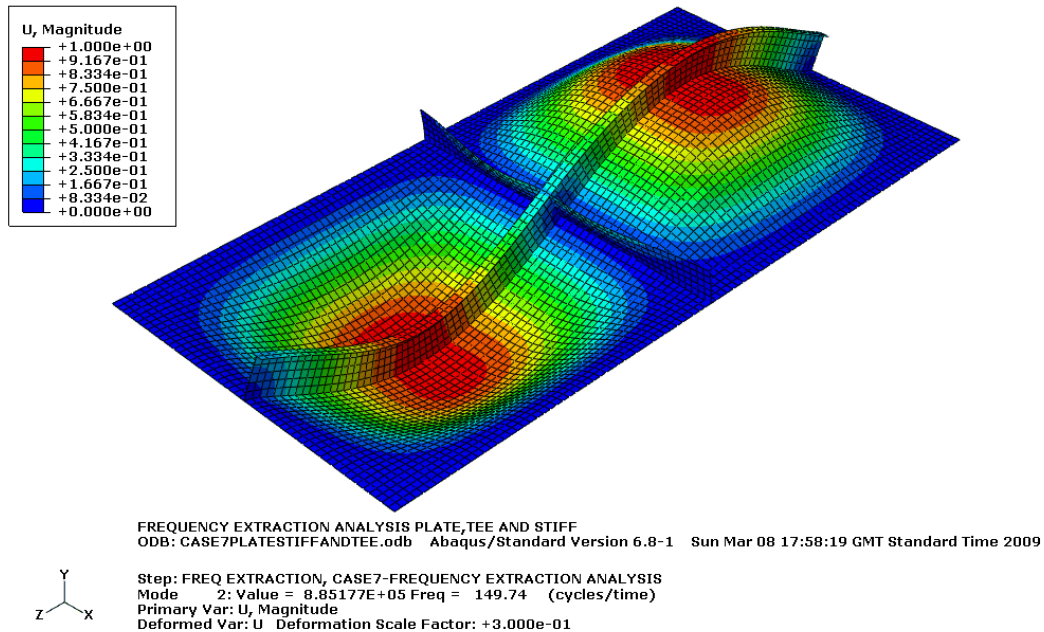


Figure 3.4: Showing the frequency extraction analysis of (1x1)-Mode 2(149.74Hz)

Comment: The frequency extraction analysis of 1x1 stiffeners in mode 1 and 2 yielded a natural frequency of about 99.85Hz and 149.74Hz respectively. However, the natural frequency generated in mode 1 is actually the most important mode as this is the natural frequency at which resonance will occur. Hence designers can design against resonance.

CASE 2

Model 2-Configuration of Stiffeners [2x2]

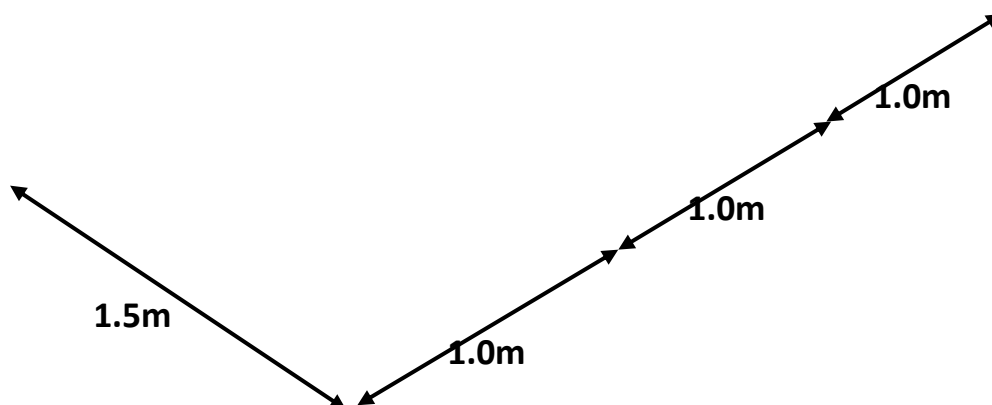


Figure 3.5 Configuration of Stiffeners-Model 2-[2x2]

CASE 2 MODE 1

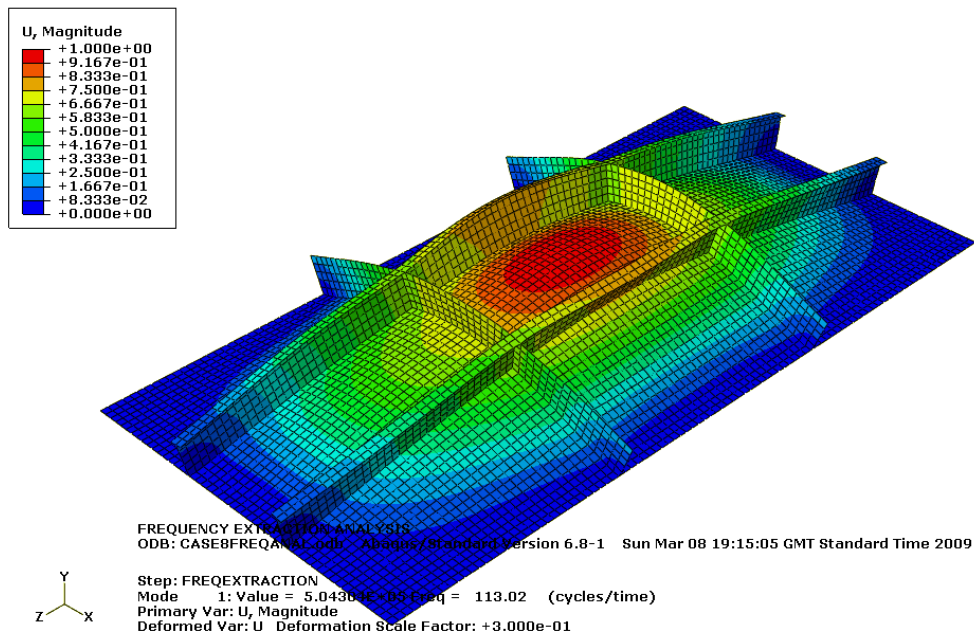


Figure 3.6: Showing the frequency extraction analysis of (2x2)-Mode 1(113.02Hz)

CASE 2 MODE 2

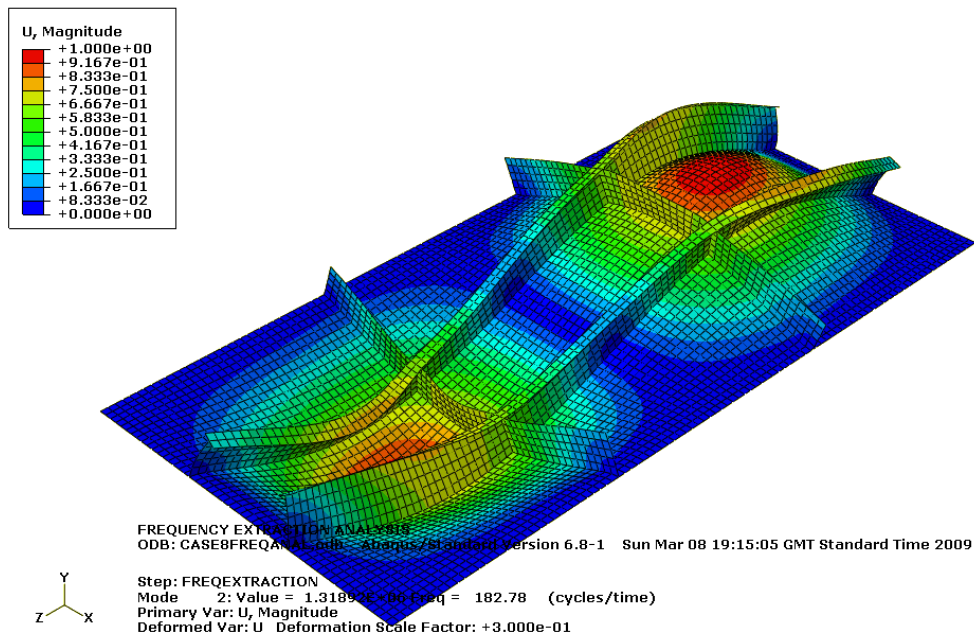


Figure 3.7: Showing the frequency extraction analysis of (2x2)-Mode 2 (182.78Hz)

Comment: The frequency extraction analysis of 2x2 stiffeners in mode 1 and 2 yielded a natural frequency of about 113.02Hz and 182.78Hz respectively. However, the natural frequency generated in mode 1 is actually the most important mode as this is the natural frequency at which resonance will occur. Hence designers can design against resonance. One important deduction here is that the more stiffened the plate, the higher the frequency required to excite the structure to resonance.

CASE 3

Model 3-Configuration of Stiffeners [3x3]

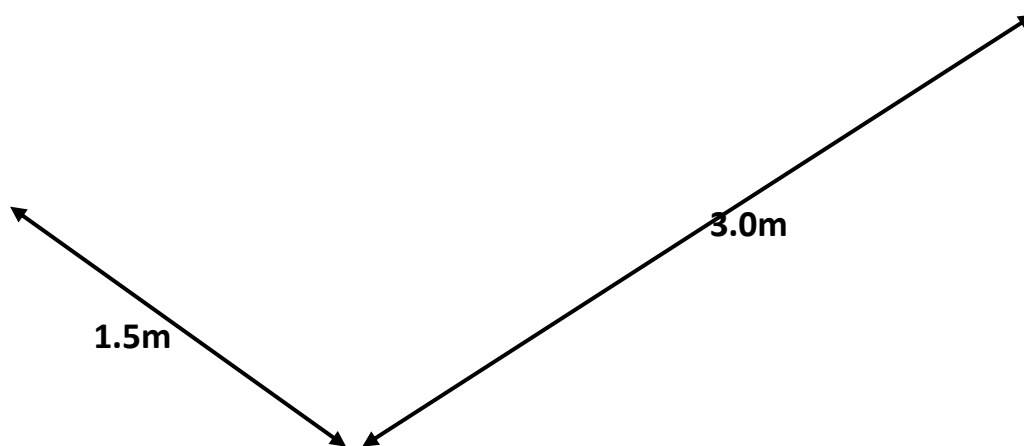


Figure 3.8: Configuration of Stiffeners-Model 3-[3x3]

CASE 3 MODE 1

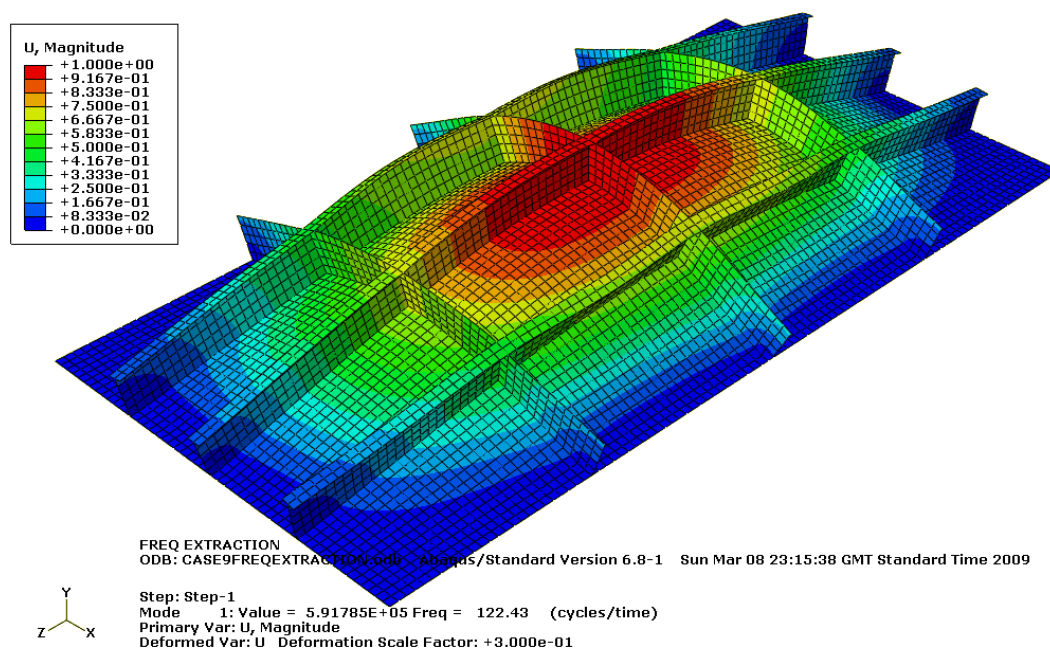


Figure 3.9: Showing the frequency extraction analysis of (3x3)-Mode 1(122.43Hz)

Summary of Natural Frequencies for FPSO Stiffened Plate

Comment: Here, only the first mode was generated. Thus, the frequency extraction analysis of 3x3 stiffeners in mode 1 yielded a natural frequency of about 122.43Hz .Also the deduction here is that the more stiffened the plate,the higher the frequency required to excite the structure to resonance. It is therefore imperative for designers to ensure their structures is well stiffened in order to produce a good design that will be able to withstand terrorist attack or to design a structure that will reduce the effect of terrorist attack to the barest minimum.

3.6 RESULT AND DISCUSSIONS

Actually, this chapter 3 is for structural analysis and frequency extraction analysis, However, before the researcher dwell into the frequency extraction for unstiffened and stiffened plates, it was very important to carry out numerical analysis by using Abaqus software code to determine the displacements and stresses of different sizes of plates with different thicknesses ranging from 5mm, 10mm, 15mm, 20mm, 25mm and 30mm. Furthermore he used classical theory (Roark's formula) to calculate the stresses and displacement of the same plates with different thicknesses that were subjected to blast pressure loading from $1e+06$ to $6e+06$ pascals. The results of the stresses and displacement from the two methods were tabulated in a table. Most importantly, It was observed that the Numerical analysis carried out on such plate under the same blast pressure loadings in order to determine the stresses and displacement correlated excellently well with those derived from the use of classical theory. The significance of these results showed that Abaqus software code has been validated by the researcher as highly reliable software that could be used and trusted in Numerical analysis. Additionally, it gives a good direction to the researcher as a validation that he has gained much confidence in the understanding of numerical software in analysis of this nature and this enable the researcher to proceed further with confidence to the next stage. Consequently, the researcher progressed to using the Abaqus software code to carry out linear perturbation analysis of plates and stiffened plates where frequency extraction analysis was determined by the calculation of the fundamental frequency of such plates and stiffened plates. These results generated from Abaqus code were further validated against those generated from classical theory.

When Plate structures are subjected to dynamic loads in real life it is periodic in nature, consequently the structures vibrate. If the operating frequency meets the natural frequency of the system then resonance occurs and it fails irrespective of its strength. Vibration also creates detrimental effect on relevant structures; human being creates irritating and annoying noise. Though It is not possible to completely avoid vibration, however it is important to design for vibration which involves keeping operating frequency away from natural frequencies of the structure and to minimize displacement, velocity and acceleration of vibrating structure within permissible and allowable limits.

In this chapter, the extraction of Natural frequencies of plates and stiffened plates were carried out using Abaqus software code. Additionally Natural frequencies for simple plates and those of the FPSO Plates were calculated through classical theories and compared

with the Abaqus software code. The result of the Natural frequencies obtained through classical theories and Abaqus software code in all cases compared favourably so well which further validated that Abaqus software code is one of the most reliable and accurate software code.

From the analysis carried out, the effect of different plate thickness on Natural frequency, the effect of boundary condition on Natural frequency and effect of aspect ratio on Natural frequency were deduced. Most importantly, the Lowest Natural frequency for the FPSO panel without stiffeners was calculated and those with stiffeners were also generated through Abaqus software in order to validate the originality of this chapter.

3.7 CONCLUSION

The Natural frequency analysis of the bare plate and stiffened plates with different thicknesses were performed. Results of the analysis gave the following information regarding Natural frequency analysis of plates.

1. The more stiffened the plate, the higher the frequency required to excite it to resonance. Thus the plated structure with 3 x 3 stiffeners would require a higher frequency to excite it than 2x2 stiffened plate and 1x1 stiffened plates.
2. Increasing the thickness of the plate increases the Natural frequency of the plate for the same boundary condition.
3. The Natural frequency of a plate with FIX FIXFIXFIX boundary condition for a plate of same size, same thickness is higher than the Natural frequency of a plate with a FIX, FREE, FREE, FREE boundary condition. Consequently, the effect of boundary condition on the frequency extraction is a very important factor.
3. The Natural frequency of a plate with FIX FIXFIXFIX boundary condition for a plate of same size, same thickness is higher than the Natural frequency of a plate with a point supported boundary condition.
4. The Natural frequency of a plate with FIX FIXFIXFIX boundary condition and the Natural frequency of a plate with FIX, FREE, FREE, FREE for a plate of same size, same thickness is higher than the Natural frequency of a plate with a point supported boundary condition.
5. The Natural frequency of a plate with a FIX, FIX, FIX, FIX boundary condition is higher than that of a plate with a PIN, PIN, PIN, PIN,

6. Addition of the stiffener to the plate has an effect of shifting natural frequencies towards higher side.
7. The plate with all edges clamped gives higher natural frequencies than the plate with all edges free for all the cases.
8. Increasing thickness of the stiffener increases the natural frequencies of the plate for all the boundary conditions.

CHAPTER 4

4. Non-linear Analysis of Stiffened Plates Subjected to Uniform Blast Pressure Load

4.1 Introduction to Non-linear Analysis of Stiffened Plates Subjected to Uniform Blast Pressure Load

Having carried out much analyses using the Abaqus code and validated the capability and accuracy of the code with all the much needed confidence, the researcher needed to progress further, thus, the researcher progressed into more complex analysis which is the Dynamic non – linear Analysis of stiffened plate by precisely taken the FPSO Panel that was considered as a case study and subjecting this FPSO panel under different loading. The aim of chapter 4 is to determine the dynamic response of a tee-stiffened rectangular plate subjected to uniform lateral blast loading with different tee-stiffened configurations. The responses of stiffeners to blast load could either be in tension or in compression. However, this chapter addressed uniform blast loading applied to the outer unstiffened surface part of the FPSO panel. The Chapter also present various results highlighting the effect of fully fixed boundary conditions and the non-linear large deflection dynamic response of the tee-stiffened plates subjected to blast loading. This includes frequency extraction to determine and obtaininig the natural frequencies of the panel but this time with the effects of damping and the high material strain rate effects as well as the effect of plasticity were considered using the finite element code ABAQUS EXPLICIT.

The displacement and responses of the stiffened panel at the central node was investigated including their energy terms. This help the researcher to understand and improve the design of tee stiffened plated structures against blast loading as studying their non-linear dynamic response of tee-stiffened plates helps in the understanding of their behaviour and potentially identify ways of improving their blast resistance nature. The results also gave a good understanding of the response of tee-stiffened rectangular plates with an aspect ratio of 2 under fixed boundary conditions subjected to lateral blast pressure loading.

4.2 INTRODUCTION

The aim of this chapter is to determine the dynamic response of a tee-stiffened rectangular plate subjected to uniform lateral blast loading with different tee-stiffened configurations. The Chapter also present various results highlighting the effect of fully fixed boundary conditions and the non-linear large deflection dynamic response of the tee-stiffened plates subjected to blast loading. This includes frequency extraction to determine and obtain the natural frequencies of the panel with the effects of damping and the high material strain rate effects as well as the effect of plasticity were considered using the finite element code ABAQUS EXPLICIT.

The displacement and responses of the stiffened panel at the central node was also investigated including their energy terms. This helped the scholar to understand and improve the design of tee stiffened plated structures against blast loading as studying their non-linear dynamic response of tee-stiffened plates helps in the understanding of their behaviour and potentially identifying ways of improving their blast resistance. The results also gave a good understanding of the response of tee-stiffened rectangular plates with an aspect ratio of 2 under fixed boundary conditions subjected to lateral blast pressure loading.

4.2.1 NUMERICAL MODELS

In order to investigate the non-linear dynamic response of the blast loaded tee-stiffened rectangular plate with an aspect ratio of 2, the non-linear finite element [FE] code Abaqus is used. The package is capable of modelling both geometric and material non-linearity, and including strain rate effects on material properties. The package is an explicit code and is very suitable in modelling transient problems where high rate dynamics and stress wave propagation effects are important. Abaqus is a suite of powerful engineering simulation programme that can solve problems ranging from relatively simple linear analyses to the most challenging non-linear simulations **Hibbit, Karlsson and Sorensen (1998)**. A large stiffness matrix does not have to be solved and does not require iteration at each time increment since iteration is not required for explicit dynamics analysis in Abaqus. Most primary structural members used in modern offshore structures comprises of high strength steel although mild steel is often used for secondary members, typically many existing plated structures consist of grade 50 steel and therefore, this has been used for the material in this study for both the plate and the stiffener components. However other marine structures may be fabricated from mild steel e.t.c including many

ships Steel which is strain-rate sensitive with high loading rates and thus significantly enhancing the yield strength, particularly mild steel and in order to account for this effect of strain rate dependent isotropic elastic-plastic material model was adopted.

4.2.2 DESCRIPTION OF PLATES

All the flat rectangular plates are 25mm thick and the overall plate size is 3000mmx1500mm and were fitted with T-stiffeners 10mm thick [flange and stiffener thickness=10mm thick] and the stiffener height is 150mm, the flange width is 50mm. They are also stiffened by a flat bar of size 1500x150x10mm and all edges are fully fixed against rotation and translation in all directions.

4.3 MODEL GEOMETRY

Abaqus has an element library which is available for utilisation on a wide range of geometric models. In this analysis, A 4 node doubly curved thin, reduced integration, hourglass control, and finite membrane strain with Quad element shape, structured with mesh minimisation has been used. The analysis was carried out under explicit code with linear geometrical order and reduced integration. Three different models consisting of shell element size of 30mm and 75mm representing fine and coarse meshes respectively were used to verify the accuracy of the finite element models of the panel.

4.4 Finite Element Modelling

This was performed using the Abaqus explicit general purpose finite element code **Hibbitt, Karlsson and Sorensen, (1998)**.

Model 1-Configuration of Stiffeners

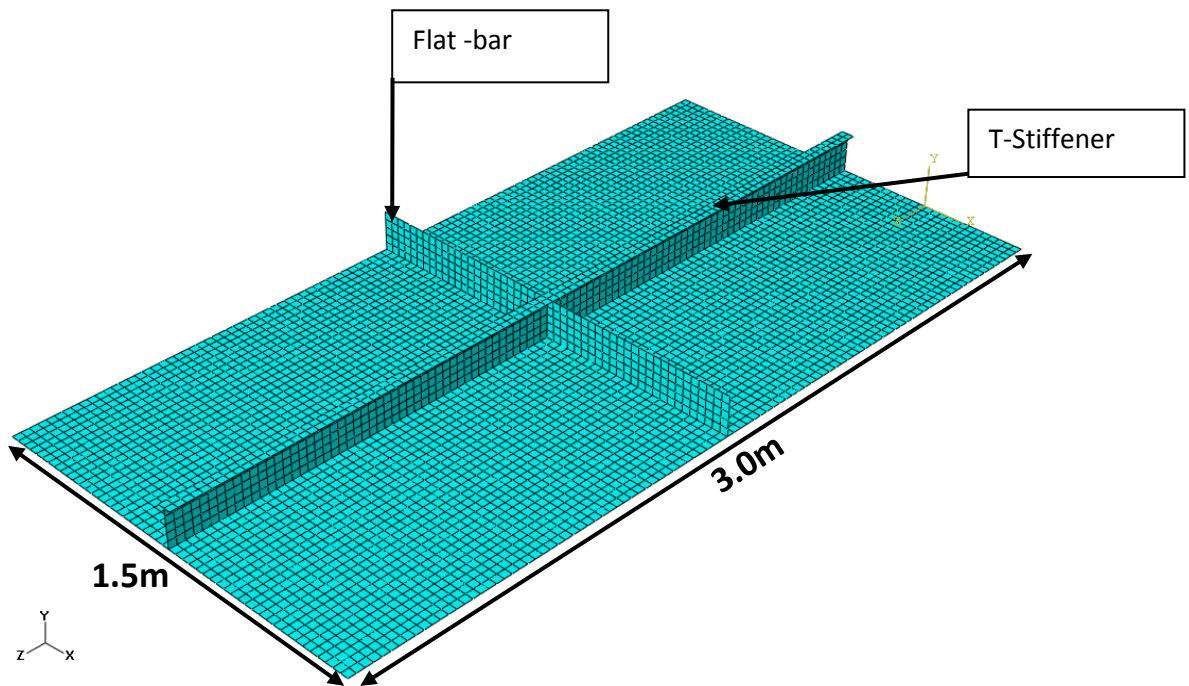


Figure 4: Model 1-Configuration of Stiffeners-(1x1)

Model 2-Configuration of Stiffeners [2x2]

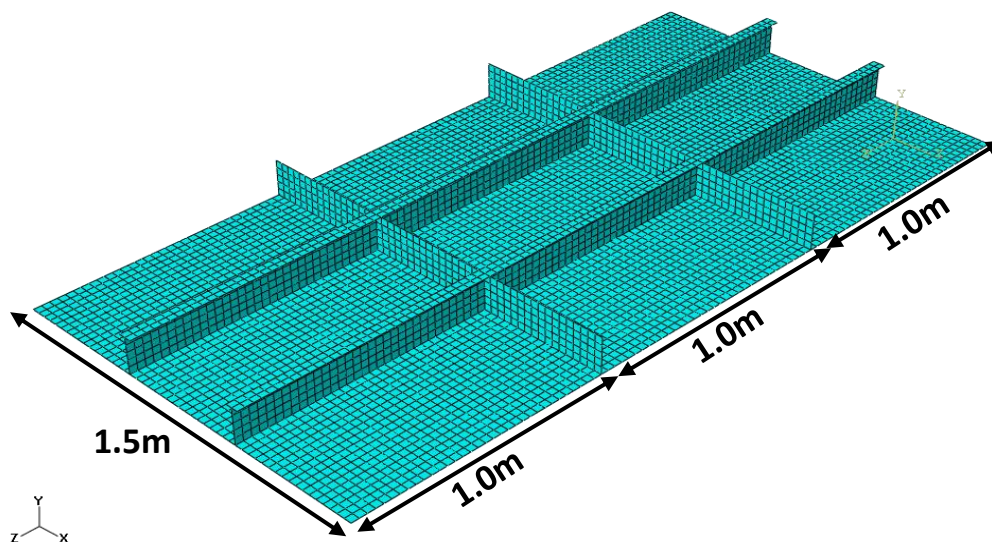


Figure 4.1 Configuration of Stiffeners-Model 2-[2x2]

Model 3-Configuration of Stiffeners [3x3]

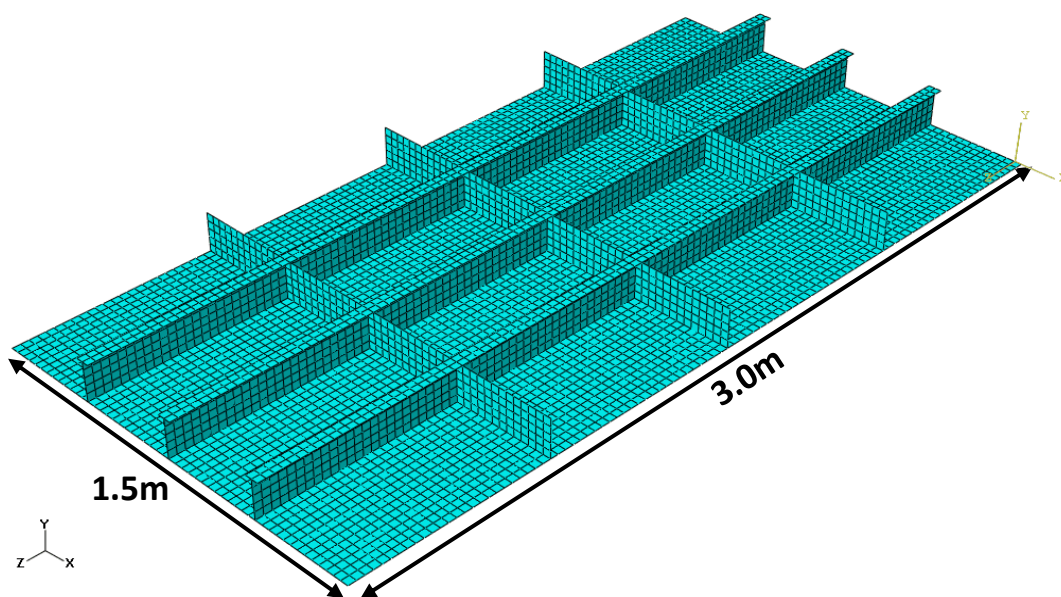


Figure 4.2: Configuration of Stiffeners-Model 3-[3x3]

4.5 FUNDAMENTAL FREQUENCY EXTRACTION AND PERIOD

The fundamental frequencies and periods of the 3 cases under observation were extracted and presented in table 4 as follows:

Table 4: Fundamental Frequencies and Period for the 3 cases in view

MODEL	1	2	3
Fn(Cycles/s)	99.86	113.02	122.43
Tn(s)	0.01	0.0088	0.0081
Tn/2(s)	0.005	0.0041	0.004

Where Fn is the fundamental frequency in cycles/s
andTn is the time in seconds

A modal analysis was carried out for the three models in order to obtain the natural frequencies of model 1 to 3. The importance of these frequency extraction analyses could not be overemphasised as this enables us to determine the ratio of the duration of loading over the natural period of the structure and to predict resonance. It is now important to discuss about the explosion to which this plates could be subjected to.

4.6 THE EXPLOSION PHENOMENON

Generally, an explosion is said to have occurred in the atmosphere if energy is released over sufficiently small time and in sufficiently small volume so as to generate a pressure wave of finite amplitude travelling away from the source **Jacinto et al(2001)**. Explosion could also be defined as a rapid chemical reaction in a substance, which converts the original material into a gas at a very high temperature and pressure evolving large amount of heat to a tune of about 4389kj/kg of trinitrotoluene popularly known as TNT explosive **Olson et al, (1993)**. Explosion phenomenon is of two stages, namely the detonation stage and the interaction stage which takes place between the product gases and the surrounding medium. Chapman-Jouguet detonation pressure is commonly used to assess the detonation performance of an explosive **Bulson, (1997)** including the temperature of **Chopra(2001)** and the detonation velocity **Jones, (1989)**. A very clear examples is a TNT explosive that has a density of 1650kg/m³, the Chapman-Jouguet detonation pressure is 21000MPa **Chopra(2001)** while the detonation temperature is 3720k **Bulson(1997)** and the detonation velocity is 6950m/s **Jones(1996)**, After the completion of detonation process, the interaction stage commence where the product gases interact with the surrounding medium and the pressure waves are generated as a result of high pressure and temperature expansion outwards. An equation of state of the explosive relating energy, pressure and volume is essential for the numerical modelling of any detonation process, the most commonly used equation to describe the state of detonation product is Jones-Wilkins-Lee which is given as **Olson et al, (1997)** :

$$P_{JWL}(V, U_{in}) = A\left(1 - \frac{Q}{R_1 V}\right)e^{(-R_1 V)} + B\left(1 - \frac{Q}{R_2 V}\right)e^{(-R_2 V)} + \frac{Q}{V} E_{in} \text{-----} (4.1)$$

Where A, B, R₁, R₂ and Q are constant **Olson et al(1997)**, P (JWL) is the pressure V is the relative volume compared to the initial volume of the explosive and U (in) is the internal energy per unit volume. The first term in JWL equation is the high pressure terms that dominates first for V close to 1, the second term is influential for V close to 2 and the last term correspond to the expanded state

4.7 Idealisation of Blast Pressure Loading

4.7.1 Air blast

A schematic diagram of a typical Blast wave time history of a blast pressure wave is shown in Fig 4.3. The diagram is an illustration of an idealisation of an explosion in free air. The shock wave has an instantaneous rise and an exponential fall. Usually; three important parameters are of interest when considering blast pressure waves. The parameters are Peak overpressure which is the pressure that is above atmospheric pressure, the positive duration with respect to scaled distance and the impulse with respect to the scaled distance. In the positive phase, maximum overpressure, P^{+s} is developed instantaneously and decay to the atmospheric pressure P_o , in the time $T+$. The maximum negative phase P_s has much lower amplitude than the positive overpressure. In most blast studies, the negative phase of the blast wave is usually ignored and only blast parameters associated with the positive phase are considered or reported however in comparison, the duration of the negative phase $T-$ is much longer compared to the positive duration. An explosion that has a higher yield will arrive at a point faster than the explosion with a lower yield; the greater the overpressure at the shock front, the higher would be the velocity of the shock wave. The instantaneous pressure $P(t)$ of the positive phase of an ideal air blast wave is generally given by Friedlander equation as

$$p(t) = p_o + p_m \left[1 - \left(\frac{t}{t_d} \right) e^{-\frac{\alpha t}{t_d}} \right] \quad \text{----- (4.2)}$$

Where P_o is the ambient pressure

t is the instantaneous time

t_d is the positive duration of the pressure pulse

α is the wave front parameter and it is dependent on the peak overpressure P_m of the shockwave

α , the waveform parameter is an adjustable parameter and it is selected in order that the overpressure-time relationship can provide that suitable values of the blast impulse

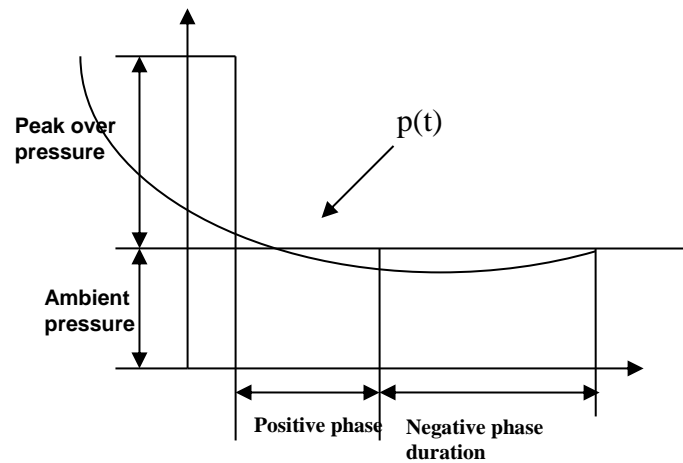


Fig: 4.3: A schematic diagram of a typical Blast wave time history of a blast pressure wave.

For purposes of references, the peak overpressure for **chemical explosion** is

Given as (4.2a):

$$\frac{P_m}{P_o} = \frac{808 \left[1 + \left(\frac{S'}{4.5} \right)^2 \right]}{\sqrt{1 + \left(\frac{S'}{0.048} \right)^2} \sqrt{1 + \left(\frac{S'}{0.32} \right)^2} \sqrt{1 + \left(\frac{S'}{1.35} \right)^2}} \text{----- (4.3)}$$

While the peak overpressures for nuclear explosions (4.2a)

$$\frac{P_m}{P_o} = 3.2 \times 10^6 S^{-3} \sqrt{1 + \left(\frac{S}{87} \right)^2} \left[1 + \frac{S'}{800} \right] \text{----- (4.4)}$$

And the scaled distance S' is given as (3, 4, and 5):

$$S' = \frac{S}{W^{1/3}} \text{----- (4.5)}$$

Where S is the stand off from the explosion in m and W is the TNT equivalent of the explosive charge weight in kg.

4.7.2 Scaling Laws

Scaling of the properties of blast wave from explosive is a common practice as scaling laws are used to predict the properties of blast waves from large scale explosions based on tests on a much smaller scale. The most common blast scaling is that of Hopkinson – Cranz or cube root scaling which states that self –similar blast waves are produced at identical scaled distance when two explosive charges of similar geometry and of the same explosive but of different sizes are detonated in the same atmosphere. The scaling laws equation is as stated in equation **Keshawarz M.H., Eta al (2006)** above. Some standard conversion factors for TNT equivalence) for calculating equivalence of high explosive charges as given by **Baker, (1973)** and Suppressive **Shields(1977)** are given below:

Table 4.1: Standard Conversion Factor for Some Explosives.

Explosives	Mass specific Energy (KJ/KG)	TNT EQUIVALENT $/(E/M)X(E/M)_{TNT}$	Density (Mg/m3)	Detonation velocity(km/s)	Detonation pressure (Gpa)
TNT	4520	1.000	1.6	6.73	21
PETN	5800	1.283	1.77	8.26	34
RDX	5360	1.185	1.65	8.70	34.0
HMX	5680	1.256	1.90	9.11	38.7
PITRIC	4180	0.926	1.71	7.26	26.5
ACID					
TETRYL	4520	1.0	1.73	7.85	26

Source: Curled from W.E. Baker

4.7.3 MATERIAL PROPERTIES

The material properties used in the analysis and as specified by the **(CCM 1977)** are as follows:

Table 4.2: Material Properties Used for the Analysis.

PROPERTY	VALUE
Density(kg/m³)	7800
Modulus of Elasticity(Pa)	210E+09
Poisson's Ratio	0.3
Initial Yield stress (Pa)	300E+06
Blast Amplitude Pressure (Pa)	8.0E+05
Material type	Mild steel ASTM A36 Steel

The material is Mild steel ASTM A36 Steel. The initial yield stress and the post yield stress behaviour for this steel is known from previous executed experiment **Abaqus user manual(2006)**, thus from the above table, the initial yield stress for this grade of mild steel is 300MPa and it increases to 400MPa at a plastic strain of 35%. This is imputed into ABAQUS.

Table 4.3: BLAST LOAD AMPLITUDE

0.00	0.00
1E-3	8E+5
10E-3	8E+5
20E-3	0.00
50E-3	0.00

SOURCE: Abaqus User Manual (2006)

4.8. Effect of Mesh Refinement on the Displacement of the central node, Energy terms of the model and Von Misses Stress.

4.8.1 Effect of Mesh Refinement on Displacement of the Central Node on Model 1

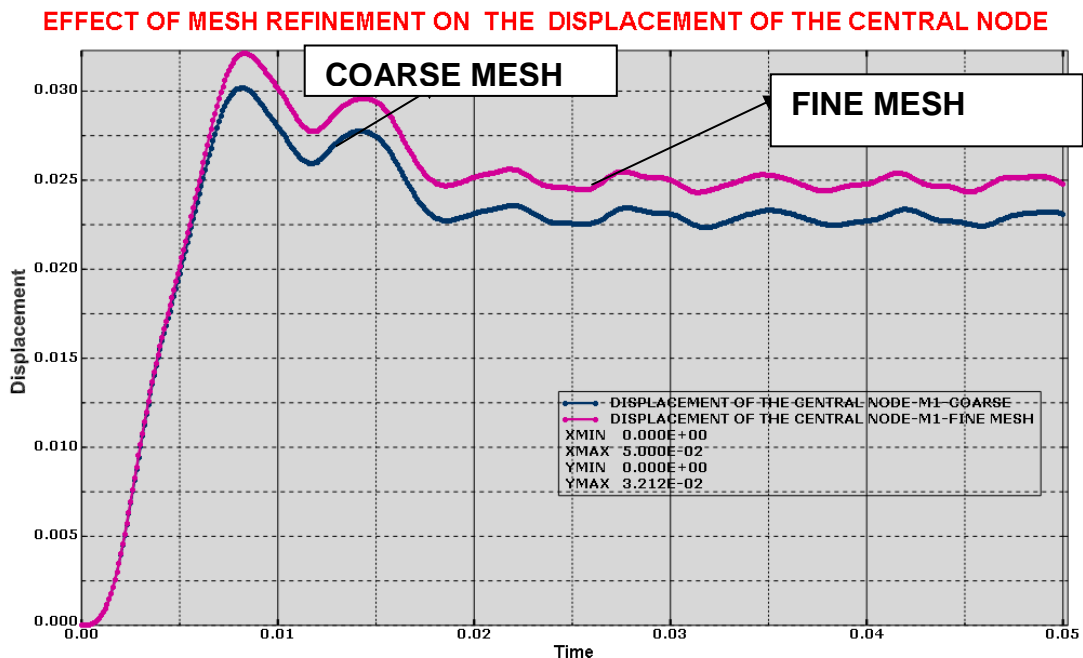


FIGURE 4.4. Showing the effect of mesh refinement on the displacement of the central node when coarse and fine meshes were considered in model 1

Comments: From the above graph in figures 4.4 above, effect of the coarse mesh on the displacement of the central node gave a displacement of the central node of 0.03 however when the mesh is made finer, the displacement of the central node went slightly higher from 0.03 to 0.035. Thus the deduction here is that the finer the mesh, the higher the displacement of the central node and the better is the result obtained from the displacement of the central node. However, the finer mesh while giving a good result of an analysis, it has a singular disadvantage of increasing the elements in a computer analysis. Consequently, computer processing time will be increased depending on the type of analysis.

4.8.2 EFFECT OF MESH REFINEMENT ON DISPLACEMENT OF THE CENTRAL NODE ON MODEL 2

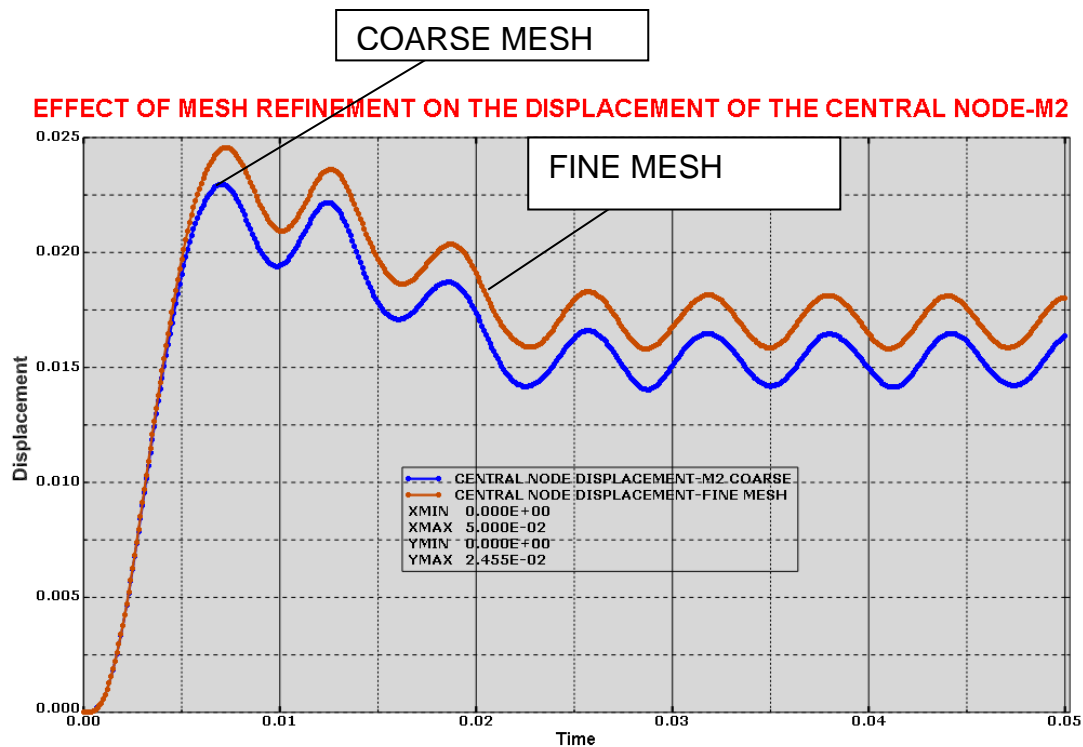


Figure 4.5 Showing the effect of mesh refinement on the displacement of the central node when coarse and fine meshes were considered in model 2

Comments: From the above graph in figures 4.5 above, the effect of the coarse mesh on the displacement of the central node gave a displacement of the central node as slightly above 0.0225 while an improvement on the refinement gave an increase of the value of the displacement of the central node as close to 0.025 in model 2 which is the 2x2 stiffener configuration. Thus again because of the increase in stiffener configuration in model 2, there was a decrease in the displacement of the central node. However, the same argument that the finer the mesh, the higher the value of the displacement of the central node. Also with a finer mesh, a more accurate results would be obtained.

4.8.3 EFFECT OF MESH REFINEMENT ON DISPLACEMENT OF THE CENTRAL NODE ON MODEL 3

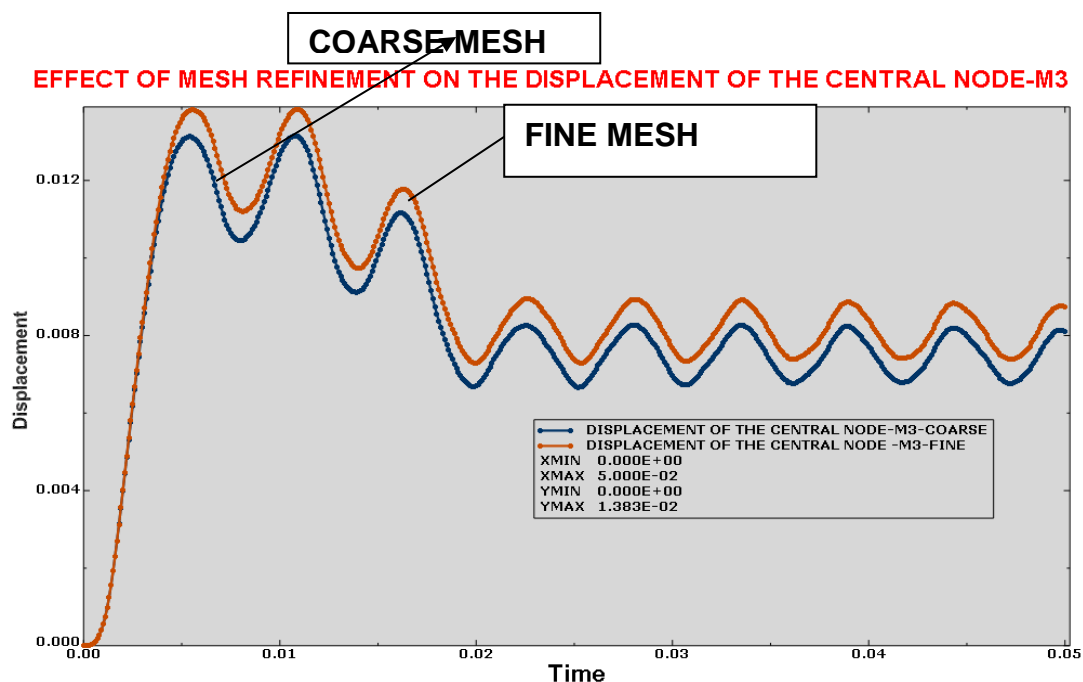


Figure 4.6: Showing the effect of mesh refinement on the displacement of the central node when coarse and fine meshes were considered in model 3.

Comments: From the above graph in figures 4.6, the effect of the coarse mesh on the displacement of the central node gave a displacement of the central node as 0.013 while an improvement on the refinement increased the displacement of the central node value to 0.014 in model 3 which is the 3x3 stiffener configuration. Thus because of the increase in stiffener configuration in model 3, there was a decrease in the displacement of the central node due to increase in stiffness hence the decrease in the value of the displacement of the central node in model 3 as compared with the value of the displacement of the central node in model 1 and model 2 respectively. It can therefore be deduced that the refinement of the mesh would generate a better result and the more stiffened the plate, the less the value of the displacement of the central node and the stronger is the panel.

4.8.4 EFFECT OF MESH REFINEMENT ON THE VALUE OF VON-MISSES STRESSES IN MODEL 1-3

Model1-3

Table 4.4: Showing the effect of mesh refinement on Von –Misses Stresses for Model 1, 2 and 3

MODEL		MESH-SIZE	ELEMENT-NO	VON-MISSES STRESS (PA)	DISPLACEMENT (M)
MODEL1	COARSE	0.075	1084	3.206E+8	3.5E-2
	FINE	0.03	6055	3.235E+8	3.712E-2
MODEL2	COARSE	0.075	1288	2.513E+8	2.02E-2
	FINE	0.03	7010	2.699E+8	2.19E-2
MODEL3	COARSE	0.075	1584	2.353E+8	9.03E-3
	FINE	0.03	8153	2.367E+8	9.753E-3

Comments: From Table 4.4 above, the effect of the coarse mesh on the displacement of the central node in model 1,2 and 3 decreases the Von Mises stresses in a particular model. However, it was observed that in a particular model, the finer the mesh, the higher is the value of the displacement of the central node, the higher is the stress and the more accurate is the overall output of the analysis. Additionally, the more stiffened a plate or panel, the stronger it is. Also, the more stiffened a plate is the less is the value of displacement of the central node and the stronger is component. The introduction of more stiffeners, leads to the decrease in the value of the displacement of central node. Stability of the plate is achieved.

4.8.5 EFFECT OF MESH REFINEMENT ON INTERNAL ENERGY AND PLASTIC DISSIPATION ENERGY OF THE SYSTEM FOR MODEL 1,2 AND 3

Table 4.5: Effect of Mesh refinement on internal energy and plastic dissipation energy of the system.

		Mesh-size	Element-no	Internal energy [j]	Plastic Dissipation energy [j]
MODEL1	COARSE	0.075	1084	5.50E+04	4.05E+04
	FINE	0.03	6055	5.964E+04	4.56E+04
MODEL2	COARSE	0.075	1288	3.26E+4	2.20E+4
	FINE	0.03	7010	3.60E+4	2.71E+4
MODEL3	COARSE	0.075	1584	1.824E+3	1.10E+4
	FINE	0.03	8153	1..525E+3	1.214E+4

Comments: From the above Table 4.5 above, The internal energy and the plastic dissipation energy generated by model 1,2 and 3 are compared. It was observed that the effect of the coarse mesh on the displacement of the central node in model 1 generated an internal energy of 5.5e+4 Joules. However, when the mesh was increased or refined, model 1 generated an internal energy of 5.964E+4 whose value is higher than when the mesh was coarse. The same observation was noted for model 2 and 3. Thus the conclusion here is that the value of the fine mesh is directly proportional to the value of the internal and dissipation energy of the system. The more stiffened a plate is, the less is the displacement of the central node and the stronger is the component or stiffened panel. There is therefore the need for designer to adequately carry more stiffened designs at a lesser weight in order to prevent against terrorism.

**4.8.6: EFFECT OF COARSE MESH ON ENERGY TERMS AS A FUNCTION OF TIME ON [MODEL 1&2]
MODEL 1-COARSE**

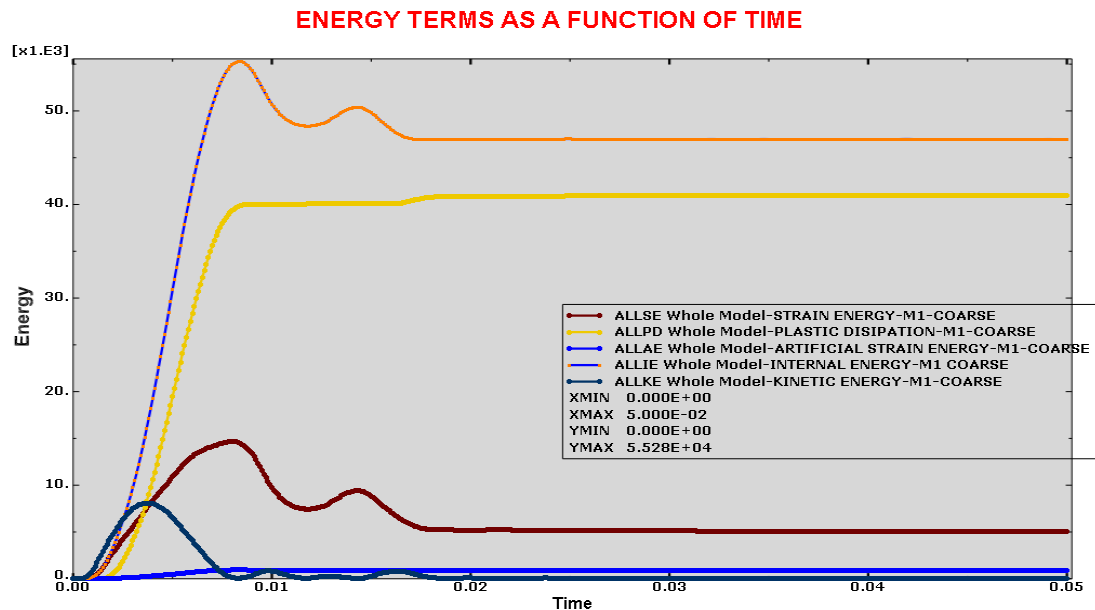


Figure 4.7: Effect of coarse mesh on internal energy and plastic dissipation energy of the system- The coarse mesh has the effect of reducing the internal and plastic dissipation energy of the plate panel

MODEL 1 FINE-MESH

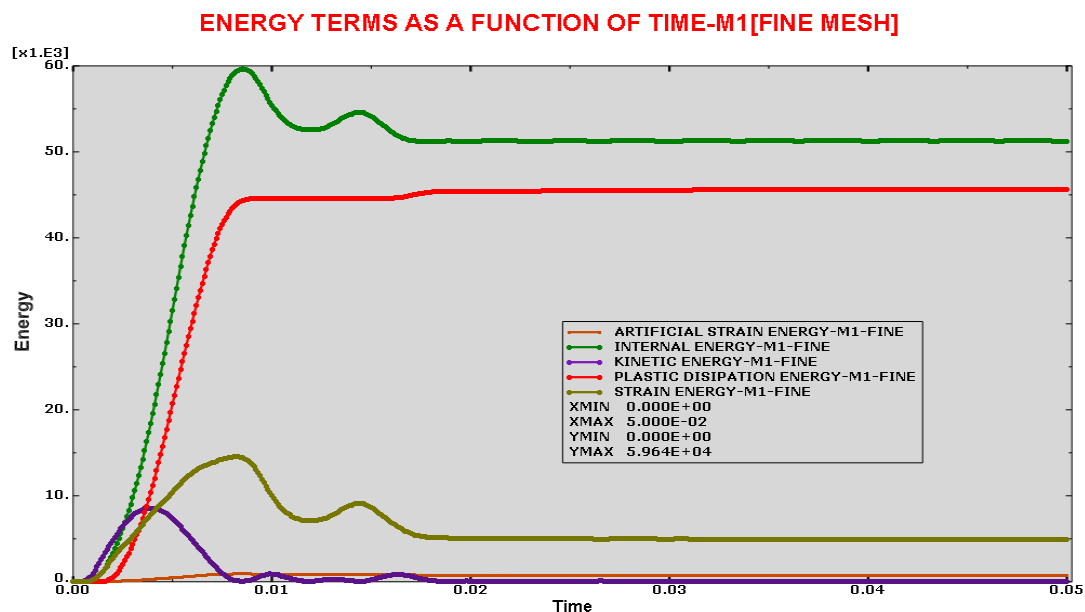


Figure 4.8: Effect of fine mesh on internal energy and plastic dissipation energy of the system-The finer mesh gave rise to a higher internal energy and plastic dissipation energy of the plate panel.

MODEL 2-COARSE

ENERGY TERMS AS A FUNCTION OF TIME[COARSE]

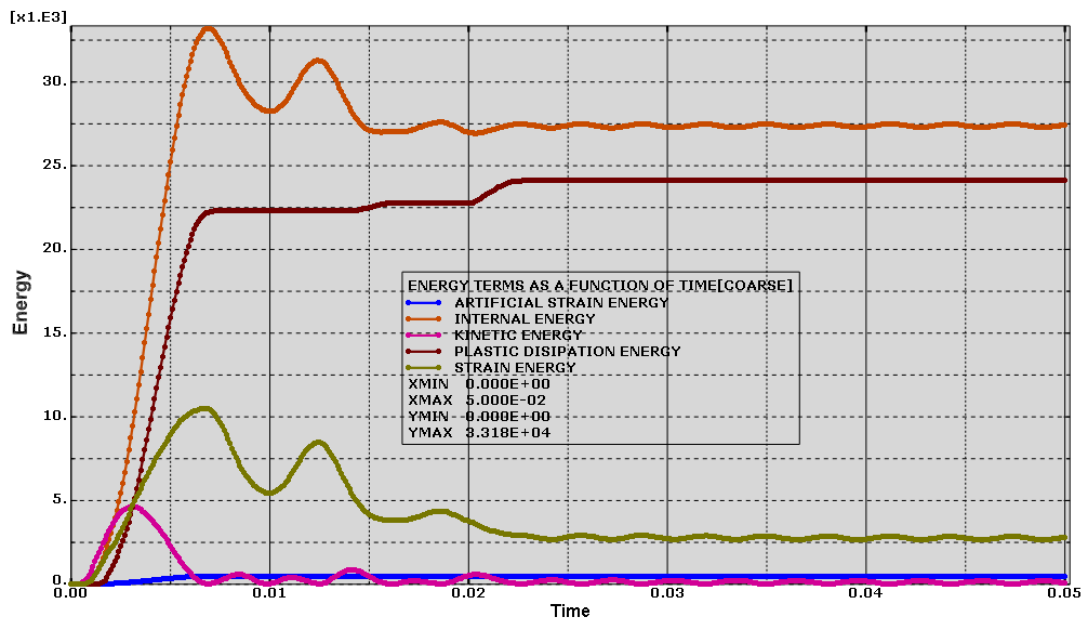


Figure 4.9 Effect of coarse mesh on internal energy and plastic dissipation energy of the system.

MODEL 2-FINE MESH

ENERGY TERMS AS A FUNCTION OF TIME[FINE]

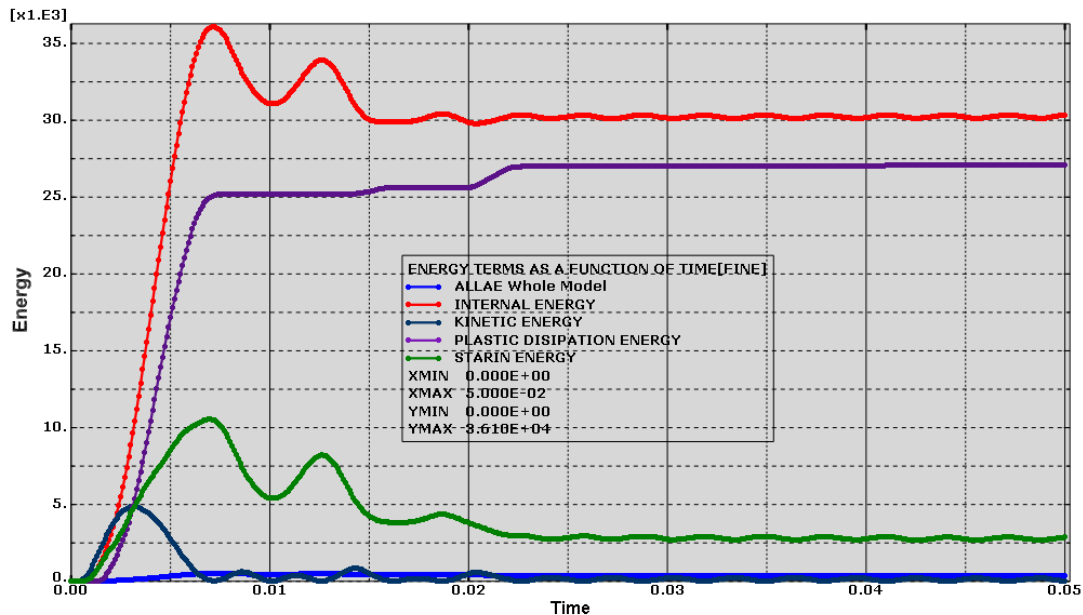


Figure 4.1.1: Showing the effect of fine mesh on internal energy and plastic dissipation energy of the system.

MODEL 3-COARSE

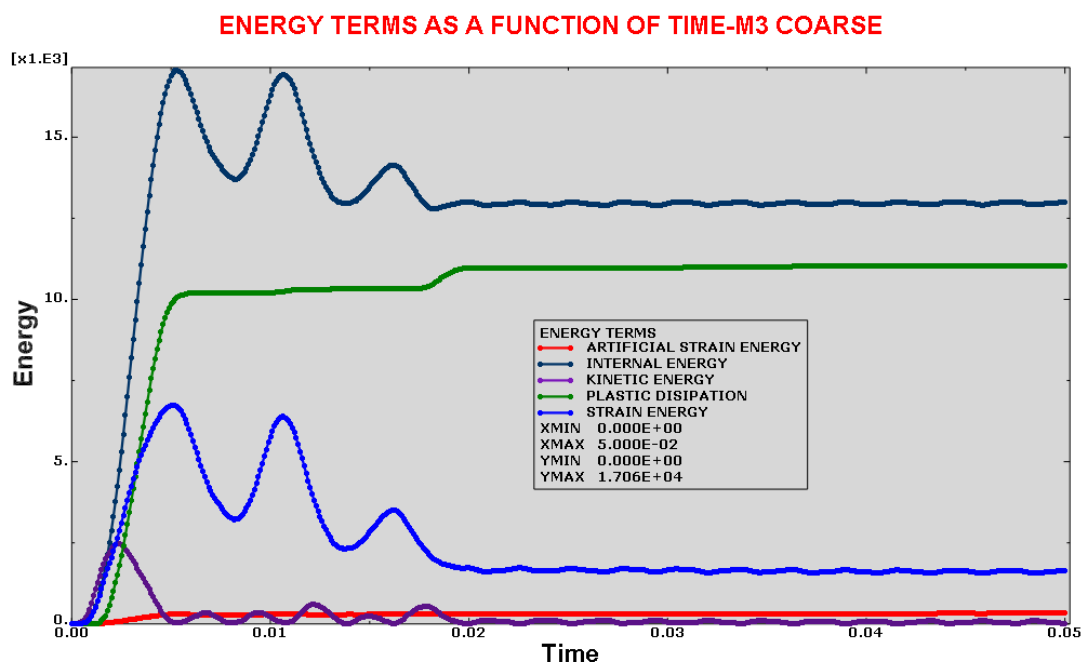


Figure 4.1.2: Effect of coarse mesh on internal energy and plastic dissipation energy of the system.

Comments: The behaviour and the effect of the coarse and fine mesh on the internal energy, plastic dissipation energy, strain energy, artificial strain energy and kinetic energy is demonstrated from the figures 4.7 to 4.1.2 above. Generally, the finer the mesh, the higher is the internal energy of the stiffened plate, the internal energy rise to its maximum and gradually oscillates and fades away while the plastic dissipation energy also increase with increase in the refinement of the mesh, it maintains a steady level for few seconds and slightly increase and fade away as could be seen from figures 4.7-4.1.2.

4.8.7: EFFECT OF MATERIAL DAMPING ON THE DISPLACEMENT OF CENTRAL NODE ON MODEL 1, 2 AND 3

Model 1

EFFECT OF DAMPING ON THE DISPLACEMENT OF THE CENTRAL NODE

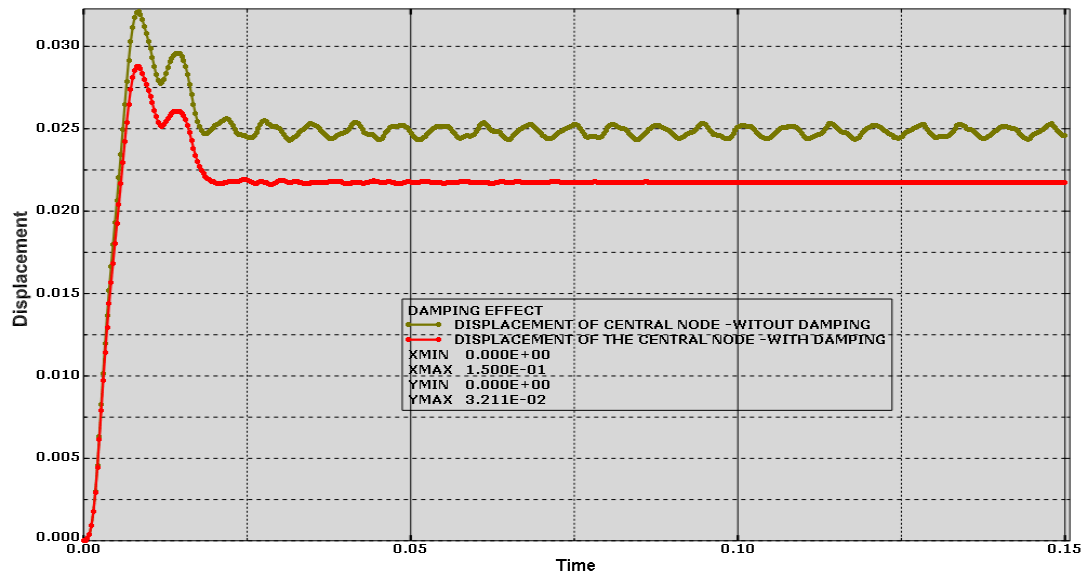


Figure 4.1.3: Showing the effect of Damping on the Displacement of the central node on model 1- Here, Damping effectively reduced the displacement of the central node and thus the vibration is reduced to a barest minimum

Model 2

EFFECT OF DAMPING ON THE DISPLACEMENT OF THE CENTRAL NODE-M2

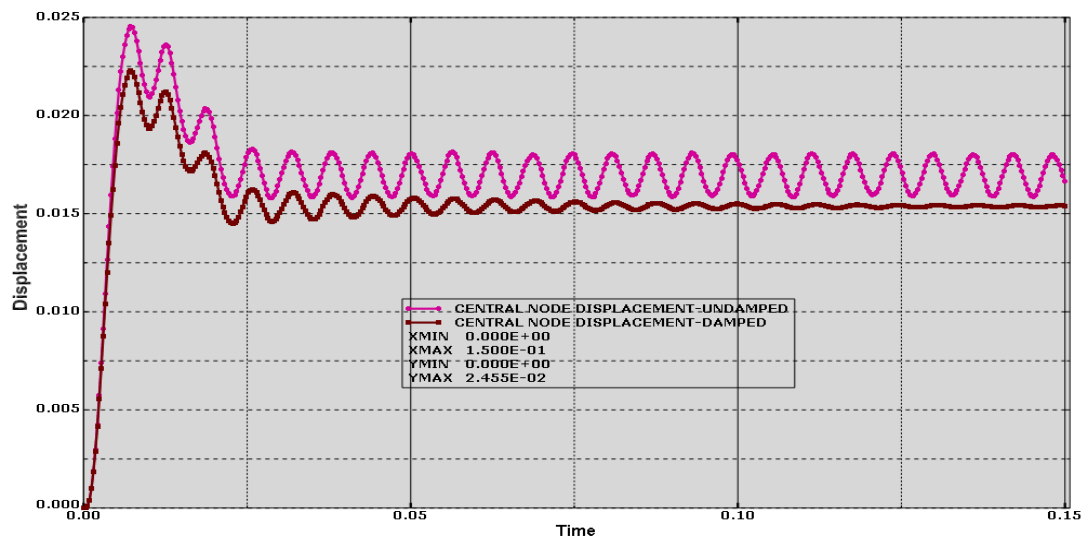


Figure 4.1.4: Showing the effect of Damping on the Displacement of the central node on model 2- also here, Damping effectively reduced the displacement of the central node and vibration automatically reduced.

Model 3

EFFECT OF DAMPING ON THE DISPLACEMENT OF THE CENTRAL NODE

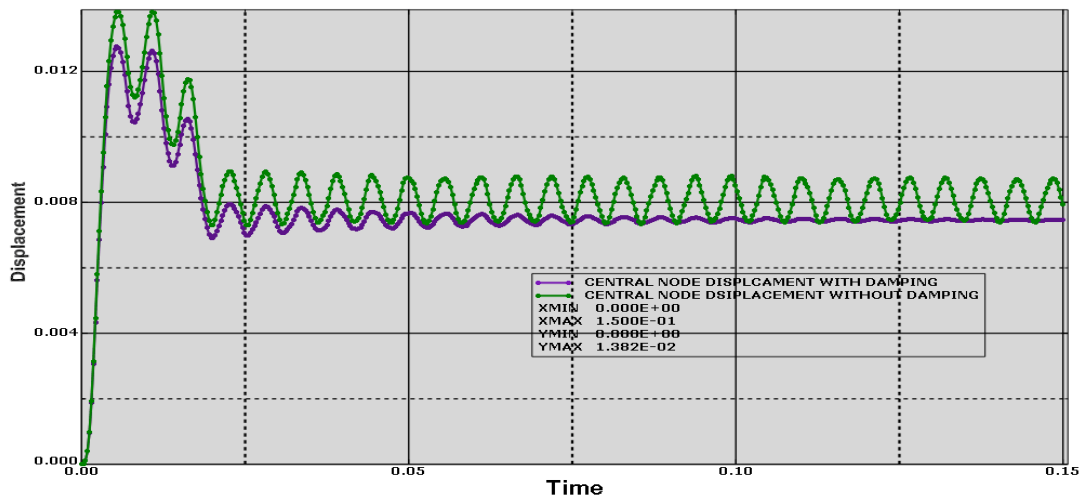


Figure 4.1.5: Effect of Damping on the Displacement of the central node on model 3 showing the effect of Damping on the Displacement of the central node on model 3- Damping effectively reduced the displacement of the central node and vibration automatically reduced.

4.8.5: EFFECT OF MATERIAL DAMPING ON INTERNAL ENERGY OF THE SYSTEM [MODEL 1, 2 AND 3]

MODEL 1

EFFECT OF DAMPING ON INTERNAL ENERGY -M1

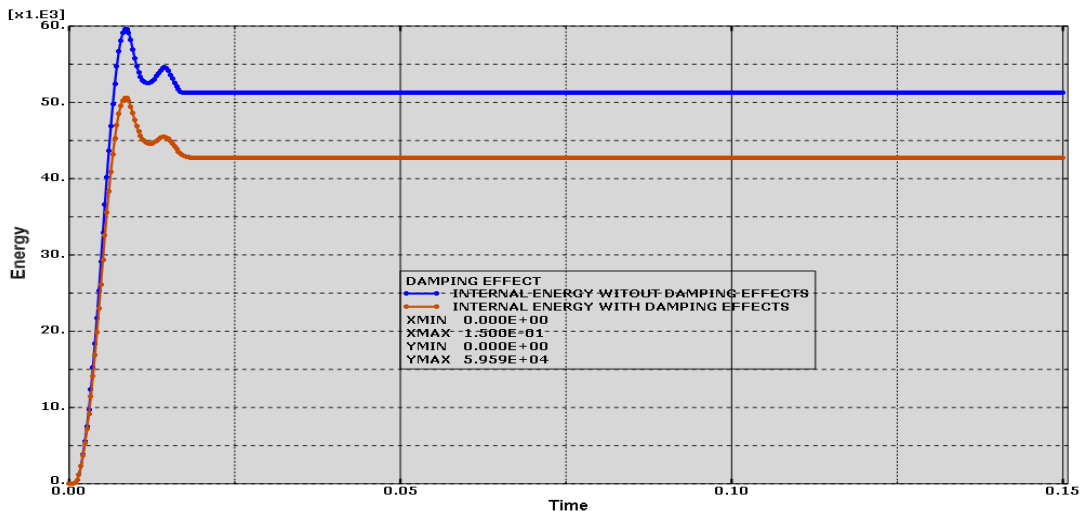


Figure 4.1.6: Effect of material damping on internal energy of the system for model 1. Because Damping was included in the modelling in Abaqus, the internal energy is seen to reduce as compared to when there is no damping as seen in the graph above (Figure 4.1.6).The value of the internal energy when there is no damping is about 60kilo joules. However when Damping value was included into the system, the value of the internal energy decreased from 60 kilo joules to 50 kilo joules.Consequently,it is concluded that the inclusion of the damping effect reduced the internal energy of the system by 10kilo joules.

MODEL 2

EFFECT OF DAMPING ON THE INTERNAL ENERGY -M2

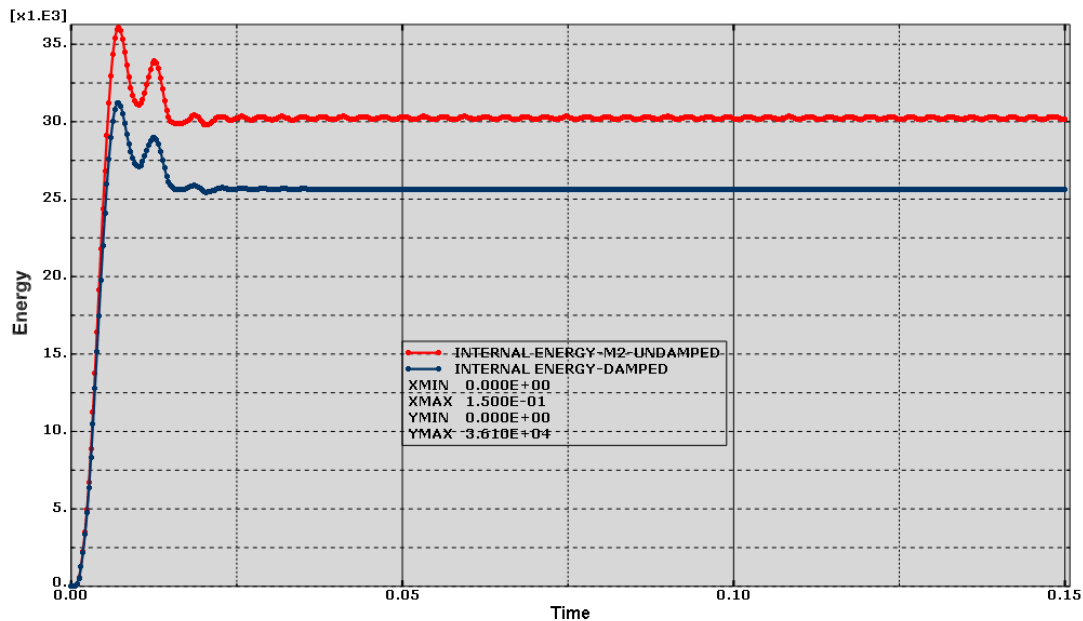


Figure 4.1.7: Showing the effect of material damping on internal energy of the system for **model 2**, first it reduces the internal energy and secondly, it damped away vibration as seen in figures 4.1.7. Here, the inclusion of the damping factor reduces the internal energy of the system from 36.5 kilo joules to 31.5 kilo joules.

MODEL 3

EFFECT OF DAMPING ON THE INTERNAL ENERGY

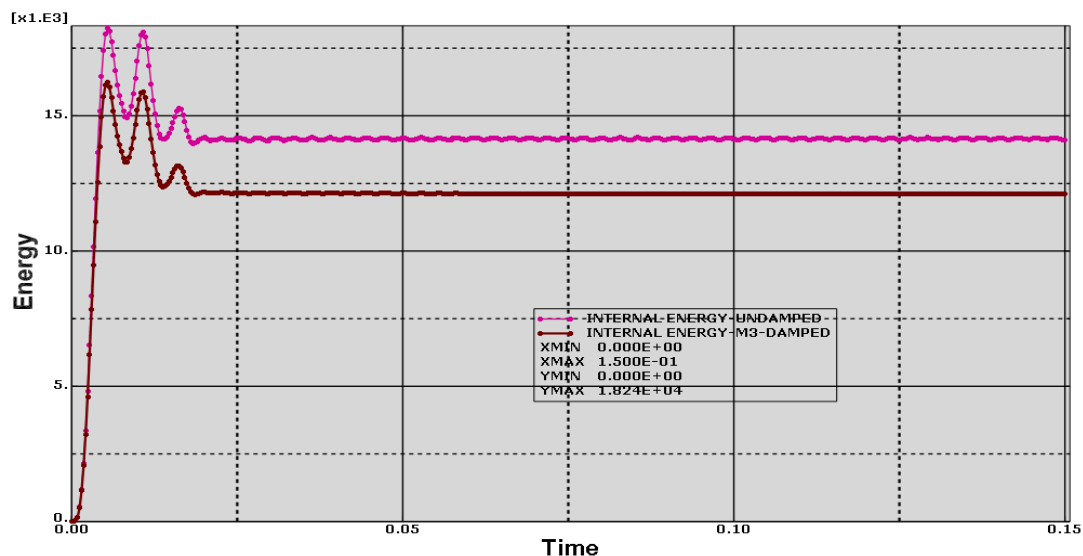


Figure 4.1.8: Showing the effect of material damping on internal energy of the system for **model 3**, first it reduces the internal energy from 18.75E+3 to 16.25E+3 joules then damped out away vibration as seen in figures 4.1.8 above. The inclusion of damping factor in the analysis has played a vital role important role. Thus, the internal energy used by the system has been reduced.

4.9 EFFECT OF DAMPING ON THE ARTIFICIAL ENERGY OF THE SYSTEM

MODEL 1

EFFECT OF DAMPING ON ARTIFICIAL STRAIN ENERGY -M1

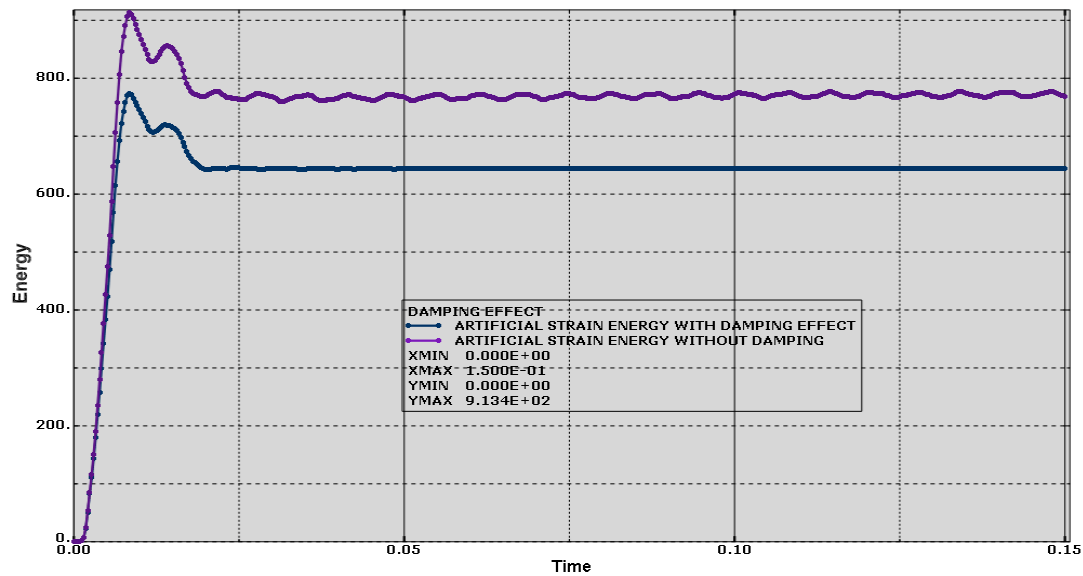


Figure 4.1.9: Showing the effect of material damping on artificial energy of the system for **model 1**, first it reduces the artificial energy from 920 joules to 780 joules and then damped away vibration as seen in figure 4.1.9 above.

MODEL 2

EFFECT OF DAMPING ON THE ARTIFICIAL STRAIN ENERGY -M2

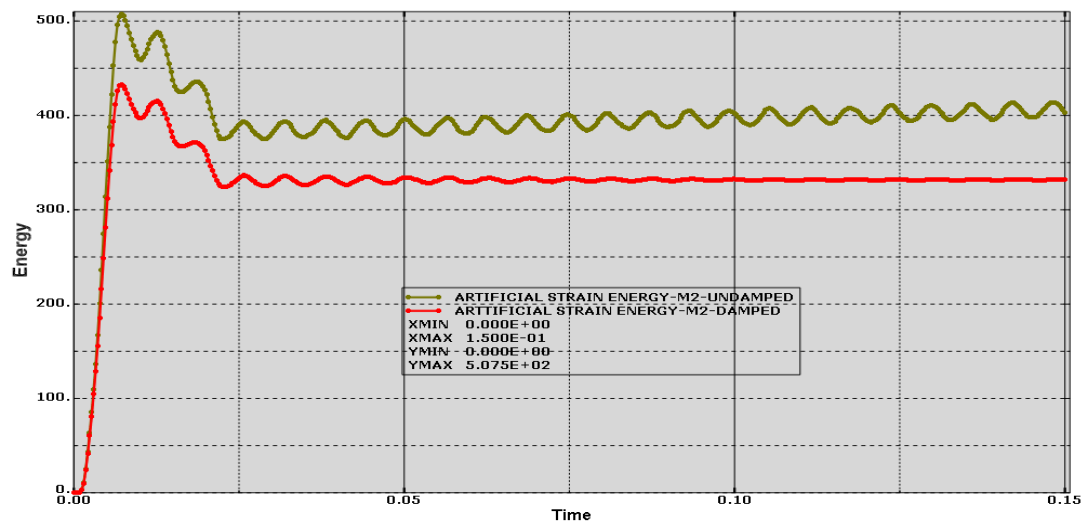


Figure 4.2.1 Showing the effect of material damping on artificial energy of the system for **model 2**, first it reduces the artificial energy from 525 joules to 430 joules in model 2 and damped away vibration as seen in figure 4.2.1 above. Generally, the introduction of damping has also reduced the amount of artificial energy generated by the system.

MODEL3

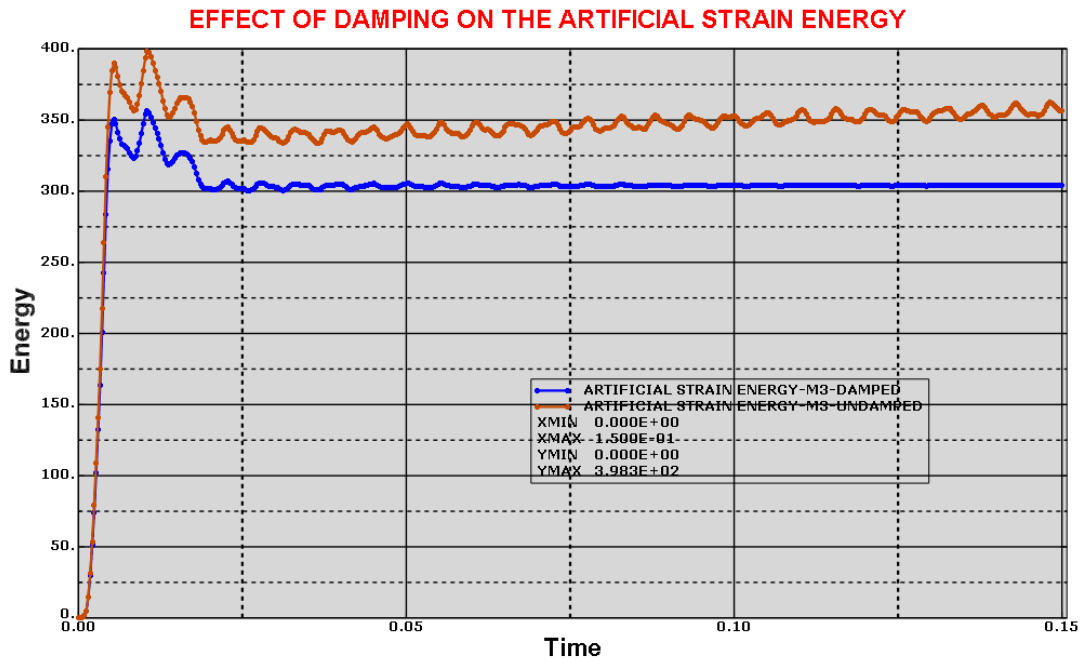


Figure 4.2.2 Showing the effect of material damping on artificial energy of the system for **model 3**, first it reduces the artificial energy and damped away vibration as seen in figure 4.2.2 above. Remarkably, the effect of damping on artificial energy of the system for model has also reduced the artificial energy in the system and damped away vibration.

4.8.7 EFFECT OF DAMPING ON PLASTIC DISSIPATION ENERGY OF THE SYSTEM

MODEL1

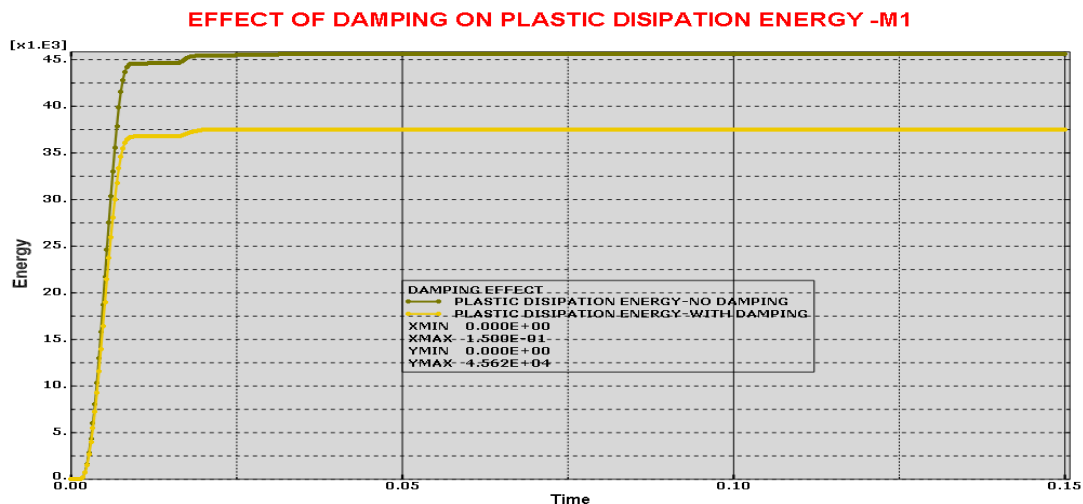


Figure 4.2.3: Showing the effect of material damping on Plastic dissipation energy of the system for model 1. Damping remarkably reduces the plastic dissipation energy of model 2 from about 47.5E+3 Joules to 37.5E+3 Joules. This has been reduced drastically by 10 kilo joules.

MODEL 2

EFFECT OF DAMPING ON THE PLASTIC DISSIPATION ENERGY -M2-DAMPED

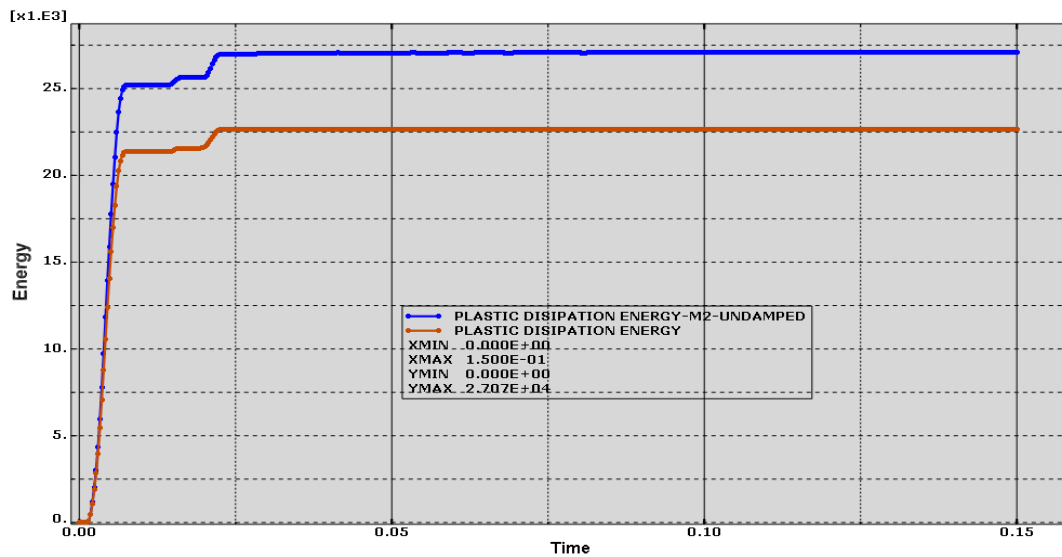


FIGURE 4.2.4 Showing the effect of material damping on Plastic dissipation energy of the system for model 2. Damping remarkably reduces the plastic dissipation energy of model 2 from about 27.5E+3 Joules to 22.0E+3 Joules. Here, the inclusion of damping has also reduced the plastic dissipation energy by about 5.5 kilo joules.

MODEL3

EFFECT OF DAMPING ON THE PLASTIC DISSIPATION ENERGY

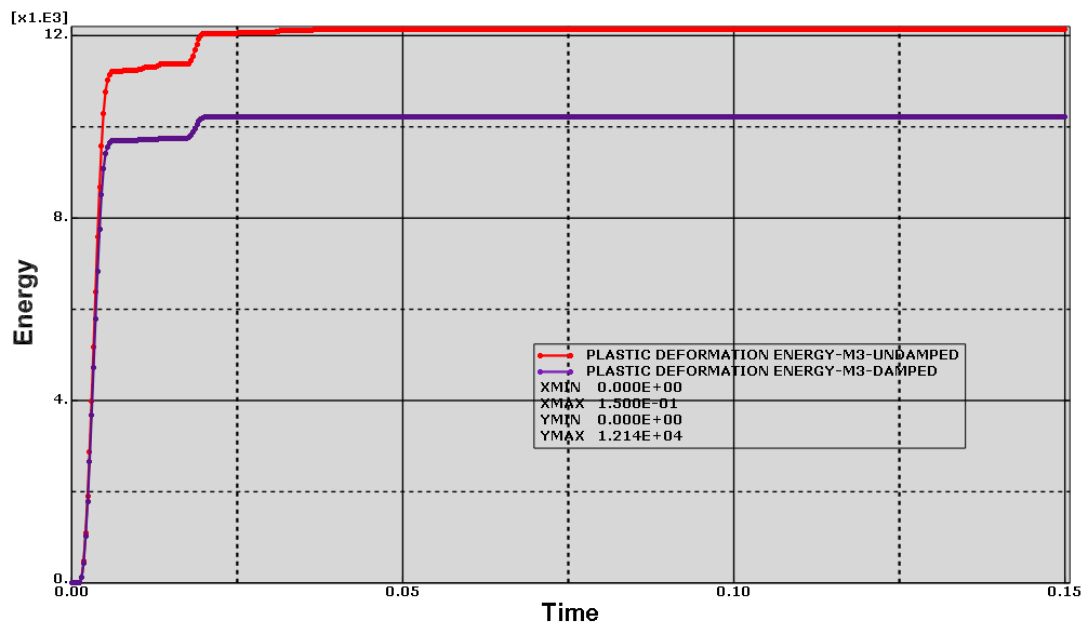


FIGURE 4.2.5 Showing the effect of material damping on Plastic dissipation energy of the system for model 3. Damping remarkably reduces the plastic dissipation energy of model 3 from about 12E+3 Joules to 10.0E+3. This is about 2 kilojoules.

4.10 EFFECT OF RATE DEPENDENCE ON CENTRAL NODE ON MODEL 1, 2 AND 3

MODEL1

EFFECT OF RATE DEPENDENCE ON THE DISPLACEMENT OF THE CENTRAL NODE-M1

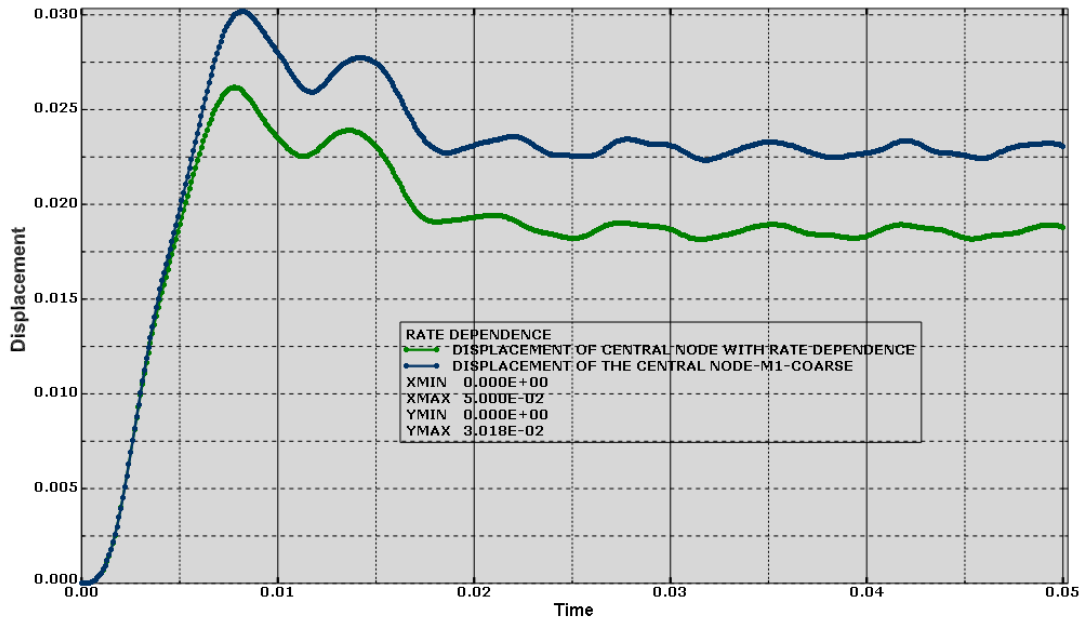


FIGURE 4.2.6 Showing the effect of rate dependence on the displacement of the central node for model 1. It reduces the displacement of the central node from about 0.03m to about 0.026m. The inclusion of rate dependence in the ABAQUS code has reduced the value of the displacement of the central node from 0.03m to 0.026m in model 1.

MODEL2

EFFECT OF RATE DEPENDENCE ON THE DISPLACEMENT OF THE CENTRAL NODE-M2

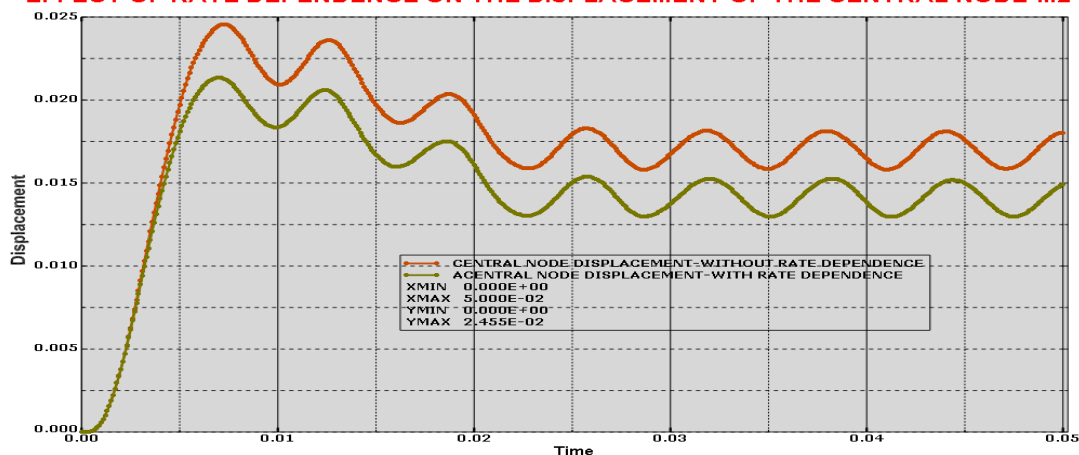


FIGURE 4.2.7 Showing the effect of rate dependence on the displacement of the central node for model 2. It reduces the displacement of the central node from about 0.025m to about 0.023m as seen on figure 4.2.7 above. In mode 2, the effect of the inclusion of rate dependency factor has also reduced the value of the displacement of the central node. The

deduction here is that the completion time for this experiment is reduced due to inclusion of rate dependency constant.

MODEL3

EFFECT OF RATE DEPENDENCE ON THE DISPLACEMENT OF THE CENTRAL NODE-M3

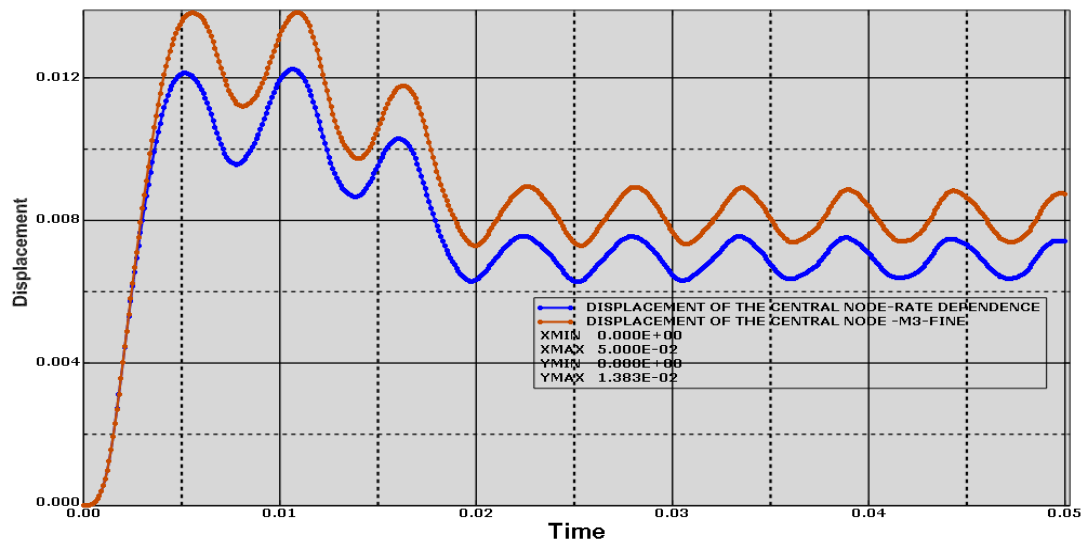


FIGURE 4.2.8 Showing the effect of rate dependence on the displacement of the central node for model 3. It reduces the displacement of the central node from about 0.012m to about 0.014m as seen on figure 4.2.8 above. In model 3 also, the effect of the rate dependency

4.10.1 - EFFECT OF RATE DEPENDENCE ON ARTIFICIAL STRAIN ENERGY-MODEL [1-3]

MODEL1

EFFECT OF RATE DEPENDENCE ON ARTIFICIAL STRAIN ENERGY

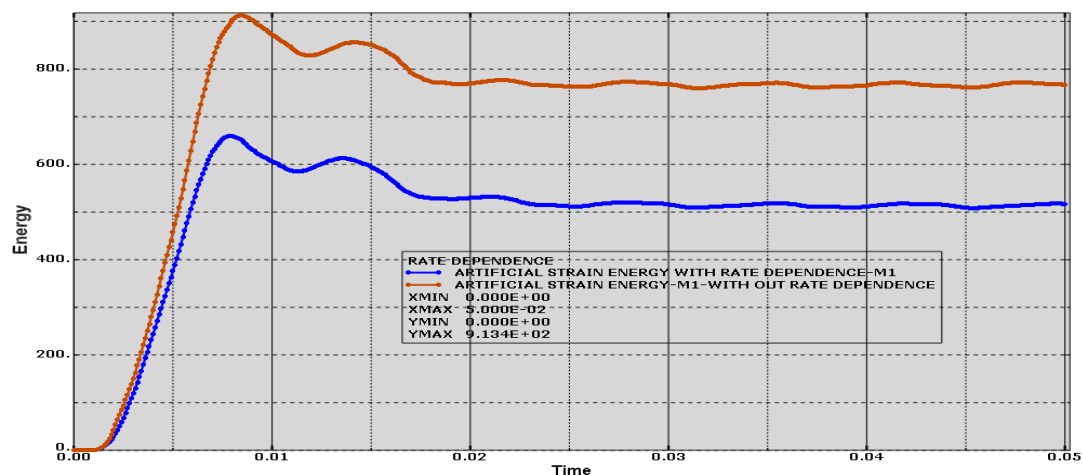


FIGURE 4.2.9 Effect of material damping on Artificial Strain dissipation energy of the system for model 1. The effect of rate dependence on artificial strain energy reduces the artificial strain energy for model 1 from about 900 Joules to about 650 Joules.

MODEL 2

EFFECT OF RATE DEPENDENCE ON THE ARTIFICIAL STRAIN ENERGY-M2

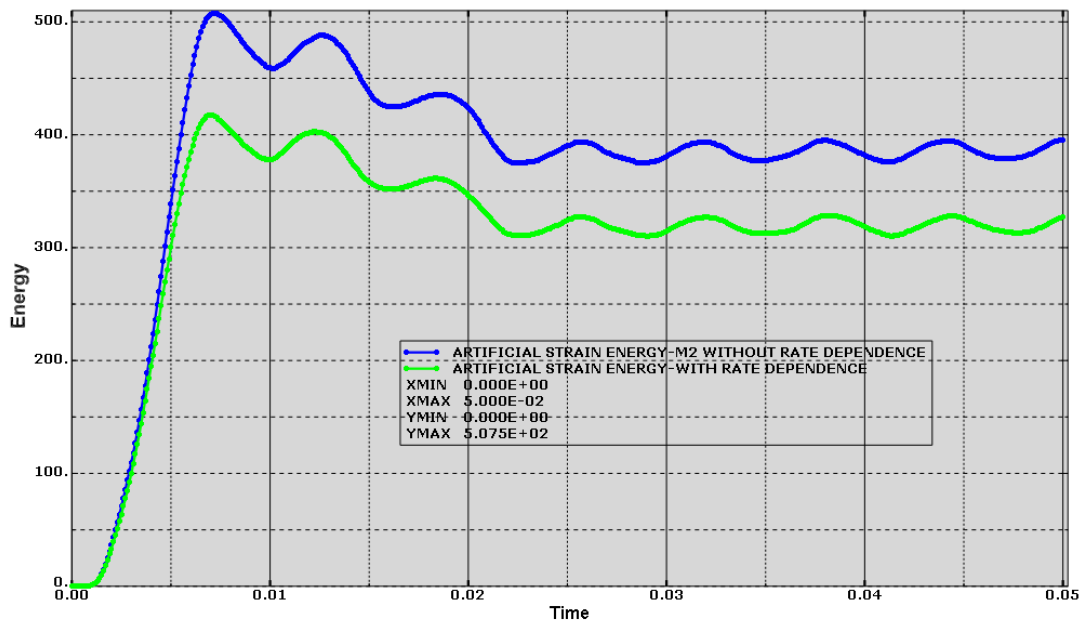


FIGURE 4.3.1 Effect of material damping on Artificial Strain dissipation energy of the system for model 2. The effect of rate dependence on artificial strain energy reduces the artificial strain energy for model 2 from about 525 Joules to about 425 Joules.

MODEL 3

EFFECT OF RATE DEPENDENCE ON THE ARTIFICIAL STRAIN ENERGY-M3

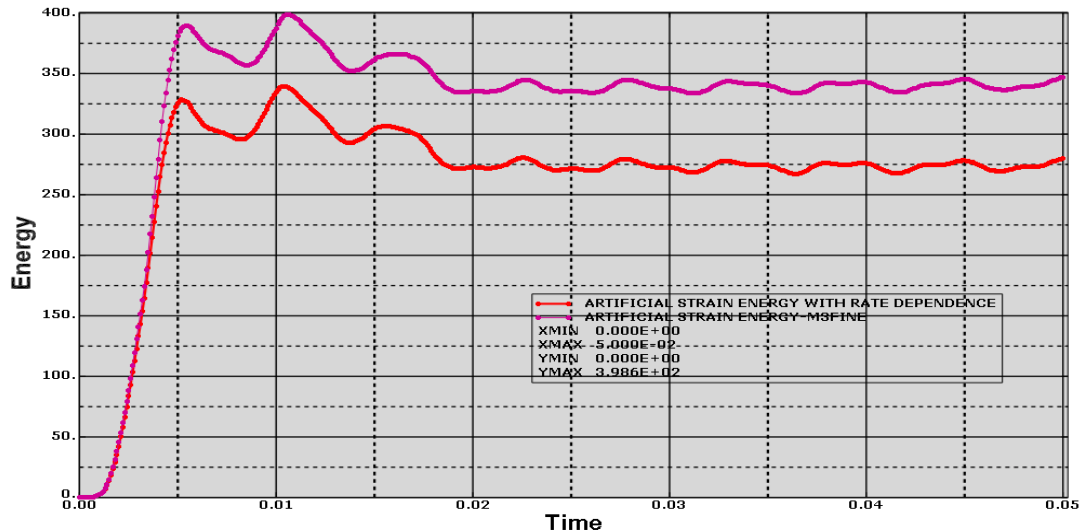


FIGURE 4.3.2 Effect of material damping on Artificial Strain dissipation energy of the system for model 3. It reduces the artificial strain energy of the system appreciably. Here, in model the effect of material damping has reduced the artificial strain energy from 400 joules to 325 joules.

4.10.2 EFFECT OF RATE DEPENDENCE ON THE INTERNAL ENERGY MODEL 1-3

MODEL 1

EFFECT OF RATE DEPENDENCE ON THE INTERNAL ENERGY-M1

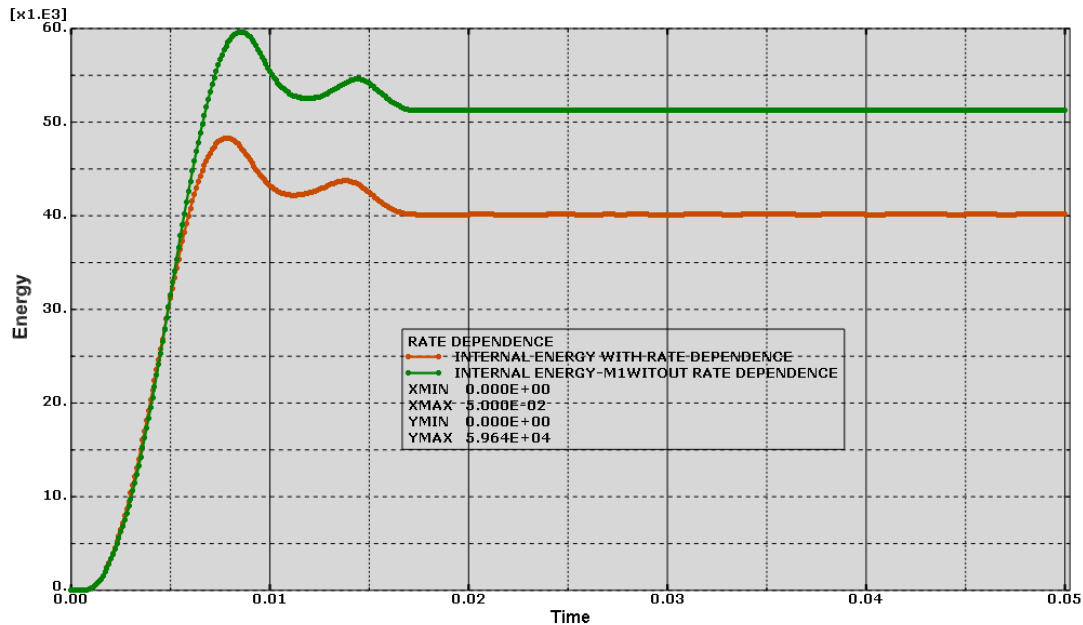


FIGURE 4.3.3 Showing the effect of material damping on Internal Energy of the system for model 1. With the inclusion of the rate dependence, the internal energy for model 1 reduced considerably. Here in model 1, the inclusions of material damping in the abaqus code during the analysis the internal energy of the system as 47 kilo joules. However, without the inclusion of the material damping constant, a very high energy of about 60kilo joules is generated.

MODEL2

EFFECT OF RATE DEPENDENCE ON THE INTERNAL ENERGY -M2

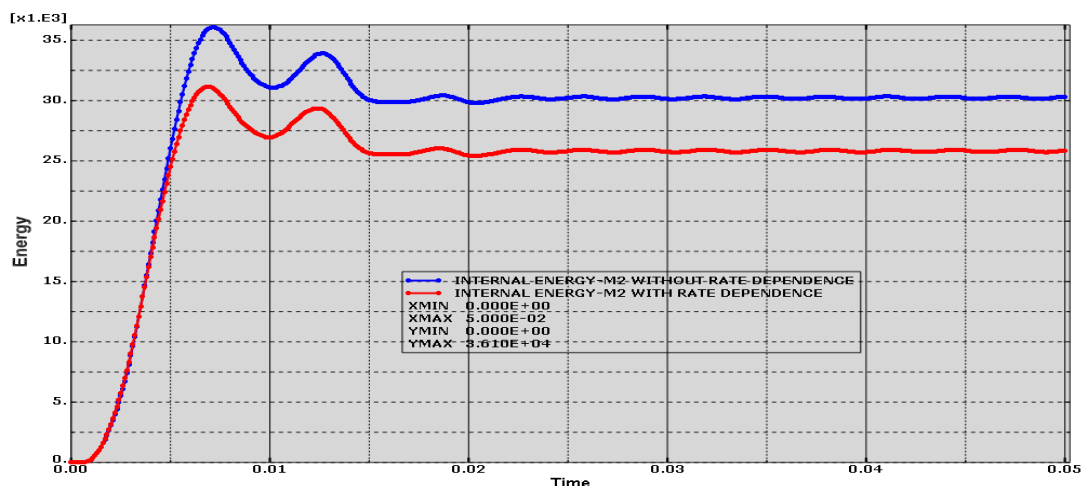


FIGURE 4.3.4 Showing the effect of material damping on Internal Energy of the system for model 2. With the inclusion of the rate dependence, the internal energy for model 2 reduced appreciably.

MODEL3

EFFECT OF RATE DEPENDENCE ON THE INTERNAL ENERGY-M3

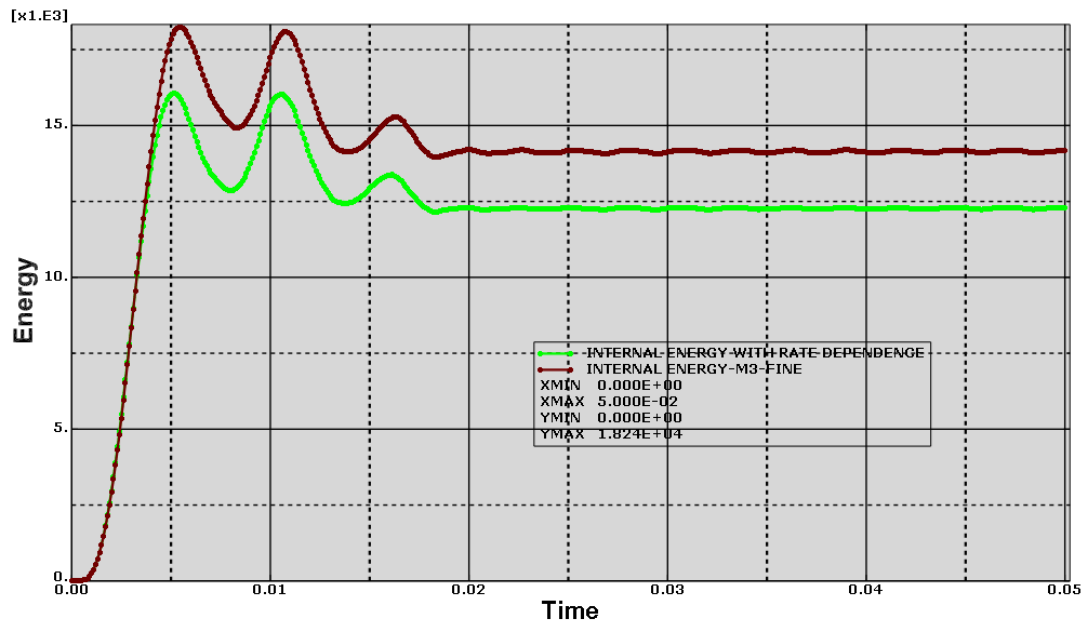


FIGURE 4.3.5 showing the effect of material damping on Internal Energy of the system for model 3. With the inclusion of the rate dependence, the internal energy for model 3 reduced appreciably.

4.10.3 EFFECT OF RATE DEPENDENCE ON THE PLASTIC DISSIPATION ENERGY MODEL [1, 2 AND 3]

MODEL 1

EFFECT OF RATE DEPENDENCE ON THE PLASTIC DISSIPATION ENERGY-M1

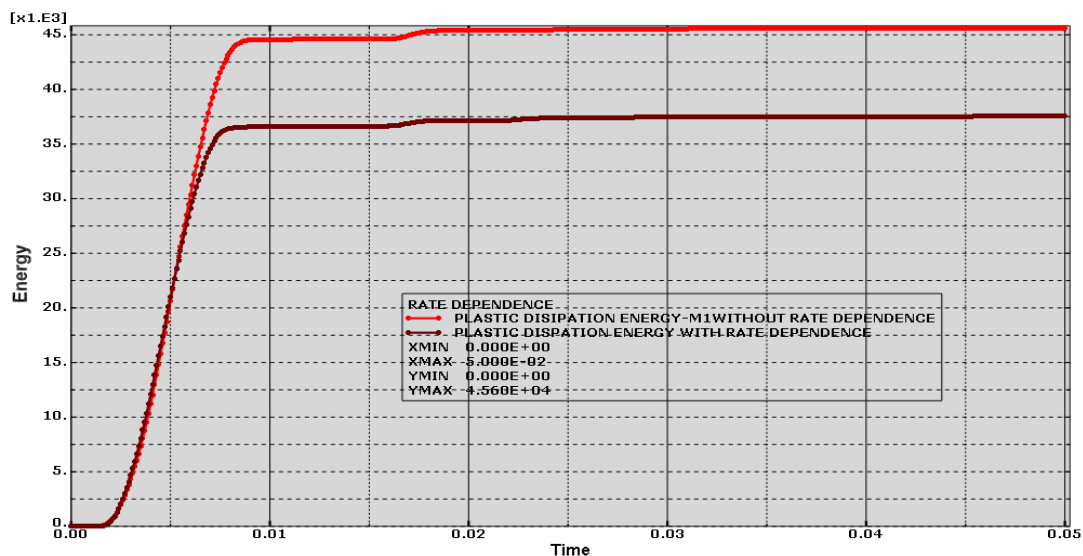


FIGURE 4.3.6 Showing the effect rate dependence on the plastic dissipation energy model 1. The plastic dissipation energy is reduced due to the inclusion of rate dependence factor in the analysis.

MODEL 2

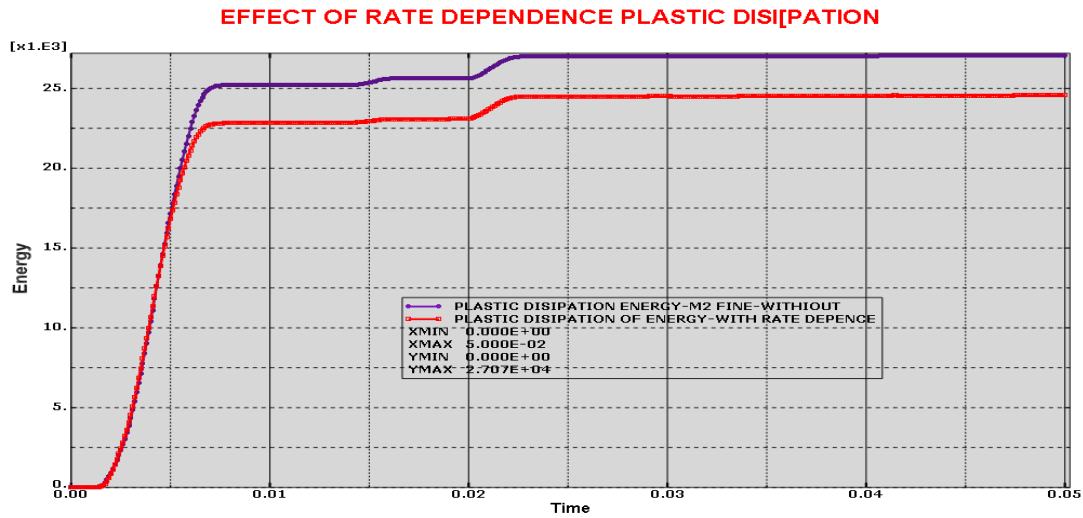


FIGURE 4.3.6 Showing the effect rate dependence on the plastic dissipation energy model 2. The plastic dissipation energy is reduced due to the inclusion of rate dependence factor in the analysis.

MODEL 3

EFFECT OF RATE DEPENDENCE ON THE PLASTIC DISSIPATION ENERGY-M3 ENERGY-M3

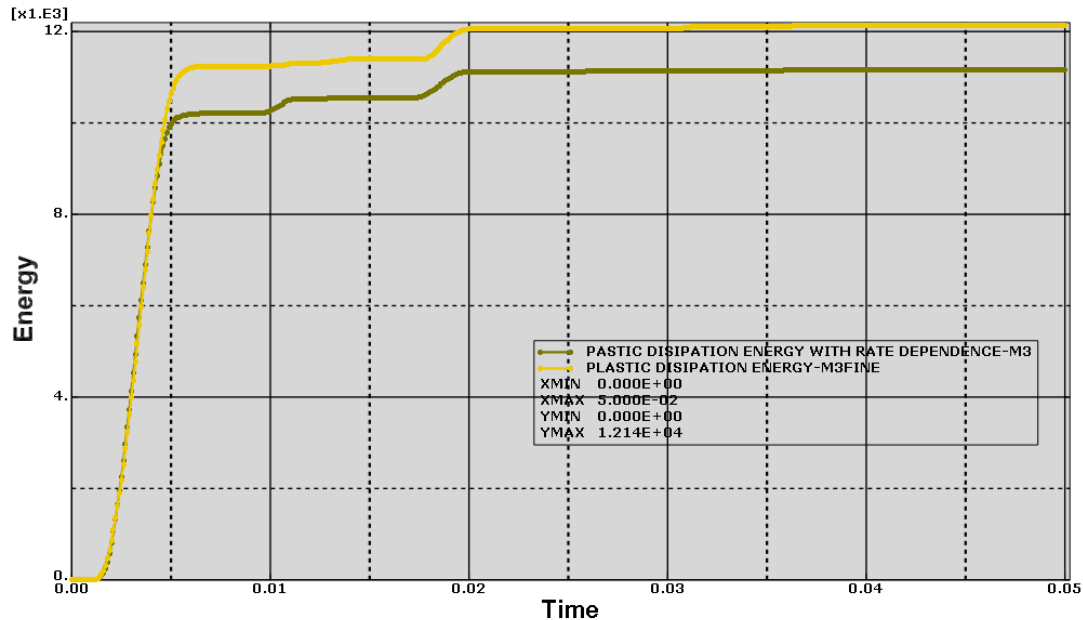


FIGURE 4.3.7: Showing the effect rate dependence on the plastic dissipation energy model 3. The plastic dissipation energy is reduced due to the inclusion of rate dependence factor in the analysis.

4.10.4 -EFFECT OF RATE DEPENDENCE ON STRAIN ENERGY- MODEL 1, 2 AND 3

MODEL1

EFFECT OF RATE DEPENDENCE ON THE STRAIN ENERGY-M1

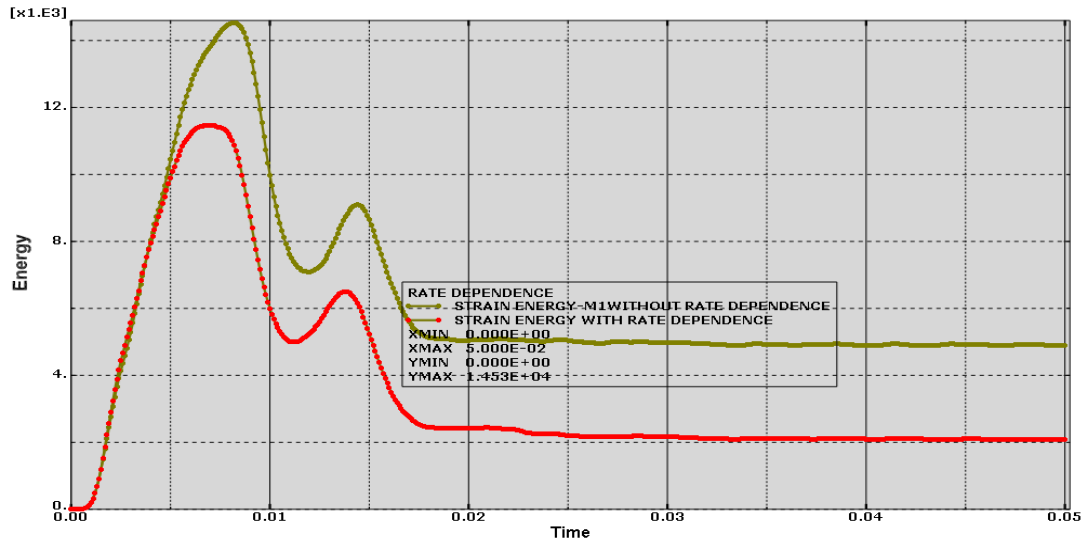


FIGURE 4.3.8. Showing the effect of material damping on Strain Energy of the system for model 1. The strain energy is reduced due to the inclusion of the rate dependence.

MODEL2

EFFECT OF RATE OF DEPENDENCE STRAIN ENERGY

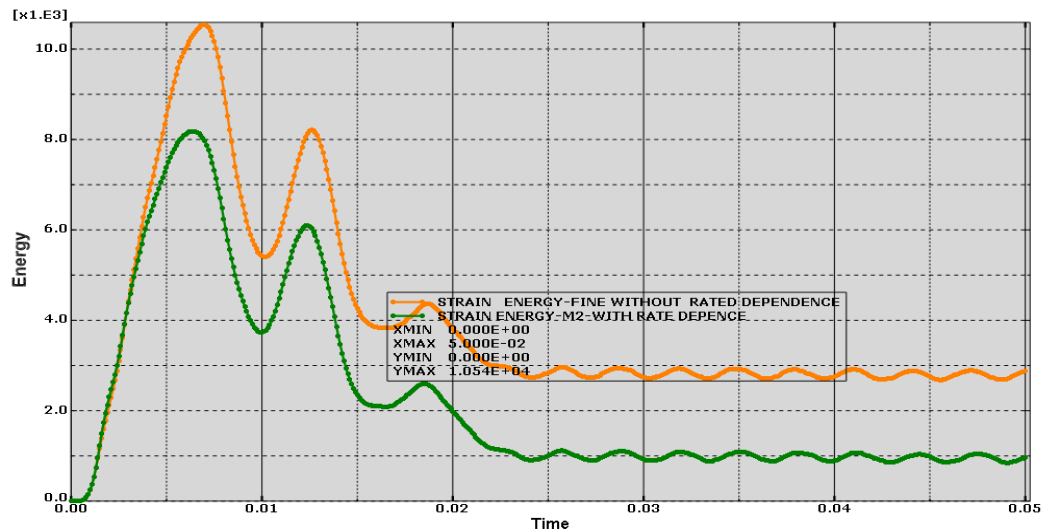


FIGURE 4.3.9 Showing the effect of material damping on Strain Energy of the system for model 2. The strain energy is reduced due to the inclusion of the rate dependence.

MODEL3

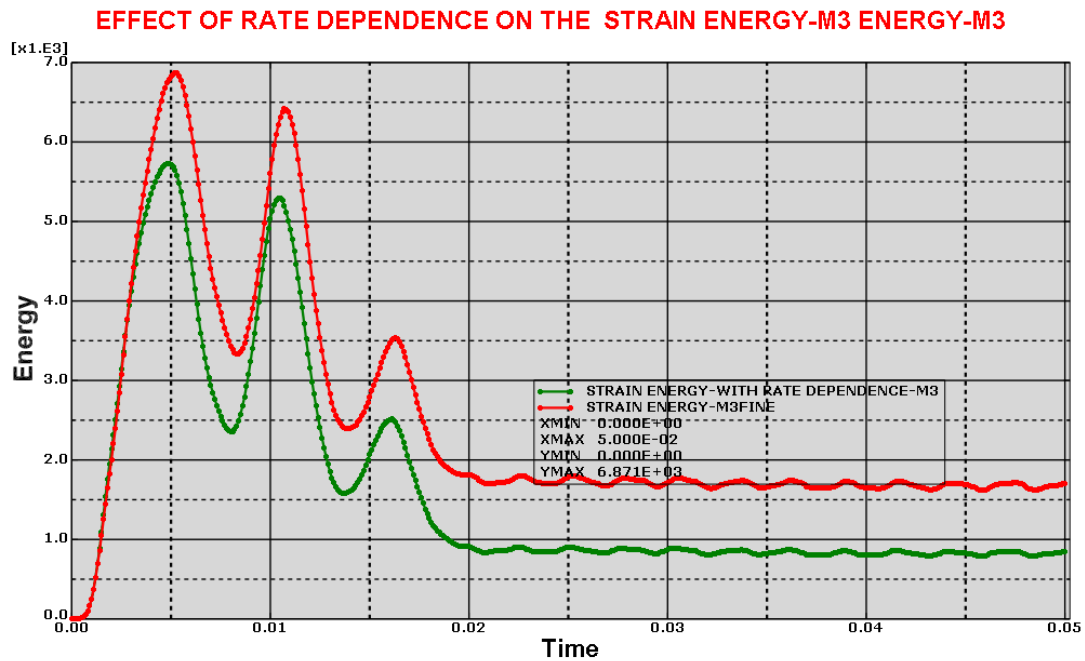


FIGURE 4.4.1 Showing the effect of material damping on Strain Energy of the system for model 3. The strain energy is reduced due to the inclusion of the rate dependence.

Summary of the effects of Rate Dependence on all the Energy terms

Table 4.6: Showing the effect of rate dependence on all the energy given terms.

		Artificial Strain energy [J]	Internal energy [J]	Plastic dissipation energy [J]	Strain energy [J]	Displacement [M]
MODEL1	With rate dependence	6.2E2	4.65E4	3.750E4	0.95E4	2.6E-2
	Without rate dependence	9.13E2	5.964E4	4.5682E4	1.45E4	3.018E-2
MODEL2	With rate dependence	4.05E2	3.20E4	2.495E4	0.81E4	2.10E-2
	Without rate dependence	5.075E2	3.610E4	2.707E4	1.054E4	2.455E-2
MODEL3	With rate dependence	3.25E2	1.650E4	1.10E4	5.81E3	1.20E-2
	Without rate dependence	3.986E2	1.824E4	1.214E4	6.871E3	1.383E-2

Comment: From the table 4.6, it could be seen that the inclusion of the rate dependence factor into the analysis lowered all the values of all the energy given terms including the value of the displacement of the central node for model 1, 2 and 3 while the non-inclusion of the rate dependence in model 1, 2 and 3 indicated an increase in the values of all the energy given terms. It was also established that the energy given terms with inclusion of the rate of dependence decreases with an increase in the number of stiffeners. Also the value of the displacement of the central node decreases with the increase in the number of stiffeners.

4.11 COMPARISON OF THE DISPLACEMENT HISTORIES MODEL 1-3

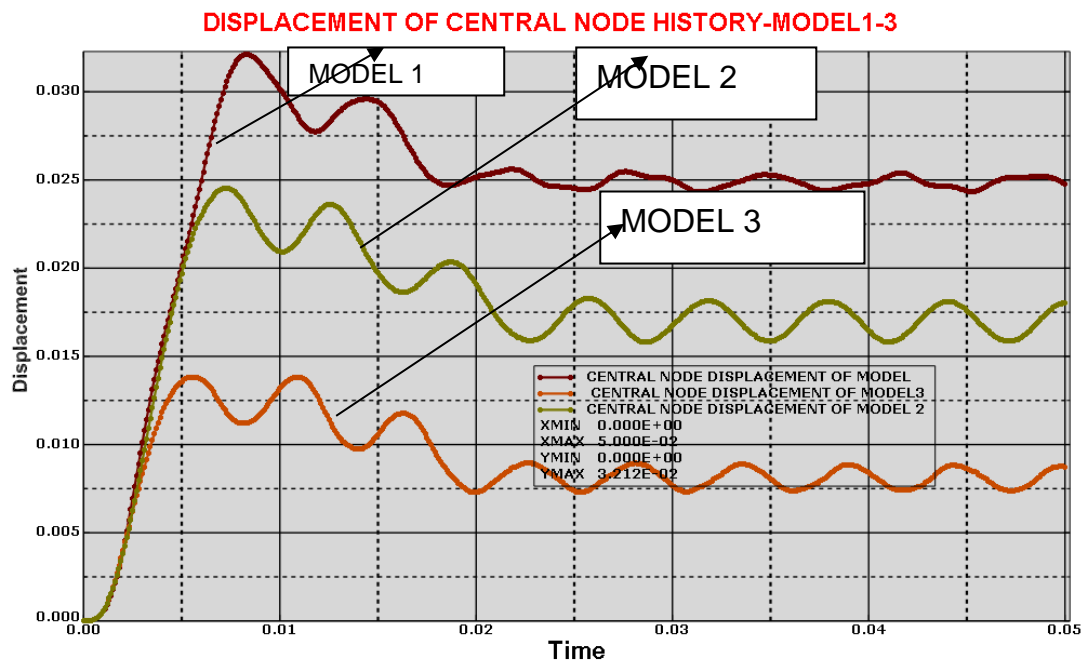


FIGURE 4.7.3 Comparison of the Displacement History of the central node for Model 1, 2 and 3.

Comment: Comparing the displacement of the central for models 1,2 and 3,in figure 4.7.3 above, it could be seen from the graph that the values for the displacement of the central nodes decreases with additional stiffeners thus in this case, model 3 has the highest number of stiffeners and hence the lowest value of the displacement of the central node followed closely by model 2 (2x2 stiffeners) and the highest values of the displacement of the central node is recorded in model 1 with (1 x 1).The deduction here is that with more stiffeners, the value of the displacement of the central node decreases and the more stiffened is the structure. Thus, model 3 is more stiffened, stronger, lowest value of the displacement of the central node.

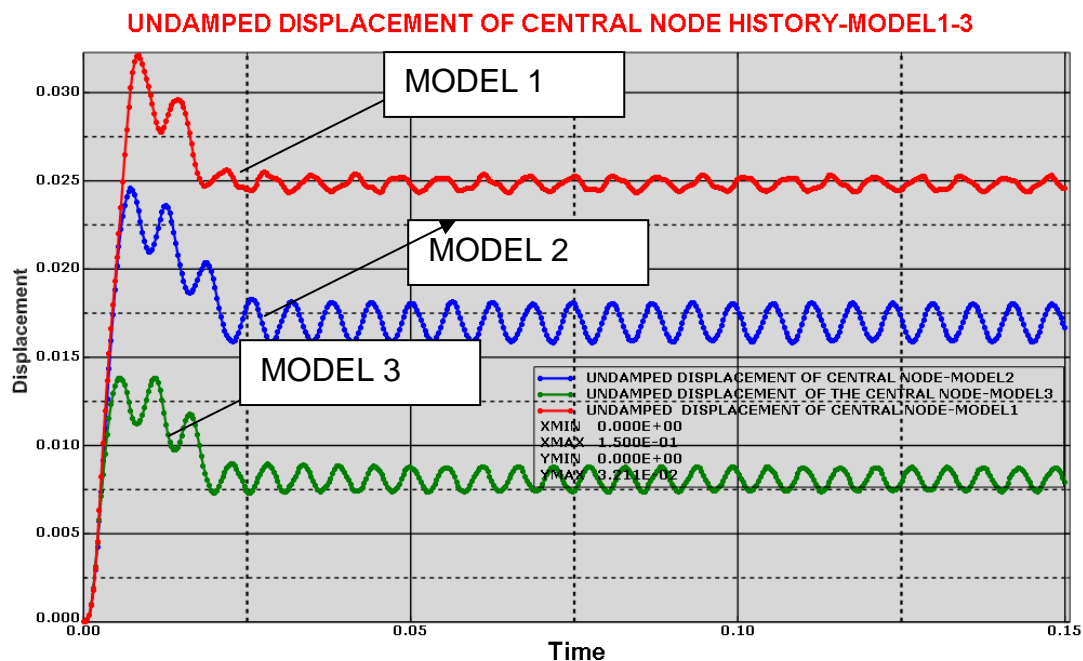


FIGURE 4.7.4 Comparison of the Undamped Displacement History of the central node For Model 1, 2 and 3.

Comment: Here comparison of the undamped displacement of the central for models 1,2 and 3,in figure 4.7.4 above is compared, Model 1 (1x1) has the highest values of the displacement of the central node followed by model 2 (2x2) and the lowest value of the displacement of the central node is model 3 (3x3). The deduction here is that, because model 3 has the highest number of stiffeners, it is going to be more stable and more resilient to blast pressure attack than model 1 and model 2. it is seen from the graph that the values for the displacement of the central nodes decreases with additional stiffeners thus in this case, model 3 has the highest number of stiffeners and will be most resilient to blast pressure attack than the 1x1 and the 2x2 stiffener configurations. This is a good guild for designers.

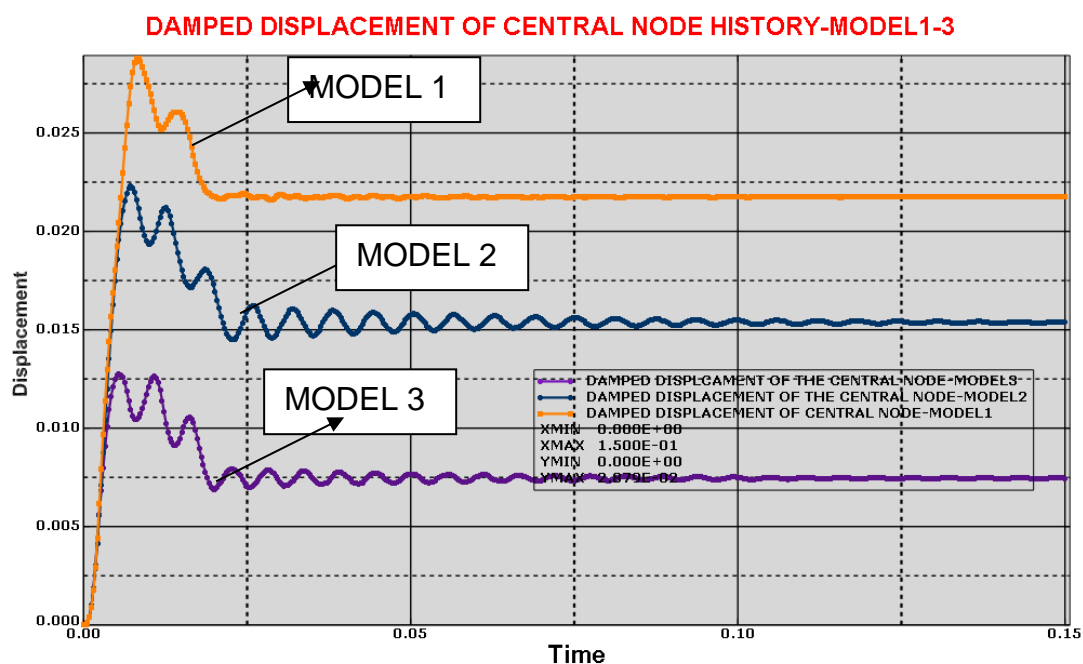


FIGURE 4.7.5 Showing comparison of the damped Displacement History of the central node For Model 1, 2 and 3.

Comment: Comparing the damped displacement of the central for models 1,2 and 3,in figure 4.7.5 above, Model 1 (1x1) has the highest values of the displacement of the central node followed by model 2 (2x2) and the lowest value of the displacement of the central node is model 3 (3x3). Because the model 3 has the highest number of stiffeners, it is going to be more stable and more resilient to blast pressure attack than the remaining model 1 and model 2. it is seen from the graph that the values for the displacement of the central nodes decreases with additional stiffeners thus in this case, model 3 has the highest number of stiffeners and will be most resilient to blast pressure attack than the 1x1 and the 2x2 stiffener configurations. Most importantly, it could be seen that the vibration is damped away due to the inclusion damped factor. Damped factor is an important constant to replicate the actual scenario in real life in a system or structure. A system cannot vibrate continuously in real life, the vibration will naturally be damped away. Therefore, the most important way to replicate the dampness of a system in real life is through the inclusion of a damped constant into the abaqus code.

EFFECT OF RATE DEPENDENCY ON DISPLACE. OF CENTRAL NODE HISTORY-MODEL1-3

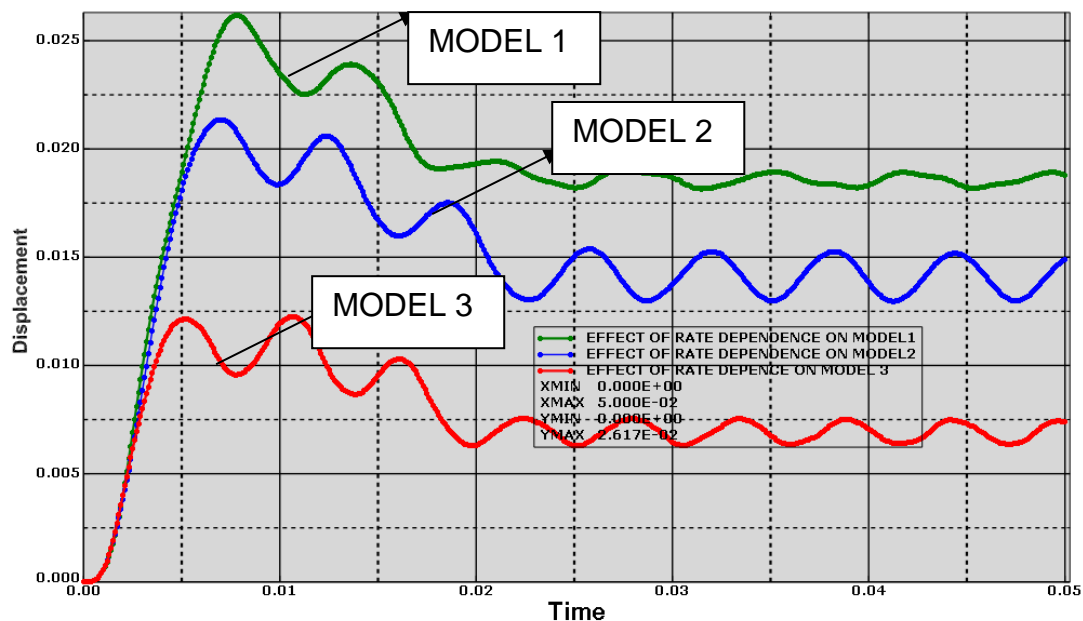


FIGURE 4.7.6 Showing the effect of Rate Dependency on the Displacement of the central node for model 1, 2 and 3.

Comment: Comparing the displacement of the central for models 1,2 and 3,in figure 4.7.6 above. The inclusion of the rate dependency lowered the values of the displacement of the central nodes for model 1, 2 and 3. Additionally, the increase in the number of stiffeners has lowered the values of the displacement of the central node. Model 1 which has (1x1) stiffener has the highest values of the displacement of the central node followed by model 2 which has a stiffener configuration of (2x2) and the lowest value of the displacement of the central node is model 3 which has a stiffener configuration of (3x3). Model 3 has the highest number of stiffeners; it is going to be more stable and more resilient to blast pressure attack than model 1 and model 2.

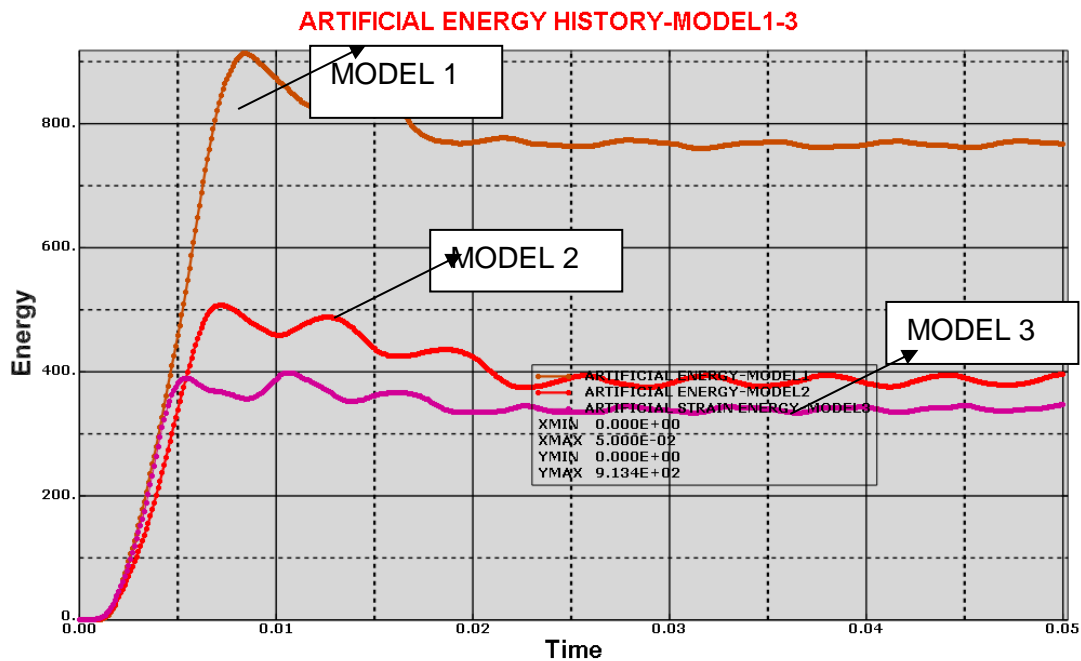


FIGURE 4.7.7 Comparison of the Effect of Artificial Energy on the Displacement of the central node for model 1, 2 and 3.

Comment: Comparing the artificial energy for models 1, 2 and 3, in figure 4.7.7 above. The artificial energy of model 1 with 1 x1 stiffener configuration has the highest value of artificial energy and model 2 with 2x2 stiffener configuration is next with the highest value of artificial energy a while model 3 with 3x3 stiffener configuration has the lowest artificial energy. The deduction here is that the more the stiffeners, the more stable will be the stiffened panel and the less the artificial energy of the system and the more stronger will be the system thus model 3 will most resilient to blast pressure attack than the other 2 models (1 & 2).

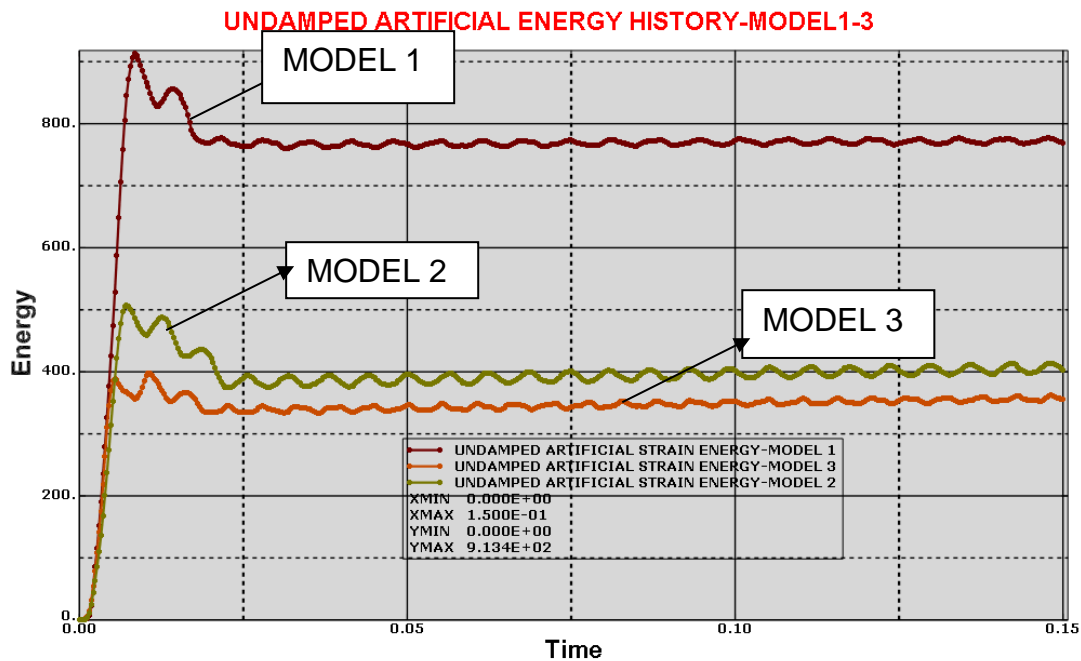


FIGURE 4.7.8 Showing comparison of the Effect of Undamped Artificial Energy on the Displacement of the central node for model 1, 2 and 3.

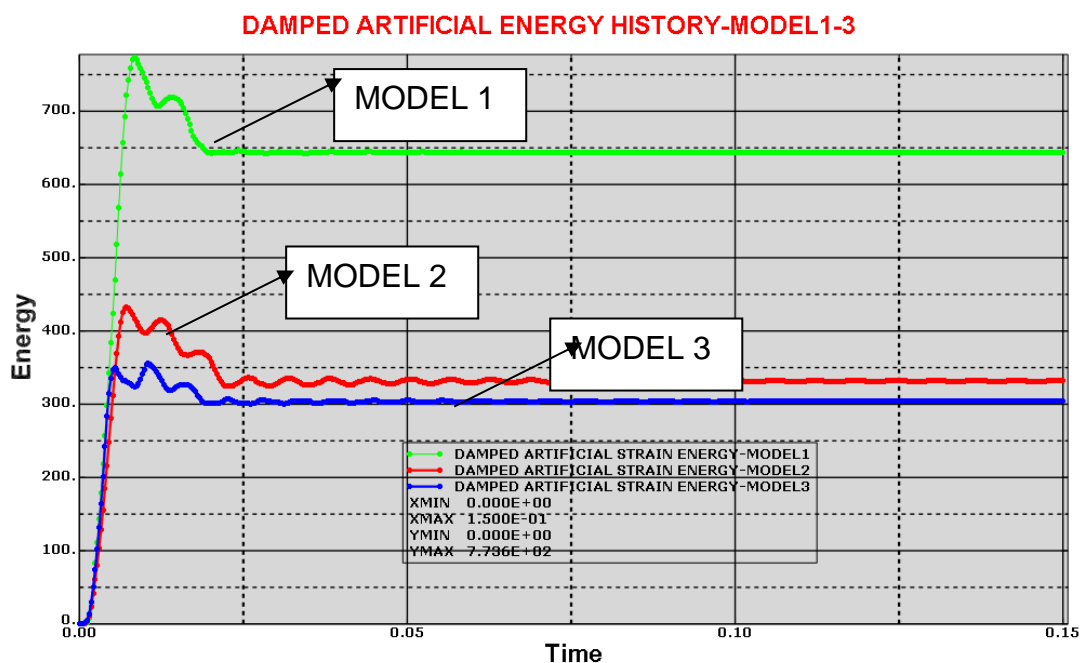


FIGURE 4.7.9 Showing comparison of the Effect of damped Artificial Energy on the Displacement of the central node for model 1, 2 and 3.

Comment: comparing the damped and undamped artificial energy term, it will be noted from figures 4.7.8 and figures 4.7.9. It was observed that the damped artificial energy generated a lower value of energy in models 1-3. The inclusion of the damped constant is to replicate a natural phenomenon as much as possible and it plays an important role in an experiment.

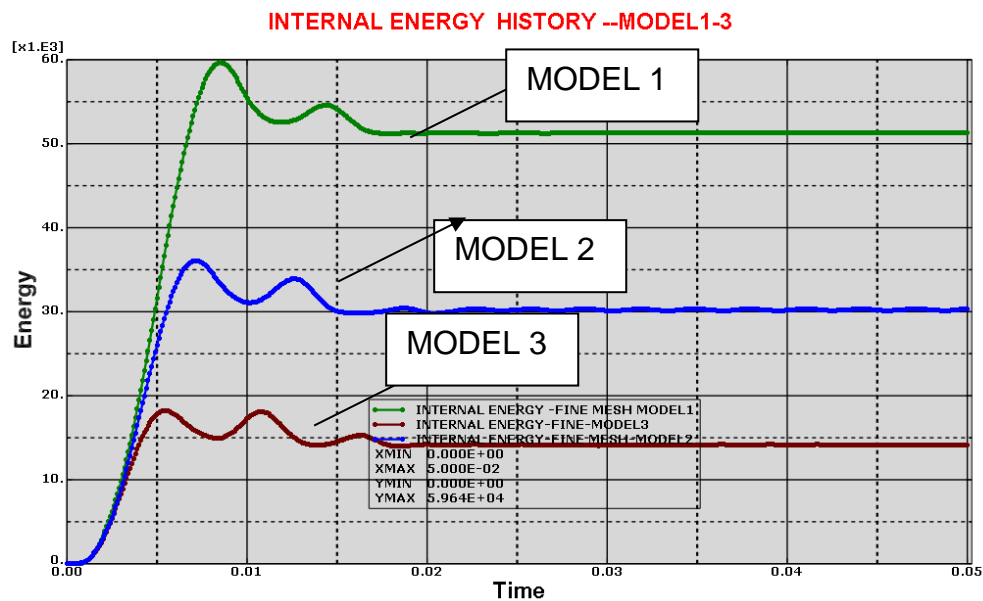


FIGURE 4.8.0 Showing comparison of the Effect of Internal Energy on the Displacement of the central node for model 1, 2 and 3

Comment: In figure 4.8.0, Comparing the internal energy of models 1,2 and 3, it was noted that because of the stable nature of the configuration of the 3x3 stiffeners of model 3, The system will exhibit less internal energy than model 1 and 2 . This is closely followed by model 2 which has 2x2 stiffeners configurations. The internal energy exhibited by Model 1 will be more than model 2 and model 3. This is because model 3 is the most stable of the 3 models, therefore, the internal energy generated by model 3 will be the lowest while the internal energy generated by model 2 will be lower than that of model 1.

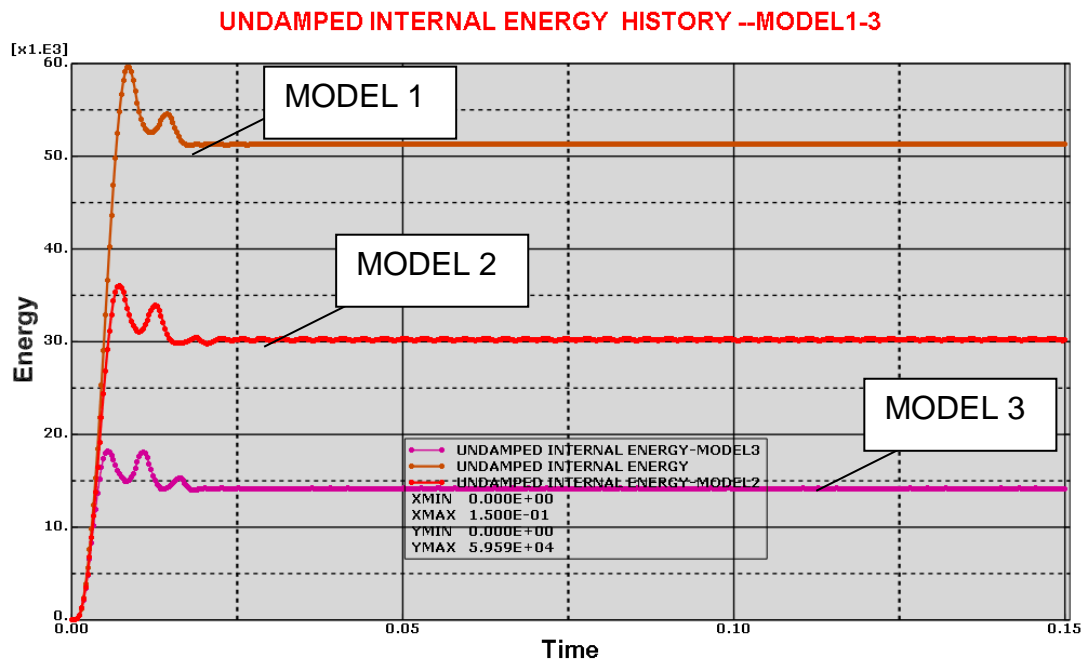


FIGURE 4.8.1: Showing comparison of the Effect of Undamped Internal Energy on the Displacement of the central node for model 1, 2 and 3

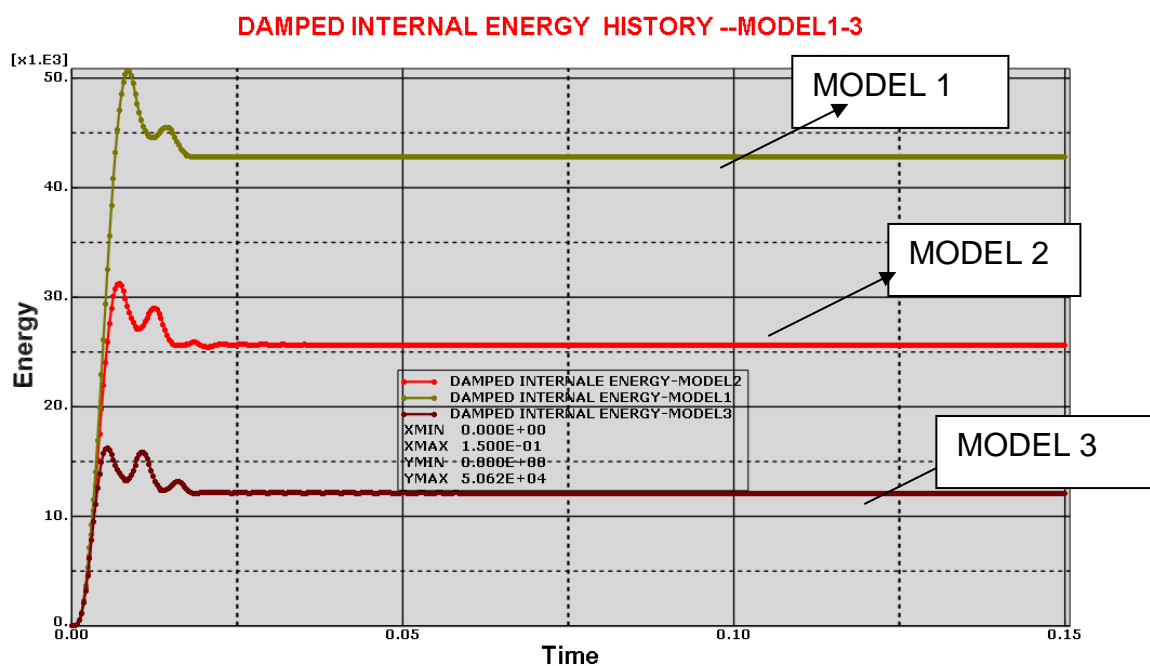


FIGURE 4.8.2 Showing the comparison of the Effect of Damped Internal Energy on the Displacement of the central node for model 1, 2 and 3.

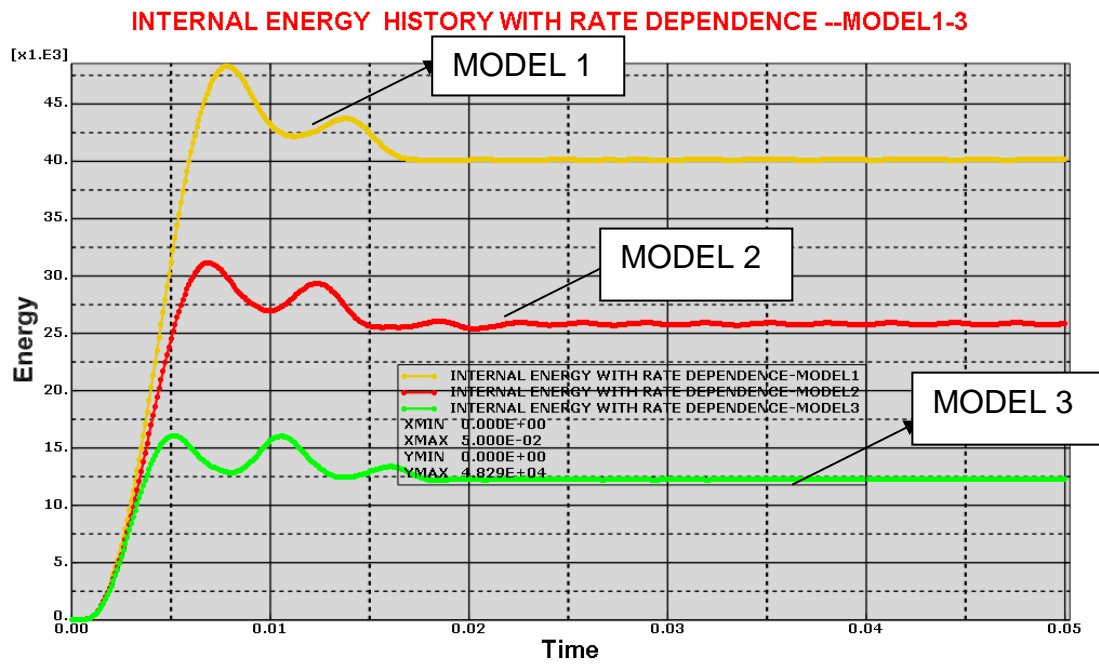


FIGURE 4.8.3 Showing the comparison of the Effect of Internal Energy with rate of Dependence on the Displacement of the central node for model 1, 2 and 3

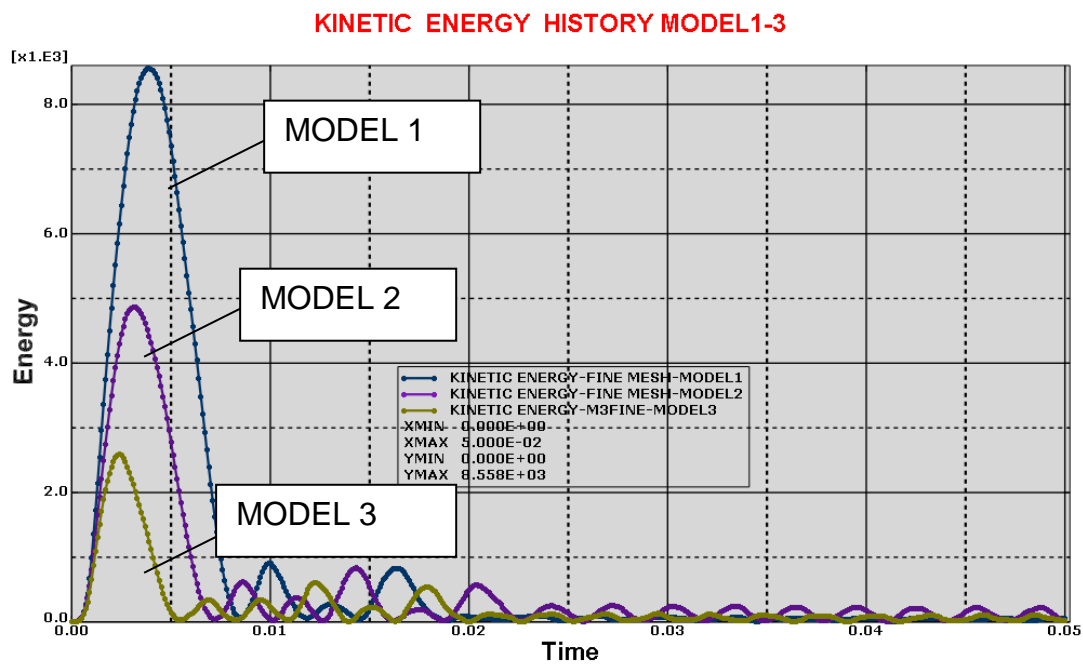


FIGURE 4.8.4 Showing the comparison of the Effect of Kinetic Energy on the Displacement of the central node for model 1, 2 and 3.

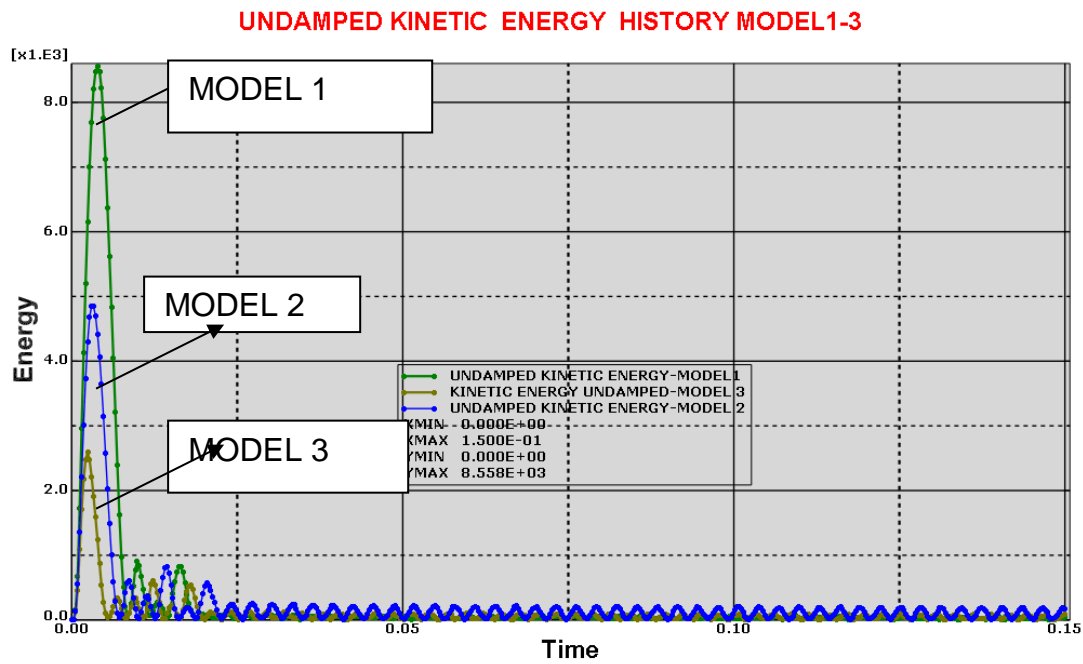


FIGURE 4.8.5 Showing the comparison of the Effect of Undamped Kinetic Energy on the Displacement of the central node for model 1, 2 and 3

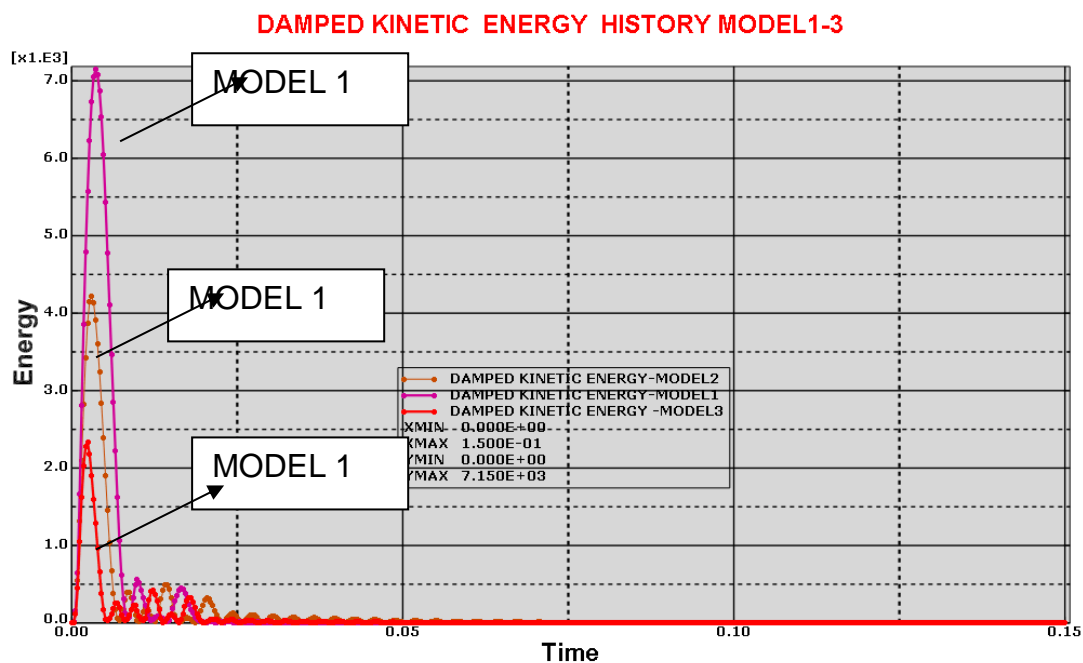


FIGURE 4.8.6 Showing the comparison of the Effect of damped Kinetic Energy on the Displacement of the central node for model 1, 2 and 3

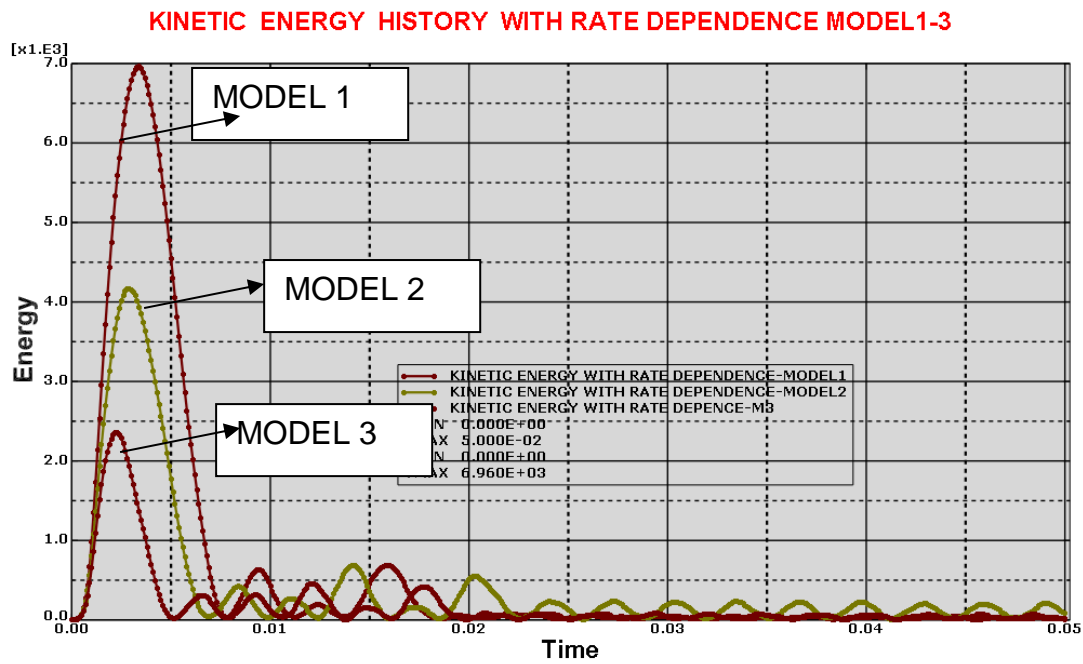


FIGURE 4.8.7 Showing the comparison of the Effect of Kinetic Energy with rate of dependence on the Displacement of the central node for model 1, 2 and 3.

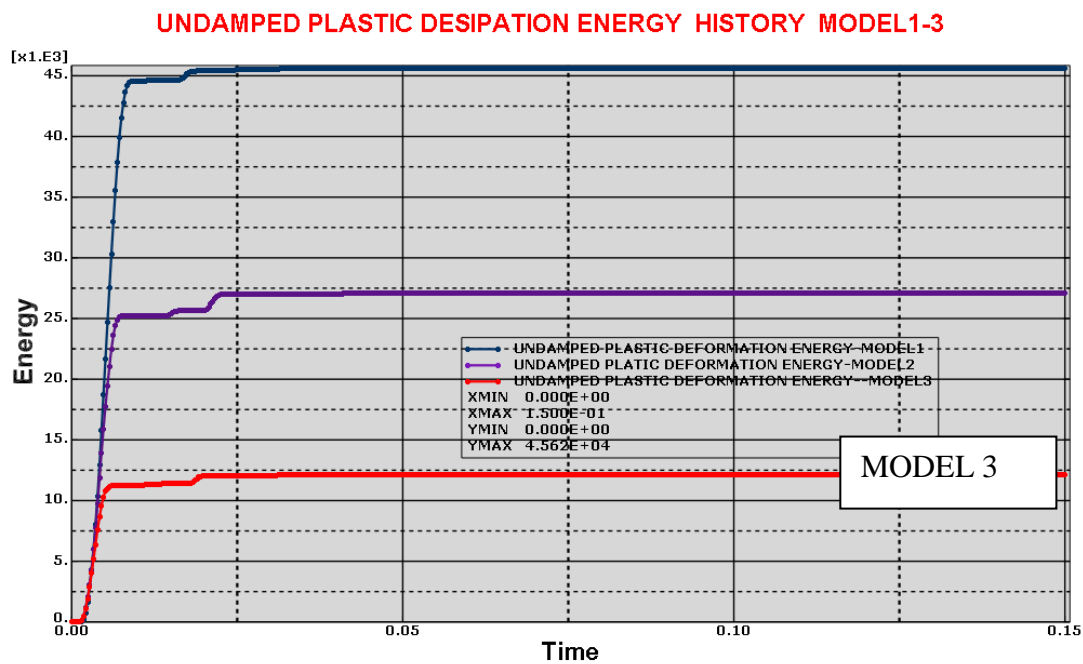


FIGURE 4.8.8 Showing the comparison of the Effect of Undamped Plastic Dissipation Energy on the Displacement of the central node for model 1, 2 and 3.

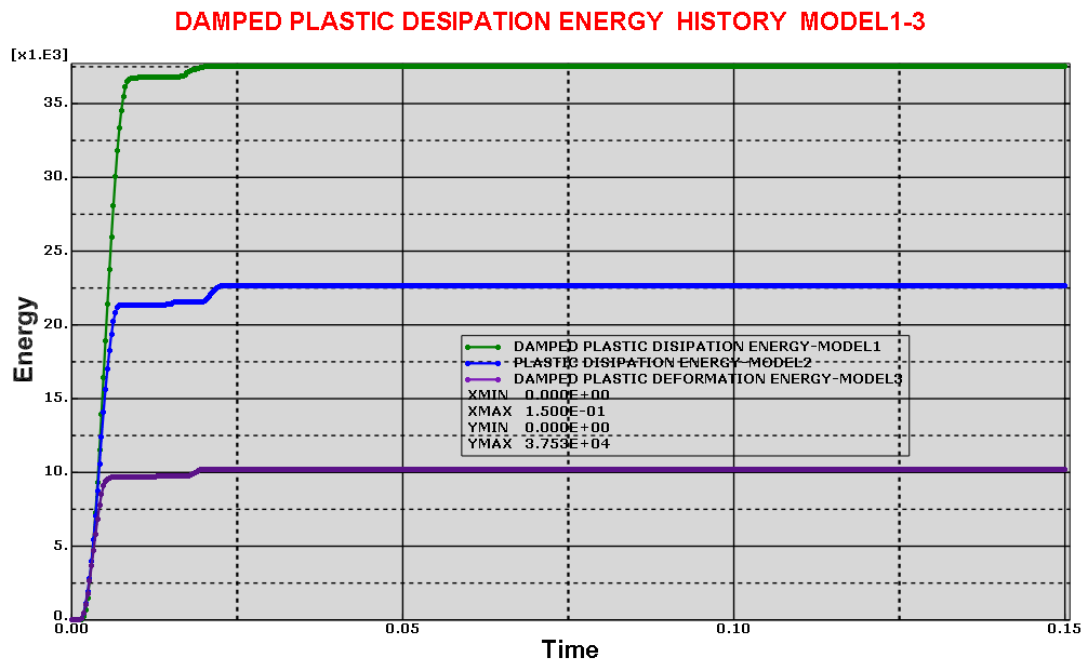


FIGURE 4.8.9 Showing the comparison of the Effect of damped Plastic Dissipation Energy on the Displacement of the central node for model 1, 2 and 3

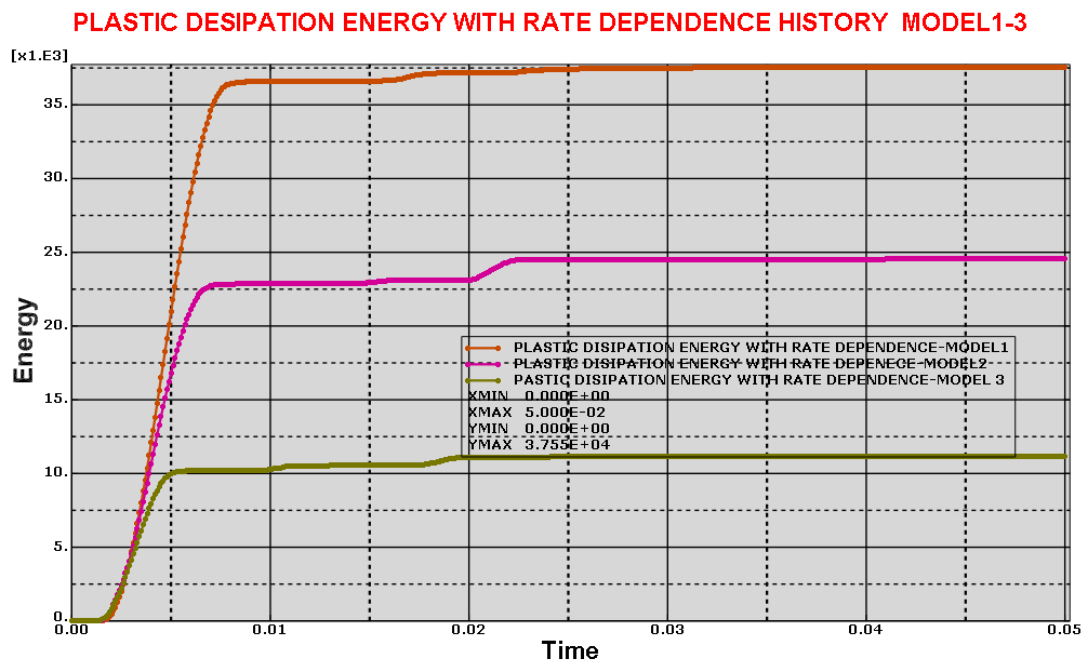


FIGURE 4.9.0 Showing the comparison of the Effect of Plastic Dissipation Energy with rate of dependence on the Displacement of the central node for model 1, 2 and 3

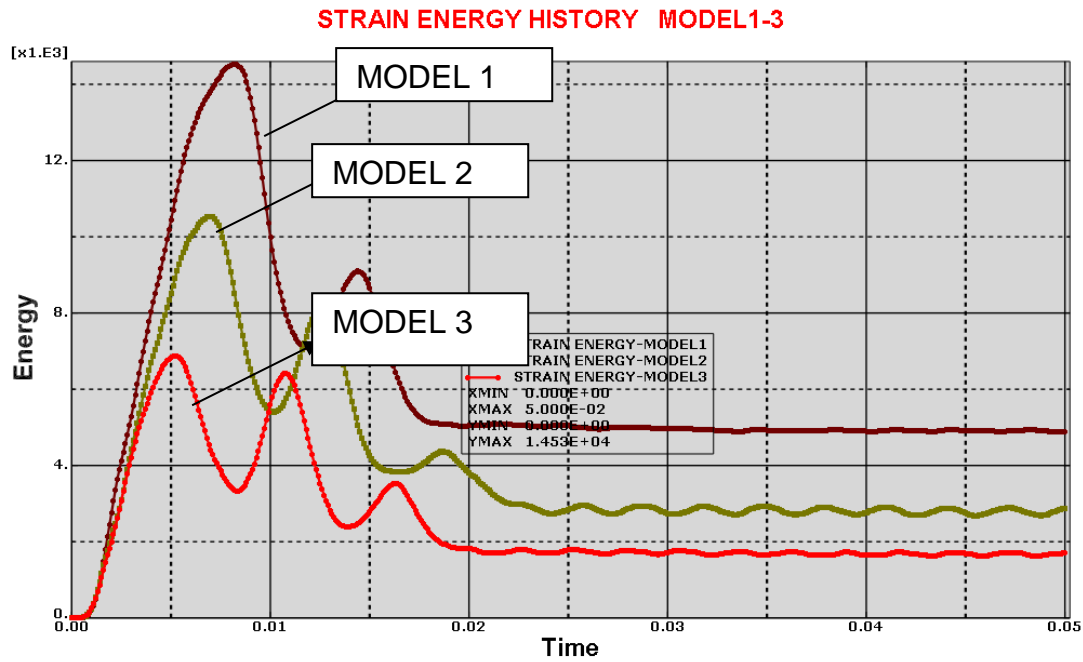


FIGURE 4.9.1 Showing the comparison of the Effect of strain Energy on the Displacement of the central node for model 1, 2 and 3

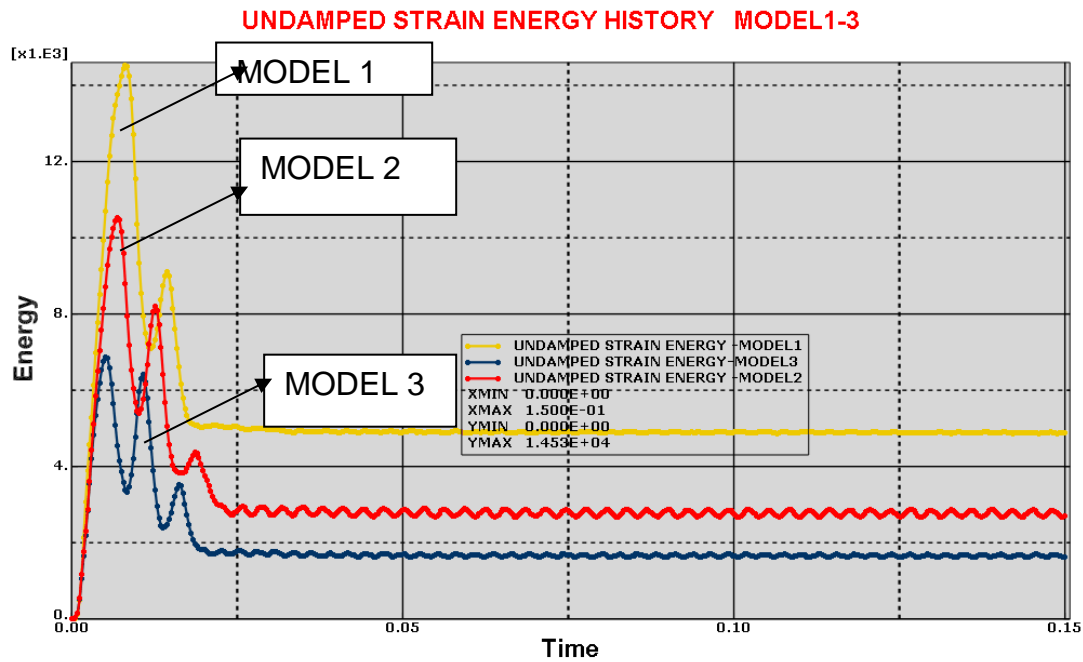


FIGURE 4.9.2 Showing the comparison of the Effect of undamped strain Energy on the Displacement of the central node for model 1, 2 and 3.

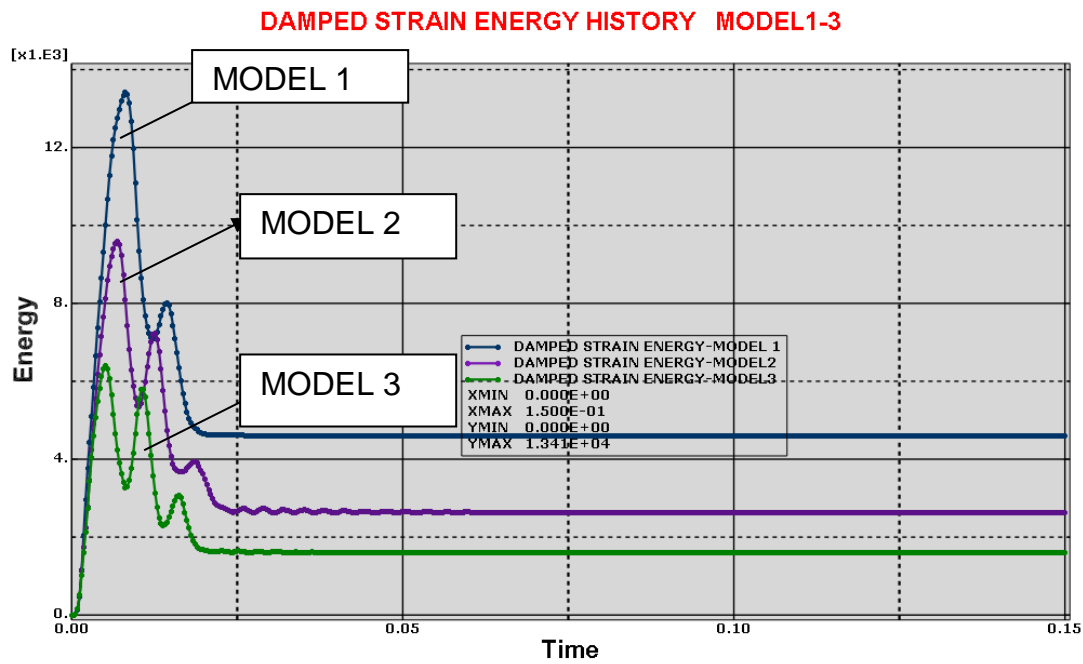


FIGURE 4.9.3 Showing the comparison of the Effect of damped strain Energy on the Displacement of the central node for model 1, 2 and 3.

Comment:

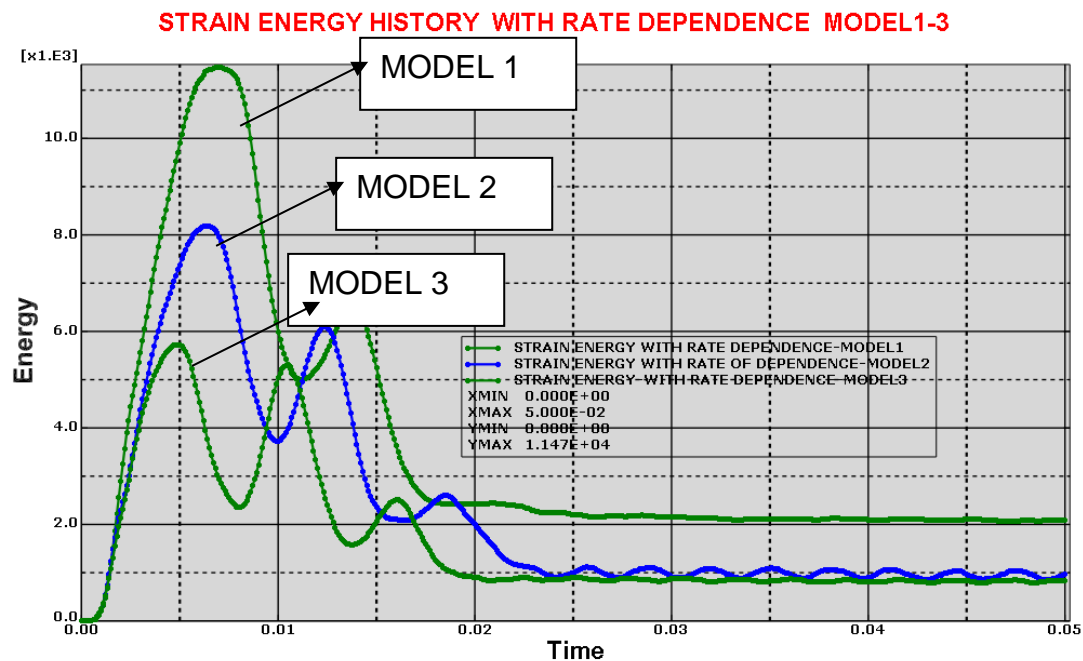


FIGURE 4.9.2 Showing comparison of the Effect of strain Energy with rate of dependence on the Displacement of the central node for model 1, 2 and 3.

Comment: The strain energy terms for the 3 models with rate dependency was compared together and it was observed that the strain energy generated by model 3 is less than that generated by model 2 which is in turn less than that generated by

model 1. This is simply due to the stability of model 3 structure which is composed of 3 x 3 stiffeners.

4.12 RESULTS AND DISCUSSIONS

It is be noted that all comparison are made with reference to fine mesh

4.12.1 Effect of Mesh Refinement

Turkmen and Mecitoglu(1999) in their research found out that refining the mesh can lead to greater changes in the response of stiffened plate. The structural responses of the displacement of the central node become sharper and leading to an increase in the value of the displacement of the central node. In figure 4.4-4.6, it was also observed that the mesh refinement from a coarse mesh of 75mm to a fine mesh of 30mm, increased the number of element generated from 1084 to 6055 elements for model1,1288 elements to 7010 elements for model 2 and 1584 elements to 8153 elements for model 3. Additionally, it was observed that the mesh refinement has increase the displacement values of the central node from 30mm to 35mm, 22.5mm to 25mm and 13mm to 14mm for model 1, model 2 and model 3 respectively. Though the increase in mesh has undoubtedly increase the solution time however the refinement has the advantage of better capturing the variation of stresses and plastic strain through the stiffeners much better and consequently good results are obtained. From model 1-3, the effect of mesh refinement also increases the Von misses stresses and the energy terms such as the internal energy and plastic dissipation energy of the system have also shown considerable increase and this will yield better results than the coarse mesh.[see figures 4.4,4.5 and 4.6].

4.12.2 Effect of stiffener configuration.

As could be seen from table 4.3 and figure 4.4-4.6, the time duration for this analysis was 50ms, thus it could also be seen that as more stiffener were been introduced into the model, the displacement of the central node decreases. The value of the central node displacement of model 1 is 35mm, the value of the central node displacement of model 2 is about 25mm and the value of the central node displacement of model3 is about 13.25mm. This further indicate that the importance of stiffener can greatly influence the

response of T-stiffened Panel, this result further enunciates and agrees with the numerical and experimental results of previous scholars. **Yuen et al(2003)** stated, that as the plates becomes stiffer with more stiffeners, the maximum displacement decreases. **Pan et al(1997)** also submitted that global displacement can be affected significantly by stiffener configuration. **Turkmen and Mecitoglu(1999)** asserted that peak strain can be reduce by stiffener from 11 to 42 %. **Abdelrimkadid(2008)** concluded that stiffener configuration could have significant effect on the mid displacement of the central node of flat bars in a square plate and asserted that the more the stiffener, the more stronger and stable a structure would become. Thus model 3 will withstand or becomes more resilient than model 2 and 1.

4.12.3 Effect of Damping

Undamped structures continue to vibrate with constant amplitude. A constant vibration is though not what would be expected in practice since the vibration of this kind of stiffened panel/plate would tend to die out over time and probably disappear after about 5-10 oscillations. Lots of energy are lost by variety of means especially and including frictional effects at the supports and damping by the air. It is therefore of vital importance to consider the presence of damping in most analysis to model the energy loss and also to have about a real scenario of how the panel will response to damping in a real life. Material damping was introduced in order to have a more realistic structural response. From figure 4.1.3-4.2.5, the introduction of damping constant has not only shown a realistic structural response, it has also reduced the displacement of the central node from model 1-3, the plastic dissipation energy and the artificial energy has also reduced considerably. It is therefore important to introduce material damping in an analysis of this nature in order to obtain a realistic structural response. However, enough time must be allowed in order that the vibration can die out hence the initial time of 50ms was increased to 150ms to allow the vibration to be damped out completely.

4.4 Effect of Rate Dependence

Material such as mild steel shows an increase in the yield stress with increasing strain rate, in the analysis of stiffened plate, strain rate dependence is important especially when the loading rate is high. In rate dependence behaviour, the ratio of the dynamic yield stress to the static yield stress (R) is given for an equivalent plastic strain rate ($\dot{\epsilon}$),

according to the equation $\sigma = D(R-1)^n$ where D and n are material constant (45 and 10 in this case), the analysis showed that with the introduction of the rate dependence, the yield stress effectively increases as the strain rate increases. Consequently because of this, the elastic modulus is higher than the plastic modulus and therefore resulted into stiffer response. The displacement history in figures 4.7.5, 4.7.6 and 4.7.7 and the plastic dissipation energy in figures 4.8.8, 4.8.9 and 4.9.0 including the strain energy also showed that the response is stiffer when the rate of dependence is included. It should be noted however that the result obtained are sensitive to material data and the values of D and n used here are typical of mild steel. **Boh et al(2004)** asserted that there are lots of uncertainties concerning the strain rate effects on steel structural response and that there are studies on rate dependence that are only applicable to their investigated domain. The effect of strain rate dependence on the displacement history, strain energy history, plastic dissipation energy and artificial strain energy from model 1-3 clearly shows that there is a decrease in their respective values.

4.5 Conclusions

Conclusively and from the analysis of non-linear tee-stiffened rectangular plate with an aspect ratio of 2 that was subjected to uniform blast pressure loading, fully clamped boundary condition which was carried out to examine the behaviour of Tee-stiffened rectangular plate, the following conclusion were drawn:

- a. The effect of mesh refinement for T-stiffened plate can significantly affect the result obtained, the von misses stresses is increased, the values of the displacement of the central node increased, and this has the advantage of capturing the variation of stresses and plastic strain through the stiffener much better. The values of the plastic strain energy and the internal energy also increased.
- b. The effect of stiffener configuration in a T-stiffened plate could not be overemphasised as this has got a considerable effect on the overall structural response of the plate. Basically as more stiffeners are been introduced, the structural response of the plate decreases and consequently the value of the displacement of the central node decreases and the plate now becomes more stiffer with the introduction of T-stiffener and flat bar.

- c. In order to obtain a realistic structural response, there is the need to introduce material damping; this has shown effect on the value of the displacement of the central node as the value decreases, the plastic dissipation energy and the artificial strain energy of the system were all reduce by the introduction of the damping coefficient. This also allows the vibration to die out realistically.
- d. In the non-linear analysis of T-Stiffened plate, the need to use strain rate dependence cannot be overemphasised especially when the loading is high. It leads into a stiffer response as could be seen in the displacement of the central node and the energy terms for models 1-3
- e. Time duration also has very greater influence on non-linear analysis of T-stiffened plate as many other parameters are dependent on it. It also has influence on the structural response of a T-stiffened plate subjected to damping. A little time increase from 50ms to 150ms showed that the dampness in models 1-3 was able to die away and this reflected in the graph gotten from the analysis. Time variation is therefore important to enable the dampness to die out vibration.

CHAPTER 5

5. Blast Analysis and Determination of Rupture Strain

5.1 Introduction to Blast Analysis and Determination of Rupture Strain

In Chapter 4, the researchers carried out extensive frequency extraction analysis to determine and obtain the natural frequencies of the FPSO panel with the effects of damping and the high material strain rate effects as well as the effect of plasticity were considered using the finite element code ABAQUS EXPLICIT. The displacement and responses of the stiffened panel at the central node was deeply investigated including their energy terms and the effects of mesh refinement, rate dependency and stiffener configuration were considered.

Consequently, chapter 5, Numerical analysis carried out in the present investigation aims to study (a) blast loading effect on 3 types of T stiffeners configurations and 3 types of L stiffeners configurations, All the 6 stiffener types have the same flange area however the width and thickness of the flanges are different in each case. (b) Part of the panel of FPSO panel code named FPSO Nigeria was extracted, modelled and the above water side of the FPSO was subjected to blast loading replica to an attack that could be inflicted by the militant of the Nigerian Niger Delta, Consequently rupture strain rate under such hostile loading was determined. Where in experimental tests are costly and dangerous. Moreover, the reproducibility of the experimental results is not always ensured because of the uncertainties involved, especially in case of the blast experiments where huge amount of money would have been invested. These shortcomings are addressed herein by using numerical simulation, which reduces the number of experimental trials and helps in better understanding of the physics of the problem. The overall aim is to proffer and recommend a good stiffener configuration type amongst the 6 types of stiffeners for the design of the above water side of FPSO Nigeria. It would also enable the researcher to appreciate the effect of the attack by the terrorist especially the militant of the Nigerian Niger Delta that are getting sophisticated day by day and causing the nation to lose millions of dollars in terms of revenue. In order to facilitate the proper understanding of

this chapter, the researcher quickly reflected on the fundamentals of stress and strain before going into the material modelling proper and blast analysis.

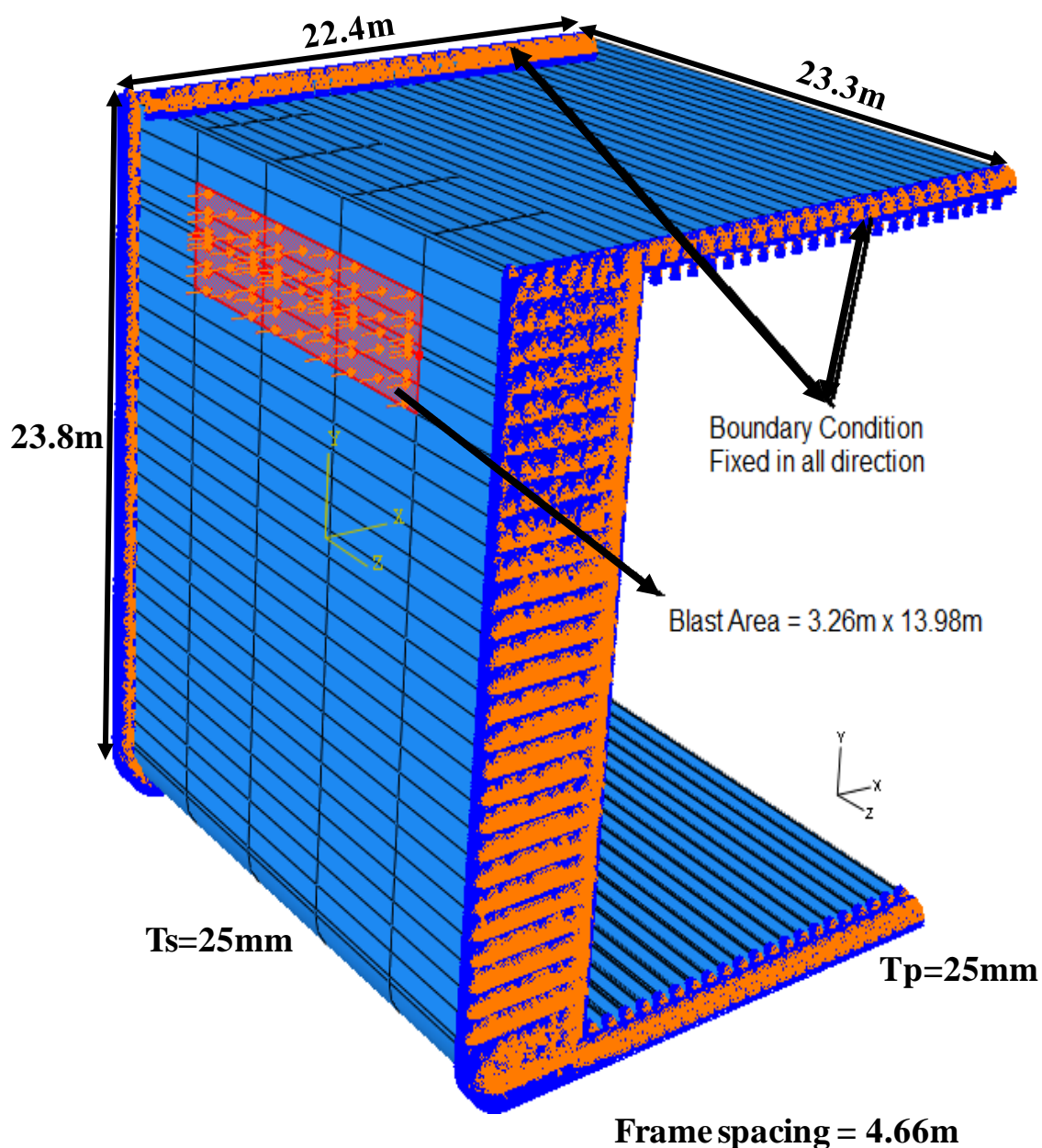


Figure 5: Panel of the FPSO Nigeria subjected to blast pressure loading

5.2 Introduction

In recent years, analysis of structures and its components under blast loading has received considerable attention due to various blast events all over the world. The blast loading results in large deformation of structures including its components. In such situations, the utmost requirements are that the structure should be safe and operative, especially in case of the ship structures like plate and scantlings. Such attacks on civil and ship structures all over the world has demanded the need for detailed analysis of structures and its components under complex loading resulting from blast loading.

Analysis involving time dependent deformations, high strain rates and nonlinear inelastic material behaviour necessitated various assumptions and approximations to simplify the models. The blast loading analysis is highly complex especially interm of time and space. This complexity supplemented with the consideration of nonlinear vibrations and strain rate effects, calls upon obtaining dynamic response by numerical techniques using commercially available finite element (FE) software such as ABAQUS/Explicit **Dassault Simulia Corporation (2006)**. Earlier research on the structures and components subjected to blast is limited to military and industrial applications, which are condensed in the form of equations and charts and are not easily accessible to structural designers **Smith et al (1994)**.

Stiffened plates are amongst the most frequently used structural elements to resist high amplitude loading such as that due to the explosions or impact. In the stiffened plates, stiffeners may either be T stiffened or L stiffened. In spite of the large number of plates designed and built, the effect of stiffeners on their behaviour under blast loading are not well understood and properly taken into account by the designers. Consequently, Numerical analysis carried out in the present investigation aims to study (a) Blast loading effect on 3 types of T stiffeners configuration and 3 types of L stiffeners and subjected to 3 types of blast pressure loading (1e+6 Pascal, 1e+7 Pascal and 1e+8 Pascal). All the 6 stiffener types have the same flange area however the width and thickness of the flanges are different in each case. (b) Rupture strain rate was determined under such hostile loading wherein experimental tests are costly and dangerous. Moreover, the reproducibility of the experimental results is not always ensured because of the uncertainties involved, especially in case of the blast experiments where huge amount of money would have been invested. These shortcomings were addressed herein by using numerical simulation using Abaqus software code which has been proved to be highly

reliable software by most researchers including the present researcher by gradually validating most numerical analysis in this thesis with classical theory and were proven to be highly accurate. Numerical analysis reduces the number of experimental trials, cost and helps in better understanding of the physics of the problem. The overall aim was to proffer and recommends a good stiffener configuration amongst the 6 types of stiffeners for the design of the above water side of FPSO Nigeria and to carry cost benefit analysis in the next chapter on the need to protect the above external waterside of an FPSO against blast pressure attacks. It would also enable the researcher to appreciate the effect of the attack by the terrorist especially the militant of the Nigerian Niger Delta that are getting sophisticated day by day and causing the nation to lose millions of dollars in terms of revenue and to make modest contribution to knowledge by carrying out a cost benefit analysis in addition to recommending the best of the 6 stiffener configurations considered where in rupture strain was determined vis a vis recommending a composite anti ballistic material for the above water side of an FPSO subjected to blast pressure attacks. In order to facilitate the proper understanding of the chapter, the researcher reflected on the fundamentals of stress and strain before going into the material modelling proper.

5.2 Definition of Stress and Strain

5.2 Stress

A material or structure subjected to an external force, will either totally comply with that force and be pushed away, or it will set up internal forces to oppose those applied from outside. Solid materials when stretched or compressed have their internal forces coming into play. A material or structure subjected to external forces that tend to stretch itself is said to be in **tension**, whereas forces which squeeze the material put it in **compression**. The term 'stress', symbol σ (Greek letter sigma), is used for the force per unit area, and has the units of pascals (Pa) with 1Pa being one Newton per square metre. However if the reference area is so large, high multiples such as the mega Pascal (**MPa = 10^6 Pa**) and gigapascal (**GPa = 10^9 Pa**) is used.

5.3 Strain

A material in tension or compression changes in length, and the change in length compared to the original length is referred to as the 'strain', symbol ϵ (**Greek letter epsilon**). Since strain is a ratio of two lengths it has no units and is frequently expressed as a percentage: a strain of 0.005 corresponds to a ½% change of the original length.

5.4 Relationship Between Stress and Strain

The relationship between the stress and strain that a material displays is known as a Stress-Strain curve and it is unique for every material and or structure. It is found by recording the amount of deformation strain at distinct intervals of tensile or compressive loading. Stress strain curves reveal the properties of a material or structures including data to establish the Modulus of Elasticity, E.

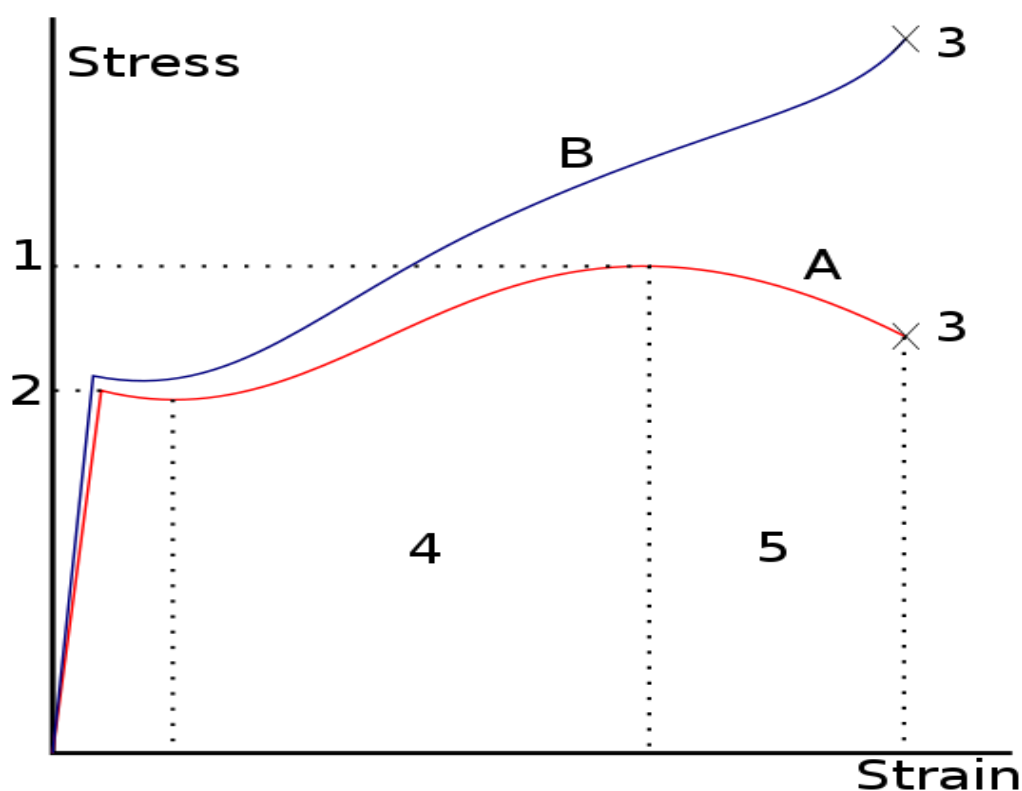


FIGURE 5.1: STRESS CURVE FOR STRUCTURAL STEEL

(Source: Stress Strain Lecture note-Newcastle University)

Reference numbers for the above stress strain curve is as follows:

- 1 - Ultimate Strength
 - 2 - Yield Strength (elastic limit)
 - 3 - Rupture
 - 4 - Strain hardening region
 - 5 - Necking region
- A: Apparent stress (F/A_0)
- B: Actual stress (F/A)

There are a number of significant points on a stress-strain curve that help one understand and predict the way every blast structure will behave, thus the below graph further explain the behavior of materials or structures under blast loading.

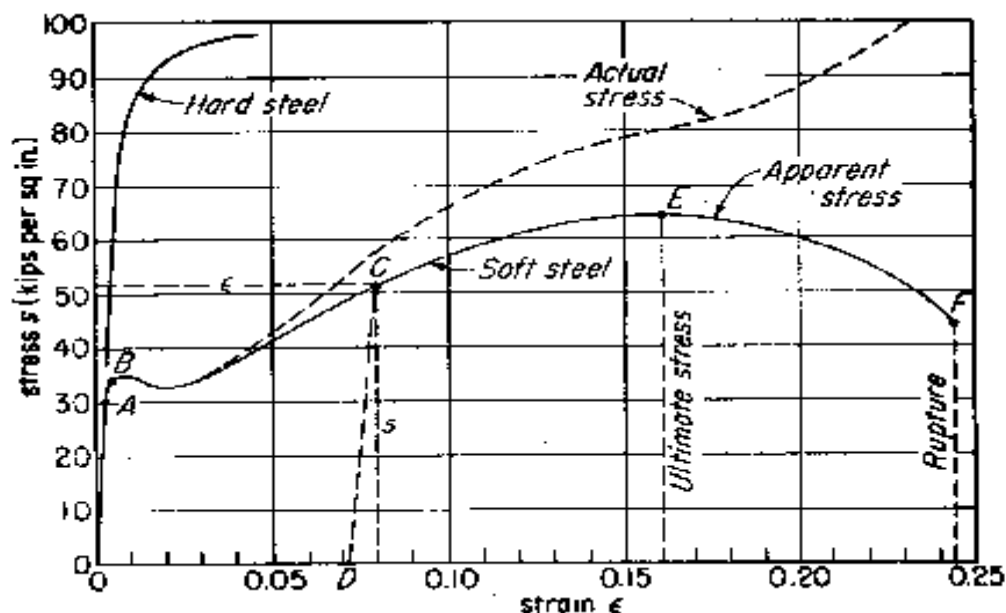


FIGURE 5.2: Example Test on 2 grades of Steel (Curled from Stress-Strain note-Newcastle University)

An example plot of a test on two grades of steel is illustrated above in figure 5.2 above. If one begins at the origin and follows the graph a number of points are indicated. Point A in Figures 5.2 is known as the proportional limit. Up to this point the relationship between

stress and strain is exactly proportional. The number which describes the relationship between the two is the Modulus of Elasticity.

Strain increases faster than stress at all points on the curve beyond point A. Up to this point, any steel specimen that is loaded or any structure that is loaded and unloaded would return to its original length. This is known as elastic behaviour. Point B is the point after which any continued stress results in permanent, or inelastic, deformation. Thus, point B is known as the elastic limit. Since the stress resistance of the material decreases after the peak of the curve, this is also known as the yield point.

The line between points C and D shows the behaviour of the steel or structure specimen for continued loading to the stress indicated as point C. When the specimen or structure is unloaded the magnitude of the inelastic deformation would be determined (in this case 0.0725 inches /inch). If the same specimen or structure was to be loaded again, the stress-strain plot would climb back up the line from D to C and continue along the initial curve. Point E indicates the location of the value of the ultimate stress which is different from the yield stress. The yield stress and ultimate stress are the two values that are most often used to determine the allowable loads for materials or structures. A material or structure is considered to have completely failed once it reaches the ultimate stress. The point of rupture, or the actual tearing of the material or structure, does not occur until point F. Changes in that body of knowledge have had large impacts on the way in which ship structures are designed and has greatly influenced the type of stiffeners to be used on plates. Thus in this analysis, the best option of the type of stiffener shall be selected.

5.4 COMPUTATIONAL MATERIAL MODEL

The Materials used in this analysis are mild steel (S235JR-EN10025) the material properties are describe in Table 5 below.

Table 5: Properties of Steel curled from **Dow et al (2010)**

Material types	K (MPa)	N	ε_{plat}	ε_f	σ_y (MPa)
S235-A	740	0.24	-	0.35	285
S235-B	760	0.225	0.015	0.35	340
S355-C	830	0.18	0.01	0.28	390

These material are assumed to be isotropic and to exhibit strain hardening properties in accordance with the true stress-strain relationship approximated by the equation below where K and n are material parameter constants proposed by **(Amdahl et al 2009)** and later **(Dow et al, 2010)**.

$$\sigma = \begin{cases} \sigma_y K (\varepsilon + \varepsilon_0)^n & \text{if } \varepsilon \leq \varepsilon_{plat} \\ \text{otherwise} & \end{cases}$$

and

$$\varepsilon_0 = \left(\frac{\sigma_y}{K} \right)^{\frac{1}{n}} - \varepsilon_{plat}$$

and

Where ε_{plat} is the plateau strain

In this study, the material failure model used is based on forming limit diagram (FLD) method which is a concept introduced by **Keeler and Backofen (1964)** to determine the amount of deformation that a material can withstand prior to the onset of necking instability. The maximum strains that sheet material can sustain prior to the onset of necking are referred to as the forming limit strains as described in the ABAQUS documentation **Abu-Bakr, (2010)**.

The forming limit strains are rate independent effects in the FLD method. In **Jie, Cheng et al (2009)** the following relationships are used:

$$\varepsilon_1 = \begin{cases} \frac{n}{(1+r_\varepsilon)} \text{ if } r_\varepsilon \leq 0 \\ \frac{3r_\varepsilon^2 + (2+r_\varepsilon)^2 n}{2(2+r_\varepsilon)(1+r_\varepsilon+r_\varepsilon^2)} \text{ if } r_\varepsilon > 0 \end{cases}$$

Where: $r_\varepsilon = \frac{\varepsilon_2}{\varepsilon_1}$ is strain ratio,

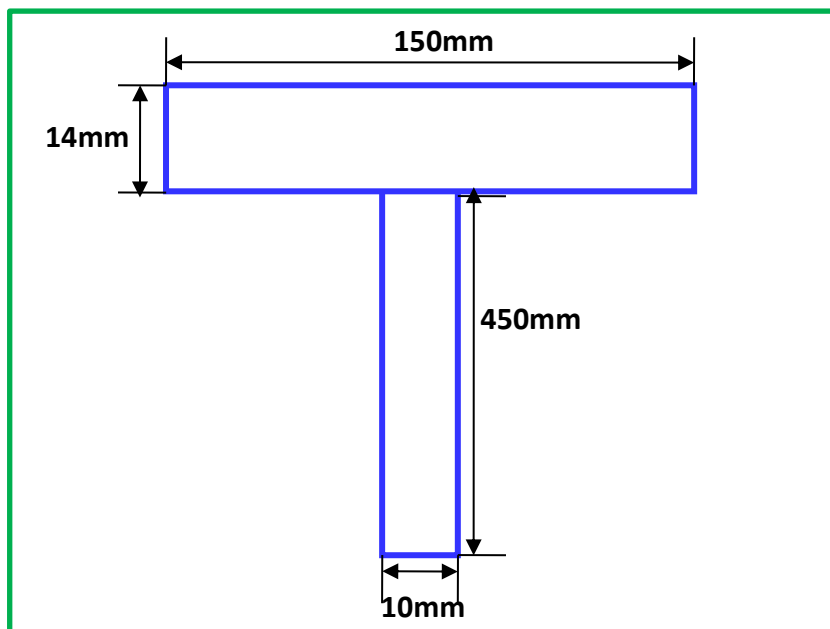
$r_\varepsilon = 0$ For plain strain,

$r_\varepsilon = -0.5$ For simple tension

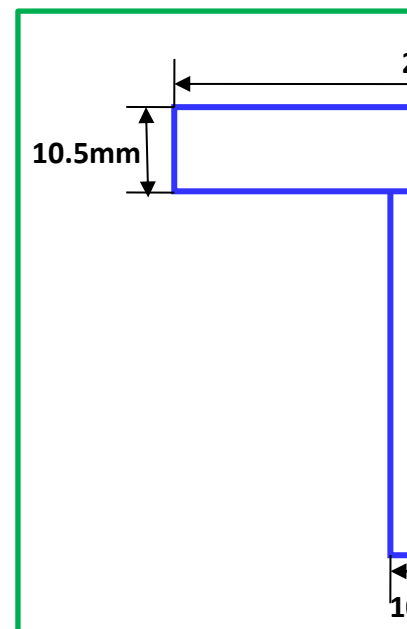
And $r_\varepsilon = 1$ biaxial tension which is the basis for localized necking failure.

For all of the simulations carried out by **Abu-Bakr et al 2010** the friction coefficient was set at 0.3 and the displacement at failure considered to be $\varepsilon_u L$. Where ε_u is ultimate strain, approximately $0.5\varepsilon_f$; ε_f is fracture strain and L is characteristic element length. The mesh size used was 80mm.

Types of Stiffener Configuration used for this analysis



Not Draw to Scale



Not Draw to Scale

Figure 5.3a-T Stiffener (150mm x14mm) Figure 5.3b: T Stiffener (200mm x10.5mm)

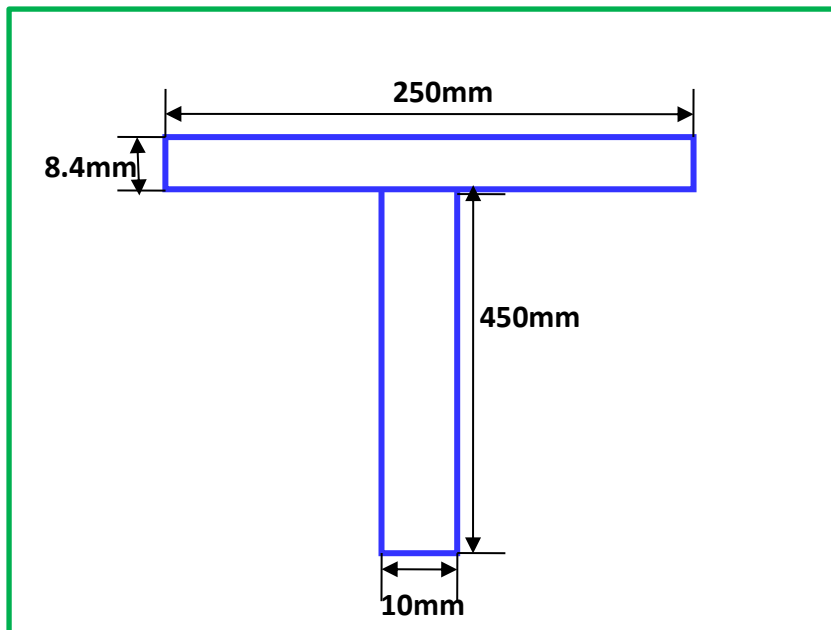
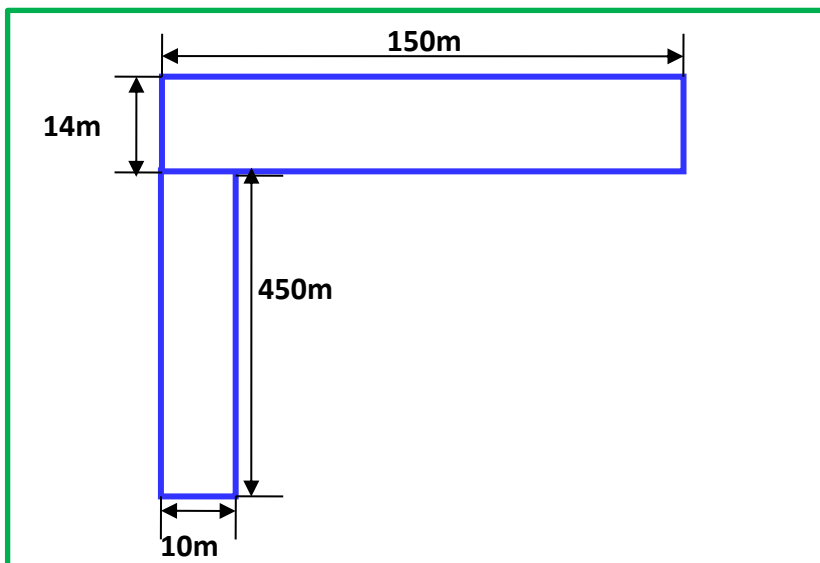
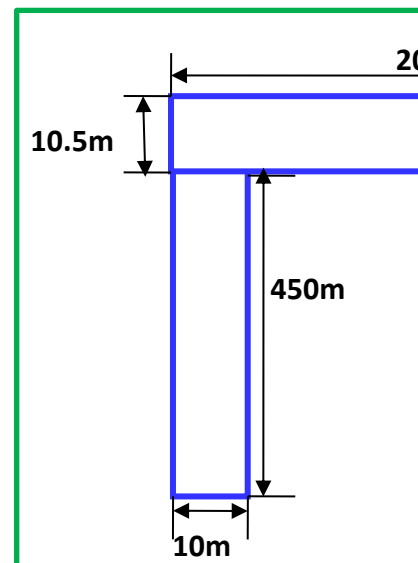


Figure 5.3C: T Stiffener (250mm x8.4mm)

L- STIFENERS

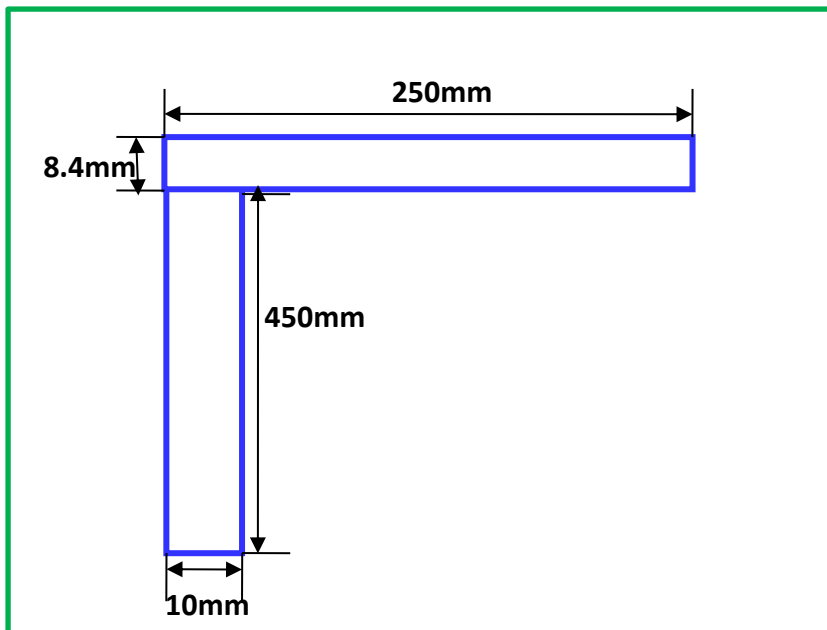


Not Draw to



Not Draw to

Figure 5.3d-L Stiffener (150mm x14mm)Figure5.3e-L Stiffener (200mm x10.5mm)



Not Draw to Scale

Figure 5.3f-L Stiffener (250mm x8.4mm)

Detailed Size of T-Stiffeners Considered on the Midship Section of FPSO Nigeria

TABLE 5.1: Detailed Size of T-stiffeners Considered

Steel Grade	T-Stiffener								
	Type-A			Type-B			Type-C		
	FB	Thk	Area	FB	Thk	Area	FB	Thk	Area
DH	150	14	2100	200	10.5	2100	250	8.4	2100
DH	150	14	2100	200	10.5	2100	250	8.4	2100
DH	150	14	2100	200	10.5	2100	250	8.4	2100
D	150	14	2100	200	10.5	2100	250	8.4	2100
D	150	14	2100	200	10.5	2100	250	8.4	2100
D	150	14	2100	200	10.5	2100	250	8.4	2100
D	150	19	2850	200	14.25	2850	250	11.4	2850
D	150	19	2850	200	14.25	2850	250	11.4	2850
D	150	22	3300	200	16.5	3300	250	13.2	3300
D	150	25	3750	200	18.75	3750	250	15	3750
D	150	25	3750	200	18.75	3750	250	15	3750
D	150	25	3750	200	18.75	3750	250	15	3750
D	150	25	3750	200	18.75	3750	250	15	3750
D	150	25	3750	200	18.75	3750	250	15	3750
D	150	28	4200	200	21	4200	250	16.8	4200
D	150	28	4200	200	21	4200	250	16.8	4200
D	150	28	4200	200	21	4200	250	16.8	4200
D	150	28	4200	200	21	4200	250	16.8	4200

D	150	28	4200	200	21	4200	250	16.8	4200
D	150	25	3750	200	18.75	3750	250	15	3750
D	150	25	3750	200	18.75	3750	250	15	3750
D	150	25	3750	200	18.75	3750	250	15	3750
D	150	25	3750	200	18.75	3750	250	15	3750
D	150	25	3750	200	18.75	3750	250	15	3750
D	150	25	3750	200	18.75	3750	250	15	3750
D	150	25	3750	200	18.75	3750	250	15	3750
DH	150	25	3750	200	18.75	3750	250	15	3750

Detailed Size of L-Stiffeners Considered on the Midship Section of FPSO Nigeria

Table 5.2: Detailed Size of L-Stiffeners Considered

Steel Grade	L-Stiffener								
	Type-D			Type-E			Type-F		
	FB	Thk	Area	FB	Thk	Area	FB	Thk	Area
DH	150	14	2100	200	10.5	2100	250	8.4	2100
DH	150	14	2100	200	10.5	2100	250	8.4	2100
DH	150	14	2100	200	10.5	2100	250	8.4	2100
D	150	14	2100	200	10.5	2100	250	8.4	2100
D	150	14	2100	200	10.5	2100	250	8.4	2100
D	150	14	2100	200	10.5	2100	250	8.4	2100
D	150	19	2850	200	14.25	2850	250	11.4	2850
D	150	19	2850	200	14.25	2850	250	11.4	2850
D	150	22	3300	200	16.5	3300	250	13.2	3300
D	150	25	3750	200	18.75	3750	250	15	3750
D	150	25	3750	200	18.75	3750	250	15	3750
D	150	25	3750	200	18.75	3750	250	15	3750
D	150	25	3750	200	18.75	3750	250	15	3750
D	150	25	3750	200	18.75	3750	250	15	3750

D	150	28	4200	200	21	4200	250	16.8	4200
D	150	28	4200	200	21	4200	250	16.8	4200
D	150	28	4200	200	21	4200	250	16.8	4200
D	150	28	4200	200	21	4200	250	16.8	4200
D	150	28	4200	200	21	4200	250	16.8	4200
D	150	25	3750	200	18.75	3750	250	15	3750
D	150	25	3750	200	18.75	3750	250	15	3750
D	150	25	3750	200	18.75	3750	250	15	3750
D	150	25	3750	200	18.75	3750	250	15	3750
D	150	25	3750	200	18.75	3750	250	15	3750
D	150	25	3750	200	18.75	3750	250	15	3750
D	150	25	3750	200	18.75	3750	250	15	3750
DH	150	25	3750	200	18.75	3750	250	15	3750

Description of Works.

In this study, an above water side of a midship section of an FPSO code named FPSO Nigeria was subjected to 3 types of blast pressure loading which are $1e+6$ Pascal, $1e+7$ Pascal and $1e+8$ Pascal. The loading is to replicate the type of an attack that could be inflicted by Nigerian Niger Delta militants on an FPSO operating in Nigerian waters. Consequently, the study considered the use of 3 types of T stiffened plate and 3 types of L stiffened plate. The stiffeners all have the same flange area however the width and thickness of the stiffeners are different. Thus even though the flanges have same area, their second moment of area is different. These stiffeners were then tested and subjected to blast pressure loading with a view to select the one that would provide better resilient or that which will reduce the effect of the blast pressure loading to the above external water side of the FPSO code named FPSO Nigeria. Comparatively, the study came out with the best type of stiffener and the size of stiffener out of the 6 different types of stiffeners considered (3T types and 3 L types). Most importantly, The rupture strain was also determined. Active and passive methods of offering better resilient to blast pressure loading on the above water side of the FPSO was also proffered.

5.5 NUMERICAL SIMULATIONS

The finite element code Abaqus (**Simulia, 2006**) was used in the analysis of the blast loading. The area of the above water side of the FPSO subjected to blast pressure loading was 3.26m x 13.98m (45.58sqm). The area of the above water side of the FPSO that was subjected to blast pressure loading is shown in figure 5.3 below.

The midship section was modelled with Abaqus code with a boundary condition of all edges being fixed. Simulations were performed using 80mm mesh and application of 3 different blast pressures loads were applied at different times in order to establish the effect of the blast pressure loads on the blast areas of the midship section of the FPSO. It is important to note that the blast area is an above water side of the FPSO. The loading was defined by an application of the above water areas of the FPSO in order to avoid the effect of hydrodynamics which will form other areas of study and would be recommended accordingly for future studies. The boundary conditions on the FE model were set as ENCASTRE.(Fully fixed) for all the blast pressure loadings considered in all the simulation. The impact of the blast pressure loading was set at the midship section of the FPSO in an area defined as an above water section of the FPSO midship section. A panel of the FPSO which constitute the midship bulkhead was selected and modelled as this will give same effect as the whole above water side of the FPSO. Two major types of stiffeners were considered namely T stiffeners and L-stiffeners. The area of the flange for the T and L stiffeners are the same however the thicknesses of the 3 types of the flanges for the T were different. The length and thickness of the web were kept constant. This study subjected the 3 types of T stiffener and 3 types of L shape stiffeners to blast pressure loading of $1e+6$, $1e+7$ and $1e+8$ pascals with a view to come out with the best type of stiffener.

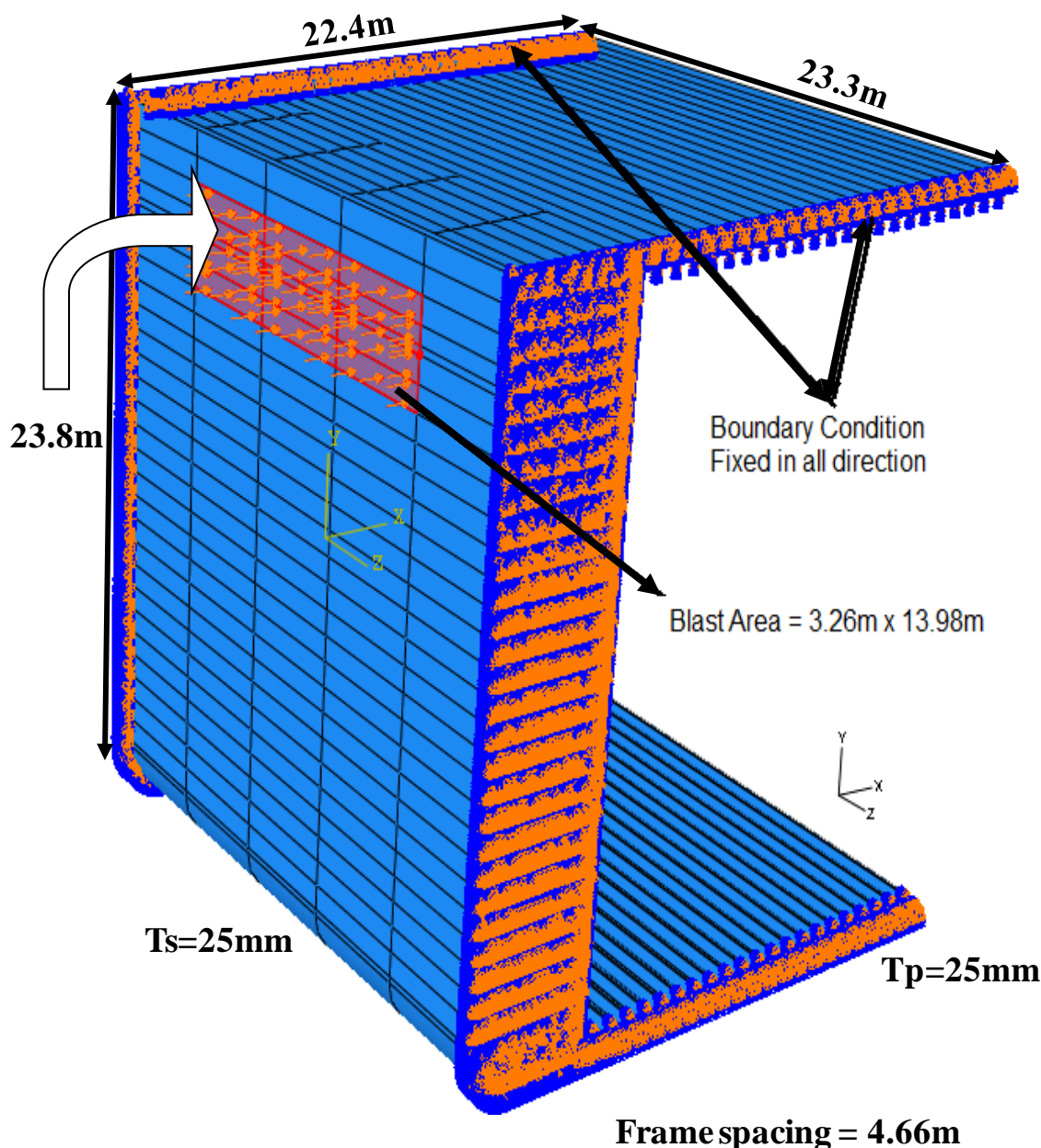


Figure 5.3: Midship section of the FPSO showing blast area and boundary condition applied which is fixed in all direction.

Conversion of Blast Pressure to TNT Equivalence

Three different blast pressures were applied to the above water side of the FPSO namely $1e+6$, $1e+7$ and $1e+8$ pascals .These blast pressures can be converted to TNT Equivalence as follows:

a. 1e+6Pa

Blast area = $13.98m \times 3.26m$
 = $45.58m^2$

Volume of Blast area

= blast area x thickness of plate

= 45.58m² x 0.025m (thickness of plate is 25mm)

= 1.14m³

Energy in joules

= blast pressure in N/m² x volume of blast area in m³

= 1e+6 N/M² X 1.14M³

= 1140000Nm

= 1140000NM

= 114000Joules

But 1 gram of TNT = 4184 Joules

Xgram of TNT= 1140000 Joules

Xgram TNT= (1140000/4184)

= 272.466 grams of TNT

= **272.5 Grams of TNT (0.2725kg of TNT)**

b. 1e+7Pa

Energy in joules would be

= 1e+7 n/m² x 1.14m³

= 11400000NM

And when converted to grams of TNT

= (11400000/4184)

= **2725 Grams of TNT (2.725KG OF TNT)**

c. 1e+8Pa

Energy in joules would be

= 1e+8 n/m² x 1.14m³

= 114000000NM

And we converted to grams of TNT

= (114000000/4184)

= **27250 Grams of TNT (27.25KG OF TNT)**

5.7 Simulation of Blast Analysis Results

Type A-Stiffeners with flange size (150mm x 14mm thick) Blast pressure (bp)- (where bp-blast pressure 1e+6, 1e+7 and 1e+8 pascal, 80mm mesh

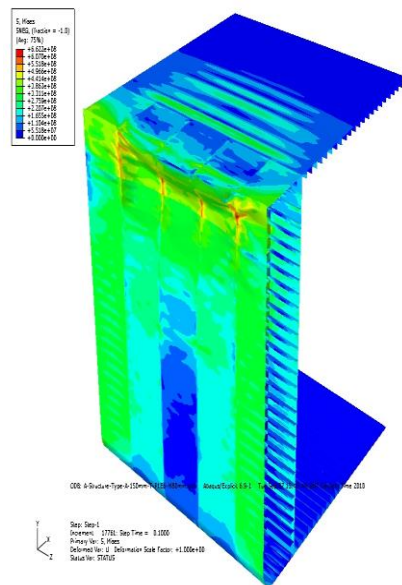


Figure 5.4(a)

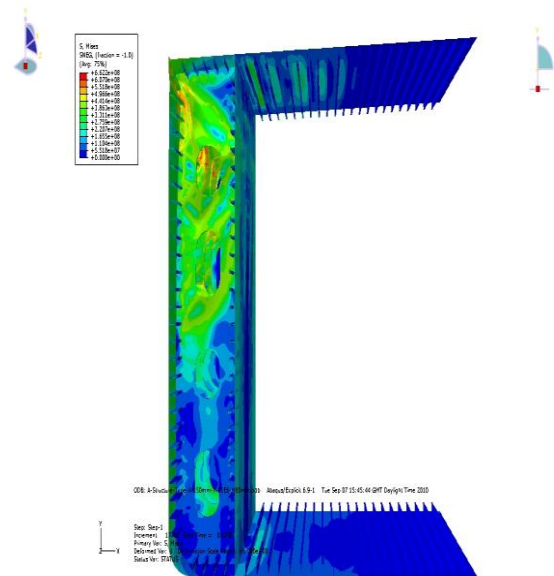


Figure 5.4(b)

Figures 5.4 (a and b): Showing blast simulation result of the impact of blast Pressure of **1e+6 Pascal** on the blast area of an above water side of the FPSO Nigeria for Type A Stiffened Plate

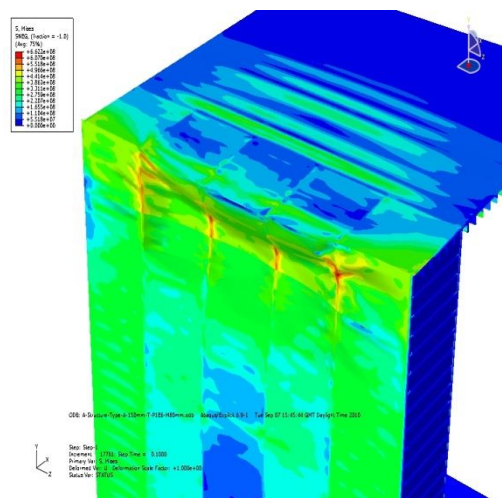


Figure 5.4(c)

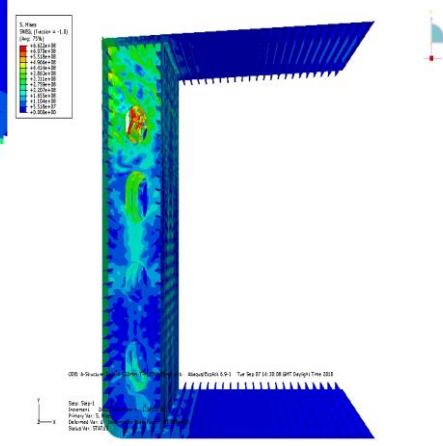


Figure 5.4(d)

Figures 5.4 (c and d)above : Showing blast simulation result of the impact of blast Pressure of **1e+7 Pascal** on the blast area of an above water side of the FPSO Nigeria on Type A Stiffened Plate.

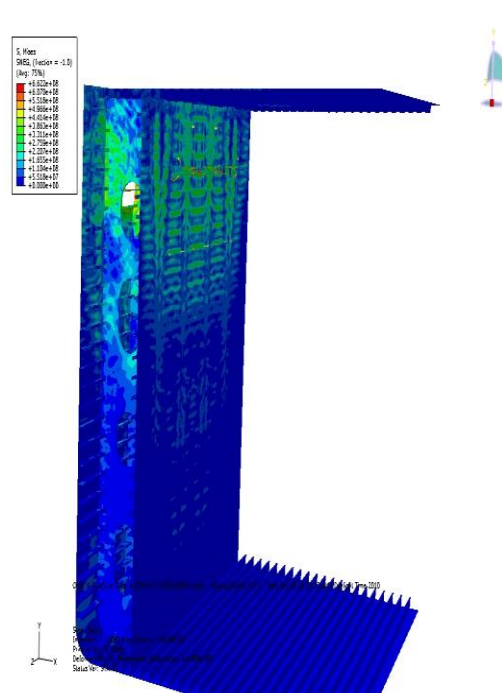
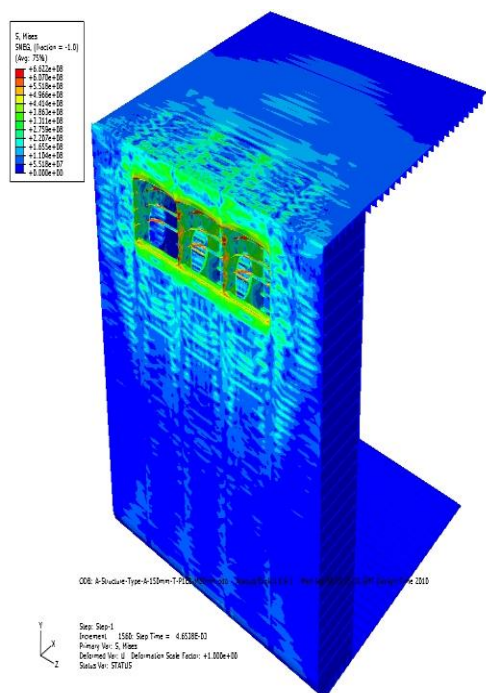


Figure 5.4(e)

Figure 5.4(f)

Figures 5.4 (c and d): Showing blast simulation result of the impact of blast Pressure of **1e+8 Pascal** on the above water side of the FPSO Nigeria (Type A Stiffened Plate)

Comment: From figures 5.4 (a-f), the Tee stiffener with the dimension 150mm x 14mm was subjected to blast pressure loading at the blast area with 80mm mesh. As could be seen, when a blast pressure of 1e+6 Pascal was applied which is equivalent to 0.2725kg of TNT, there was a slight indentation on the blast area. Additionally in figures 5.4c and 5.4d, when a blast pressure of 1e+7 Pascal was applied which is equivalent to 2.725kg of TNT, further indentation was observed on the blast area. However, further application of blast pressure of about 1e+8 Pascal equivalent to 27.25kg of TNT, there was a remarkable change in the blast analysis as seen in figures 5.4e and 5.4f. There was structural failure due to increase in imposed loading which causes structural failure of the plate and on individual stiffeners. The type of failure would be predicted by the applied blast pressure and on the strength of the plate and the stiffener type.

Type B (TB)-Stiffeners with flange size (200mm x 10.5mm thick) Applied Blast pressure (where bp-blast pressure 1e+6, 1e+7 and 1e+8 pascal, 80mm mesh)

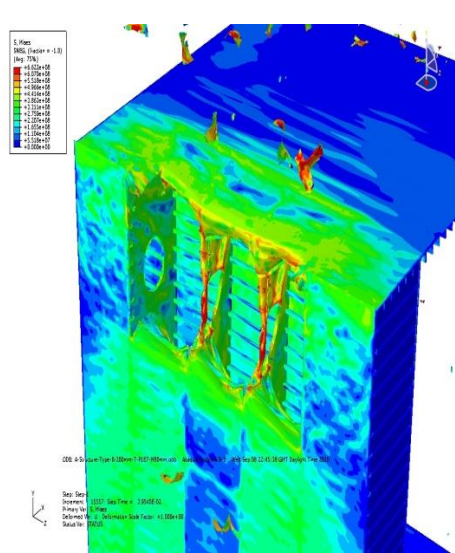
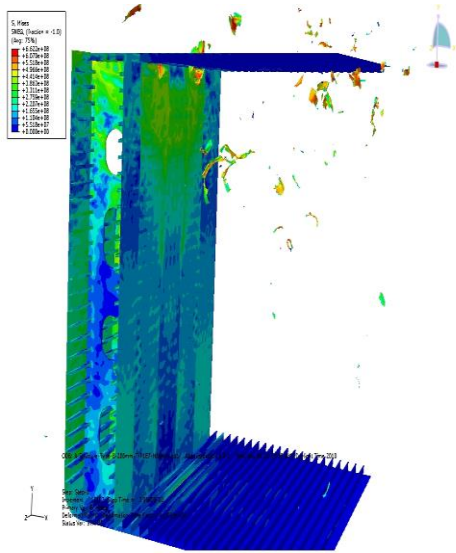


Figure 5.5(a)

Figure 5.5(b)

Figures 5.5 (a and b): Showing blast simulation result of the impact of blast Pressure of **1e+7 Pascal** on the above water side of the FPSO Nigeria (Type B Stiffened Plate)

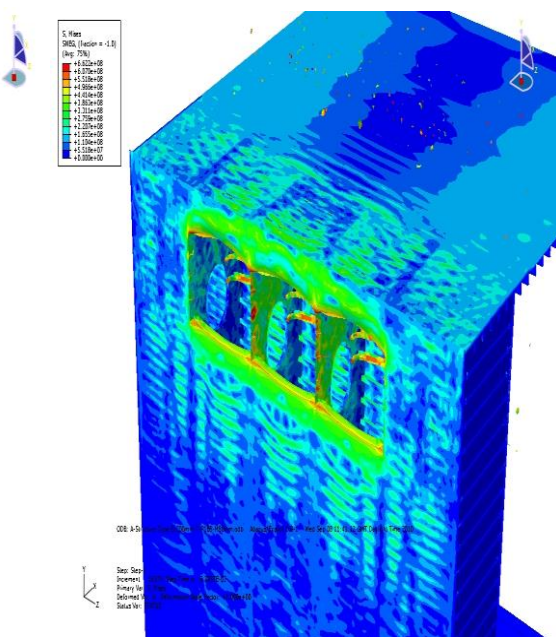
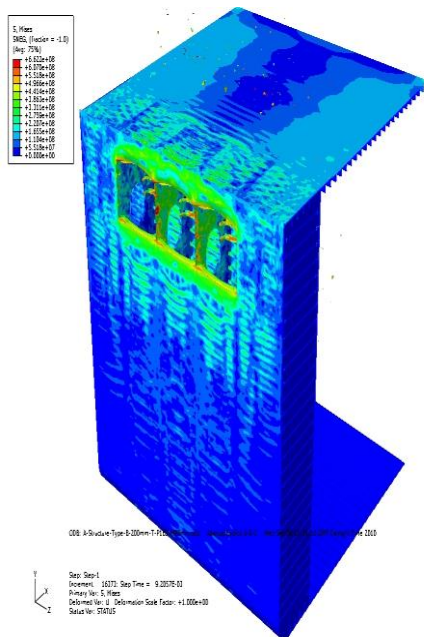


Figure 5.5(e)

Figure 5.5(f)

Figures 5.5 (e and f): Showing blast simulation result of the impact of blast Pressure of **1e+8 Pascal** on the above water side of the FPSO Nigeria (Type B Stiffened Plate)

Comment: From figures 5.5 (a-d), the Tee stiffener with the dimension 200mm x 10.5mm was subjected to blast pressure loading at the blast area with 80mm mesh. As could be seen, when a blast pressure of 1e+6 Pascal was applied which is equivalent to 0.2725kg of TNT,

there was a slight indentation on the blast area. Additionally in figures 5.5c and 5.5d, when a blast pressure of $1e+7$ Pascal was applied which is equivalent to 2.725kg of TNT, further indentation was observed on the blast area. However, further application of blast pressure of about $1e+8$ Pascal equivalent to 27.25kg of TNT, there was a remarkable damage the late and the stiffener as seen in figures 5e and 5f. There was structural failure due to increase in imposed loading which causes structural failure of the plate and on individual stiffeners. The damage here is slightly more intense than 5.4(a-f). This is due to the thickness of the flange and the length of the flange.

Type C (TC)-Stiffeners with flange size (250mm x 8.4mm thick) Applied Blast pressure (where bp-blast pressure $1e+6, 1e+7$ and $1e+8$ pascal, 80mm mesh)

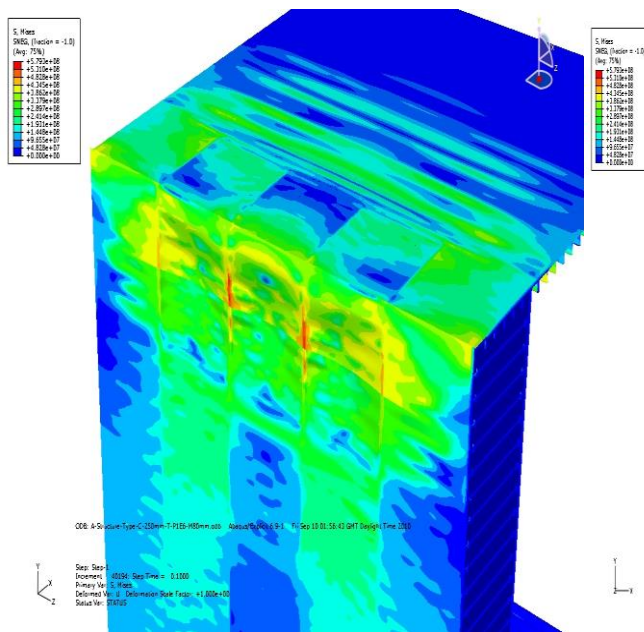


Figure 5.7(a)

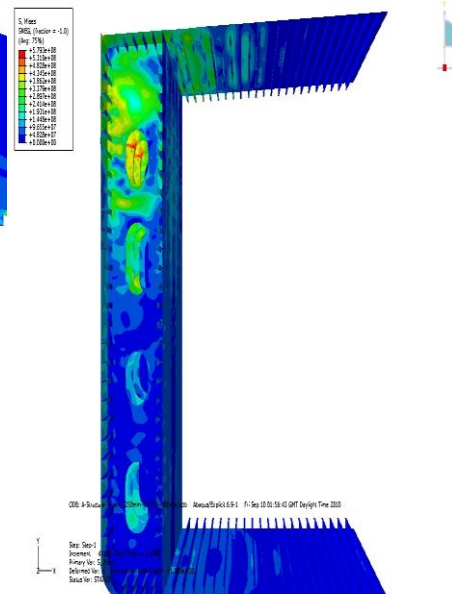


Figure 5.7(b)

Figures 5.7 (a and b): Showing blast simulation result of the impact of blast Pressure of **$1e+6$ Pascal** on the above water side of the FPSO Nigeria (Type C Stiffened Plate)

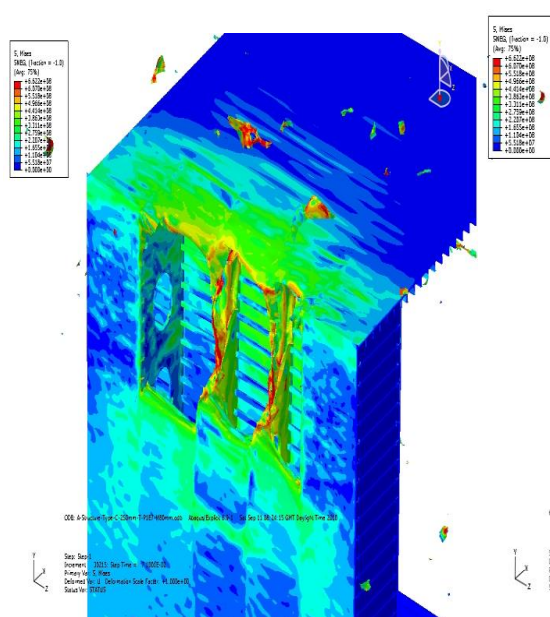


Figure 5.7(c)

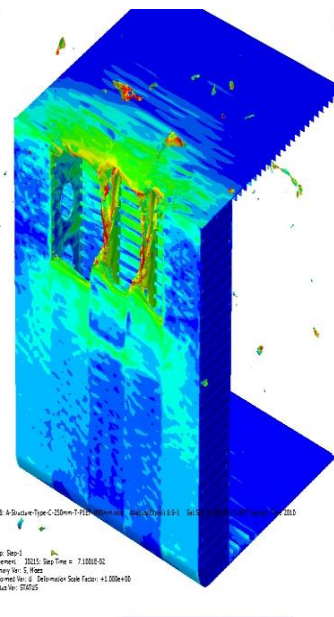


Figure 5.7(d)

Figures 5.6 (a and b): Showing blast simulation result of the impact of blast Pressure of **1e+7 Pascal** on the above water side of the FPSO Nigeria (Type C Stiffened Plate)

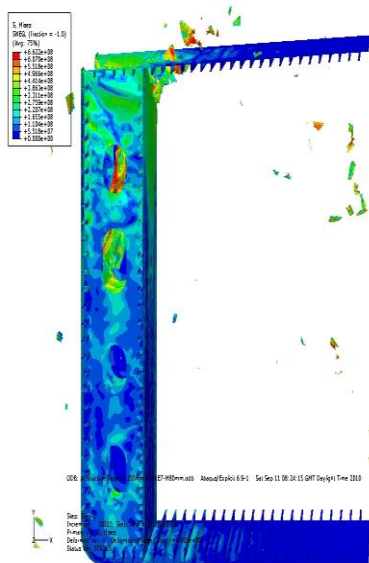


Figure 5.(e)

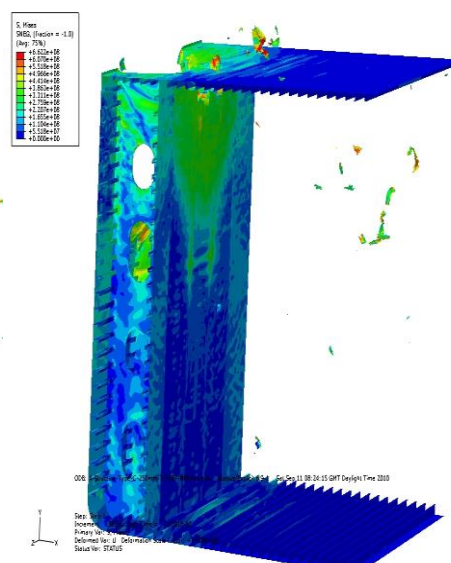


Figure 5.(f)

Figures 5.7 (e and f): Showing blast simulation result of the impact of blast Pressure of **1e+8 Pascal** on the above water side of the FPSO Nigeria (Type C Stiffened Plate)

Comment: Figures 5.7(a-f) is showing the blast simulation resulting from the application of blast pressure of 1e+6, 1e+7, 1e+8 Pascal which is equivalent to 0.2725kg, 2.725kg and 27.25kg of TNT applied to a midship section of the FPSO made up of a T stiffener size 250mm x 8.4mm. The FPSO is subjected to blast analysis using ABAQUS code. It was observed that the failure rate of

this particular type of stiffener ruptured faster than the other types of T stiffeners with flange thickness of 10.5mm and 14mm. The deduction here is that flange thickness is an important Parameter to be considered in the design and choice of a Tee stiffener. Now the L stiffeners would also be subjected to the same condition as the Tee stiffeners.

L STIFFENERS

Type D (TD)-L Stiffeners with flange size (150mm x 14mm thick) Applied Blast pressure (where bp-blast Pressure 1e+6, 1e+7 and 1e+8 pascal, 80mm mesh)

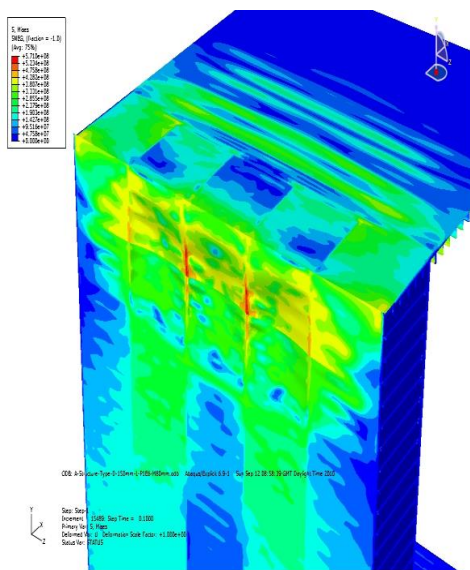


Figure 5.8 (a)

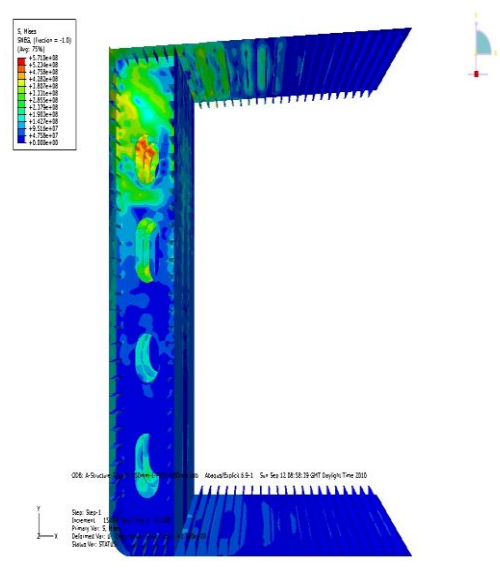


Figure 5.8 (b)

Figures 5.8 (a and b): Showing blast simulation result of the impact of blast Pressure of 1e+6 Pascal on the above water side of the FPSO Nigeria (Type D Stiffened Plate)

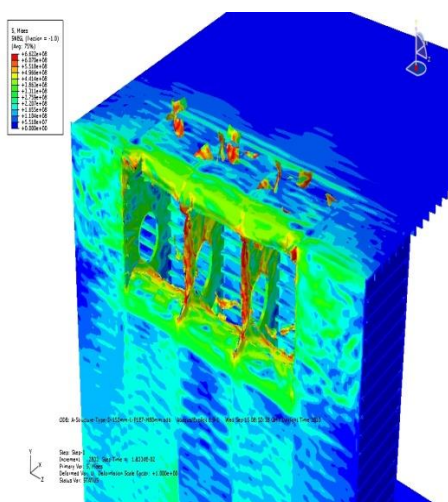


Figure 5.8 (c)

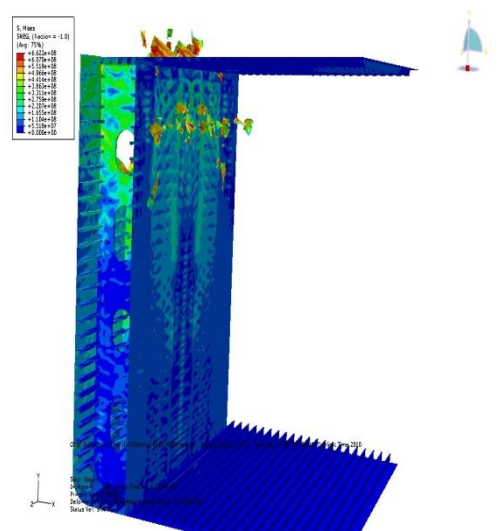


Figure 5.8(d)

Figures 5.8 (c and d): Showing blast simulation result of the impact of blast Pressure of **1e+7Pascal** on the above water side of the FPSO Nigeria (Type D Stiffened Plate)

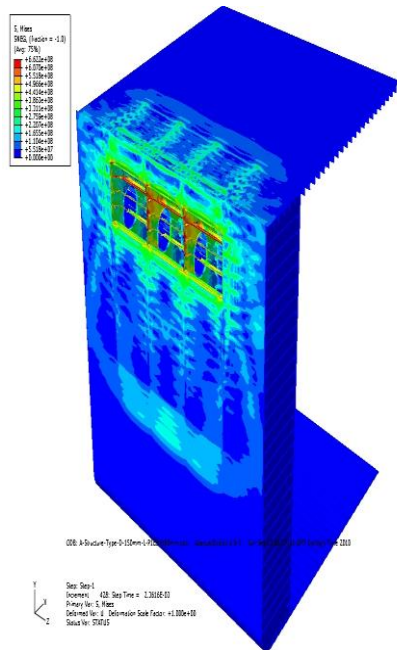


Figure 5. 8(e)

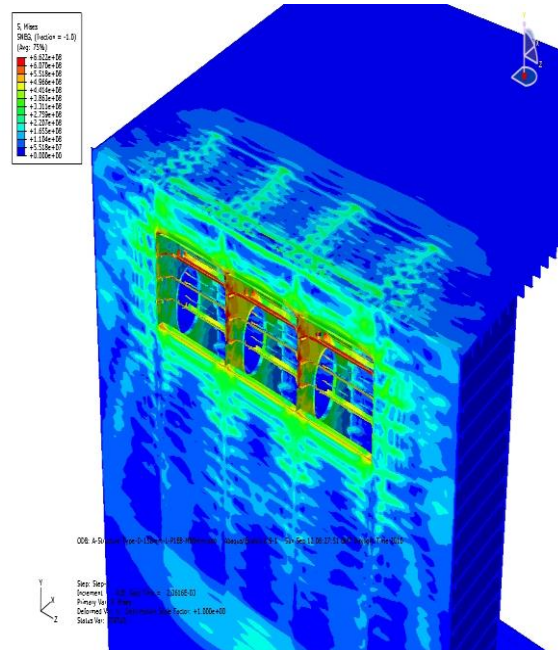


Figure 5.8(f)

Figures 5.8 (e and f): Showing blast simulation result of the impact of blast Pressure of **1e+8Pascal** on the above water side of the FPSO Nigeria (Type D Stiffened Plate)

Comment: Figures 5.8(a-f) is showing the blast simulation resulting from the application of blast pressure of 1e+6, 1e+7, 1e+8 Pascal which is equivalent to 0.2725kg, 2.725kg and 27.25kg of TNT applied to a midship section of the FPSO made up of a L (type D) stiffener size 150mm x 14mm. The FPSO is subjected to blast analysis using ABAQUS code. It was observed that the L stiffener with this size was able to withstand the blast pressure of 1e+6 Pascal to a particular state. However, when subjected to 1e+7 and 1e+8 ,it begins to gradually fail until its finally rupture. Parameter to be considered in the design and choice of a L stiffener is its ability of such stiffeners to withhold imposed loads.

Type E (TE)-L Stiffeners with flange size (200mm x 10.5mm thick) Applied Blast pressure (where bp-blast Pressure $1e+6, 1e+7$ and $1e+8$ pascal, 80mm mesh)

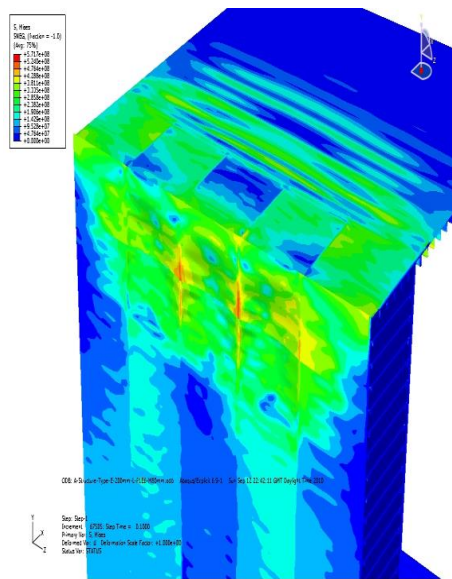


Figure 5. 9(a)

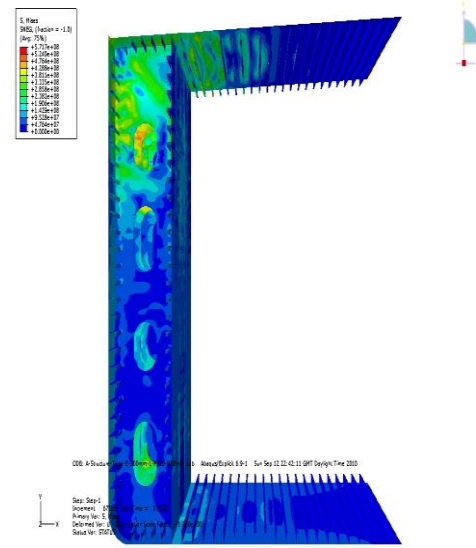


Figure 5.9(b)

Figures 5.9 (a and b): Showing blast simulation result of the impact of blast Pressure of **1e+6 Pascal** on the above water side of the FPSO Nigeria (Type D Stiffened Plate)

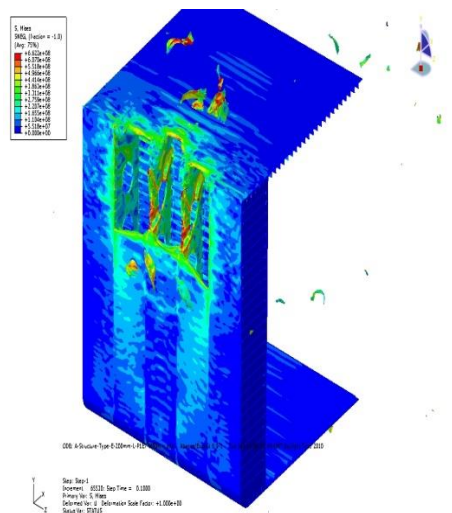


Figure 5. 9(c)

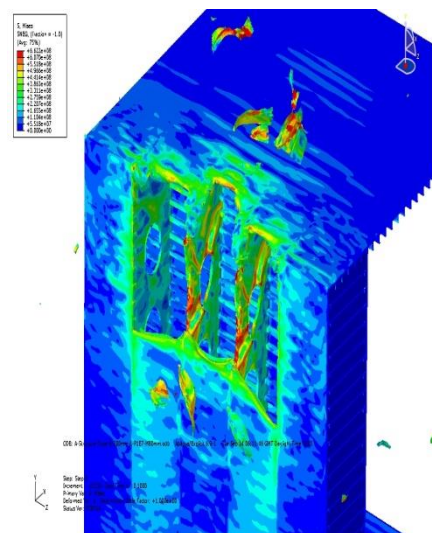
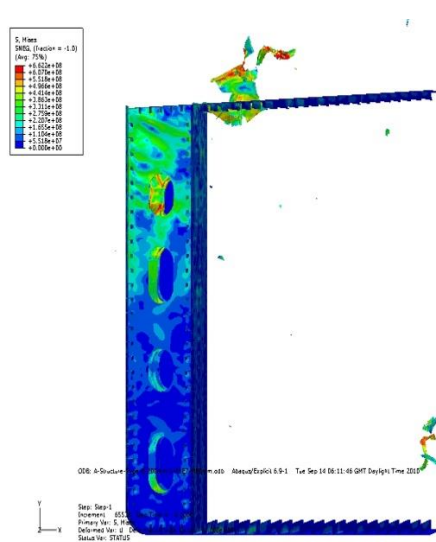


Figure 5.9(d)

Figures 5.9 (c and d): Showing blast simulation result of the impact of blast Pressure of **1e+7 Pascal** on the above water side of the FPSO Nigeria (Type D Stiffened Plate)



(Figure 5. 9(e))

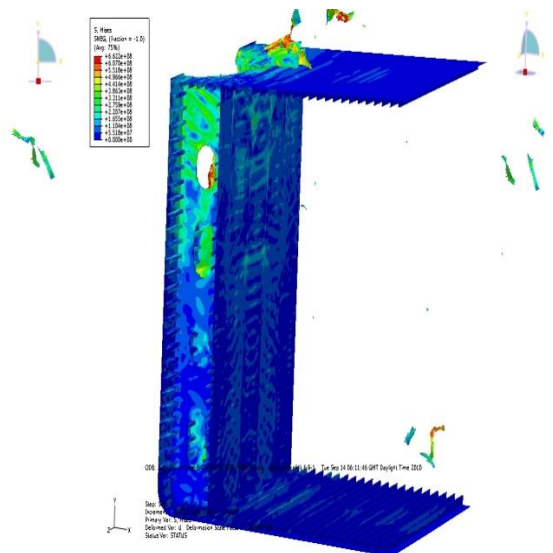
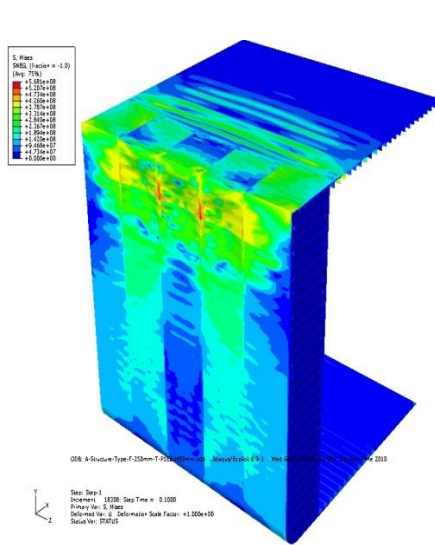


Figure 5.9(f)

Figures 5.9 (e and f): Showing blast simulation result of the impact of blast Pressure of **1e+8 Pascal** on the above water side of the FPSO Nigeria (Type E Stiffened Plate)

Comment: Figures 5.9(a-f) is showing the blast simulation resulting from the application of blast pressure of 1e+6, 1e+7, 1e+8 Pascal which is equivalent to 0.2725kg, 2.725kg and 27.25kg of TNT applied to a midship section of the FPSO made up of a L stiffener size 200mm x 10.5mm. The FPSO is subjected to blast analysis using ABAQUS code. It was observed that the failure rate of this particular type E stiffener took a slightly faster time to rupture than the L stiffeners with flange size of 10.5mm and 14mm. The deduction here is that flange thickness is an important Parameter to be considered in the design and choice of an L stiffener.

Type F (TF)-L Stiffeners with flange size (250mm x 8.4mm thick) Applied Blast pressure (where bp-blast Pressure $1e+6, 1e+7$ and $1e+8$ pascal, 80mm mesh)



(Figure 5. 91(a))

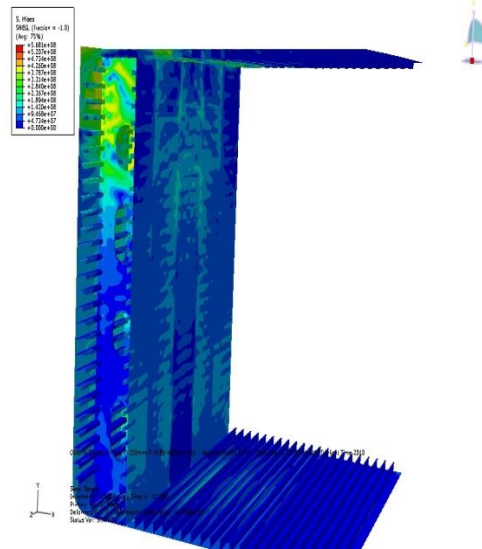
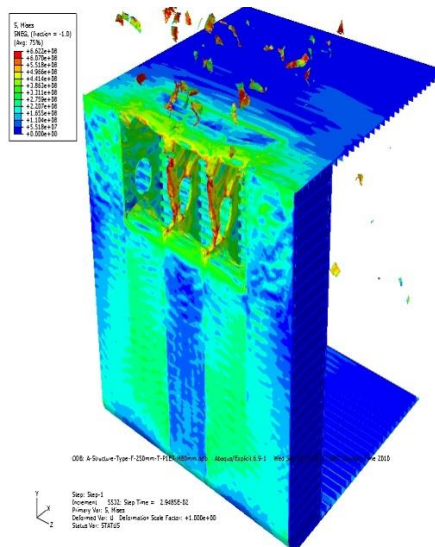


Figure 5.91(b)

Figures 5.91 (a and b): Showing blast simulation result of the impact of blast Pressure of **$1e+6$ Pascal** on the above water side of the FPSO Nigeria (Type F Stiffened Plate)



(Figure 5. 91(c))

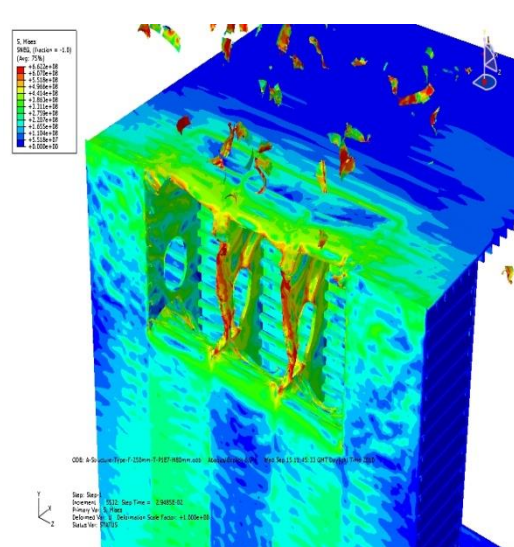


Figure 5.91(d)

Figures 5.91 (a and b): Showing blast simulation result of the impact of blast Pressure of **$1e+7$ Pascal** on the above water side of the FPSO Nigeria (Type F Stiffened Plate)



FIGURE 5.91: A TRUE STRESS STRAIN CURVE OF THE AREA BLASTED (FOR T STIFFENERS)

Where

- TAT-150-1PE7-M80 = Type A, T Stiffener (150mm x 14mm) with Blast Pressure 1E7 PA with 80mm Mesh.
- TAT-150-1PE6-M80 = Type A, T Stiffener (150mm x 14mm) with Blast Pressure 1E6PA with 80mm Mesh.
- TAT-150-1PE8-M80 = Type A, T Stiffener (150mm x 14mm) with Blast Pressure 1E8PA with 80mm Mesh.
- TBT-200-1PE8-M80 = Type A, T Stiffener (200mm x 10.5mm) with Blast Pressure 1E8 PA with 80mm Mesh.
- TBT-200-1PE7-M80 = = Type B, T Stiffener (200mm x 10.5mm) with Blast Pressure 1E7PA with 80mm Mesh.

The true stress–true strain curve which is also known as a flow curve increases continuously up to fracture. A comparison of the engineering stress –strain curves (E235A,E-S235B,E-2355) and a true stress-strain curves (S235A,S235B,S355)carried out by (Dow etal 2010) is shown below.

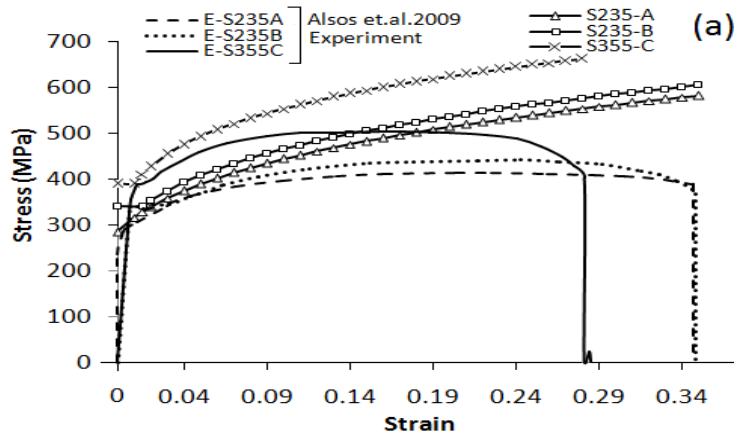


Figure 5.93: a. The stress strain curve (Curled from Abu-Bakr and Dow(2010)).

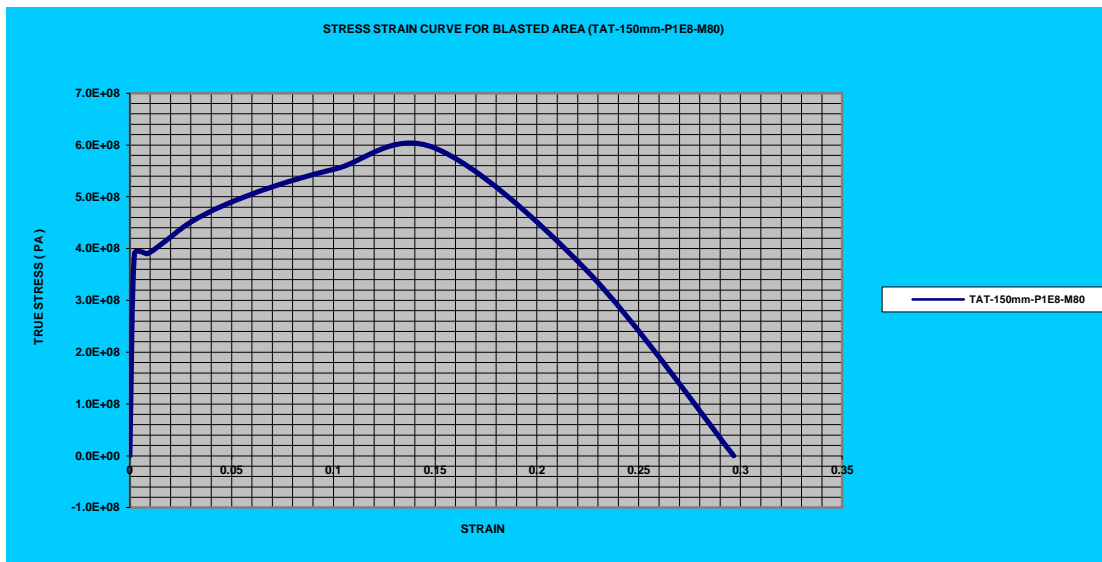


FIGURE 5.94: A TRUE STRESS STRAIN CURVE OF THE AREA BLASTED (FOR TYPE A STIFFENERS-150mm x 14mm with application of Blast Pressure 1e8 Pa)

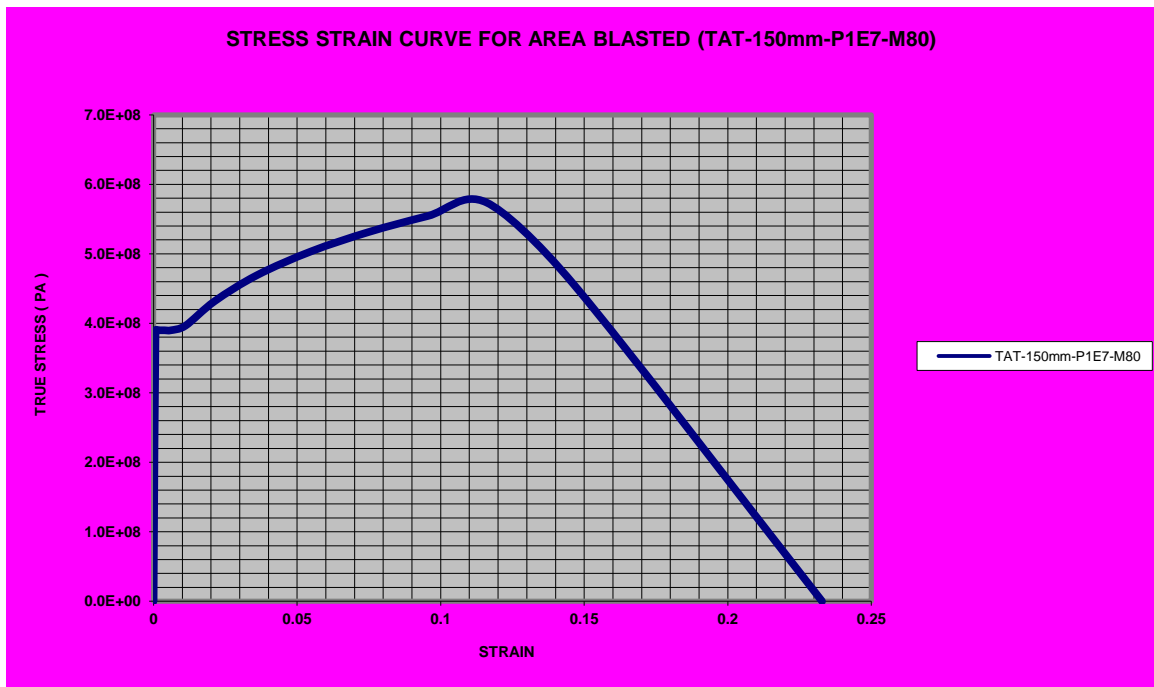


FIGURE 5.95: True Stress-strain curve for type A –T stiffener-150mm x14mm with the application of 1e7pascal blast pressure.

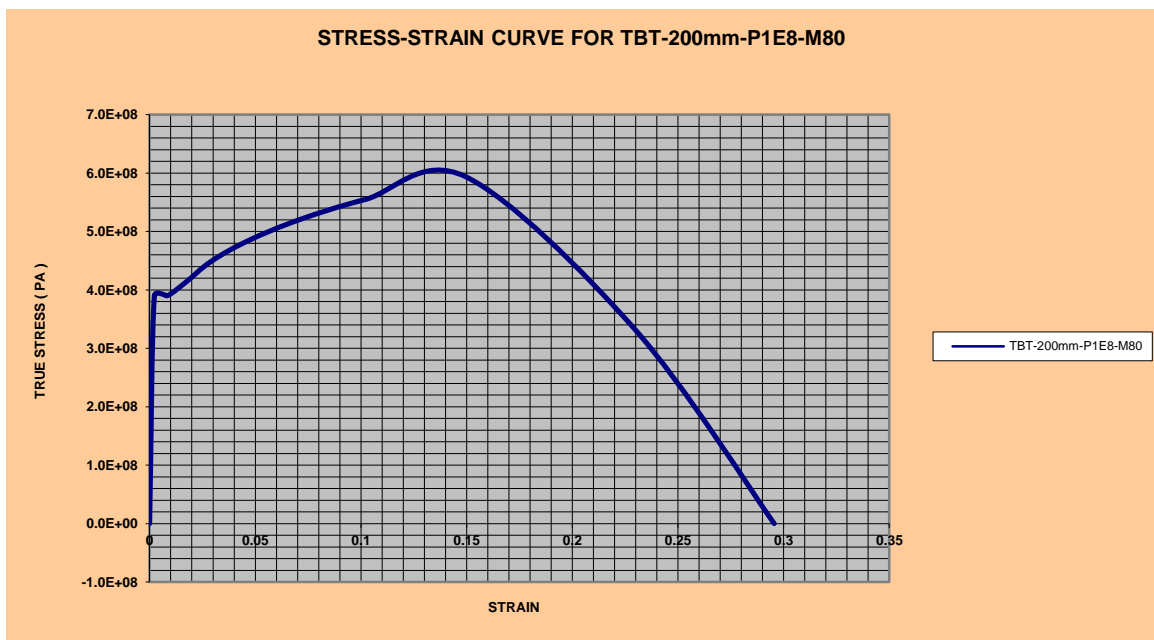


FIGURE 5.96: True Stress-strain curve for type A –T stiffener-200mm x10.5mm with the application of 1e8pascal blast pressure

A combined Energy graph for all the cases when a blast pressure of 1E8 Pascals was applied to T and L stiffeners is shown below.

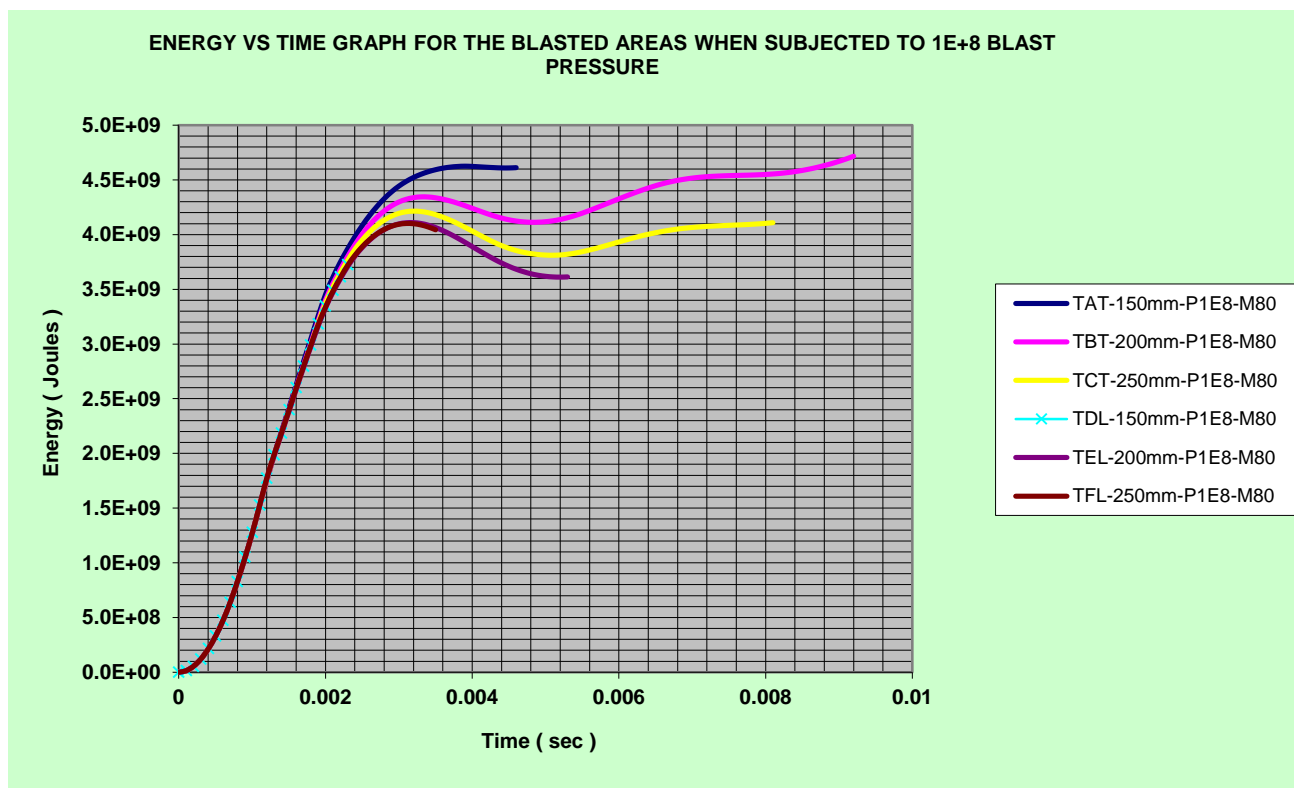


FIGURE 5.97: COMBINED ENERGY GRAPH FOR STIFFENNER T AND L when Blast Pressure of 1e8 Pascal was applied

Where

- TAT-150-1PE8-M80 = Type A, T Stiffener (150mm x 14mm) with Blast Pressure 1E8 PA with 80mm Mesh.
- TBT-200-1PE8-M80 = Type B, T Stiffener (200mm x 10.5mm) with Blast Pressure 1E8 PA with 80mm Mesh
- TCT-250-1PE8-M80 = = Type C, T Stiffener (250mm x 8.4mm) with Blast Pressure 1E8PA with 80mm Mesh.
- TDL-150-1PE8-M80 = Type D, L Stiffener (150mm x 14mm) with Blast Pressure 1E7PA with 80mm Mesh.
- TEL-200-1PE8-M80 = = Type E, L Stiffener (200mm x 10.5mm) with Blast Pressure 1E8 PA with 80mm Mesh

- TFL-250-1PE8-M80 = Type E, L Stiffener (250mm x 8.4mm) with Blast Pressure 1E8 PA with 80mm Mesh

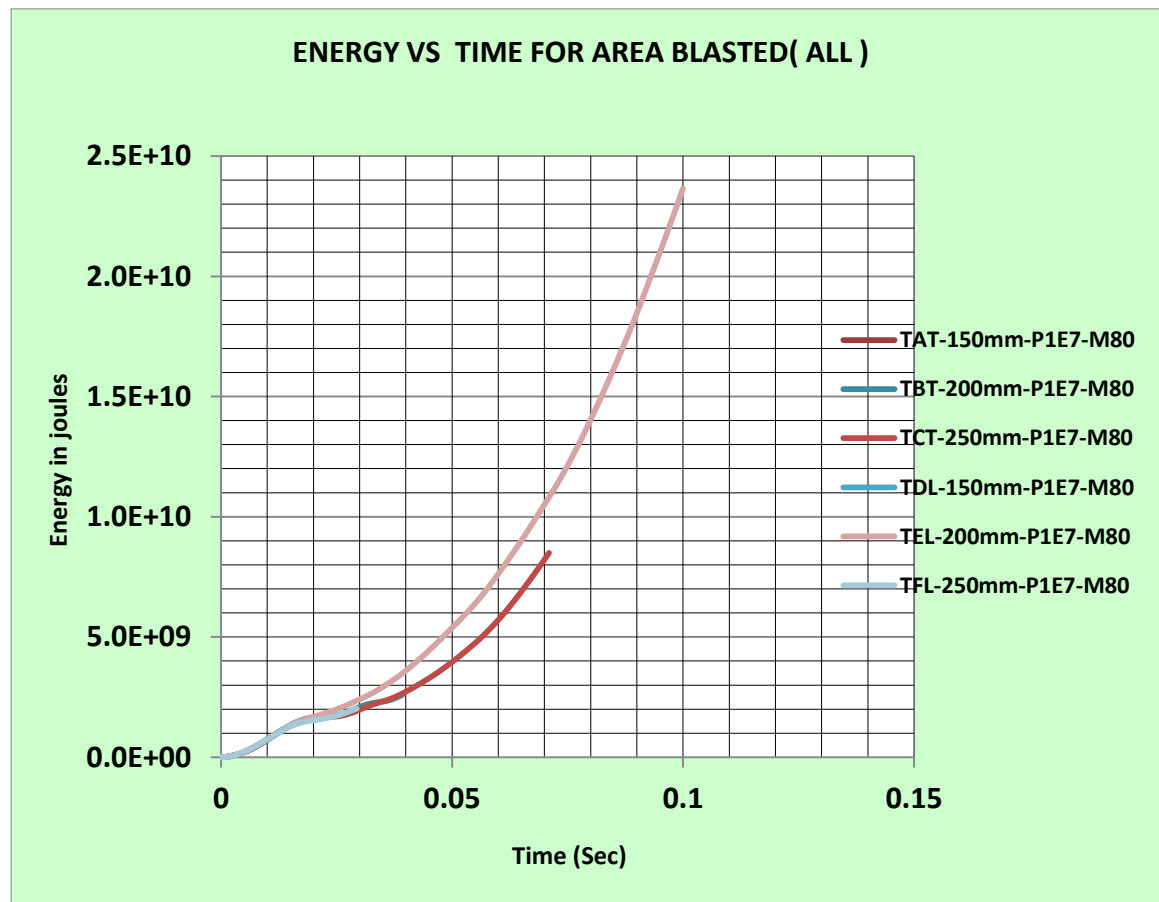


FIGURE 5.98: COMBINED ENERGY GRAPH FOR STIFFENNER T AND L when Blast Pressure of 1e7 Pascal was applied

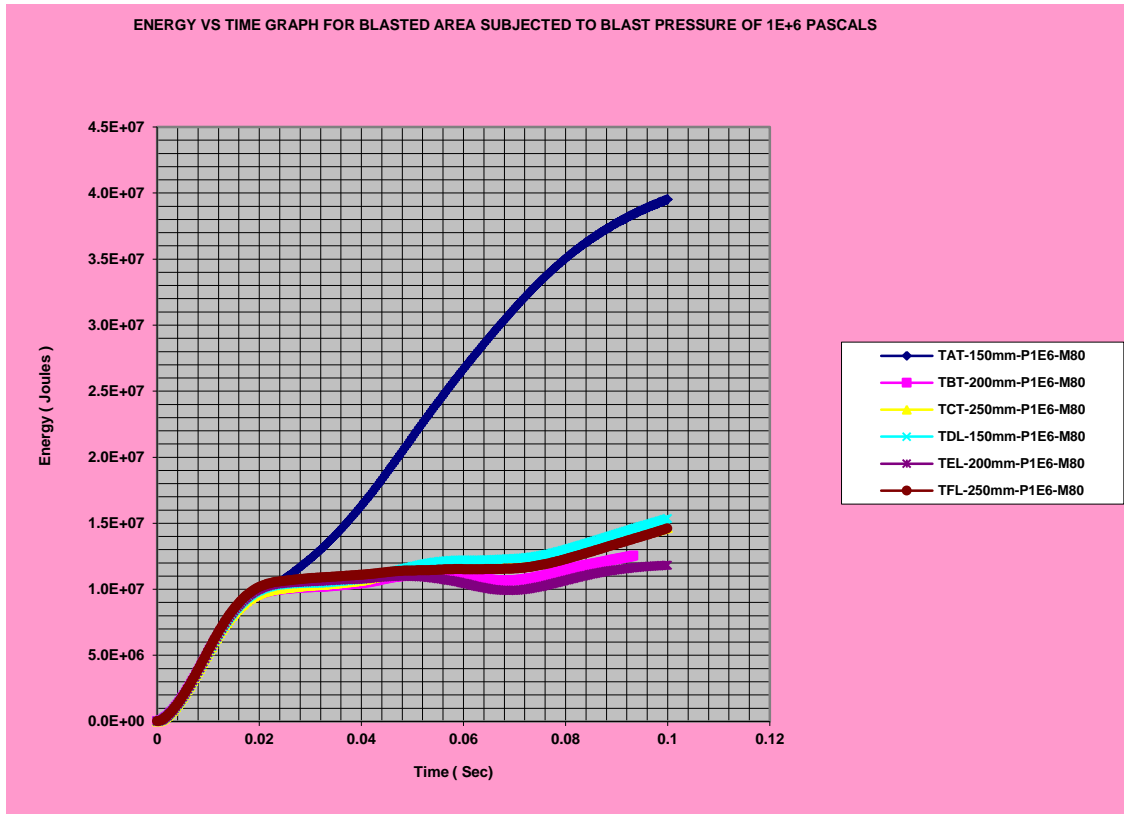


FIGURE 5.99: COMBINED ENERGY GRAPH FOR STIFFENNER T AND L when Blast Pressure of 1e6 Pascal was applied

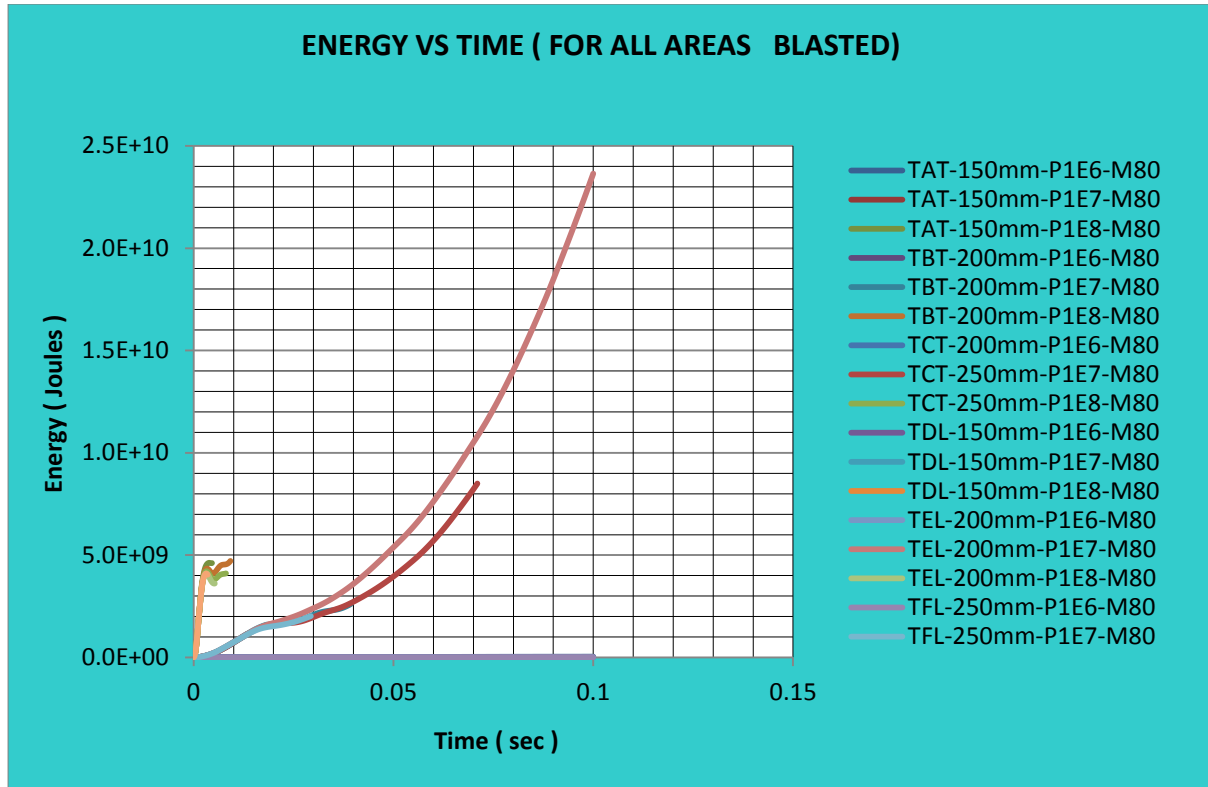


FIGURE 5.9.1: COMBINED ENERGY GRAPH FOR STIFFENNER T AND L when Blast Pressure with 1e6Pascals, 1e7Pascals and 1e8 Pascal was applied

5.8 DISCUSSION AND CONCLUSION

5.8.1 Determination of Rupture Strain

The rupture strain determined from this study from Figure 5.91 above fell between 0.24-0.30 and which correlates with the general range of rupture strain for mild steel which is between 0.21-0.35 and which depends on the strain rate which in the case of explosive impulse loading is very high. These rupture strain values fall within the range of values that was obtained for the same grade of steel by **Dow et al (2010)** as reflected in figures 5.92. Normally, the stronger the steel or high tensile steel, the lower the rupture strain because higher tensile steel is strain rate dependent. The tensile properties of structural steel are usually determined at relatively slow strain rates in order to obtain information appropriate for the designing of structures subjected to static or essentially quasi static loads, however, in the designing of structures that are subjected to high loading rates, such as those caused by high speed impact loads, the variation of tensile properties with strain rate may be considered.

5.8.2 Selection of Best Stiffener of the 6 Stiffener Type and Size Considered for Fpso Nigeria.

A stiffened panel is an assembly of plating and stiffeners (support Members). Even if the stiffened panel or its parts initially buckle in the elastic or even inelastic regime, the stiffened panel will normally be able to sustain further applied loads. The ultimate strength of the stiffened panel is eventually reached by excessive plasticity and or stiffener failure. Many researchers have contributed various approaches to the response capability of ship plating using conventional stiffeners for example **Timoshenko and Gere (1963)**, **Bleich (1952)**, **Paik et al (1998)** and **Paik and Thayamballi (2003)** especially on the elastic buckling coefficients of stiffeners under suitable selected conditions. However in the current wave of terrorism across the globe, there is the need for more in-depth studies on the need to carry out a stiffened arrangement or design that could be resilient to or reduce the effect of an above water attack explosive force on FPSOs operating in the Nigeria water by militants of the Nigerian Niger delta and to offer good solutions to ensure that the structural consequences of such an attack are reduced to the barest minimum, if not completely eliminated due to the volume of money being lost by the Nigerian

Government every month by this associated menace. Consequently during the analysis, 6 types of stiffener design were considered. Of the 6 stiffeners, 3 were T-section stiffeners while 3 were L-section stiffeners. All the 6 stiffeners had a constant web sizes and for flange areas, however the thickness and the sizes of the flanges varied in order to make a best selection for the FPSO Nigeria. The sizes of the flange for the T and L section stiffeners are as follows:

- a. TYPE A-150mm x 14mm = 2100mm² –T Section
- b. TYPE B-200mm x 10.5mm= 2100mm²-T-Section
- c. TYPE C-250mm x 8.4mm = 2100mm²-T-Section
- d. TYPE D-150mm x 14mm = 2100mm² –L Section
- e. TYPE E-200mm x 10.5mm= 2100mm²-L Section
- f. TYPE F-250mm x 8.4mm = 2100mm²-L Section

All the 6 stiffeners connected at different time to the same size rectangular plate and same web size were subjected to 3 different blast pressure loads at different times as could be seen from the blast results from FIGURES 5.5(a-f) -5.91(a-f). The 3 blast pressure forces that the stiffeners were subjected to were 1e+6 Pascal, 1e+7 Pascal and 1 e+8 Pascal this corresponded to 272.5grams(TNT), 2725 grams(TNT) and 27250 grams(TNT) respectively. They all responded in a different manner to the blast pressures as can be seen above in the blast results. However it was observed that even though the area of the flanges of the 6 stiffeners was the same, the blast pressure energy required to take the stiffeners to rupture differed considerably as can be seen from the energy-time graphs for the stiffeners. In figure 5.97 above, it can be seen that T stiffener type A with 150mm wide flange and 14mm thickness flange subjected to a blast pressure load of 1e+8 pascal (TAT 150mm-p1e+8 Pascal) required more energy to get to the rupture strain level than did the 5 other type of stiffeners (about 4.6e+09 Joules), this was followed by another T stiffener 200mm wide with flange thickness 10.5mm with the same blast pressure of 1e+8 pascal (4.3 e+09 Joules) while the T stiffener type 3 with flange width of 250mm and 8.4mm thickness required about 4.2e+09 to get to rupture. Expectedly, the L section stiffeners were damaged earlier than did the T-stiffeners. In that particular order, the stiffener type T with flange size 150mm x 14mm thick came to best, followed by

stiffener type T with flange size 200mm x 10.5mm thick and this was followed by stiffener type T with flange size 250mm x 8.4mm and this selection procedures aside from justification from numerical analysis, could be further validated from simple classical theory by the calculation of the second moment of area of the T stiffeners flange sizes which is calculated below. Strength of resistance to blast analysis of a stiffener is directly proportional to the second moment of area of the flange which is denoted by I. Thus the second moment of area of the 3 types of stiffener could be calculated as follows:

- For flange size 150mm x 14mm, $I = 1/12 \times bt^3 = 1/12 \times 150\text{mm} \times 14^3\text{mm}^3 = \mathbf{34300\text{mm}^4}$.
- For flange Size 200mm x 10.5mm, $I = 1/12 \times bt^3 = 1/12 \times 200\text{mm} \times 10.5^3\text{mm}^3 = \mathbf{19,293\text{mm}^4}$.
- For flange Size 250mm x 8.4mm, $I = 1/12 \times bt^3 = 1/12 \times 250\text{mm} \times 8.4^3\text{mm}^3 = \mathbf{12,348\text{mm}^4}$

5.9 Conclusions

Consequently, based on the above study and in order for Naval architects to design structures that are strong enough and capable of allowing the above water sides of an FPSO operating in the Nigerian Niger Delta being potentially subjected to a blast pressure attack, this section of the study was able to validate and establish the following:

- a. Of the 6 stiffeners configuration considered, it was observed that the stiffener with flange size 150mm x 14mm thick will require greater take energy to rupture than the other stiffeners did and by implication will be more resilient to blast loading than the other stiffeners considered in this study.
- b. T-Stiffeners whose flange area are the same with other stiffeners but with higher second moment of area still would be more resilient to blast pressure attack than those with same flange area but with lower second moment of area. This implies increasing the thickness and decreasing the width.
- c. The true stress-stress curve was established to conform to some past studies

and rupture strain for the blast area for the mild steel used was determined from the graph to have fallen within the 0.24-0.30 range and which correlates with the results from existing studies of the rupture strain of mild steel which falls between 0.21-0.30.

d. The FPSO plate could further be reinforced with extra large stiffener to make more it resilient to blast pressure loading.

e. Having selected the best T-stiffener for FPSO Nigeria in Chapter 6, the researcher went further in Chapter 7 to recommend the addition of ballistic protection of the above water sides of FPSO Nigeria in Chapter 7 in order to ensure a higher level of resilient of the FPSO Nigeria to blast pressure loading replica to the attack by the militant of the Nigerian Niger Delta in order to save the nation from the huge loss in foreign currency and the attendant consequences of danger that could results from this attack. Therefore, a cost benefit analysis was carried out by the researcher to justify the need for the use of ballistic protection of the above water sides of FPSO operating in the Nigerian Niger Delta.

f. As a general note ,the naval ship designers seems to prefer T-section stiffeners in the hull as they are less susceptible to damage due to an underwater attack e.g torpedo that explodes below the hull, etc.

CHAPTER 6

6. A Cost Benefit Analysis of Installing Anti Ballistic Material on the above water sides of FPSO Nigeria

6.1 Introduction

In this chapter, the researcher discusses the position of Nigeria as one of the larger oil producers in the world and of the importance of FPSO vessels which are being largely used in the Nigerian Niger Delta for oil explorations and extraction by the Nigerian Government and most of the multinationals that are operating in Nigeria. Furthermore the current wave of different types of criminality and of the vulnerability of these platforms leads to the necessity for the above water sides of these platforms to be well protected against potential blast pressure and other projectiles attacks resulting from the use of different types of explosive munitions are discussed. A cost benefit analysis was also carried out to further indicate that protection of the above water side surfaces of an FPSO is a necessity in the Nigerian waters and will largely result in a positive pay-off for the protection of lives and property and avoid pollution due to oil spillage.

6.2 Nigeria as an Oil Producing Nation

Nigeria is a major player in the world energy market. It is the seventh largest producer of oil in the world and it provides a fifth of the United States oil imports. Further, it is becoming an important supplier in the world list producers of global liquefied natural gas (LNG). Table 6 below shows Nigeria as one of the top world oil producers. Instability in world supplies and the critical importance of oil to the international economy has made Nigerian and more generally African oil to be a more strategic producer of oil and gas products due to its geographical location and the favourable relationship it has among the committee of nations **Augustine (2004)**. Consequently oil and gas and its product has become the life blood of the nation's revenues, its economic and national survival as well as the Armed forces of Nigeria which is one of the best trained in Africa and which is also financed from part of the nation's revenue and the Tax collections **Ogbomodia (2009)**. Between 2003 and 2010, oil and gas accounted for about 80.6% of the Federal Government receipts **Lawal (2011)**. However, the Nigerian oil belt which is located in the Nigerian Niger Delta region is embroiled in an armed the resistance against the Nigerian state and the multinational oil companies. The region is generally restive with lots of insurrections, armed rebellion, attack of oil and gas installations, platforms, wells and equipment such as fixed site oil tankers (FPSO) and oil pipelines, to mention but few.

of income for them to buy weapons. The direct link between bunkering, militancy, and conflict was demonstrated in the May 12–14, 2009, attacks on the camp of Tom Polo, a MEND leader and a bunkering kingpin in Delta State. The militants and the military had clashed over the protection of Tom Polo's bunkering interests, which was a trigger for massive air and land attacks by Nigerian armed forces (Army, Navy and Airforce) on the militants' strong hold before they were overcome **Maj General Dan Bazau (2010)**. These details further necessitate the need for the following analyses on the effects of explosive devices on FPSO vessels. It is perhaps useful to note that any future attacks on offshore oil installations including FPSO vessels, will probably employ a combination of weapons such as the ubiquitous rocket propelled grenades (a so called shaped charge device) and simple masses of explosive material e.g.(TNT e.tc) and which may includes solid particles forming shrapnel.

CHAPTER 6: A Cost Benefit Analysis of Installing Anti Ballistic Material on the above water sides of FPSO Nigeria

Table 6: Showing Top World Oil Producers, Exporters, Consumers, and Importers as at 2006
(Millions of barrels per day)

Producers ¹	Total oil production	Exporters ²	Net oil exports	Consumers ³	Total oil consumption	Importers ⁴	Net oil imports
1. <i>Saudi Arabia</i>	10.72	1. <i>Saudi Arabia</i>	8.65	1. United States	20.59	1. United States	12.22
2. Russia	9.67	2. Russia	6.57	2. China	7.27	2. Japan	5.10
3. United States	8.37	3. Norway	2.54	3. Japan	5.22	3. China	3.44
4. <i>Iran</i>	4.12	4. <i>Iran</i>	2.52	4. Russia	3.10	4. Germany	2.48
5. Mexico	3.71	5. <i>United Arab Emirates</i>	2.52	5. Germany	2.63	5. South Korea	2.15
6. China	3.84	6. <i>Venezuela</i>	2.20	6. India	2.53	6. France	1.89
7. Canada	3.23	7. <i>Kuwait</i>	2.15	7. Canada	2.22	7. India	1.69
8. United Arab Emirates	2.94	8. <i>Nigeria</i>	2.15	8. Brazil	2.12	8. Italy	1.56
9. <i>Venezuela</i>	2.81	9. Algeria	1.85	9. South Korea	2.12	9. Spain	1.56
10. <i>Norway</i>	2.79	10. <i>Mexico</i>	1.68	10. Saudi Arabia	2.07	10. Taiwan	0.94
11. <i>Kuwait</i>	2.67	11. Libya	1.52	11. Mexico	2.03		
12. <i>Nigeria</i>	2.44	12. <i>Iraq</i>	1.43	12. France	1.97		
13. Brazil	2.16	13. Angola	1.36	13. United Kingdom	1.82		
14. <i>Iraq</i>	2.01	14. Kazakhstan	1.11	14. Italy	1.71		

(source: Energy Information Administration-EIA)

NOTE: OPEC members in italics.

1. Table includes all countries with total oil production exceeding 2 million barrels per day in 2006. Includes crude oil, natural gas liquids, condensate, refinery gain, and other liquids.

2. Includes all countries with net exports exceeding 1 million barrels per day in 2006.

3. Includes all countries that consumed more than 2 million barrels per day in 2006.

4. Includes all countries that imported more than 1 million barrels per day in 2006.

6.3 Floating Production Storage and Offloading (FPSO).

A floating production, storage and offloading unit FPSO is a MOORED floating vessel used by the offshore oil and gas industry for the partial processing of hydrocarbons and for storage of oil. An FPSO vessel is designed to receive hydrocarbons produced from nearby platforms or subsea templates, partially process them, and store the crude oil until it can be offloaded onto a shuttle tanker or, less frequently, transported through a pipeline to the shore. FPSOs are preferred in frontier offshore small regions as they are easy to install, and do not require a local pipeline infrastructure to export oil. FPSOs can be a conversion of an existing oil tanker or can be a vessel built specially for the application. A vessel used only to store oil (without processing it) is referred to as a floating storage and offloading vessel **Wikipedia (2012)**. The technical advantages of FPSOs for oil field development are given below.

6.4 Technical Advantages of FPSO For Oil Field Development

The use of moored FPSO vessels for oil field development has several advantages compared to other types of production facilities such as fixed platforms, subsea-processing or other floating facilities such as semi-submersible platforms, tether leg platform, SPAR, etc. The main features of FPSOs are:

- a. **Mooring:** It can be installed in any water depth from 200 to 2,500 metres
- b. **Crude oil storage:** The hulls of the FPSO contains several large capacity tanks where crude oil is stored until an offloading operation to another tanker. This renders the development of a remote marginal field much easier as it is almost a stand-alone unit. Exporting the extracted crude oil does not require expensive subsea pipelines and nearby onshore port facilities.
- c. **Large area and payload for oil processing facilities.** The typically large main deck area offers more physical space than on other platforms. For an Oil Company, this means increased flexibility. Initially not all deck space may be needed for the processing modules. Later on the unused space can be used to add new equipment or modules. The possible modification of the FPSO during the production may therefore allow the increase in the production of the oil field or to connect to another field located nearby.
- d. **Relocation.** Once the production a field is completed, the FPSO may be relatively easily moved to another field. This operation is called a re-deployment as normally some

modifications on the FPSO may be required to cope with the new field peculiarities. On the contrary, fixed non floating platforms may only be transferred to a new location at a very high cost which renders this operation not economically viable.

Overall, those four main features create numerous opportunities for offshore field development. One of the main consequences is that an FPSO is not irrevocably associated to a specific field as a fixed platform is. The existence of a potential second life beyond the production of the specific field for which it has been designed gives an FPSO its own economic advantage over other oil and gas drilling and production platforms. Hence, the use of FPSOs in Nigerian waters for oil and gas exploration has been the country's choice and its advantages can not be overemphasised. For instance FPSO Bonger operating in the Nigerian water is one of the world's largest FPSO's. It receives crude from the production wells on the seabed. The oil is processed on board, stored and then sent to the single point mooring i.e a buoy anchored nearby that is used to transfer the crude to the receiving tankers for transport and export. When fully laden, Bonger weighs 300,000 tonnes **Shell (2012)**. In view of the enormous importance of these platforms to the Nigerian Government and indirectly to the world, there is, therefore the outmost need for the above water side surfaces of an FPSO operating in Nigerian waters to be well protected against possible terrorist attacks. Most importantly, production of oil and gas in Nigeria has helped to meet global demand for energy long into the future **Shell (2012)**. A further analysis of the importance of this study is highlighted in the Cost Benefit Analysis laid out below in section 6.5. Some of the FPSOs that are operating in the Nigerian waters also are listed in the table 6.1 below.

Table 6.1: Some of the FPSOs operating in the Nigerian Water

S/No	FPSO Description	Current-Operator	Field Operator	Location	Capacity	Remarks
(a)	(b)	(c)	(d)	(e)	(f)	(g)
1.	ABO	PROSAFE	AGIP	ABO	932	
2.	AGBAMI (CHEVRON)	STAR DEEPWATER JV	NNPC	AGBAMI OPL 216,217	1800	
3.	AKPO	TOTAL	TOTAL	AKPO OPL 246,OML 130	2000	
4.	ARMADA PERKASA	BUMI ARMADA	BUMI ARMADA	OKORO-SETU	400	
5.	BW OFFSHORE	BW OFFSHORE	SHELL	BONNY RIVER	472	
6.	BONGA(SHELL)	SHELL	SHELL	BONGA	1400	
7.	KNOCK ADOON	FRED. Olsen Production	ADDAX PETROLEUM	ANTAN	1700	
8.	MYSTRAS	AGIP ENERGY &NATURAL RESOURCES	AGIP NIGERIA	OKONO&OKONO FIELDS	1035	
9.	SEA EAGLE	SHELL	SHELL	EA (OML)	920	
10.	SENDJE BERGE	BW OFFSHORE	ADDAX	OKWORI,OKWORI SOUTH	920	
11.	TRINITY SPIRIT	CONOCO PHILIPS	Shebahe&p services	Ukpokiti	1700	
12.	USAN/UKOT	Total	Total	OPL 222-Usan	2000	

6.5 Cost Benefit Analysis on whether to Protect the Above Water Side of an FPSO Operating In Nigerian Water or not

Over the past few years, countries are being encouraged to make decisions on the design planning, and development of the safety of their future energy sources as well as to suggest strategies on how they intend to reach their objectives in order to eliminate and or reduce the potential effects of the wave of terrorism which is assuming increasing sophistication by the day especially in countries like Nigeria and other African countries. As a result, efforts have been on the increase to try to reduce to the minimum the consequences of the aggressive and ever growing wave of terrorism in the Nigerian Niger Delta **Abdulsallam (2009)**. Consequently this chapter provides a cost benefit analysis which is aimed at contributing to knowledge on the need to incorporate blast resistance materials on the above water side of an FPSO operating in Nigerian water. Cost-benefit analysis (CBA) - is a systematic process for calculating and comparing both the benefits and the costs of a project, of a government policy or of a decision. Thus as an example for over twenty years, in the United States, American presidents have required agencies

to perform CBA for major regulations; and one of the conditions to regulate is that only if the benefits of a regulation justifies its costs **USIS (2004)**. Consequently this study outlines a cost benefit analysis in order to show the cost implications and whether or not it is beneficial to incorporate blast resistance structures and materials in the FPSOs. The decision criteria for a cost benefit analysis is that for a project to be worthwhile to a nation, community, organisation and the resulting benefit must be greater than 1(one) and the net present value must be positive **Weston (2009)**.

6.6 Parameters of FPSO Vessel Nigeria in which Cost Benefit Analysis was Carried out and other Related Parameters

The important parameters of the FPSO Nigeria used in this cost Benefit Analysis are as follows:

- a. Name of FPSO = FPSO NIGERIA
- b. Length overall = 231.6m
- c. Breadth = 44.8m
- d. Depth = 23.8m
- e. Loaded Draught = 16.65m
- f. Oil storage capacity = 850,000 bbls
- g. Accommodation=55 persons
- h. Exposed side shell areas having loaded to capacity the FPSO
 $= (23.8-16.65) m=7.15m$
- J. Areas to be covered with anti ballistic material length wise = $(231.8m \times 2 \text{sides} - (\text{port and starboard}) \times 7.15m) = 3314.74m^2$
- K. Areas to be covered with anti-ballistic material width wise = $(44.80m \times 2 \text{sides} (\text{forward and aft}) \times 7.15m) = 640.64m^2$
- L. Total area to be covered with anti-ballistic material = $(J + k) = 3955.38m^2$

CHAPTER 6: A Cost Benefit Analysis of Installing Anti Ballistic Material on the above water sides of FPSO Nigeria

- L. Upper limit of Cost of anti ballistic material/m²=\$10,000/m²
- M. Lower limit of cost of anti ballistic material/m² =\$5,750/m²
- N. Current cost of crude oil per barrel in Nigeria as at September 2012 is \$102 per barrel
- M. Current cost of an FPSO of this standard and size i.e 850,000 barrel storage/tonnage=\$700,000,000.00
- N. Value of cargo content when at full load= 850,000 barrels x\$102 par barrel =\$82,110,000.
- O. Insurance of 55 maritime personnel @\$15,000,000 each=\$825,000,000.00
- P. Cleaning cost for oil spillage and damage to equipment (UN suggested \$1.5b for 30yrs which is \$50,000,000 per yr)
- Q. Production Gains- Currently Nigeria losses \$9,000,000,000/20=\$450,000,000 (3:6-losses to gain ratio per annum) =\$300,000,000,000
- R. Production Losses- currently Nigeria losses \$9,000,000,000/20=\$450,000,000 (3:6-losses to gain ratio per annum) =\$150,000,000.00
- S. Docking cost of FPSO per year including cost of fittings (5% of cost purchase) = \$35,000,000.00.
- T. Cost of anti ballistic and blast resistance materials including cost of delivery and fittings at upper limits of \$10,000/m² x 8712.20m²) = \$87,122,000.00
- W. Losses to the community through secondary bunkering (10%)=\$8,670,000.00
- X. Losses to treasury inform of Tax to state and federal Government (15% x (850,000x102) x12 =\$208,080,000.00

Table 6.2 Annual Benefits

S/No	Annual Benefit	Amount(\$)
(a)	(b)	(c)
1.	Averted loss of ship	700,000,000.00
2.	Averted loss of maritime personnel(insured for 55 personnel @ \$15,000,000.00	825,000,000.00
3.	Reduced safety insurance premium on ship	35,000,000.00
4.	Averted loss of cargo-content in-case of attack(850,000x102)	86,700,000.00
5.	Averted cost of environmental degradation (10%)	8,670,000.00
6.	Averted cleaning cost and damage to equipments	50,000,000.00
7.	Production gains	300,000,000.00
	Annual total benefit	2,005,370,000

Table 6.3 ANNUAL COST (OUTGOINGS)

S/No	Annual Cost	Amount(\$)
(a)	(b)	(c)
1.	Cost of docking FPSO	35,000,000.00
2.	Cost of anti ballistic materials(10,000x8712m2)	87,122,000.00
3.	Reduced safety insurance premium on ship	35,000,000.00
4.	Loss to the community in terms of secondary bunkering (10%)	8,670,000.00
5.	Loss to treasury inform of tax to state, federal govt and local government.(15% x850,000 x 102)x12	208,080,000.00
6.	Production losses.	150,000,000.00
7.	Other miscellaneous losses	100,000,000.00
	Total Annual cost	623,872,000.00

6.7 Decision Criteria for this Project

If the discounted present values of the benefits exceeds that of the discounted present value of the costs then the project is worthwhile. One of the conditions is that the net benefit must be positive .Another equivalent condition is that the ratio of the present value of the benefit to the present level of the cost must be greater than one.

Therefore from Tables 6.2 and 6.3

The present value of the benefits = \$2,005,370,000 ----- (1)

The Present Cost = 623,872,000.00----- (2)

Thus Present Value of the Benefit = (Present cost of the benefit/present cost)
= (2,005,370,000/623,872,000.00)
= 3.21>1(Condition 1 satisfied)

Condition 2 stipulates that the Annual Benefit must exceed the Annual Cost

=**\$2, 005,370, 000**>**\$623,872,000.00**

This is further tabulated below:

Present Value of the Benefit

Table 6.4 : Present Value of Benefit

Present cost of the benefits/present cost = 2,005,370,000/623,872,000.00 =3.21 which is greater than 1 = Project is viable and worth it.

6.9 Benefits Expected from the Study

The following benefits are expected to be gained by the Nigerian Government if carried out in order to prevent the potential consequences of the aggression of militants in the Nigerian Niger delta. The benefits are summarized as follows:

- a. As the lifespan of an FPSO ranges from 25yrs and above, hence the protection of the above water side of the FPSO with anti ballistic and anti blast material would offer a great greater resistance to blast pressure effects to a reasonable extent sufficient to avoid complete disintegration and material lost to the nation.
- b. Being resistant to blast means no significant loss of crude oil in the event of sabotage.

- c. Being resistance to blast means no local oil pollution and by extension no costly environmental degradation and threat to ecological status of the ocean. Currently, Nigerian Government and shell are having a case being held in the world court pertaining to current environmental degradation of Nigerian water
- d. No loss of revenue potentially resulting to billions of dollars which could have arisen due to vulnerability attacks by the Niger delta militants.
- e. Increase in the export capacity leading to more revenue income to Nigerian Government which would lead to more developmental projects and also increase in the foreign earning of the nation.
- f. Docking activities to effect repairs and install the anti ballistic material would attract foreign exchange to participating shipyards and enable technology transfer and create job opportunity for the locals.
- g. Enhancement of cooperation between local and international companies would be brought to bear.

6.10 Ballistic Protection Material

Very mechanically hard material have increasingly found utility in ballistic projectile protection as armour materials .Such hard materials often include metals and ceramics. Such hard materials functions, in part, by helping to break up an impacting a projectile into fragments (e.g in fighting vehicles) **Normandiaetal (2004)**.Although metals are theoretically well suited for ballistic protection application because they are generally dense and have high impact resistance properties, metals are also very heavy and thus of limited usefulness even if providing a hull strength structural function for weight critical applications however in contrast certain ceramic materials ,such as boron carbide, Luminas and silica have impact resistance properties on a par with metals but are lower in density and thus can serve as relatively lightweight ballistic protection materials e g body armour. Though light weight ceramic materials can be difficult to fabricate and thus can be of very high cost however the importance and cost savings that would be provided by the usage of this materials on the above water side of FPSO Nigeria vis a vis of the threat far outweighs the cost. Ballistic resistant materials are usually rigid but may be supple if in small overlapping plate form. They may also be complex such as Kevlar, lexan and carbon fibre composite materials as used in bullet proof jacket. It is therefore suggested that ballistic material such as composite material such as baron carbide,

Luminas and silica may be used. Additionally blast pressure resistance materials such as dyneema hard ballistic protection materials could be employed to counteract improvised explosive devices (IED) or the insertion of spall liners e.g. between the inner and outer hulls in order to stop fragment penetration and to reduce cone reduction in case of stress wave penetration e.g. HESH. Above all, the upgrading the FPSO to include a very high level protection is very possible by installing only at an acceptable extra weight and there by maintaining the vessels load carrying capacity. However, it would be desirable to have lightweight ballistic protection material that are easy to fabricate into final armour components at a reasonable cost, yet still offers ballistic protection properties on par with heavier armour materials. Such materials would find ready use in a number of applications especially the above water side of the FPSO Nigeria in order to make it completely resilient in conjunction with the vessel's structure to blast attack or at least to the barest minimum. The Nigerian government should approach the armour or ballistic protection manufacturer related industry to usefully prepare do with more robust design tools in order to design composite ballistic protection and forms of spaced armour for the threat levels as applicable to FPSOs operating in Nigeria water with a view to better manufacturing systems to provide that ballistic protection cost effectively. A typical ballistic resistance material composition is as shown below

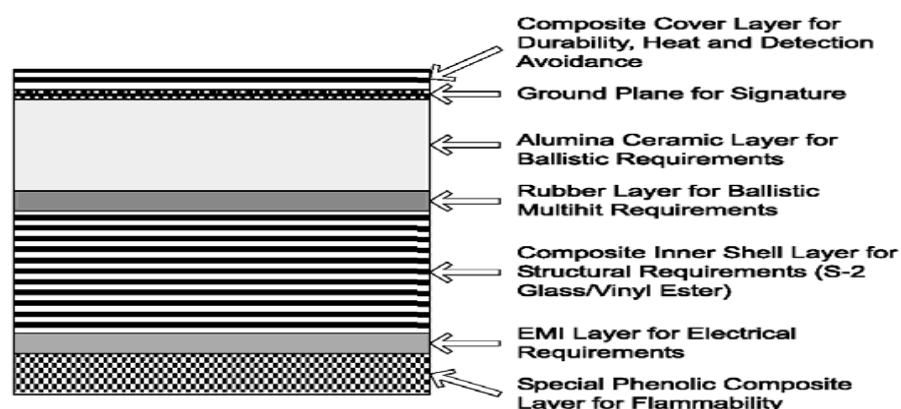


Figure 6.2: Typical arrangement of a composite ballistic protection material
(Source: United States Army Armament library)

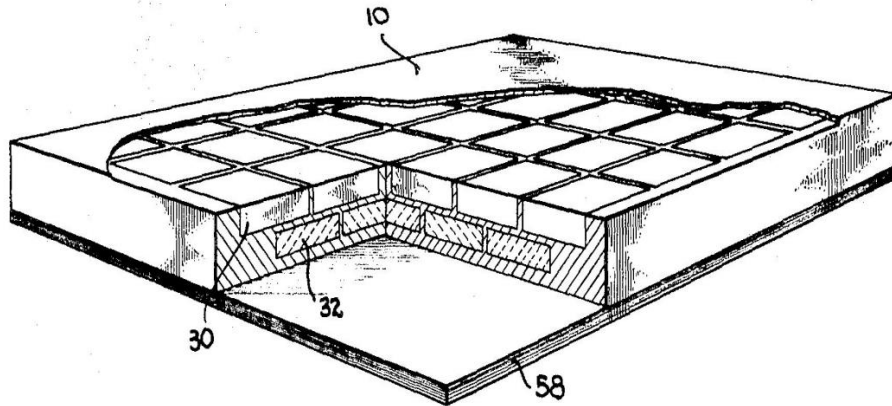


Figure 6.3: Isometric view of the typical arrangement of a composite ballistic protection material.
(Source: United States Army Armament library)

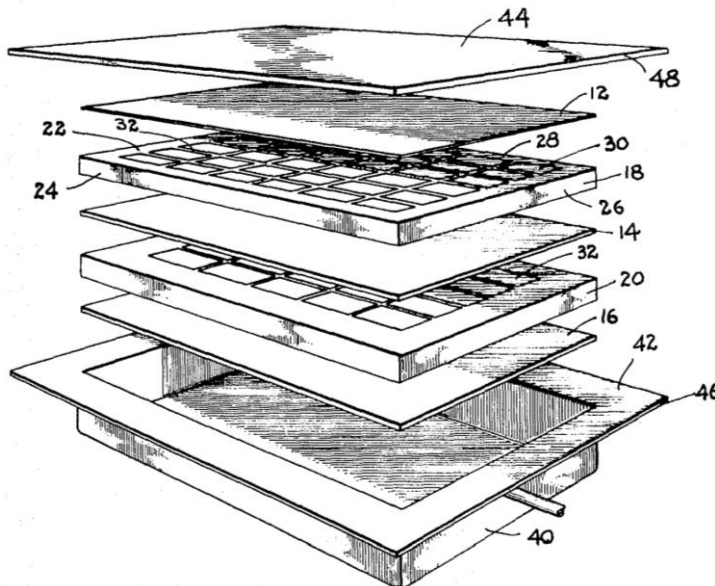


Figure 6.4: Vertical view of a typical arrangement of a composite ballistic protection material.
(Source: United States Army Armament library)

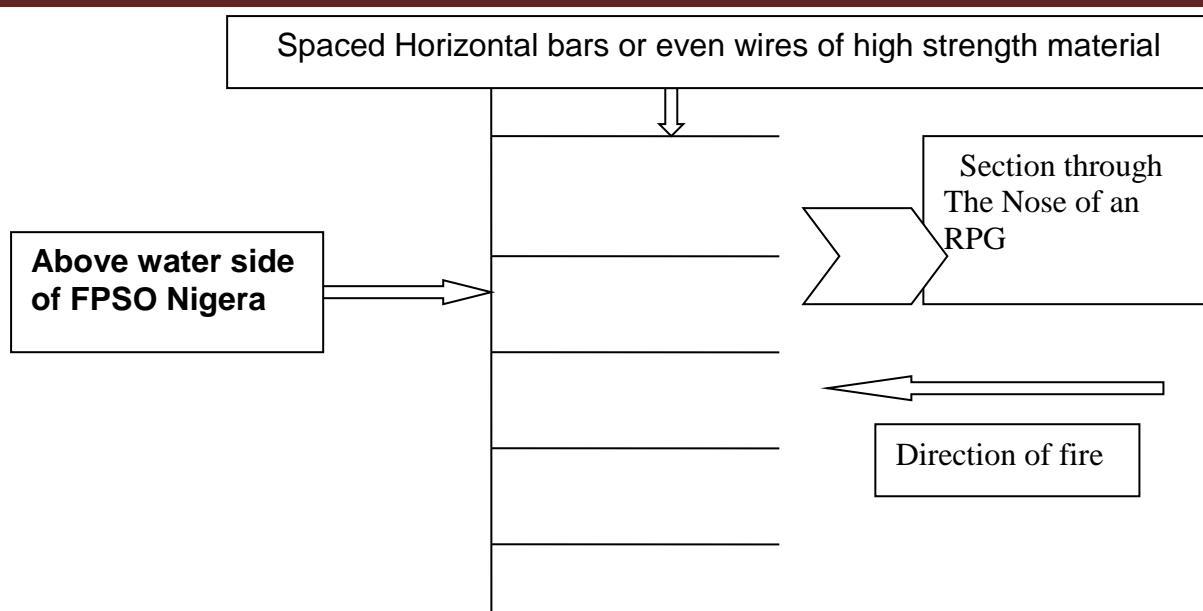


Figure 6.5: Simple Schematic diagram of a bar armour for the protection against shaped charger

6.11 Conclusion

The global political situation with the threats of direct conflicts and terrorist attacks is increasing the interest in ballistic protection for marine structures and armour for people, vehicles, oil and gas installations and other structures. The market for composites in marine structure is growing hence the potential for applications of composite materials in non-military use is also enormous and should be extended to the above water side of an FPSO and possible to top side structures and process equipment to counter RPG attacks and resultant damage and fires operating in Nigeria water in order to forestall an unexpected attack in the ever growing violent arena of the Nigerian Niger Delta where oil exploration and extraction is taking place. Positive efforts should therefore be initiated by the Nigerian Government towards the incorporation of some form of ballistic protection on its operational FPSOs in order to reduce the potential dangers highlighted earlier in this section, Hence projects should be initiated in the armour or ballistic protection industry in order to provide robust and composite design which highlights the incorporation of the ballistic protection materials according to the specific threats in a cost effective manner. The researcher was to ascertain through a Cost Benefit analysis that there was the need to carry out this task by the Nigerian Government and also suggested some composite ballistic material and other forms of protection for consideration however, mention was only

made on such areas as such areas would be recommended as areas for future studies. Most terrorist will employ either a simple mass of explosive material or a rocket propelled grenade ,a RPG and not more sophisticated projectiles .The fitting of bar armour ,as seen on many military vehicles in combat zones, provides at a minimum weight ,a high level of protection against HEAT ,shaped charge, attacks e.g RPGs (Rocket propelled grenades) e.g. The simple bar armour ,and other against HEAT projectiles and not against the extreme blast pressures as caused by the simple detonation of a mass of explosive material along side a vessel. Hence the needs for both exclusion zones (Using offset fenders) and hull structures that are less damaged by large over pressures, etc.

CHAPTER 7

7. Conclusion and Recommendations for further work

7.1 Introduction

This chapter presents an overall summary of the research that was conducted in this thesis, including the main conclusions that were obtained from the research as well as providing some recommendation for further research.

In Section 7.2, the researcher presents his rationale from a different perspective for the research conducted in this research. Based upon his rationale, an overall summary of the work conducted in each chapter is presented including the re-statements of the aim and specific objectives of the work in a logical sequence and that are given in Section 7.3, Finally in Section 7.4, the main conclusions obtained from the thesis are presented while recommendations are proposed for future work in Section 7.5

7.2 Rationale of the Research

The scholars' main motivation in conducting the research presented in this thesis stems from his desires to make a contribution to the following:

- a. The design of the above water side of an FPSO in order for it to withstand blast pressure attack that could possibly be inflicted on them by the militants of the Nigerian Niger Delta or other invaders. FPSO is a major component of oil and gas exploration and extraction in Nigeria and Nigeria is a major world oil player.
- b. Carry out a Cost Benefit analysis on the need to use composite anti ballistic protection material on the above water sides of an FPSO in order to make it resilient to blast pressure attacks or at least to reduce the effects of such an attack to the barest minimum. More over the researcher is a serving in the Nigerian Navy who was sponsored by the Petroleum Trust Development Fund (PTDF) for this topic.

At the start of this research studies, an average of 400,000 barrels of crude oil per day is missing in Nigeria daily. It means that Nigeria and her operating partners may be losing a cumulative estimate of \$40m (about N6bn) per day at a current price of \$100 per barrel of crude oil. This translates to an estimated N2.184 trillion per annum or \$480,000,000.00 per annum. These losses are so huge to a developing nation like Nigeria and it results from different sources and the sophistication is increasing day by day. Therefore there was a need for this study.

7.3 Summary

Based upon the above rationale, the aims and objectives of this research was specified to *come out with a modest improvement in the design of an FPSO so that it would be more resilient to a larger extent, to a possible above water crude attack by considering different sizes of T section Stiffeners and L section Stiffeners, to carry out a cost benefit analysis of the need to use an anti ballistic composite component on the above water sides of an FPSO and to focus on how to minimize the effects of an air blast pressure attack on an FPSO, and then to recommend further passive means and strategies in order to further achieve a design that would negates the potential activities of terrorist potential in the Niger Delta of Nigeria.*

In order to achieve the stated aims and objectives, the researcher identified his tasks in the following sequence:

- a. *The first objective was to carry out a critical literature review of the blast analysis methods on structures and specifically on plain plates and on stiffened flat plates.*
- b. *The second objective was to apply the finite element analysis techniques using the commercially available ABAQUS software to analysis the non linear displacement and stresses of plates and stiffened panels of an FPSO under different boundary conditions and aspect ratios in order to then validate the results obtained from ABAQUS software code with that obtained from classical theory (Roark's formula)*
- c. *The third objective was to further carry out plate and stiffened plate analysis with much emphasis on the actual side shell panels of the representative FPSO considered and to carry out Frequency Extraction Analysis of plate and stiffened plate again using the Abaqus software code and validate with those generated from classical theory in order to avoid resonance.*
- d. *The fourth objective was to carry out a Nonlinear Analysis of stiffened plates of the midship section side shell of FPSO Nigeria subjected to various blast pressure loadings in an explicit non linear dynamic analysis state*
- e. *The fifth objective was to identify the unique blast pressure loads that are capable of causing economic damage to the structural members of the midship section of an FPSO considered when attacked or exploded from the above water point specifically the stiffened plate panel and to identified the best stiffener configuration amongst the various*

types of stiffeners considered at the midship section of the FPSO by carrying out an assessment of standard FPSO structure using the Abaqus finite element analysis.

g. The sixth objective was to determine the steel material's rupture strain level.

h. The seventh and final objective was to under take cost benefit analysis on the consequences to Nigeria as a nation on the need to use anti ballistic composite components on the above water part on an FPSO vis a vis the amount that would be lost to Nigerian Government should an attack be carry out on the FPSO by militants of the Niger Delta.

The above aims and objectives have been satisfied through the work that has been undertaken and presented in eight chapters of this thesis.

Chapter One included the author's motivation, aims and specific objectives of the thesis as already summarized in Section 7.1 of this thesis from a different point of view as well as layout so as to familiarize the reader with the progressive research presented in this thesis.

Chapter Two Addresses the first objective and specifically dwells on providing a review of explosion and blast loading effects on structures especially on stiffened plates.

Chapter Three specifically addressed the second objective where the finite element analysis was carried out using ABAQUS software in order to analysis the displacements and stresses of plates under different boundary conditions and aspect ratio loading in order to validate the results obtained from ABAQUS software code with that obtained from classical theory (Roark's formula) in order to ensure that results are consistent with those of classical theory.

Chapter Four specifically addressed the third objective where the finite element analysis was carried out undertaking Frequency Extraction Analysis of plates and stiffened plates from the actual panels of FPSO Nigeria using ABAQUS software code under different boundary conditions and aspect ratios in order to validate the results obtained from ABAQUS software code with those obtained from classical theory (Roark's formula) in order to ensure that results generated by ABAQUS is also consistent with those of classical theory and as a guide against resonance developing.

Chapter Five specifically addressed the fourth objective where Nonlinear Analysis of stiffened plate of the midship section of FPSO Nigeria subjected to blast pressure loading in an explicit non-dynamic analysis state and undertaken using the ABAQUS software code under different boundary condition was carried out. It included further frequency extraction analysis to obtain natural frequencies with effects of damping and high material strain rate effects as the well as effects of plasticity using ABAQUS Explicit Finite element code

Chapter Six specifically addresses the fifth and sixth objectives which was to examine the effects of blast pressures loading on the midship section of the FPSO by considering different sizes of T section stiffened and L section stiffened plates with a view to determine the best stiffener size amongst the ones considered that would be able to withstand blast pressure loading to a greater extent and to determine that blast pressure load capable of causing rupture and to determine the associated rupture strain, limit of the steel.

Chapter Seven: specifically addressed the seventh objective where s cost benefit analysis was carried on the benefits of using an anti ballistic composite component on the above water side hull part on an FPSO vis a vis the financial amount that would be lost to the Nigerian Government should an attack be carried out on the FPSO by militants of the Niger Delta.

Chapter Eight: Concludes the thesis and presents an overall summary of the research that was conducted in this thesis, the principal discussions and main conclusions obtained from the research, as well as recommendations for further research on the subject.

7.3 Main Conclusions

Based upon the work carried out in this research study, the following main conclusion are obtained

1. In order for naval architects to design structures that are strong enough and capable of allowing for the potential effects on the above water sides of an FPSO operating in the Nigerian Niger Delta and that may be subjected to a very close by

explosive blast pressure attack, this section of the study was able to validate and establish the following:

- a. Of the 6 stiffeners configuration considered (T section and L section stiffeners having flange sizes-150mm x 14mm, 200mm x 10.5mm and 250mm x 8.4mm) used in FPSO Nigeria and subjected to blast pressures of $1e+6$, $1e+7$ and $1e+8$ Pascal, it was observed that the T-stiffener with a flange size of 150mm x 14mm thick will take a longer energy pressure and pulse to reach rupture than the others and by implication will be more resilient to blast loading than other stiffeners considered in these studies.
- b. T section -Stiffeners whose flange area are the same with other stiffeners that were examined but with a higher second moment of area of the flange on its own would be more resilient to a blast pressure attack than those with same flange area but with lower second moment of area i.e. of a lesser thickness.
- c. The true stress-stress curve of the hull steel was established to conform to some past studies.
- d. The rupture strain for the blast area of the mild steel used was determined from the graph to have fallen within a range of 0.24-0.30 and which correlates with earlier studies of the rupture strain, at high strain rate of mild steel which falls between 0.21-0.30.
- e. The FPSO side shell plates could further be reinforced with super stiffener to make them more resilient to blast pressure loading.
- f. Frequency Extraction Analysis for the midship section of FPSO Nigeria was established and therefore resonance can be avoided.
- g. ABAQUS software was validated to be an excellent software code for considering forces due to blast in structural analysis.
- h. All validated stress and displacement calculations are good reference point for new students and researchers to this area.
- i. A Cost Benefit Analysis was generated by the researcher on the need for the Nigerian Government to incorporate composite ballistic protection material on the above water side of all FPSO operating in the Nigerian Niger Delta.
- j. High strength ballistic protection could be incorporated on its operational FPSOs in order to reduce the potential dangers highlighted earlier in this thesis.

7.4 PASSIVE PROTECTION

K. Introduction of a continuous ring of water booms positioned at about 1000m round the operational areas of FPSOS to prevent small craft laden with explosives from reaching the FPSO and with installation of aircraft detection equipment

I. 24hrs surveillance by highly formidable forces, well trained and formed up anti terrorist squad through cooperation of super powers to deter terrorists from approaching installaions

m. Showing of more presence and introduction of death penalty for terrorist amongst others.

n. Training of military and infrastructural protection development for oil community areas.

7.5 Recommendations

Because of the limited resources and time, the boundaries of the research have been restricted to the objectives stated. Based upon these facts and the main conclusions stated, further research work can be recommended in mainly five areas:

- a. Underwater attack that was not covered in this thesis
- b. Consideration of other shapes of stiffeners other than T and L stiffeners
- c. Intensive research in areas of composite ballistic component that would reduce effect of weight.
- d. The installation of bar armour and more recent similar development, to both the hulls and topside to provide some passive resistant to rocket projectiles, e.g RPGs
- e. Examine the intrinsic resistance capabilities of double hull tankers forms to rocket projectiles attacks, e.g RPGs.
- f. Other areas are the introduction of a bar armour as being a modern above water form of anti-torpedos below water nets that were used on some naval ships when in harbour in the early 1900. This could be an areas for further research.

Appendix

Appendix A

FREQUENCY EXTRACTION ANALYSIS FROM ABAQUS VALIDATION CASE (1-8)

Here the frequency extraction analysis reflected below in this appendix are frequency modes for modes 4 and 6 for plates thickness

5mm,8mm,10mm,12mm,15mm,18mm,20mm,25mm and 30mm thickness reflected as cases 1-8 for different boundary condition carried out by using abaqus software codes

CASE 1. 2mX2mX0.005M- FIX FIX BOUNDARY CONDITION

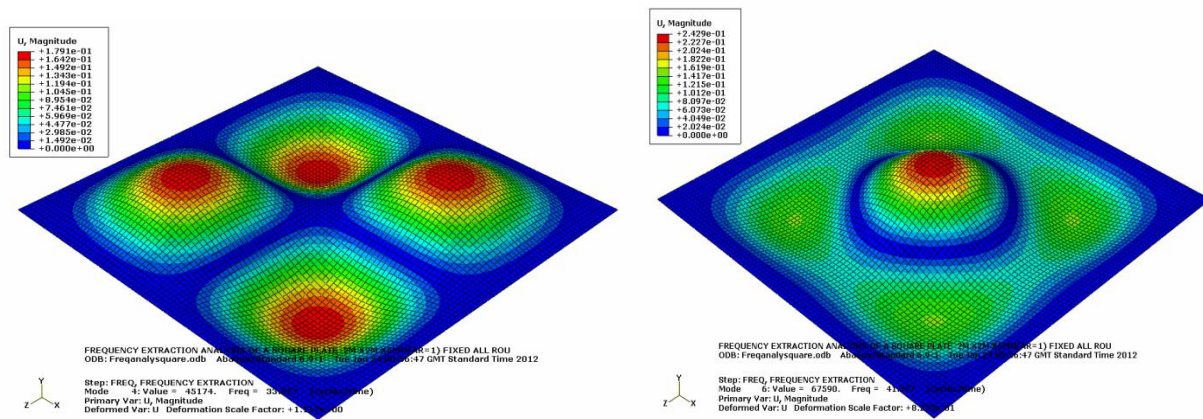


Figure A-1:Frequency extraction analysis of a 2mx2mx5mm plate showing mode4-6

CASE 2. 2mX2mX0.008M- FIX FIX BOUNDARY CONDITION

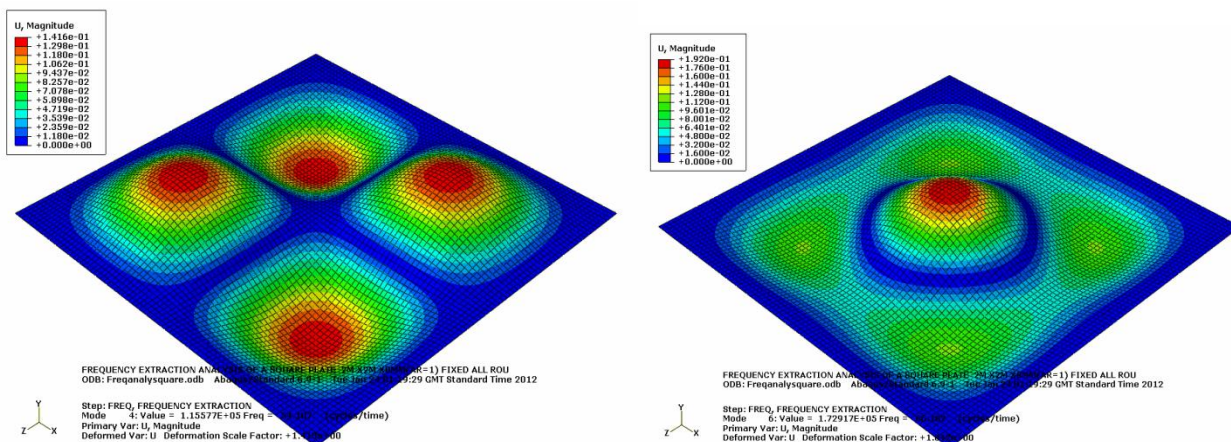


Figure A-2: Frequency extraction analysis of a 2mx2mx8mm plate showing modes 4-6

CASE 3. 2mX2mX.001m - FIX FIX BOUNDARY CONDITION

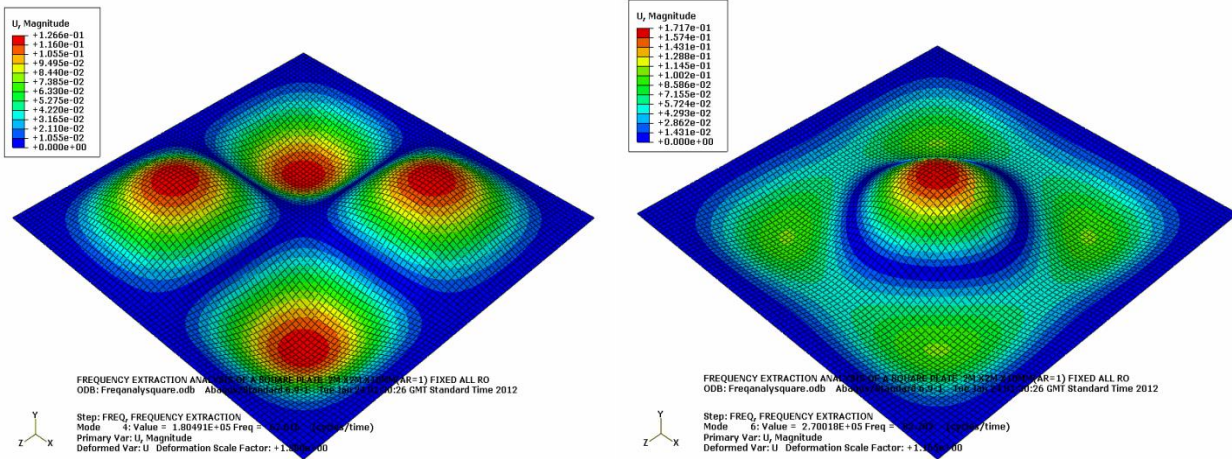


Figure A-3: Frequency extraction analysis of a 2mx2mx10mm plate showing modes 4-6

CASE 4. 2mX2mX0.0012m-FIX-FIX

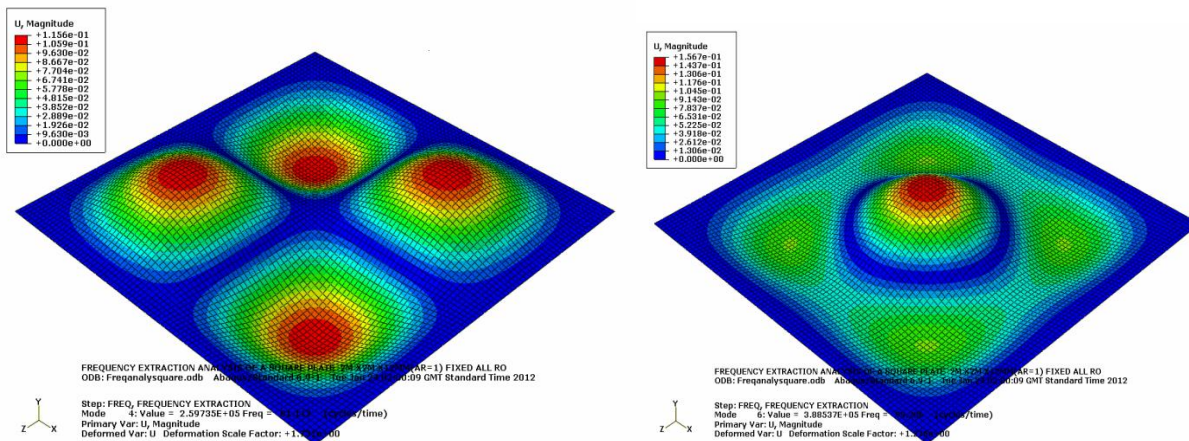


Figure A-4: Frequency extraction analysis of a 2mx2mx12mm plate showing modes 4-6

CASE 7. 2mX2mX0.02m- FIX FIX

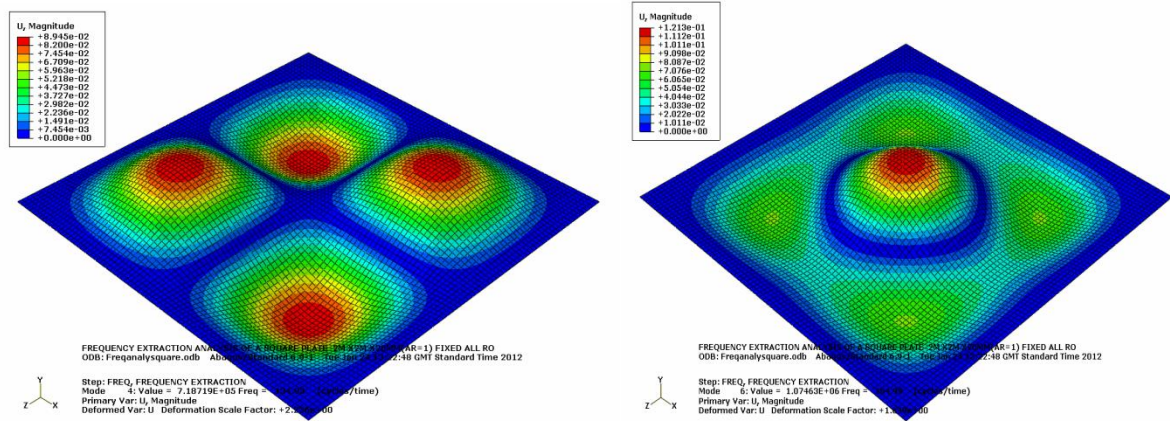


Figure A-7: Frequency extraction analysis of a 2mx2mx20mm plate showing modes 4-6

CASE 7. 2mX2mX0.025m-FIX FIX

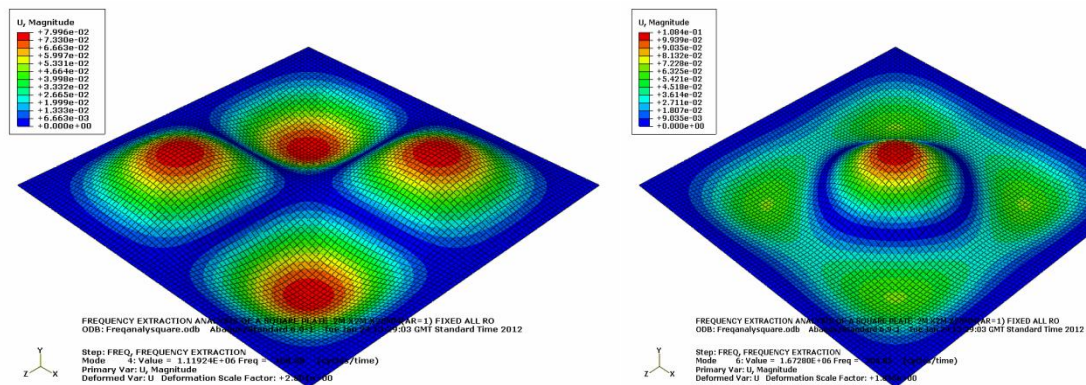


Figure A-7: Frequency extraction analysis of a 2mx2mx25mm plate showing modes 4-6

CASE 8. 2mX2mX0.30m FIX FIX

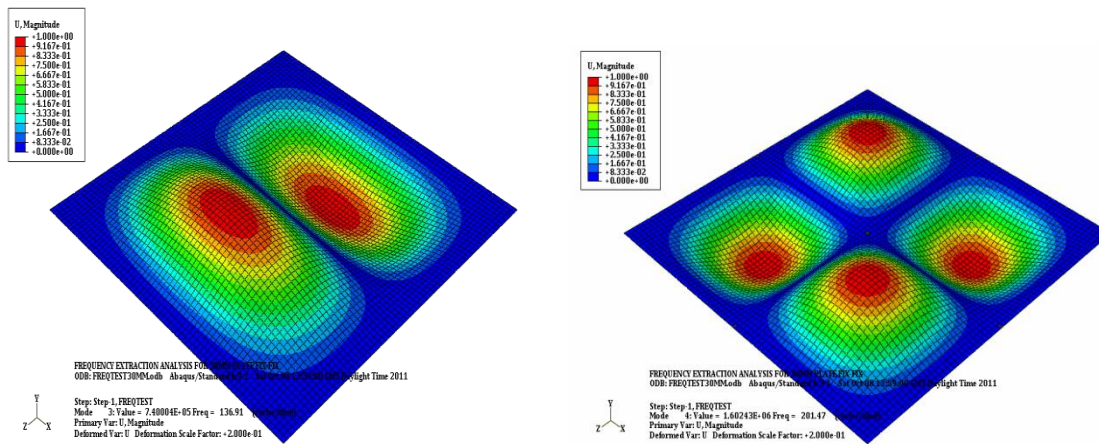


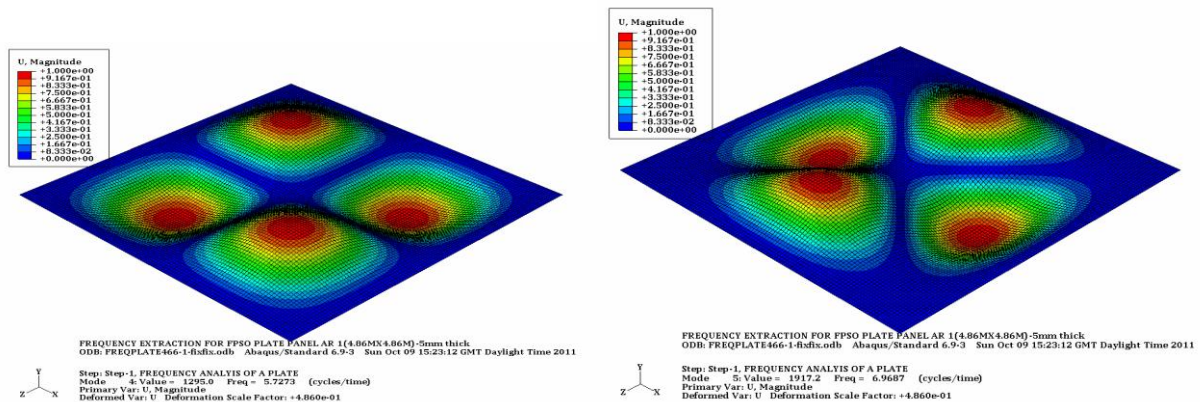
Figure A-8: Frequency extraction analysis of a 2mx2mx25mm plate showing modes 3-4

Appendix B

FREQUENCY EXTRACTION ANALYSIS FROM ABAQUS VALIDATION
CASE (1-8)

Here the frequency extraction analysis reflected below in this appendix are frequency modes for modes 4 to 7 for FPSO Panel plates thickness 5mm,8mm,10mm,12mm,15mm,18mm,20mm,25mm and 30mm thickness reflected as cases 1-9 for different boundary condition carried out by using abaqus software codes

CASE 1: 4.86mx 4.86m x5mm thick plate-All edges Fixed



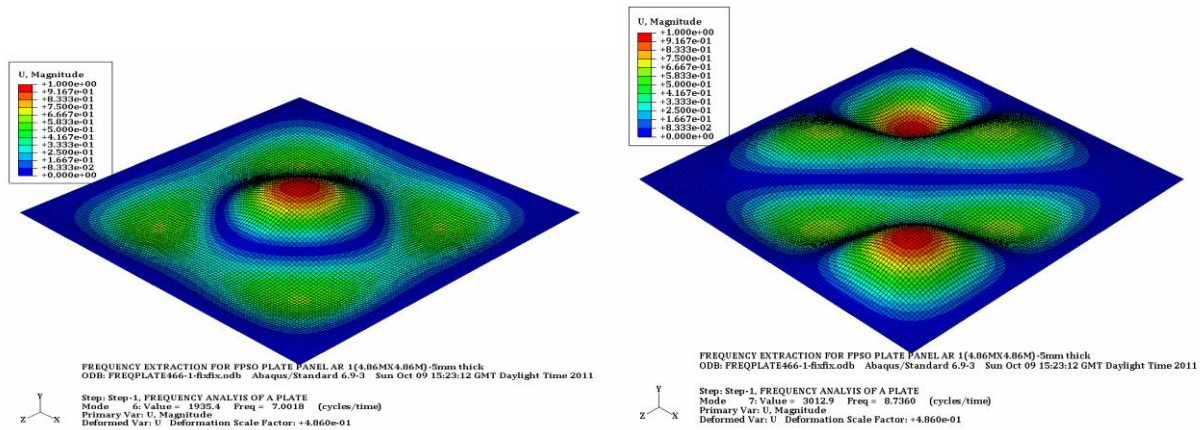


Figure B-1: Frequency extraction analysis of a 2mx2mx5mm plate showing modes 4-7

CASE 2: 4.86m X 4.86mx8mm thick plate

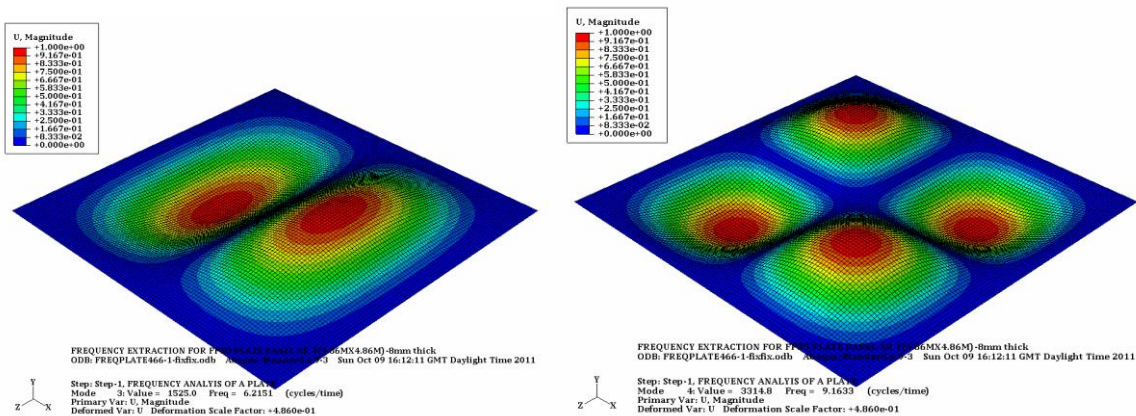


Figure B-2: Frequency extraction analysis of a 2mx2mx8mm plate showing modes 3-4

CASE 3: 4.86m x4.86m x10mm thick plate

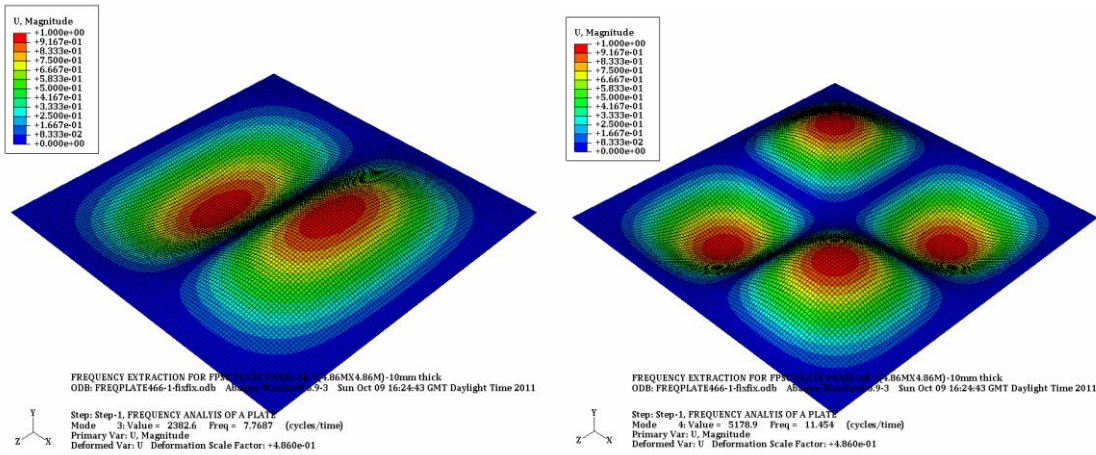


Figure B-3: Frequency extraction analysis of a 2mx2mx10mm plate showing modes 2-4

CASE 4: 14.86m x4.86m x2mm thick plate

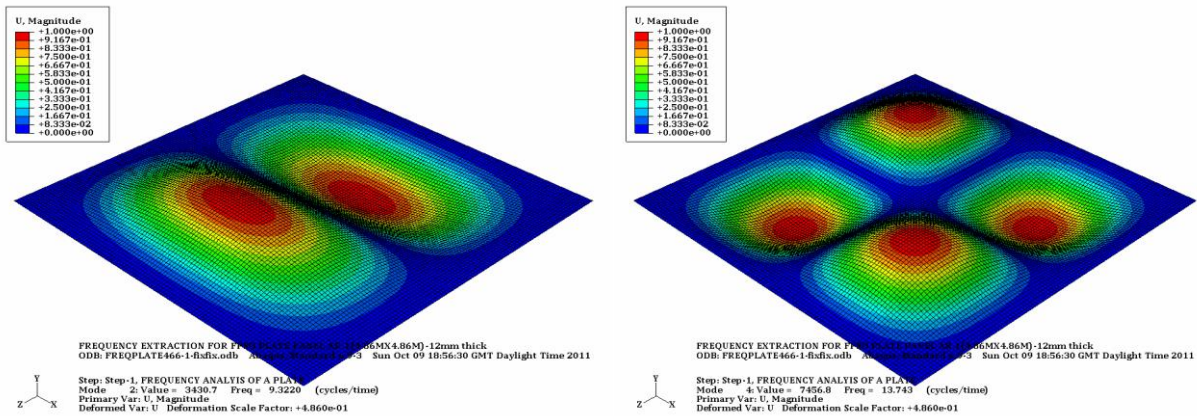


Figure B-4: Frequency extraction analysis of a 2mx2mx12mm plate showing modes 2-4

CASE 5: 4.86m x4.86m x 5mm thick plate

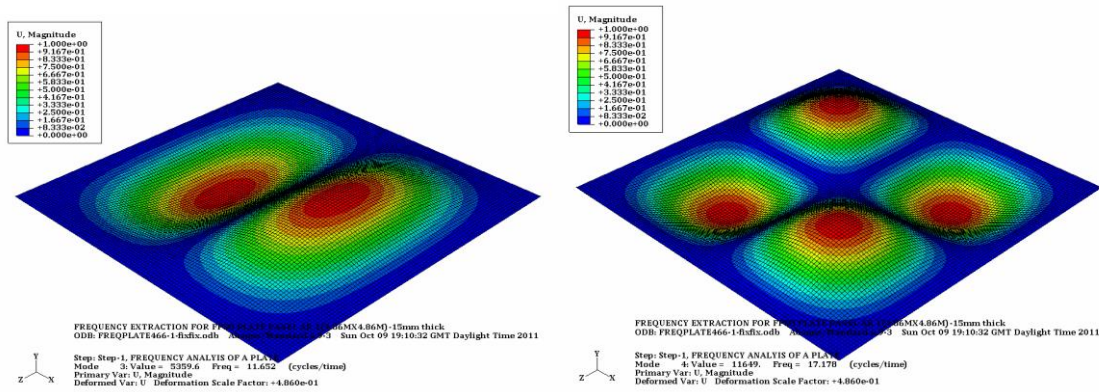


Figure B-5: Frequency extraction analysis of a 2mx2mx15mm plate showing modes 3-4

CASE 6: 4.86m x4.86m x18mm thick plate

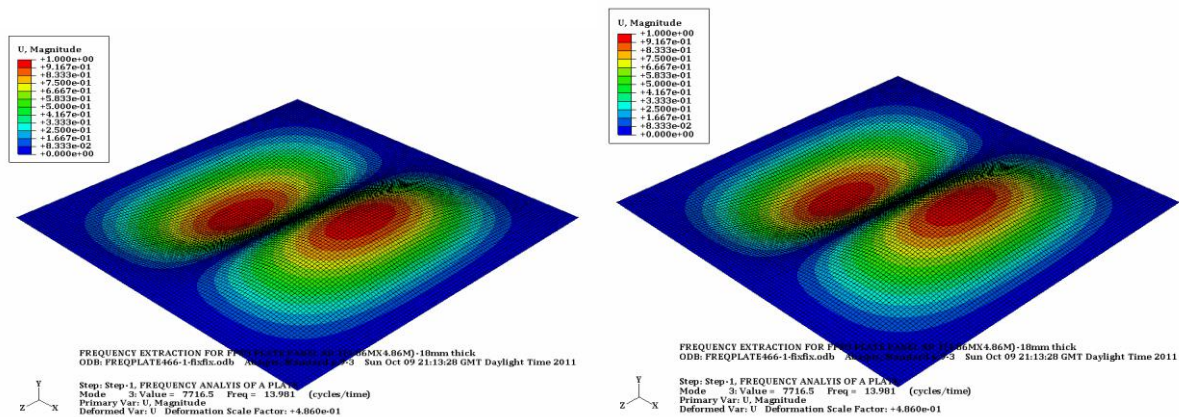


Figure B-6: Frequency extraction analysis of a 2mx2mx18mm plate showing modes 2-4

CASE 7: 4.86m x4.86m x20mm thick plate

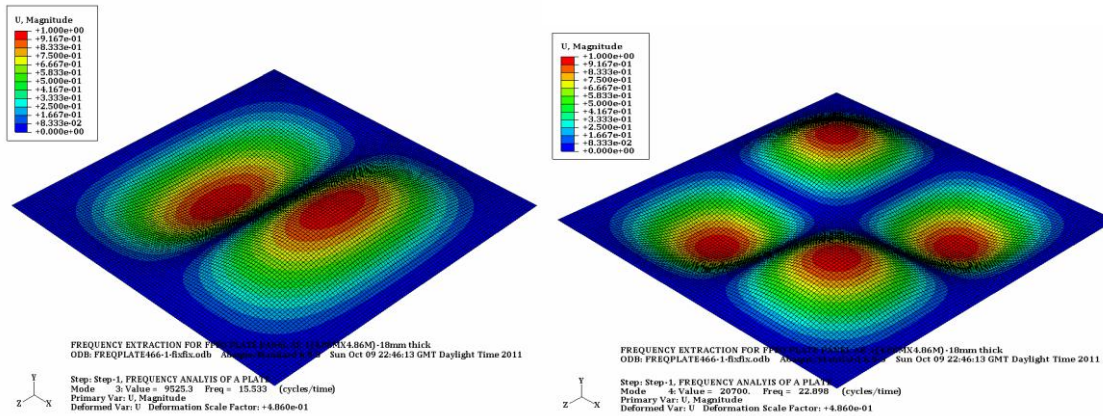


Figure B-6: Frequency extraction analysis of a 2mx2mx20mm plate showing modes 2-4

CASE 8: 4.86m x4.86m x 25mm thick plate

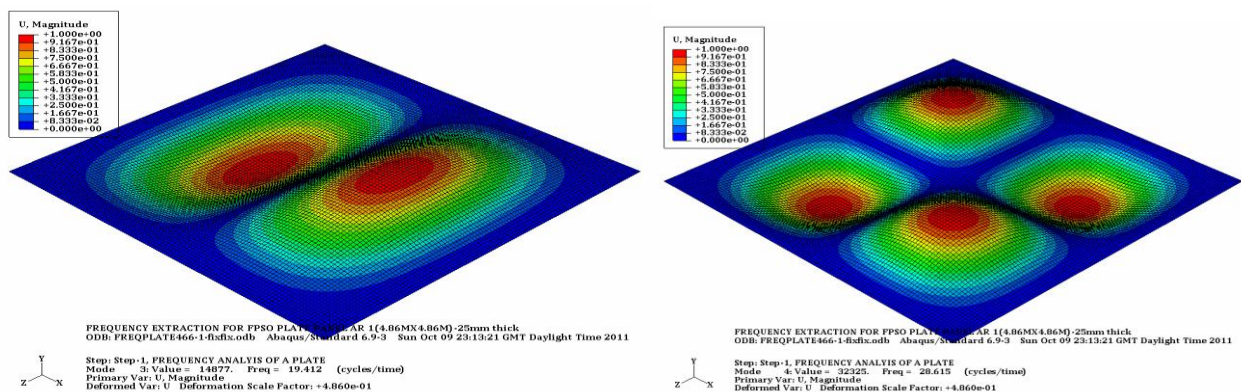


Figure B-7: Frequency extraction analysis of a 2mx2mx25mm plate showing modes 2-4

CASE 8: 4.86m x4.86m x30mm thick plate

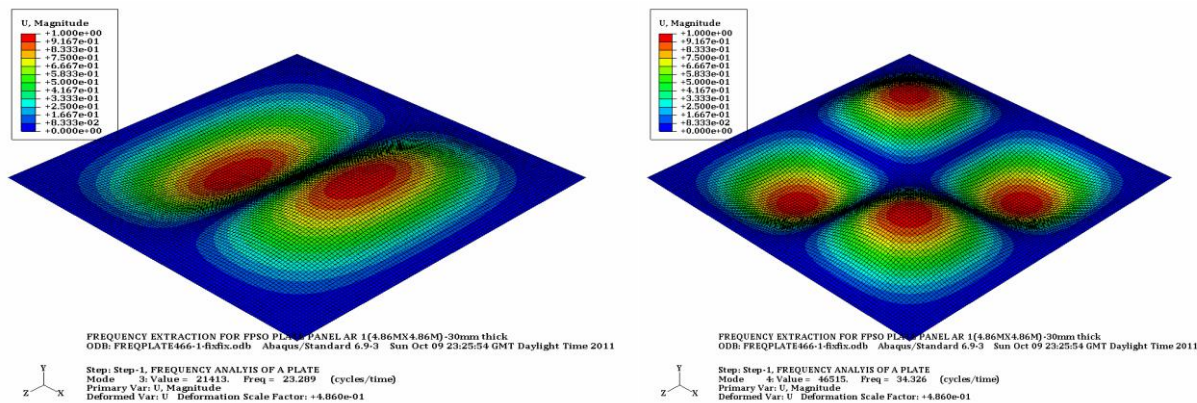


Figure B-8: Frequency extraction analysis of a 2mx2mx30mm plate showing modes 2-4

Appendix C

FREQUENCY EXTRACTION ANALYSIS FROM ABAQUS VALIDATION CASE (1-8)

Here the frequency extraction analysis reflected below in this appendix are frequency modes for modes 4 to 7 for FPSO Panel plates thickness 5mm,8mm,10mm,12mm,15mm,18mm,20mm,25mm and 30mm thickness reflected as cases 1-9 for different boundary condition carried out by using abaqus software codes

CASE 1: 4.86mx 4.86m x30mm thick Plate

Boundary condition: FIX, FREE, FREE, FREE

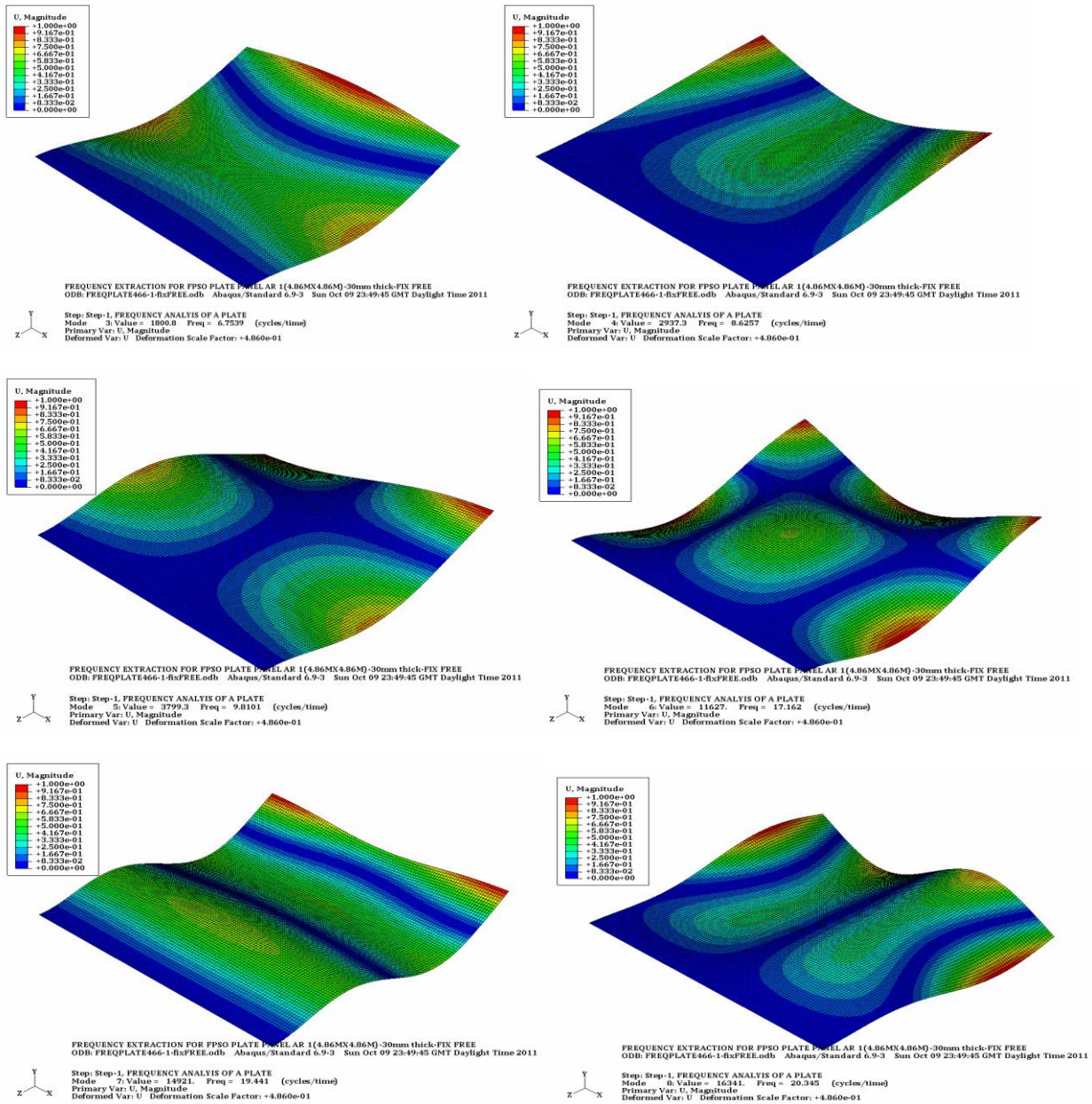


FIGURE C-1: Frequency extraction analysis of a 2mx2mx30mm plate showing modes 4-8

CASE 2: 4.86mx 4.86m x 25mm thick plate

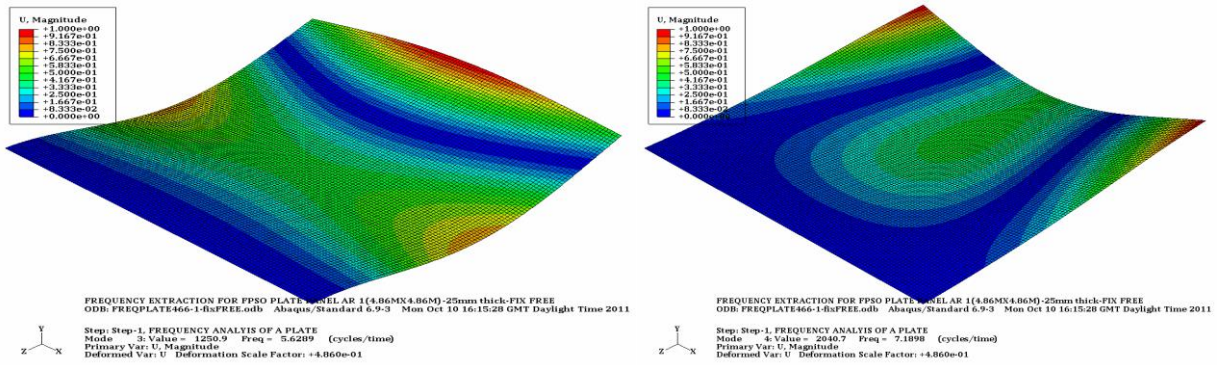


FIGURE C-2: Frequency extraction analysis of a 2mx2mx25mm plate showing modes 2-4

CASE 3: 20mm thick plate

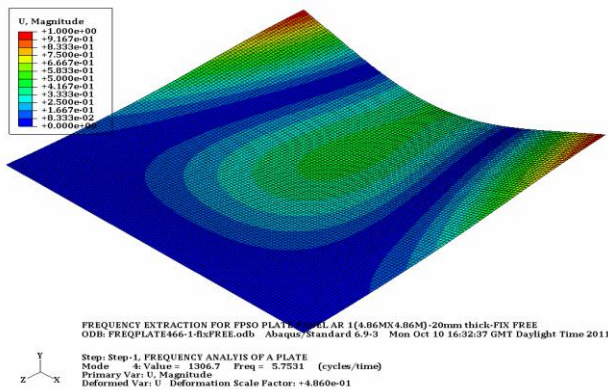


FIGURE C-3: Frequency extraction analysis of a 2mx2mx20mm plate showing modes 4

CASE 4: 4.86mx 4.86m 15mm thick plate

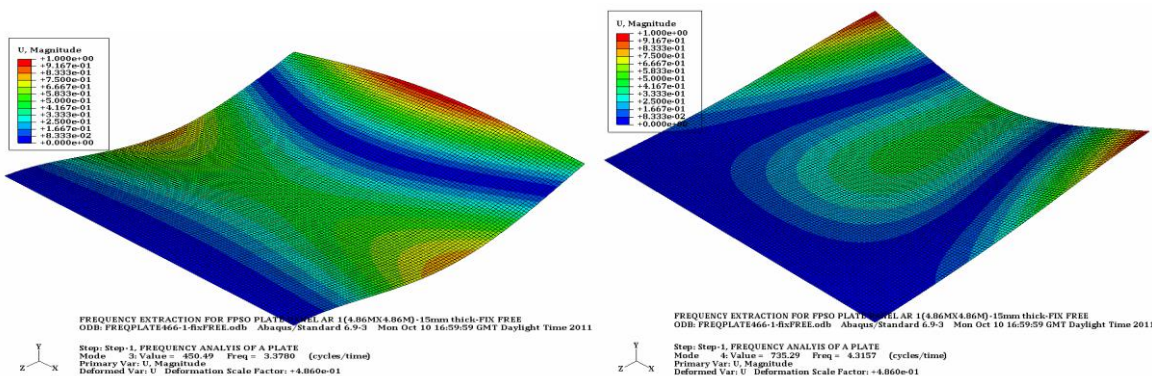


FIGURE C-4: Frequency extraction analysis of a 4.86mx4.86mx15mm plate showing modes 3-4

CASE 5: 4.86mx 4.86m x 10mm thick plate

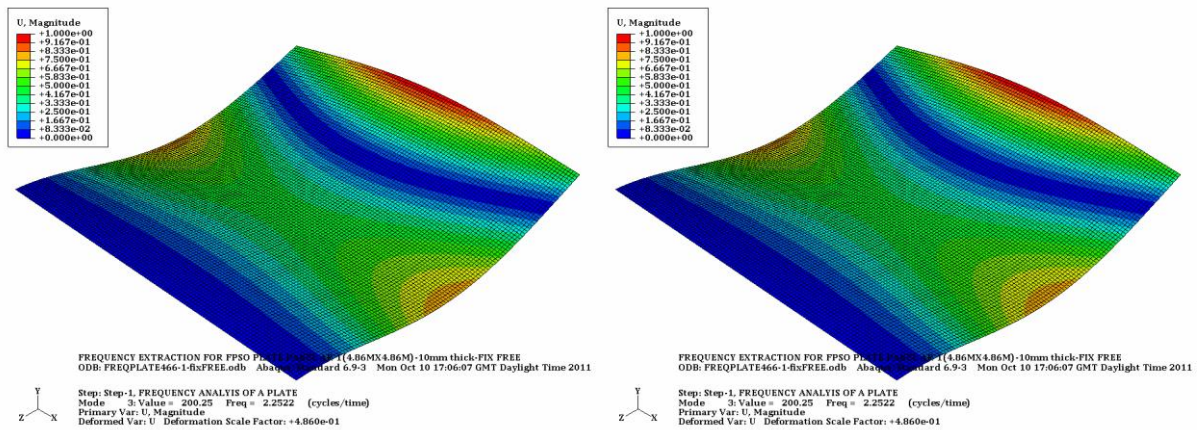


FIGURE C-5: Frequency extraction analysis of a 4.86mx4.86mx10mm plate showing modes 2-4

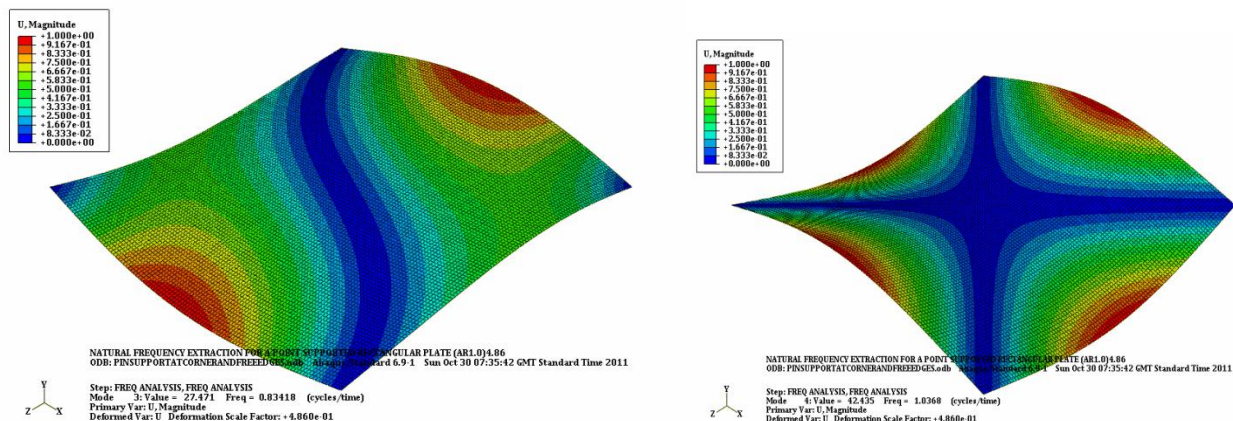
Appendix D

FREQUENCY EXTRACTION ANALYSIS FROM ABAQUS VALIDATION CASE (1-8)

Here the frequency extraction analysis reflected below in this appendix are frequency modes for modes 4 to 7 for FPSO Panel plates thickness 5mm,8mm,10mm,12mm,15mm,18mm,20mm,25mm and 30mm thickness reflected as cases 1-9 for different boundary condition carried out by using abaqus software codes

- **BOUNDARY CONDITION: POINT SUPPORTED AT THE EDGES**
- **FPSO Plate Panel is of size 4.86m x 4.86m**

Case 1-4.86 x4.86m-5m Plate



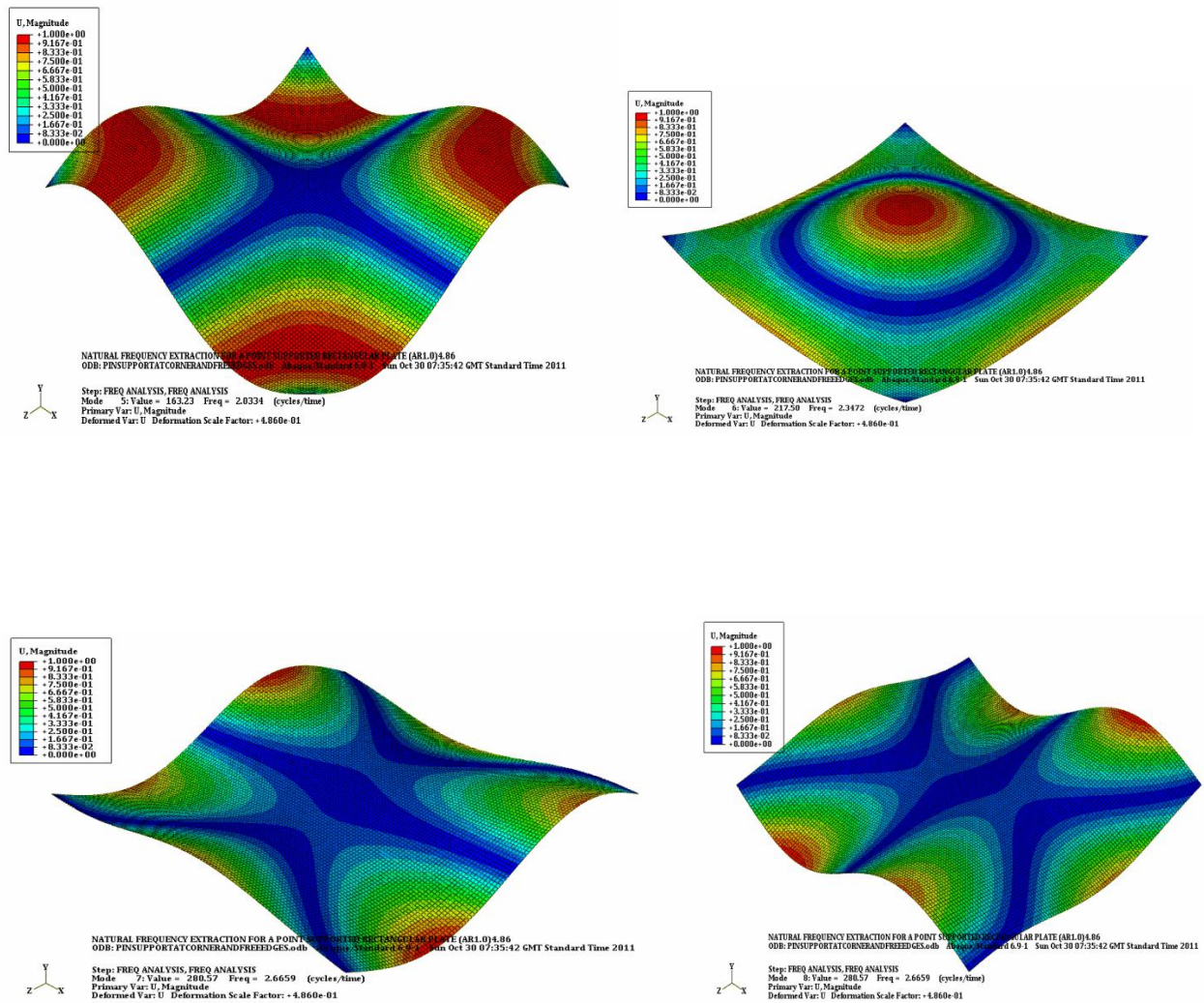


FIGURE D-1: Frequency extraction analysis of a 4.86mx4.86mx5mm plate Showing modes 1-8-Point Supported load.

CASE 2-10mm Plate (4.86x4.86m)

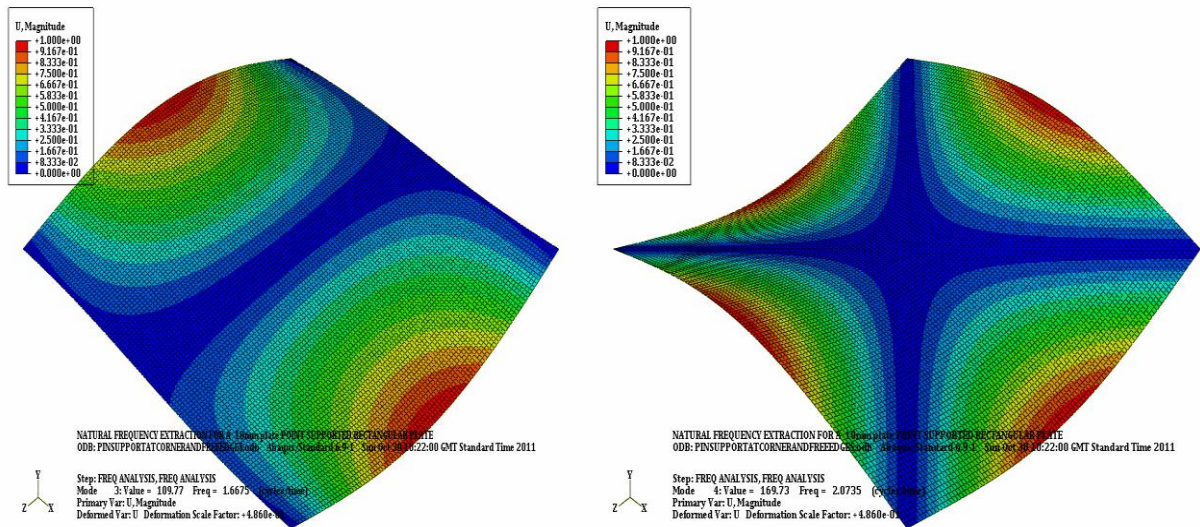


FIGURE D-2: Frequency extraction analysis of a 4.86mx4.86mx10mm plate Showing modes 2-4-Point Supported load

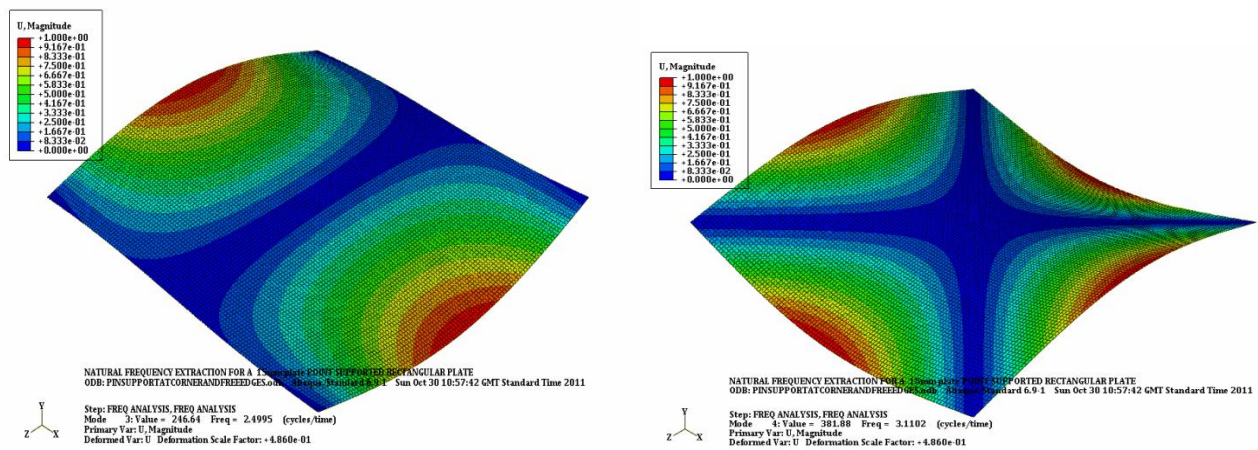


FIGURE D3-: Frequency extraction analysis of a 4.86mx4.86mx15mm plate Showing modes 3-4-Point Supported load

CASE 4-20mm Plate (4.86x4.86m)

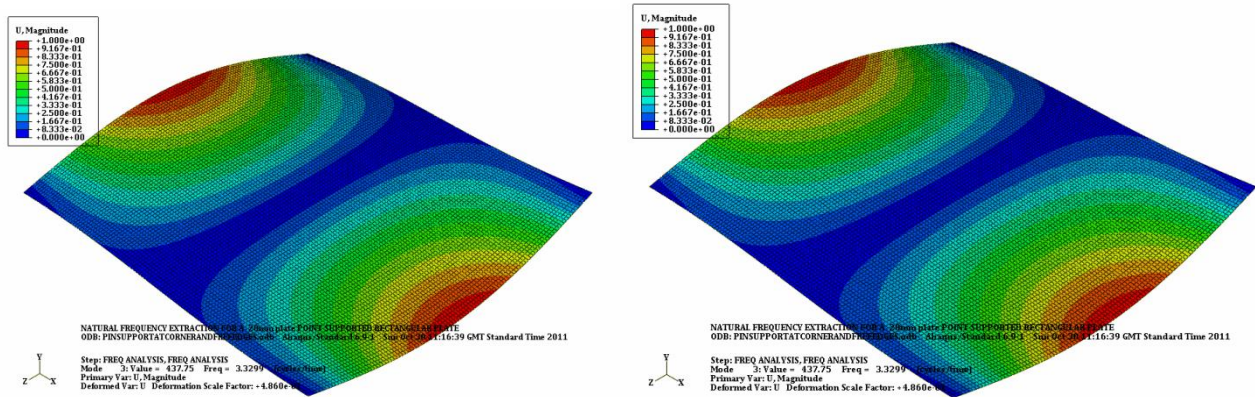


FIGURE D-4: Frequency extraction analysis of a 4.86mx4.86mx20mm plate Showing modes 1-4-Point Supported load

CASE 5-25mm Plate (4.86x4.86m)

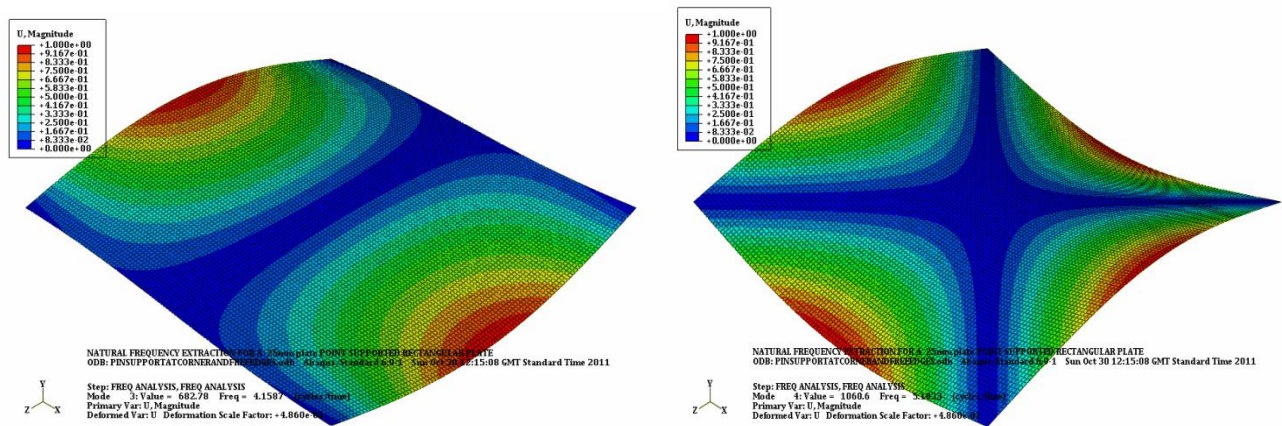


FIGURE D-5: Frequency extraction analysis of a 4.86mx4.86mx25mm plate Showing modes 3-4-Point Supported load

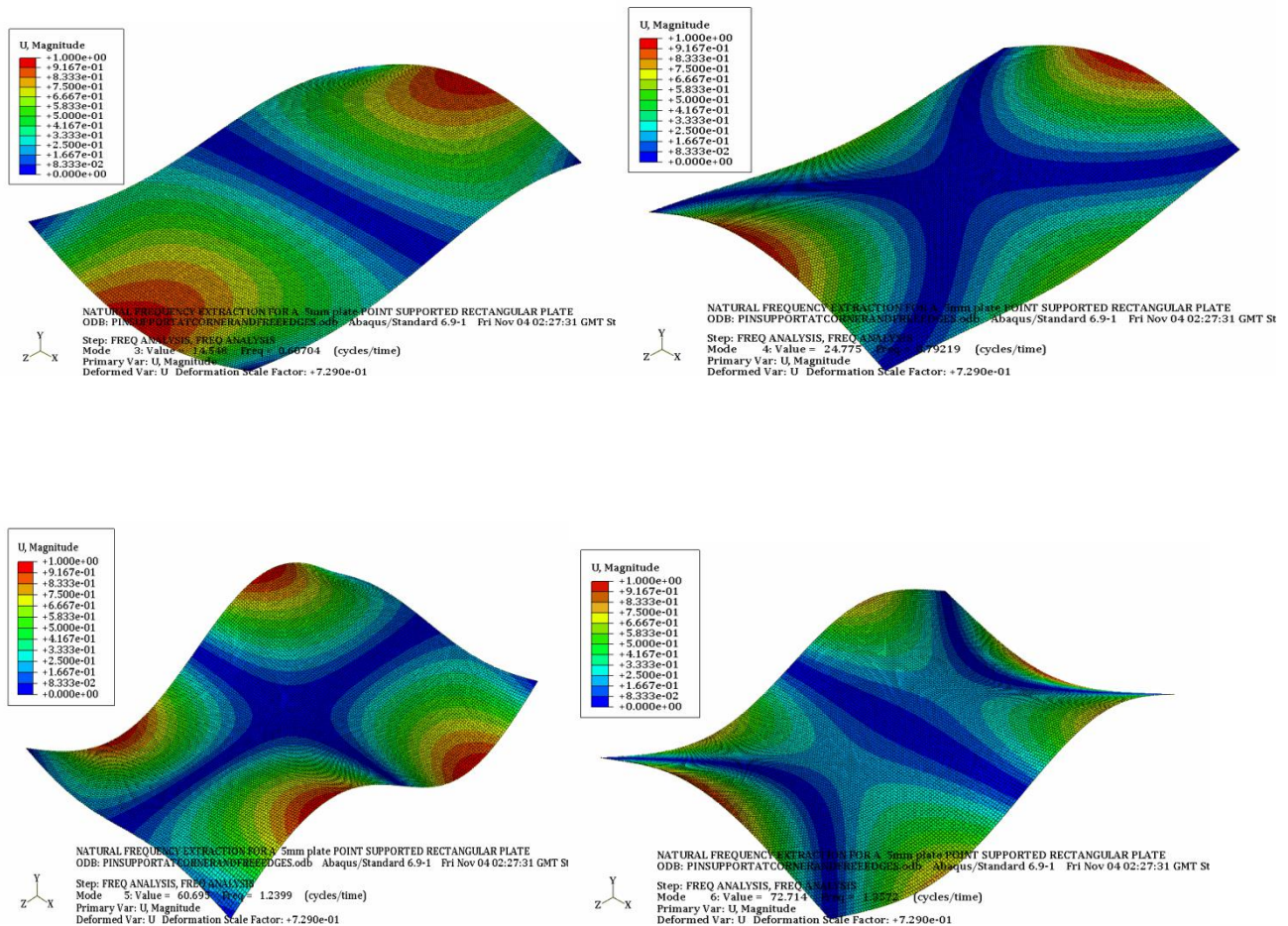
Appendix E

FREQUENCY EXTRACTION ANALYSIS FROM ABAQUS VALIDATION CASE (1-8)

Here the frequency extraction analysis reflected below in this appendix are frequency modes for modes 4 to 7 for FPSO Panel plates thickness 5mm,8mm,10mm,12mm,15mm,18mm,20mm,25mm and 30mm thickness reflected as cases 1-9 for different boundary condition carried out by using abaqus software codes

- **BOUNDARY CONDITION: POINT SUPPORTED AT THE EDGES**
- **FPSO Plate Panel is of size 4.86m x 4.86m**
- **ASPECT RATIO=1.5**

CASE 1-5mm Plate (4.86x7.29m)



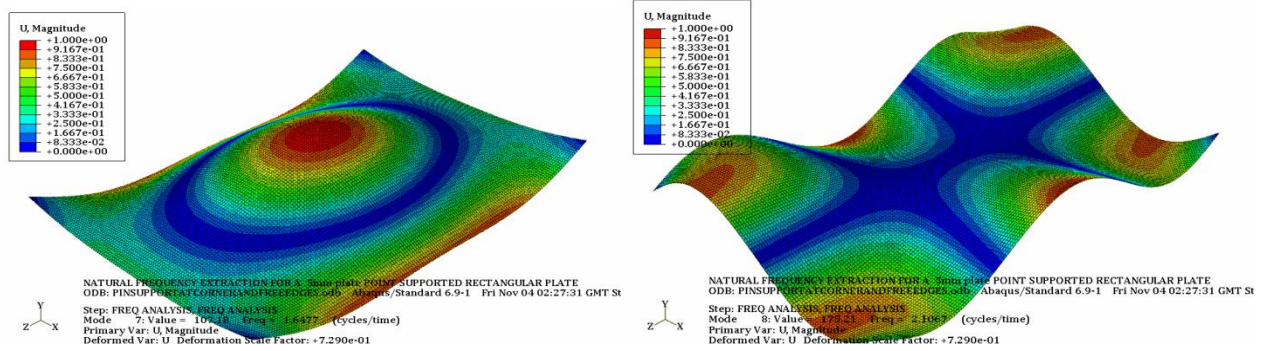


FIGURE E-1: Frequency extraction analysis of a 4.86mx7.29mx5mm plate Showing modes 3-8-Point Supported load

CASE 2-10mm Plate (4.86x7.29m)

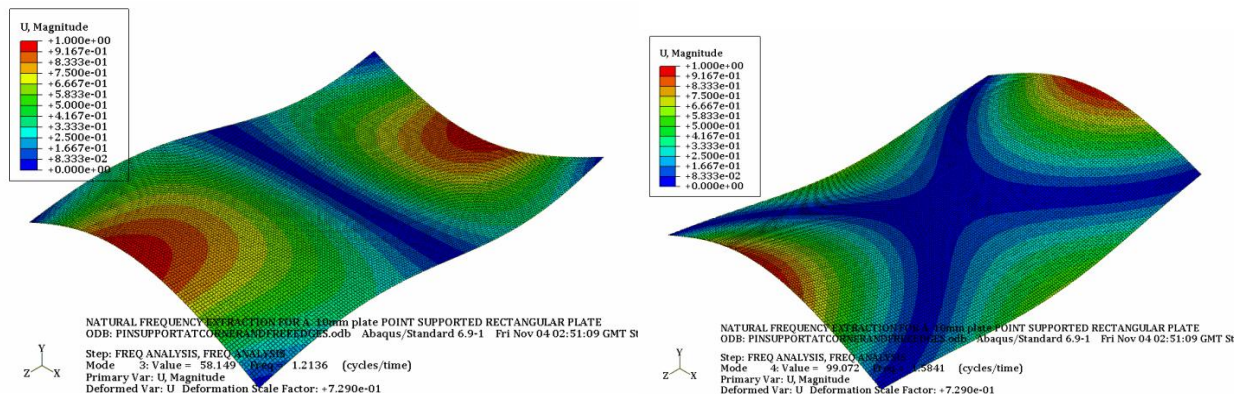
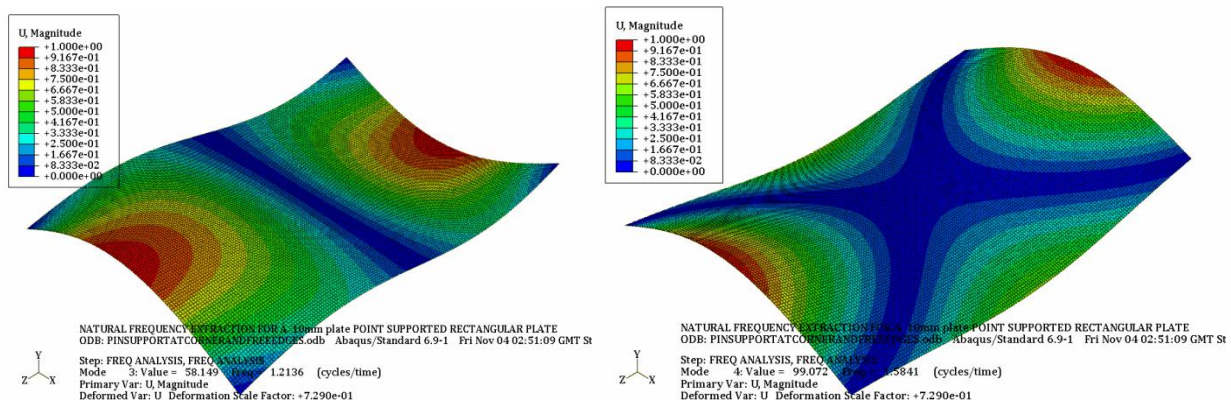


FIGURE E-2: Frequency extraction analysis of a 4.86mx7.29mx10mm plate Showing modes 3-4-Point Supported load

CASE 3-15mm Plate (4.86x7.29m)



**FIGURE E-3: Frequency extraction analysis of a 4.86mx7.29mx15mm plate
Showing modes 1-4-Point Supported load**

CASE 4-20mm Plate (4.86x7.29m)

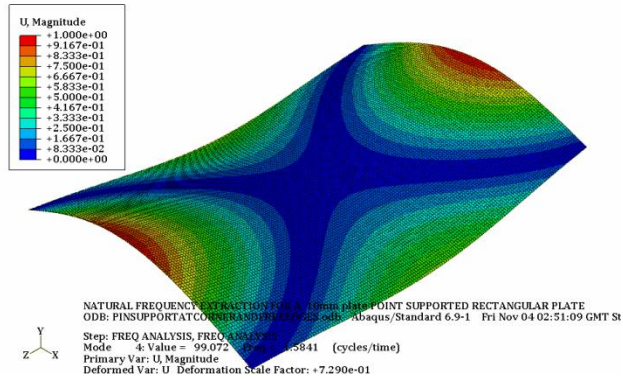


**FIGURE E-4: Frequency extraction analysis of a 4.86mx7.29mx20mm plate
Showing modes 1-4-Point Supported load**

CASE 5-25mm Plate (4.86x7.29m)

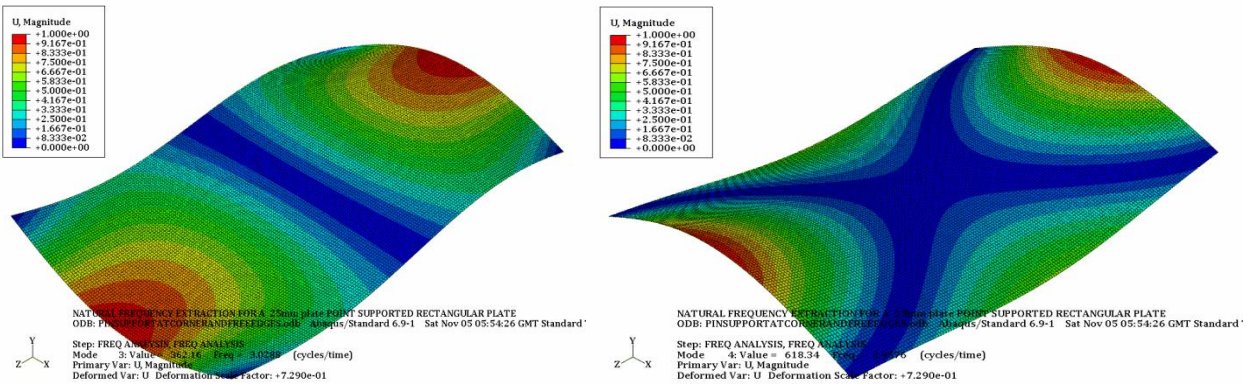
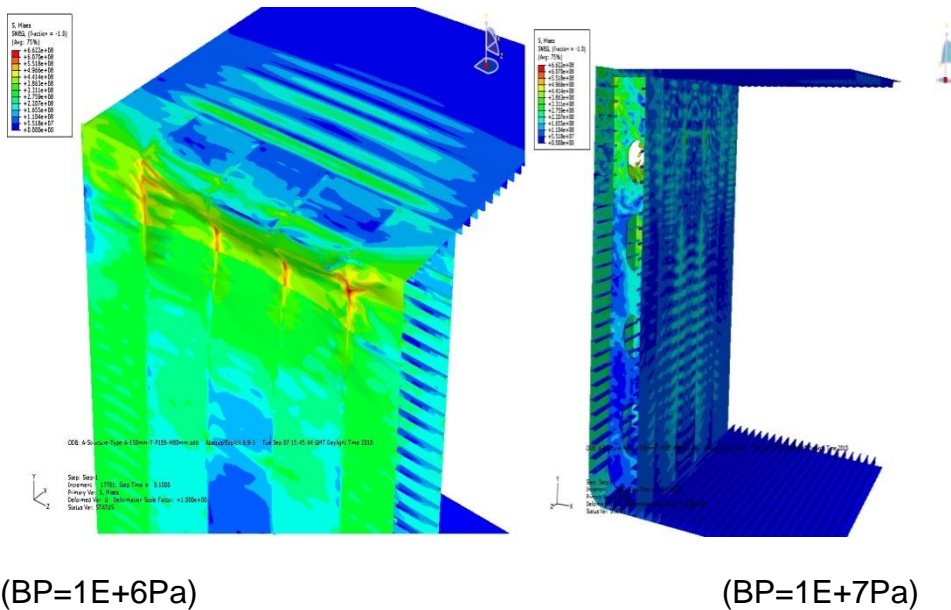


FIGURE E-5: Frequency extraction analysis of a 4.86mx7.29mx20mm plate Showing modes 3-4-Point Supported load

Appendix F

SOME SIMULATION OF BLAST ANALYSIS RESULTS

TYPE A(TA)-stiffeners Flange Size (150mm x 14mm thick) Blast Pressure (BP)-1E+6-1E+8 PASCAL,80mm Mesh (Where BP-BLAST PRESSURE



TYPE C- T STIFFENERS WITH FLANGE SIZE (250mm x 8.4mm thick)-Type C (TC)

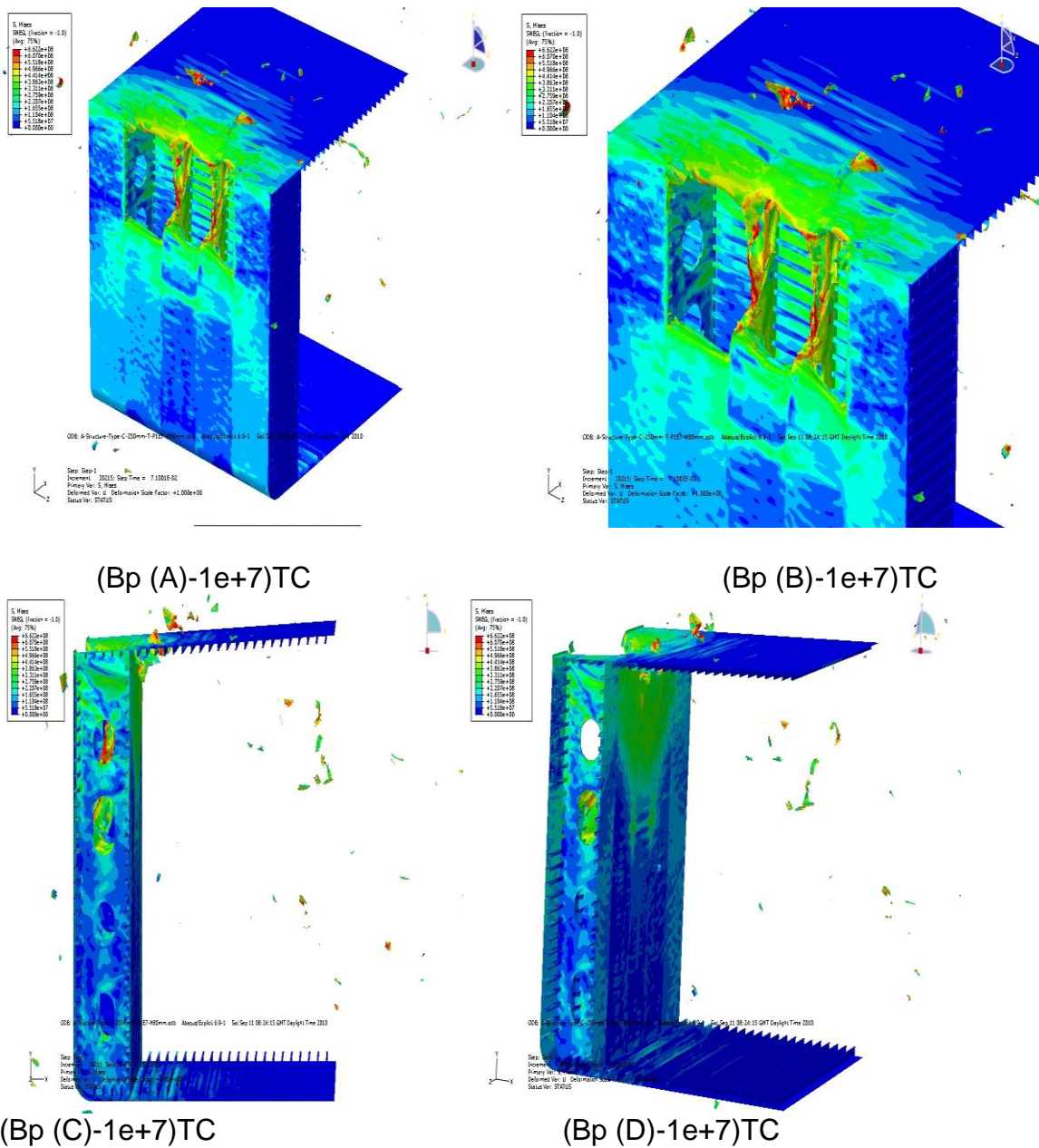
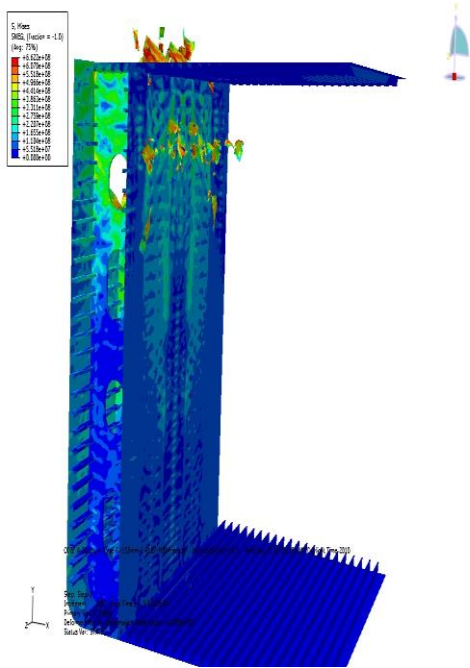


FIGURE J-3 : Showing some blast simulation results for Type C stiffeners

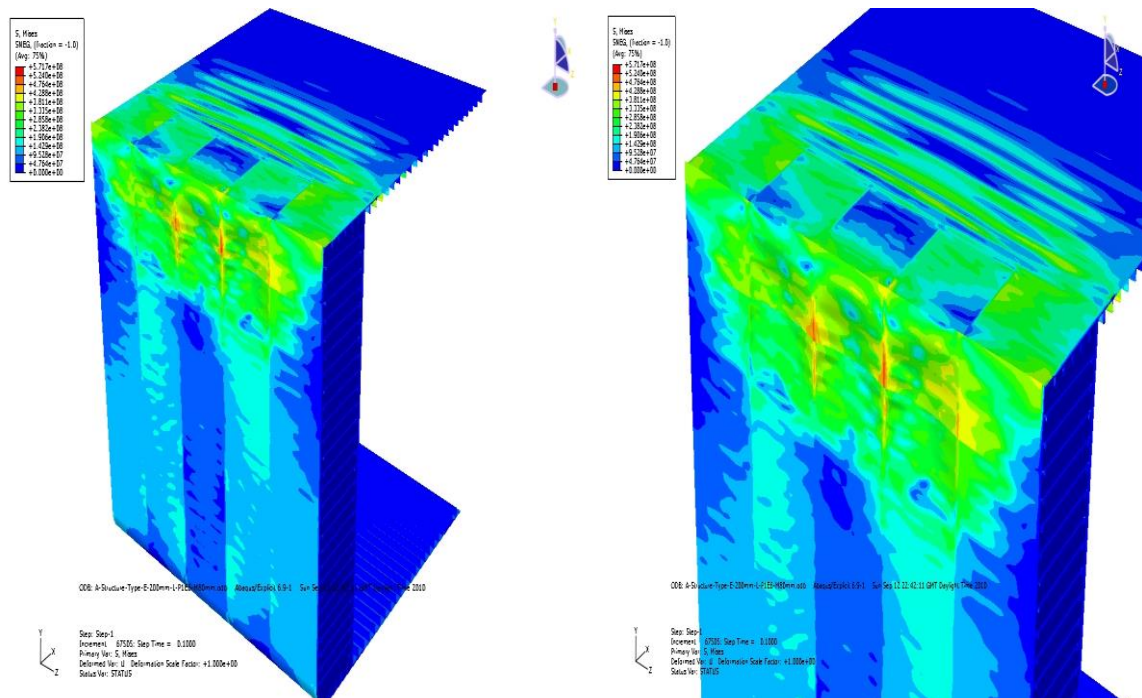
TYPE D- L-STIFFENERS WITH FLANGE SIZE (150mm x 14mmmm thick)-TYPE D(TD)



(Bp (C)-1e+7)TD

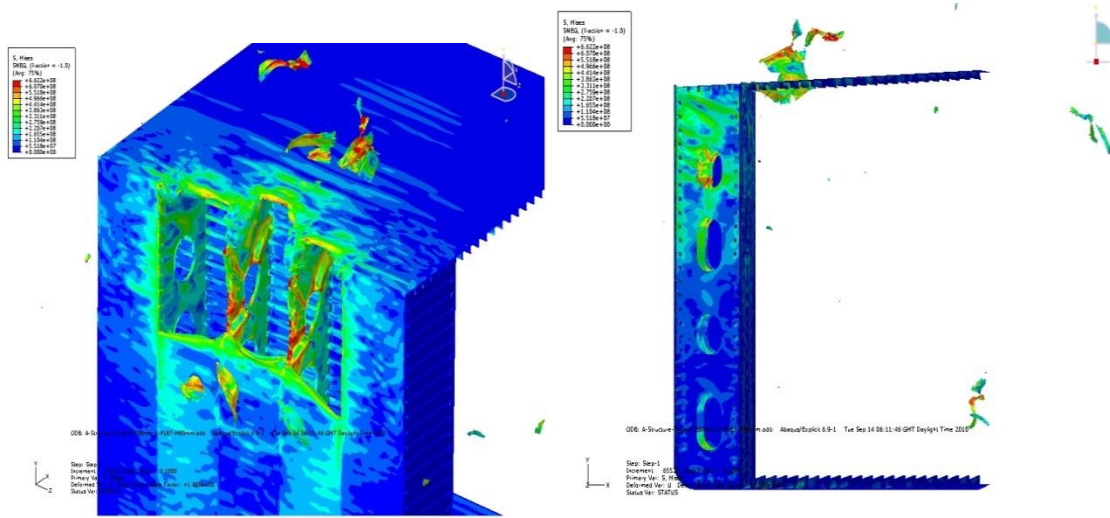
FIGURE F-4 : Showing some blast simulation results for Type D

TYPE E-STIFFENERS WITH FLAGE SIZE (200mm x 10.5mm thick)-L SHAPE



(Bp (a)-1e+6)TE

(Bp (b)-1e+6)TE



(Bp (a)-1e+7)TE

(Bp (a)-1e+7)TE

FIGURE F-5 : Showing some blast simulation results for Type E

TYPE F-STIFFENERS WITH FLAGE SIZE (250mm x 8.4mm thick)-L SHAPE

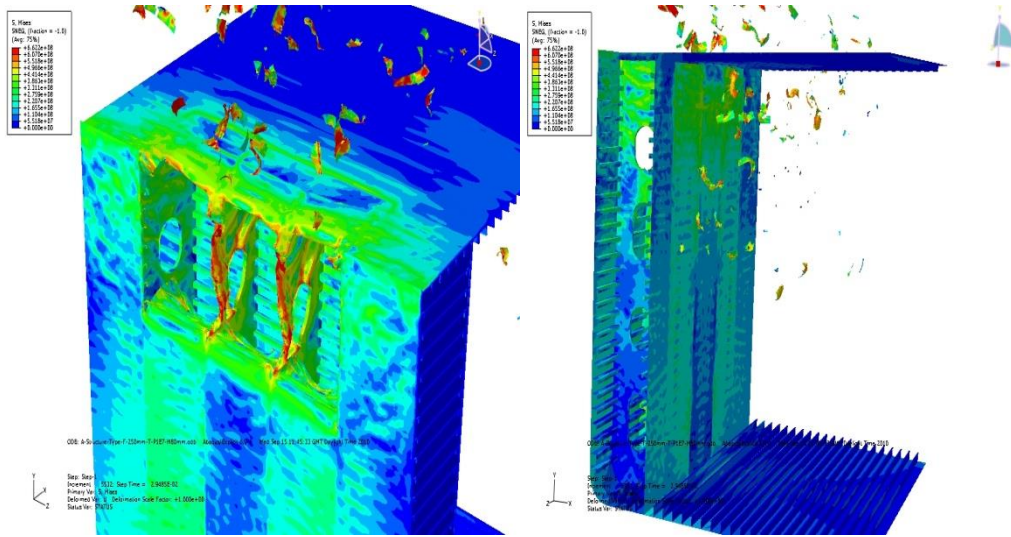


FIGURE F-6 : Showing some blast simulation results for Type F

References

- Alexander M. Remennikov, (2003) “A review of methods for predicting bomb blast effects on buildings”, *Journal of battlefield technology*, vol 6, no 3. pp 155-161.
- Alia A, Souli M. High explosive simulation using multimaterial formulations. *Applied Thermal Engineering* 2006;26: 1032–42.
- Alonso FD, Ferradas EG, Perez SJF, Gimeno JR, Alonso JM. Characteristic overpressure–impulse–distance curves for the detonation of explosives, pyrotechnics or unstable substances. *Journal of Loss Prevention in the Process Industries* 2006; 19(6):724–8.
- American Society for Civil Engineers 7-02 (1997), “Combination of Loads”, pp 239-244. ANSYS Theory manual, version 5.6, 2000.
- Baker WR, Cox PA, Westine PS, Kulesz JJ, Strehlow RA. *Explosion hazards and evaluation*. New York: Elsevier Scientific Publishing Company; 1983.
- Balden VH, Nurick GN. Numerical simulation of the post-failure motion of steel plates subjected to blast loading. *International Journal of Impact Engineering* 2005;32(1–4):14–34.
- Batra RC, Dube RN. Impulsively loaded circular plates. *International Journal of Solids and Structures* 1971;7(8):965–78.
- Batra RC, Dube RN. Impulsively loaded circular plates. *International Journal of Solids and Structures* 1971;7(8):965–78.
- Biggs JM. *Introduction to structural dynamics*. New York: McGraw-Hill; 1964.
- Biggs, J.M. (1964), “Introduction to Structural Dynamics”, McGraw-Hill, New York.
- Bjerketvedt D, Bakke JR, Wingerden KV. Gas explosion handbook. *Journal of Hazardous Materials* 1997;52:1–150.
- Bjerketvedt D, Bakke JR, Wingerden KV. Gas explosion handbook. *Journal of Hazardous Materials* 1997;52:1–150.
- Bjorno L, Levin P. Underwater explosion research using small amount of chemical explosives. *Ultrasonics* 1976:263–7.
- Bjorno L, Levin P. Underwater explosion research using small amount of chemical explosives. *Ultrasonics* 1976:263–7.

Bodner SR, Symonds PS. Experiments on viscoplastic response of circular plates to impulsive loading. *Journal of Mechanics and Physics of Solids* 1979;27(2):91–113.

Bodner SR, Symonds PS. Experiments on viscoplastic response of circular plates to impulsive loading. *Journal of Mechanics and Physics of Solids* 1979;27(2):91–113.

Clough RW, Penzien J. *Dynamics of structures*. New York: McGraw-Hill; 1975.

Clutter JK, Stahl M. Hydrocode simulations of air and water shocks for facility vulnerability assessments. *Journal of Hazardous Materials* 2004;106(1):9–24.

Cole RH. *Underwater explosions*. New York: Dover Publications Inc.; 1948.

Craig RR. *Structural dynamics*. New York: Wiley; 1981. pp. 251–261.

D.L. Grote et al. (2001), “Dynamic behaviour of concrete at high strain rates and pressures”, *Journal of Impact Engineering*, Vol. 25, Pergamon Press, New York, pp. 869-886,

Dannis M. McCann, Steven J. Smith (2007), “Resistance Design of Reinforced Concrete Structures”, *STRUCTURE* magazine, pp 22-27, April issue

Demeter G. Fertis (1973), “Dynamics and Vibration of Structures”, A Wiley-Interscience publication, pp. 343-434.

Deshpande VS, Fleck NA. One-dimensional response of sandwich plates to underwater shock loading. *Journal of Mechanics and Physics of Solids* 2005;53(11):2347–83.

Ezra AA. *Principles and practice of explosive metal working, Part I*, Industrial Newspapers Ltd.. Adelphi, London, WC2N 6JH: John Adams House; 1973.

Florence AL. Circular plates under a uniformly distributed impulse. *International Journal of Solids and Structures* 1966; 2(1):37–47.

Florence AL. Circular plates under a uniformly distributed impulse. *International Journal of Solids and Structures* 1966;2(1):37-37

Formby SA, Wharton RK. Blast characteristics and TNT equivalence values for some commercial explosives detonated at ground level. *Journal of Hazardous Materials* 1996;50(2–3):183–98.

Fox EN. A review of underwater explosion phenomena. *Compendium of Underwater Explosion Research*, ONR 1947;1: 1-83

Gifford LN, Carlberg JR, Wiggs AJ, Sickles JB. Explosive testing of full thickness pre-cracked weldments. In: Gudas JP, Joyce JA, Hockett EM, editors. Fracture mechanics twenty first symposium, ASTM-STP-1074. Philadelphia: ASTM; 1990. p. 157–77.

Gifford LN, Dally JW. Fracture resistance of metal structures loaded into plastic regime. In: Smith CS, Dow RS, editors. Advances in marine structures-2. Elsevier Applied Science; 1991. p. 23–41.

Glasstone S, Dolan PJ. Effects of nuclear weapons. Washington, DC: US Department of Defence and the Energy Research and Development Administration; 1977.

Gong SW, Lam KY, Lu C. Structural analysis of a submarine pipeline subjected to underwater shock. International Journal of Pressure Vessels and Piping 2000;77(7):417–23.

Gupta NK, Nagesh. Deformation and tearing of circular plates with varying support conditions under uniform impulsive loads. International Journal of Impact Engineering 2007;34(1):42–59.

Hartbower CE, Pellini WS. Explosion bulge test studies on deformation of weldments. Welding Journal 1951:307s–18s.

Hartbower CE, Pellini WS. Investigation factors which determine the performance of weldments. Welding Journal 1951: 499s–511s.

Hung CF, Hsu PY, Fuu JJH. Elastic shock response of an air-backed plate to underwater explosion. International Journal of Impact Engineering 2005;31(2):151–68.

Idczak W, RymarzCz, Sychala A. Studies on shock-wave loaded circular plates. Journal of Technical Physics 1981;22(2): 175-84

Idczak W, RymarzCz, Sychala A. Studies on shock-wave loaded circular plates. Journal of Technical Physics 1981;22(2): 175-84

IS 456:2000 Indian Standard Plain and Reinforced Concrete Code of Practice.

J.M. Dewey (1971), “The Properties of Blast Waves Obtained from an analysis of the particle trajectories”, Proc. R. Soc. Lond. A.314, pp. 275-299.

J.M. Gere and S.P. Timoshenko (1997.), “Mechanics of materials”, PWS publishing company, Boston, Massachusetts,

Jacinto AC, Abrosini RD, Danesi RF. Experimental and computational analysis of plates under air blast loading. International Journal of Impact Engineering 2001;25(10):927–47.

Jacob N, Yuen CH, Nurick GN, Bonorchis D, Desai SA, Tait D. Scaling aspects of quadrangular plates subjected to localised blast loads – experiments and predictions. International Journal of Impact Engineering 2004;30(7–8):1179–208.

Johnson W. Impact strength of materials. London: Edward Arnold; 1972.

Jones N. Structural impact. Cambridge University Press; 1989.

Keil AH. The response of ships to underwater explosions. Transactions of Society of Naval Architects and Marine Engineers 1961;69:366–410.

Keil. Introduction to underwater explosion research. Portsmouth, Virginia: UERD, Norfolk Naval Shipyard; 1956.

Kennard AH. The effect of pressure wave on a plate diaphragm. Compendium of Underwater Explosion Research, ONR 1944;3:11–64.

Keshawarz MH, Nazari HR. A simple method to assess detonation temperature without using any experimental data and computer code. Journal of Hazardous Materials 2006;133(1–3):129–34.

Keshawarz MH, Pouretedal HR. An empirical method for predicting detonation pressure of CHNOFCl explosives. ThermochimicaActa 2004;414:203–8.

Keshawarz MH. Detonation velocity of pure and mixed CHNO explosives at maximum nominal density. Journal of Hazardous Materials 2007;141(3):536–9.

Khadid, A. et al. (2007), “Blast loaded stiffened plates” Journal of Engineering and Applied Sciences, Vol. 2(2) pp. 456-461.

Kinnery GF, Graham KJ. Explosive shocks in air. Berlin: Springer Verlag; 1985.

Kirk A. Marchand, FaridAlfawakhiri (2005), “Blast and Progressive Collapse” fact for Steel Buildings, USA.

Langdon GS, Cantwell WJ, Nurick GN. The blast response of novel thermoplastic-based fibre-metal laminates – some preliminary results and observations. Composites Science and Technology 2005;65(6):861–72.

Langdon GS, Schleyer GK. Inelastic deformation and failure of clamped aluminium plates under pulse pressure loading. International Journal of Impact Engineering 2003;28(10):1107–27.

Lee YW, Wierzbicki T. Fracture prediction of thin plates under localized impulse loading. Part-I: dishing. International Journal of Impact Engineering 2005;31(10):1253–76.

Lee YW, Wierzbicki T. Fracture prediction of thin plates under localized impulse loading. Part-II: discing and petalling. International Journal of Impact Engineering 2005;31(10):1277–308.

Liang CC, Tai YS. Shock response of a surface ship subjected to non-contact underwater explosions. *Ocean Engineering* 2006;33(5–6):748–72.

Luccioni B, Ambrosini D. Blast load assessment using hydrocodes. In: Larreteguy A, editor. *Mechanica Computational*, vol. XXIV; 2005. p. 329–44. Buenos Aires, Argentina.

Luccioni B, Ambrosini D. Blast load assessment using hydrocodes. In: Larreteguy A, editor. *Mechanica Computational*, vol. XXIV; 2005. p. 329–44. Buenos Aires, Argentina.

M. V. Dharaneepathy et al. (1995), “Critical distance for blast resistance design”, *computer and structure* Vol. 54, No.4.pp.587-595.

Ma GW, Shi HJ, Shu DW. P–I diagram method for combined failure modes of rigid-plastic beams. *International Journal of Impact Engineering* 2007;34(6):1081–94.

Makinen K. Cavitation models for structures excited by a plane shock wave. *Journal of Fluids and Structures* 1998;12(1):85-101

Makinen K. The transverse response of sandwich panels to an underwater shock wave. *Journal of Fluids and Structures* 1999;13(5):631–46.

Nelson Lam et al. (2004), “Response Spectrum Solutions for Blast Loading”, *Journal of Structural Engineering*, pp 28-44.

Nurick GN, Gelman ME, Marshall NS. Tearing of blast loaded plates with clamped boundary conditions. *International Journal of Impact Engineering* 1996;7–8:803–27.

Nurick GN, Martin JB. Deformation of thin plates subjected to impulsive loading—a review. Part-I: theoretical considerations. *International Journal of Impact Engineering* 1989;8(2):159–69.

Nurick GN, Martin JB. Deformation of thin plates subjected to impulsive loading—a review. Part-I: theoretical considerations. *International Journal of Impact Engineering* 1989;8(2):159–69.

Nurick GN, Martin JB. Deformation of thin plates subjected to impulsive loading—a review. Part-II: experimental studies. *International Journal of Impact Engineering* 1989;8(2):171–86.

Nurick GN, Martin JB. Deformation of thin plates subjected to impulsive loading—a review. Part-II: experimental studies. *International Journal of Impact Engineering* 1989;8(2):171–86.

Nurick GN, Olson MD, Fagnan JR, Levin A. Deformation and tearing of blast-loaded stiffened square plates. *International Journal of Impact Engineering* 1995;16(2):273–91.

Nurick GN, Pearce HT, Martin JB. Predictions of transverse deflections and in-plane strains in impulsively loaded thin plates. *International Journal of Mechanical Sciences* 1987;29(6):435–42.

- Nurick GN, Pearce HT, Martin JB. Predictions of transverse deflections and in-plane strains in impulsively loaded thin plates. *International Journal of Mechanical Sciences* 1987;29(6):435–42.
- Nurick GN, Radford AM. Deformation and tearing of clamped circular plates subjected to localised central blast loads. In: Reddy BD, editor. *Recent developments in computational and applied mechanics, A volume in honour of J.B.Martin*; 1997. p. 276–301.
- Nurick GN. A new technique to measure the deflection-time history of a structure subjected to high strain rates. *International Journal of Impact Engineering* 1985;3(1):17–26.
- Nurick GN. A new technique to measure the deflection-time history of a structure subjected to high strain rates. *International Journal of Impact Engineering* 1985;3(1):17–26.
- Nurick GN. An empirical solution for predicting the maximum central deflection of impulsively loaded plates. In: *International conference on mechanical properties of materials at high rates of strain*. Oxford: Institute of Physics Society; 1989. p. 457–63. No.12, Session: 9.
- Nurick GN. The measurement of deformation response of a structure subjected to an explosive load using light interference technique. In: *Proceedings of 1986 SEM spring conference on experimental mechanics*. The Society of Experimental Mechanics Inc.; 1986. p. 105–14.
- Nurick GN. The measurement of deformation response of a structure subjected to an explosive load using light interference technique. In: *Proceedings of 1986 SEM spring conference on experimental mechanics*. The Society of Experimental Mechanics Inc.; 1986.p. 105–14.
- Nurick GN. Using photo voltaic diodes to measure the deformation response of a structure subjected to an explosive load, SPIE. *High-speed Photography* 1986;674:215–25.
- Nurick GN. Using photo voltaic diodes to measure the deformation response of a structure subjected to an explosive load, SPIE. *High-speed Photography* 1986;674:215–25.
- Olson MD, Nurick GN, Fagnan JR. Deformation and rupture of blast loaded square plates – predictions and experiments. *International Journal of Impact Engineering* 1993;13(2):279–91.
- P. Desayi and S. Krishnan (1964), “Equation for the stress-strain curve of concrete”. *Journal of the American Concrete Institute*, 61, pp 345-350.
- Pan Y, Louca LA. Experimental and numerical studies on the response of stiffened plates subjected to gas explosions. *Journal of Constructional Steel Research* 1999;52(2):171–93.
- Pandey, A. K. et al. (2006) “Non-linear response of reinforced concrete containment structure under blast loading” *Nuclear Engineering and design* 236. pp.993-1002.
- Park BW, Cho SR. Simple design formulae for predicting the residual damage of unstiffened and stiffened plates under explosion loadings. *International Journal of Impact Engineering* 2006;32(10):1721–36.

- Porter JF, Morehouse DO. Development of the DREA underwater single shot explosion bulge procedure. In Canadian fracture conference, Halifax, Nova Scotia; 1990.
- Porter JF. Response of SMA and narrow gap SMA weldments to explosive shock. Technical Memorandum 88/206, DREA, Atlantic, Canada; 1988.
- Rajendran R, Narasimhan K. A shock factor based approach for the damage assessment of plane plates subjected to underwater explosions. *Journal of Strain Analysis for Engineering Design* 2006;41(6):417–25.
- Rajendran R, Narasimhan K. Damage prediction of clamped circular plates subjected to contact underwater explosion. *International Journal of Impact Engineering* 2001;25(4):373–86.
- Rajendran R, Narasimhan K. Deformation and fracture behaviour of plate specimens subjected to underwater explosion – a review. *International Journal of Impact Engineering* 2006;32(12):1945–63.
- Rajendran R, Narasimhan K. Linear elastic shock response of plane plates subjected to underwater explosion. *International Journal of Impact Engineering* 2001;25(5):493–506.
- Rajendran R, Narasimhan K. Performance evaluation of HSLA steel subjected to underwater explosion. *Journal of Materials Engineering and Performance* 2001;10(1):66–74.
- Rajendran R, Narasimhan K. Underwater shock response of circular HSLA steel plates. *Shock and Vibration* 2000;7:251–62.
- Rajendran R, Paik JK, Kim BJ. Design of warship plates against underwater explosions. *Ships and Offshore Structures* 2006; 1(4):347–56.
- Rajendran R, Paik JK, Lee JM. Of underwater explosion experiments on plane plates. *Experimental Techniques* 2007;31(1):18–24.
- Rajendran R. Response of thin HSLA steel plates to underwater explosive shock loading. Ph.D. thesis, Indian Institute of a review. *International Journal of Impact Engineering* 2006;32(12):1945–63.
- Ronald L. Shope (2006), “Response of wide flange steel columns subjected to constant axial load and lateral blast load”. Civil Engineering Department, Blacksburg, Virginia.
- Rudhrapatna RS, Vaziri R, Olson MD. Deformation and failure of blast loaded square plates. *International Journal of Impact Engineering* 1999;22(4):449–67.
- Rudhrapatna RS, Vaziri R, Olson MD. Deformation and failure of blast loaded stiffened plates. *International Journal of Impact Engineering* 2000;24(5):457–74.
- S.Unnikrishna Pillai and Devdas Menon (2003) , “Reinforced Concrete Design”, Tata McGraw-Hill, pp 121-196.

- S.UnnikrishnaPillai and DevdasMenon (2003), “Reinforced Concrete Design”, Tata McGraw-Hill.
- Schleyer GK, Hsu SS, White MD, Birch RS. Pulse pressure loading of clamped mild steel plates. *International Journal of Impact Engineering* 2003;28(2):223–47.
- Schleyer GK, Lowak MJ, Polcyn MA, Langdon GS. Experimental investigation of blast wall panels under shock pressure loading. *International Journal of Impact Engineering* 2007;42(6):1095–118.
- Schmidt, Jon A. (2003), “Structural Design for External Terrorist Bomb Attacks”, *STRUCTURER* magazine, March issue.
- Shin YS. Ship shock modeling and simulation for far field explosion. *Computers and Structures* 2004;82(23–26):2211–9.
- Stoffel M, Schmidt R, Weichert D. Shock wave-loaded plates. *International Journal of Solids and Structures* 2001;38(42–43):7659–80.
- Stoffel M. An experimental method for measuring the buckling shapes of thin-walled structures. *Thin-walled Structures* 2006;44(1):69–73.
- Stoffel M. An experimental method to validate viscoplastic constitutive equations in the dynamic response of plates. *Mechanics of Materials* 2005;37(12):1210–22.
- Stoffel M. Sensitivity of simulations depending upon material parameter variations. *Mechanics Research Communications* 2005;32(3):332–6.
- Stoffel M. Shape forming of shock wave loaded viscoplastic plates. *Mechanics Research Communications* 2006;33(1):35–41
- Sumpter JDG. Design against fracture in welded joints. In: Smith CS, Clarke JD, editors. *Advances in marine structures*. Elsevier Applied Science Publishers; 1986. p. 326–46.
- Sumpter JDG. Design against fracture in welded joints. *Journal of Naval Science* 1987;13(4):258–70.
- Sumpter JDG. Prediction of critical crack size in plastically strained weld panels. *ASTM-STP-995*; 1989. p. 415–432.
- T. A. Rose et al. (2006), “The interaction of oblique blast waves with buildings”, Published online: 23 August 06 © Springer-Verlag, pp 35–44.
- T. Borvik et al.(2009) “Response of structures to planar blast loads – A finite element engineering approach” *Computers and Structures* 87, pp 507–520,

T. Ngo, P. Mendis, A. Gupta & J. Ramsay, “Blast Loading and Blast Effects on structure”, The University of Melbourne, Australia, 2007.

Taylor GI. The pressure and impulse of submarine explosion waves on plates. *Compendium of Underwater Explosion Research*, ONR 1941;1:1155–74.

Teeling-Smith RG, Nurick GN. The deformation and tearing of thin circular plates subjected to impulsive loads. *International Journal of Impact Engineering* 1991;11(1):77–91.

TM 5-1300(UFC 3-340-02) U.S. Army Corps of Engineers (1990), “Structures to Resist the Effects of Accidental Explosions”, U.S. Army Corps of Engineers, Washington, D.C., (also Navy NAVFAC P200-397 or Air Force AFR 88-22).

U.S. Navy. Standard procedure for explosion bulge testing of ferrous and non-ferrous metallic materials and weldments. MIL-STD-2149A (SH); 1990.

Veldman RL, Ari-Gur J, Clum C, DeYong A, Folkert J. Effect of pre-pressurization on blast response of clamped aluminium plates. *International Journal of Impact Engineering* 2006;32(10):1678–95.

Wai-Fah Chen and Atef F. Saleeb (1994), “Constitutive Equations for Engineering Materials- Volume 1: Elasticity and Modeling”, Elsevier Science B.V.

Wierzbicki T, Florence AL. A theoretical and experimental investigation of impulsively loaded clamped circular viscoplastic plates. *International Journal of Solids and Structures* 1970;6:553–68.

Wierzbicki T, Florence AL. A theoretical and experimental investigation of impulsively loaded clamped circular viscoplastic plates. *International Journal of Solids and Structures* 1970;6:553–68.

Wierzbicki T, Nurick GN. Large deformation of thin plates under localized impulse loading. *International Journal of Impact Engineering* 1996;18(7–8):899–918.

Wierzbicki T. Petalling of plates under explosive and impact loading. *International Journal of Impact Engineering* 1999; 22(9–10):935–54.

Worznicza K, Pennetier O, Renard J. Experimental and numerical simulations on thin metallic plates subjected to explosions. *Journal of Engineering and Materials Technology* 2001;123(2):203–9.

Xue Z, Hutchinson JW. A comparative study of impulse resistant metal sandwich plates. *International Journal of Impact Engineering* 2004;30(10):1283–305.

Xue Z, Hutchinson JW. Preliminary assessment of sandwich plates subject to blast loads. *International Journal of Mechanical Sciences* 2003;45(4):687–705.

Yuen SCY, Nurick GN. Experimental and numerical studies on the response of quadrangular stiffened plates. Part I: subjected to uniform blast load. *International Journal of Impact Engineering* 2005;31(1):55–83.

MIDSHIP SECTION

RAKE OF PLATING

MAIN DECK (CAMBER)	50/1000
BOTTOM SHELL (RISE OF FLOOR)	0
TRANS. FRAME SPACE	4660
MAIN DECK LONG.	
IN C.D.C. TK.	V 400X1 ² F 180X16 (T)
IN V.B.S. TK.	350 X 20 ² F.B.
BOTTOM LONG.	V 550X12 ² F 150X25 ² (T)

